MARTIN MARIETTA ENERGY SYSTEMS LIBRARIES
3 4456 0134585 6

LIBRARY
TION

3

ORNL-3573
UC-80 – Reactor Technology

THE HIGH FLUX ISOTOPE REACTOR ACCIDENT ANALYSIS

CENTRAL RESEARCH LIBRARY
DOCUMENT COLLECTION
LIBRARY LOAN COPY
DO NOT TRANSFER TO ANOTHER PERSON
If you wish someone else to see this document, send in name with document and the library will arrange a loan.

OAK RIDGE NATIONAL LABORATORY
operated by
UNION CARBIDE CORPORATION
for the
U.S. ATOMIC ENERGY COMMISSION

Printed in the United States of America. Available from Clearinghouse for Federal
Scientific and Technical Information, National Bureau of Standards,
U.S. Department of Commerce, Springfield, Virginia 22151
Price: Printed Copy $3.00; Microfiche $0.65

LEGAL NOTICE

This report was prepared as an account of Government sponsored work. Neither the United States, nor the Commission, nor any person acting on behalf of the Commission:

A. Makes any warranty or representation, expressed or implied, with respect to the accuracy, completeness, or usefulness of the information contained in this report, or that the use of any information, apparatus, method, or process disclosed in this report may not infringe privately owned rights; or

B. Assumes any liabilities with respect to the use of, or for damages resulting from the use of any information, apparatus, method, or process disclosed in this report.

As used in the above, "person acting on behalf of the Commission" includes any employee or contractor of the Commission, or employee of such contractor, to the extent that such employee or contractor of the Commission, or employee of such contractor prepares, disseminates, or provides access to, any information pursuant to his employment or contract with the Commission, or his employment with such contractor.

ORNL-3573
UC-80 – Reactor Technology

Contract No. W-7405-eng-26

THE HIGH FLUX ISOTOPE REACTOR ACCIDENT ANALYSIS

Edited by
F. T. Binford
T. E. Cole
E. N. Cramer

APRIL 1967

OAK RIDGE NATIONAL LABORATORY
Oak Ridge, Tennessee
operated by
UNION CARBIDE CORPORATION
for the
U. S. ATOMIC ENERGY COMMISSION

MARTIN MARIETTA ENERGY SYSTEMS LIBRARIES
3 4456 0134585 6

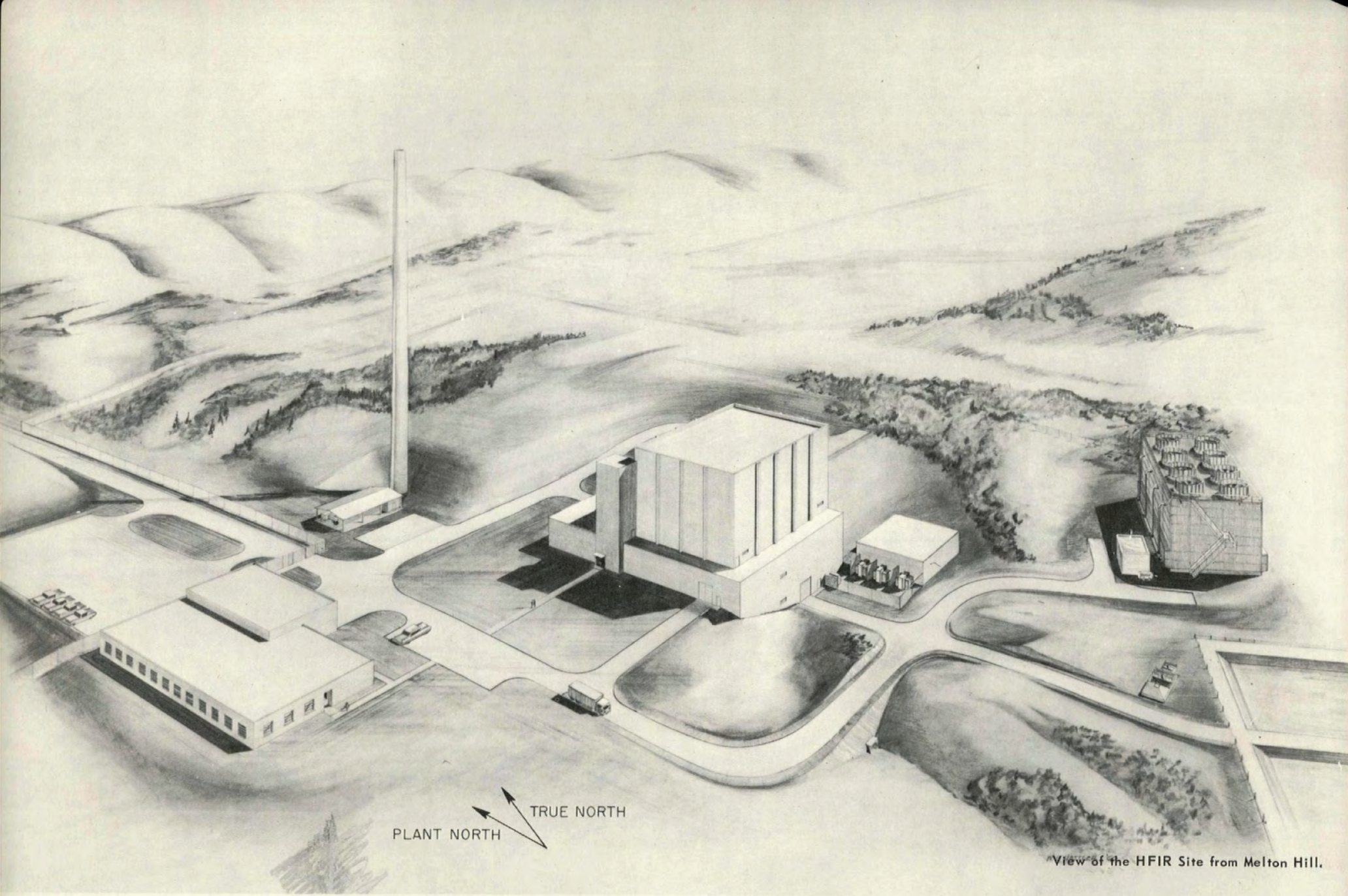

View of the HFIR Site from Melton Hill.

FOREWORD

This Accident Analysis includes the original *draft* Accident Analysis (dated February 1965) as Part I and subsequent formal AEC Safety Review Questions and ORNL Answers (as Part II) as submitted to obtain authorization to operate HFIR at the nominal 100-Mw (thermal) design power level. The various portions of the accident analysis are left as originally submitted for the reader to follow such changes in thought or design as occurred and to record the reasons why the changes were made. Footnotes were added to the earlier work referring to the later comments. The HFIR Functional Description referred to as ORNL-3572 in the accident analysis is the original version dated May 1964. This was revised in March 1965; however, topic headings were the same. Safety review questions and answers refer to this first revision.

The HFIR functional description ORNL-3572 will be revised to reflect the reactor that exists at about March 1, 1967. Thus, this second revision provides the necessary background material for this Accident Analysis, ORNL-3573.

Volume I of ORNL-3572 is basically descriptive in nature and is for the purpose of acquainting the reader with just what the HFIR is and how it operates. Except where necessary for clarity, little emphasis is placed on the design calculations. The interested reader will find in Appendix C of ORNL-3572 a list of HFIR reports which constitute the detailed basis for the design. The various operating parameters cited include both design numbers and the actual values if they differ from them to some extent.

Volume II of ORNL-3572 contains a selected group of HFIR design drawings which, if used in conjunction with text and figures in Vol. I, will materially aid in gaining an understanding of the system.

The information contained herein is primarily the result of studies performed by F. T. Binford and other members of the HFIR project, which was directed by C. E. Winters until December 1961 and since then by A. L. Boch and T. E. Cole as Director and Technical Associate Director respectively. Among those who have contributed either by supplying analysis or assisting in the review of the manuscript are F. T. Binford, R. D. Cheverton, T. E. Cole, W. K. Ergen, M. J. Kelley, J. O. Kolb, J. P. Nichols, T. M. Sims, G. M. Watson, W. R. Wise, and their co-workers.

The Editors

ABSTRACT

The High Flux Isotope Reactor is a light-water moderated and cooled, beryllium-reflected flux-trap reactor designed and built to operate at 100 Mw (thermal) for the primary purpose of producing significant quantities of the transplutonium isotopes.

The reactor system is equipped with two types of containment. The primary containment consists of the reactor primary coolant system, including the reactor vessel and associated high-pressure piping. This system alone is capable of containing the more likely and more serious accidents. The secondary containment is accomplished by controlled leakage into, and the constant discharge from, the reactor building of ~28,600 cfm of air through appropriate filters to the 250-ft HFIR stack.

The accident analysis (Part I) reveals that radiation doses following the maximum credible accident, taken to be a 50% core meltdown, would not exceed the guidelines set forth in 10 CFR, part 100. These doses would be almost entirely due to iodines and noble gases.

The safety review questions and answers (Part II) record the various additional information requested by the USAEC and such design changes as occurred following the *draft* Accident Analysis.

CONTENTS

Figure List xii

Table List xv

PART I. THE HIGH FLUX ISOTOPE REACTOR – ACCIDENT ANALYSIS

Preface 1

1. Introduction 2
2. Method of Analysis 4
3. Consequences of the Emission of Fission Products from the HFIR Stack Following an Accidental Release 5
4. Integrity of the Containment System 11
   - 4.1 Integrity of the Primary Coolant System 16
   - 4.2 Sources and Magnitudes of Energy Releases 17
5. Accidents Involving the Reactor Fuel 20
   - 5.1 Accidents Involving Fuel Within the Primary Containment 20
   - 5.2 Accidents Involving Fuel Outside the Primary Containment 21
6. The Maximum Credible Accident 23
   - 6.1 Local Consequences of the Maximum Credible Accident 25
7. Accidents Other Than to the Fuel 27
   - 7.1 Accidents to the Target 27
   - 7.2 Accidents to Experiments 29
   - 7.3 Miscellaneous Accidents 29
8. Routine Release of Activity 32
9. Relationship of HFIR to Other Facilities 33
   - 9.1 Interrelationship with Other Facilities 35
   - 9.2 Effect of Accidents in Other Facilities 35
10. Summary and Conclusions 35

APPENDIX A. CONSEQUENCES OF THE RELEASE TO THE ATMOSPHERE OF FISSION PRODUCTS FROM THE HIGH FLUX ISOTOPE REACTOR 36

1. Introduction 36
2. Atmospheric Concentrations Downwind Due to Accidental Releases 37
   - 2.1 Concentration of Daughter Products 41
3. Ground-Level Doses 43
   - 3.1 Calculation of Internal Doses 43
   - 3.2 Calculation of External Doses 44

4. Numerical Results for the Accident Cases 46
4.1 Internal Doses 47
4.1.1 Internal Doses Due to Iodines 47
4.1.2 Internal Doses Due to Other Fission Products 48
4.2 External or Submersion Dose 49
4.2.1 External Doses from Fission Products Other than Noble Gases 51
5. Continuous Release of Activity 53
Acknowledgment 53
APPENDIX B. HFIR EXCURSION CONTAINMENT POTENTIAL 63
1. Foreword 63
2. Introduction 63
3. Tentatively Postulated MCA's 64
4. Characteristics of Marginally Contained TNT Accident 64
5. Excursion Containment Bounds 65
6. Containment Qualifications 66
7. Summary Conclusions 67
APPENDIX C. REACTIVITY CONSIDERATIONS 68
1. Transient Behavior 69
1.1 Method of Analysis 69
1.2 Modes of Operation 73
1.3 Reactivity Addition Accidents 75
1.3.1 Introduction 75
1.3.2 Control Plate Accidents 75
1.3.3 Voids in the Central Target Region 80
1.3.4 Reactivities Associated with Experiments 82
1.3.5 Cold-Water Accidents 82
1.4 Significance of SPERT Data 83
2. Shutdown Margin 88
2.1 Introduction 88
2.2 Shutdown Margin Criteria 88
2.2.1 Occurrence of an Optimum Void in the Trap Region 88
2.2.2 Removal of the Target 88
2.2.3 Complete Withdrawal of Any One Control Element 89
2.2.4 One Control Plate Fails to Scram 89
2.2.5 Occurrence of a Startup Accident 89
2.3 Measurement of Shutdown Margin 90
2.4 Critical Experiment Results 90
2.5 Reactivity Accountability 91
APPENDIX D. MAXIMUM ENERGY RELEASE FROM CORE FLOW BLOCKAGE IN THE HFIR 93
1. Introduction 93
2. Energy Sources 94
3. Determination of the Maximum Credible Energy Release 95

3.1 Small Flow Blockage 96
3.2 Large Flow Blockage 96
3.3 Energy Release Time Scale 98
4. Summary 98

APPENDIX E. MAXIMUM PERMISSIBLE CONCENTRATIONS OF THE TRANSURANIC ISOTOPES 98

APPENDIX F. MISCELLANEOUS CALCULATIONS 100

1. Calculation of the Initial Iodine Dose Rate Within the Building 100
2. Calculation of the External Dose Rate Within the Building 100
3. Estimate of the Bone Dose from the Target 101

PART IIa. SAFETY REVIEW QUESTIONS AND ANSWERS 1–41

Abstract 103

Contents 105

Questions* and Information Requests on the HFIR 109

1. Applicability of Flat Terrain Meteorology Formulae 109
2. Additional Meteorology Data 111
3. Filter Effectiveness Against Organic Iodides 114
4. Manufacture and Test Experience on Fuel 115
5. Coolant Velocity to Cause Fuel Plate Collapse 116
6. Integrity (Mechanical and Fission Product Retention) of Fuel Plates 116
7. Attachment Between Drive Tubes and Shim-Safety Elements 117
8. Hydraulic Shim Cylinder Rate Limiter 119
9. Control Element Test Program 120
10. Variation with Time of Reactivity Coefficients 122
11. Target Reactivity Limits 122
12. Xenon Burnout Causing Reactivity Overshoot 122
13. Response Time of Safety System 123
14. Response Time of Neutron Flux Amplifier 124
15. Accuracy of and Input Errors to Heat Power Calculator 124
16. Beryllium Photoneutron Effect on Control Problems 124
17. Loss of Electricity Effect on Coolant Flow and Reactor Power 125
18. Capacity of and Design Criterion for Pressure Relief Valves 125
19. Effects of Scram Initiated by Overpower Instead of Rate Trip 127
20. No Void Considered During Startup Accident 128
21. Fuel Melting if Core Drops During Handling 128
22. Backup Reactivity Control System Requirements 129

*Questions 1–41 were originally answered in ORNL-CF-65-11-29, dated November 12, 1965.

23. Adequacy of the Core Cooling System, and Extent of Metal-Water Reaction 131
24. Horizontal Beam Tube Design 135
25. Reactor Control Room Shielding and Evacuation 138
26. Fuel Movement Reactivity Effects 139
27. Control Room Fires 139
28. Reactor Instrumentation and Control System 140
29. Alternate or Additional Stack Monitoring and Containment 144
30. Latest Effectiveness of Filtering Against Radioiodine 150
31. Reactor Vessel and Structural NDT Problems 150
32. Experiment Review Criteria 153
33. Evacuation of Nearby Facilities Following HFIR Accident 153
34. Criteria and Review of Possible New Core Design 154
35. Effect of Beryllium Reflector Expansion on Control Rod Motion 155
36. Choice of Overpower Scram Setpoint, and Accidents Effective in 155
37. Hazard Associated with the Target 156
38. Analysis of Reactivity Transients Considerably More Severe Than Previously Treated 156
39. Procedures if Fuel Sticks or Is Damaged 160
40. Reliability of Emergency Air Supply to Control Rod Drives 161
41. Control Room Shielding and Alternate Emergency Control Center 161

APPENDIX G. USE OF TENSILE SPECIMENS 162

PART IIb. SAFETY REVIEW QUESTIONS AND ANSWERS 42–53

Abstract 165

Contents 167

Questions* and Information Requests on the HFIR 169
42. Additional Information on Backup Reactivity Control 169
43. Details of Loss-of-Pressure Accident Calculation 172
44. Details of Beam Tube Design and Integrity 175
45. 100% Noble Gas Release During Fumigation Conditions, and Alternate Dose Limiting Schemes 178
46. Latest Effectiveness of Filtering Against Radioiodine 180
47. Error Associated with Vessel Integrated-Neutron-Flux, Failure Consequences of In-Vessel Structures 183
48. Evacuation of MSRE Following HFIR Accident 184
49. Increase in Fission Product Inventory with Changed Fuel or Irradiation Time 184
50. Detailed Criteria for New Core Design and Review 185
51. Analysis of Reactivity Transients Considerably More Severe Than Previously Treated 185
52. Operating Experience at Power Levels Up to 20 Mw (thermal) 188
53. Significant Changes Since Commencement of Operation 191

*Questions 42–53 were originally answered in ORNL-CF-65-11-29, Supplement 1, dated Feb. 1, 1966.

PART IIc. SAFETY REVIEW QUESTIONS AND ANSWERS 54–60

Abstract 195

Contents 197

Introduction and Summary 199

Questions* and Answers 201

54. Reanalysis of 1.3% $\Delta k/k$ 30-msec Reactivity Ramp Without Control Rod Action 201

55. Further Detailed Analysis of Reactivity Transients Considerably More Severe than Previously Treated 203

56. Rate of and Total Energy Release Necessary to Rupture Primary Coolant System 205

57. Phenomena Which, when Coupled with Various Chemical Reactions, Release Energy Enough to Rupture Primary Coolant System and Endanger Building Integrity 206

58. Validity of Various Analyses if No Control Motion Occurs 206

59. Consequences of Reactor Vessel Failure on Pool Walls and on Building and Secondary Containment 206

60. Interim Steps Taken Until Backup Reactivity Control System Installed 207

APPENDIX H. THE "ULTIMATE" SHUTDOWN MECHANISM OF THE HFIR 207

APPENDIX I. ENERGY RELEASES FROM Al-H_2O REACTIONS IN THE HFIR 210

APPENDIX J. CONTAINMENT POTENTIAL OF THE HFIR PRESSURE VESSEL AND PRIMARY COOLANT SYSTEM 227

APPENDIX K. CONTAINMENT POTENTIAL OF THE HFIR BUILDING 245

APPENDIX L. DETAILED DISCUSSION OF QUESTIONS 54, 55, AND 58 252

---

*Questions 54–60 were originally answered in ORNL-CF-65-11-29, Supplement 2, dated Aug. 15, 1966.

FIGURE LIST

Figure No.	Title	Page
I.3.1	Internal Doses Resulting from an Unfiltered Fission Product Release from HFIR – Infinite Exposure and Rapid Emission	6
I.3.2	External γ Dose from Noble Gases Following a Fission Product Release from HFIR – Infinite Exposure	7
I.3.3	External γ Dose from Noble Gases Following a Fission Product Release from HFIR – 2-hr Exposure	8
I.3.4	External β Dose from Noble Gases Following a Fission Product Release from HFIR – Infinite Exposure	9
I.3.5	External β Dose from Noble Gases Following a Fission Product Release from HFIR – 2-hr Exposure	10
I.3.6	External Dose Due to Fission Products Other than Noble Gases Following a Fission Product Release from HFIR – Infinite Exposure and Rapid Emission	11
I.4.1	Schematic Diagram of HFIR Containment Systems	12
I.4.2	Upper Bound Containment Potential of HFIR Under Normal Operating Conditions	16
I.5.1	Maximum Fuel Plate Heat Flux of HFIR Fuel Following 15-day Operation at 100 Mw	22
I.6.1	Doses to Be Expected Downwind Following the HFIR MCA	25
I.7.1	High Flux Isotope Reactor Melton Valley Drainage	30
I.9.1	Location of ORNL Facilities with Respect to HFIR	34
I.A.1	Horizontal Dispersion Parameters	38
I.A.2	Vertical Dispersion Parameters	39
I.A.3	Internal Dose Due to Iodines – Infinite Exposure and Rapid Emission	48
I.A.4	Internal Dose Due to Bone Seekers – Infinite Exposure and Rapid Emission	50
I.A.5	Internal Dose Due to Fission Products Other than Iodines and Bone Seekers – Infinite Exposure and Rapid Emission	51
I.A.6	External Dose Due to Noble Gases – Rapid Emission	54
I.A.7	External γ Dose Due to Noble Gases – Emission Through Reactor Bay	55
I.A.8	External γ Dose Due to Noble Gases – Emission Through CHOG System	56
I.A.9	External β Dose Due to Noble Gases – Rapid Emission	57
I.A.10	External β Dose Due to Noble Gases – Emission Through Reactor Bay	58
I.A.11	External β Dose Due to Noble Gases – Emission Through CHOG System	59
I.A.12	HFIR Stack Factor	60
I.A.13	External Doses Due to Fission Products Other than Noble Gases – Infinite Exposure and Rapid Emission	61
I.A.14	Average Downwind Fission Product Concentration Due to Continuous Release of One Curie per Minute	62
I.B.1	Upper Bound Containment Potential of HFIR Under Normal Operating Conditions	68
I.C.1	Typical Transient Curves for a Ramp Reactivity Accident	79
II.1.1	Noble Gas Gamma Dose. Infinite exposure, rapid emission ($\alpha = 0.5$)	112
II.1.2	Internal Iodine Dose. Infinite exposure, rapid emission ($\alpha = 0.5$)	112

Figure No.	Title	Page
II.2.1	Wind Speeds Used to Compute "Worst Average" Noble Gas Gamma Dose. Infinite exposure	113
II.7.1	HFIR Shim-Safety Element	118
II.17.1	HFIR Flow Coastdown Studies	126
II.23.1	Variation of Reactor Power and Core Temperature with Time Following a Step Loss in Pressure	134
II.29.1	Comparison of Ground Release (330 ft^3/min) Doses to Present MCA 2-hr Doses	145
II.29.2	Comparison of Ground Release (330 ft^3/min) Doses to Present MCA Infinite Exposure Doses	146
II.38.1	Void Coefficient in the HFIR for Uniform Local Void Distribution	160
II.43.1	Energy Absorption as a Function of Time Following Pressure Loss	173
II.43.2	Extent of Metal-Water Reaction as a Function of Energy Input	174
II.43.3	Metal-Water Reaction as a Function of Time	175
II.46.1	Effect of Iodine Concentration on the Equilibrium Partition Coefficient for Iodine at 25°C	181
II.46.2	Effect of Residence Time on Methyl Iodide Penetration of Treated and Untreated Coconut Charcoal at 40 fpm, 25°C, and 70% Relative Humidity	182
II.H.1	Decrease in Reactivity for Spherical and Cylindrical Core Expansion, Assuming Weight of Materials Remains Constant	208
II.I.1	Energy Releases During Combustion	216
II.I.2	Rate of Energy Generation by Combustion of 10^5 g of Molten Aluminum Subdivided into Drops of Various Sizes	216
II.I.3	TREAT Results with HFIR Fuel Samples	222
II.I.4	Vapor Pressure of Al(*l*)	224
II.I.5	Specific Volume of Aluminum vs Temperature	225
II.J.1	True Stress-Strain Relations for A335-22 and A212-B Steels and Nominal Circumferential Stress–Nominal Strain as Measured for an A335-22 Cylinder and as Assumed for the HFIR Pressure Vessel. Cylindrical vessels with rigid ends. $L/D = 2$	230
II.J.2.	True Stress-Strain Relation for 304 Stainless Steel and Nominal Circumferential Stress–Nominal Strain as Measured for a Vessel Having $L/D = 3$	231
II.J.3	The Effect of Steam Temperature and Nuclear Energy Pulse on the Strain Energy in the HFIR Pressure Vessel. "Steam explosion" only – assumes no metal-water reaction	234
II.J.4	The Effect of Gas Temperature and Prompt Energy Release in the HFIR Pressure Vessel. Nuclear excursion plus prompt reaction of any vaporized aluminum	237
II.J.5	The Effect of Aluminum Particle Size and Magnitude of the Prompt and Delayed Energy Release on the Strain Energy Deposited in the Primary Coolant System	243
II.K.1	Moles of Steam vs Temperature Rise Required to Increase Building Pressure by 0.8 psi	247
II.K.2	Moles of Water Vapor Which Can Be Accommodated by the Air in the HFIR Reactor Bay	248

Figure No.	Title	Page
II.K.3	Maximum Building Overpressure as a Function of Nuclear Excursion Energy	249
II.K.4	Fraction of Building Volume Which Escapes	250
II.L.1	Reactivity vs Uniform Reduction in Control Region and Removable Beryllium Water Content (End of Cycle)	259
II.L.2	Reactivity vs Decrease in Fuel Plate Density Resulting from Longitudinal Extension of Core or Uniform Removal of Fuel Plate	261
II.L.3	Reactivity vs Inward Radial Movement of Inner Element Inner Diameter (Water Content of Inner Element Increases Correspondingly)	264
II.L.4	Power and Temperature vs Time for 1.3% $\Delta k/k$, 30-msec Ramp Reactivity Addition; End of Cycle	266
II.L.5	(*a*) Power vs Time for 1.5% $\Delta k/k$, 30-msec Ramp Reactivity Addition; End of Cycle. (*b*) Temperatures vs Time for 1.5% $\Delta k/k$, 30-msec Ramp Reactivity Addition; End of Cycle	267
II.L.6	(*a*) Power vs Time for 2% $\Delta k/k$, 30-msec Ramp Reactivity Addition; End of Cycle. (*b*) Temperatures vs Time for 2% $\Delta k/k$, 30-msec Ramp Reactivity Addition; End of Cycle	268
II.L.7	Increase in Pressure at Horizontal Midplane for 1.3% $\Delta k/k$, 30-msec Ramp Reactivity Addition	269
II.L.8	Increase in Pressure at Horizontal Midplane for 1.3% $\Delta k/k$, 30-msec Ramp Reactivity Addition	269
II.L.9	Increase in Pressure at Horizontal Midplane for 1.3% $\Delta k/k$, 30-msec Ramp Reactivity Addition	270
II.L.10	Increase in Pressure at Horizontal Midplane for $t = 5$ msec (All Heat in Plate)	271

TABLE LIST

Table No.	Title	Page
I.3.1	HFIR Decontamination Factors	10
I.6.1	Downwind Doses Following the Maximum Credible Accident at Various Locations	26
I.7.1	Characteristics of the Long-Lived Fission Products	31
I.A.1	Dimensions of the Parameters Which Appear in the Concentration Equation	40
I.A.2	Parameters Used for Iodine Dose Calculations	47
I.A.3	Parameters Used to Compute Internal Dose Due to Fission Products Other than Iodine	49
I.A.4	Parameters Used to Compute External Dose from Noble Gases	52
I.A.5	Frequency of Wind Direction at ORNL	62
I.C.1	Nomenclature	71
I.C.2	Safety System Level and Rate Trips	74
I.C.3	Characteristics of the HFIR Analog Model	76
I.C.4	Summary of Pertinent Analog Results for Reactivity Addition Accidents	78
I.C.5	Characteristics of SPERT (DU-12/25) and HFIR Cores	84
I.C.6	Comparison of Experimental and Calculated SPERT (DU-12/25) Results	84
I.C.7	Comparison of SPERT and HFIR Calculated Transient Characteristics	87
I.C.8	Cases for Which Core Must Be Subcritical	90
I.C.9	Excess Shutdown Margin at 20°C for Cases I Through IV of Table I.C.8	91
I.C.10	Summary of Reactivity Accountability for the Second Production Core	92
I.D.1	Potential Energy Releases Following HFIR Flow Blockage Accident for One Fuel Element Plate	95
I.D.2	Computation of Fraction of Core Required to Override One-Dollar Reactivity Addition from Servo-Control Action Following Small Flow Blockage	97
I.D.3	Computation of Fraction of Core Required to Override One-Dollar Reactivity Addition from Servo-Control Action Following Large Flow Blockage	97
I.E.1	Maximum Permissible Concentrations	99
II.4.1	Summary of Plate Spacing Measurements on HFIR Fuel Assemblies	116
II.29.1	Internal Iodine Doses and Whole-Body Gamma Doses Following the HFIR MCA	147
II.31.1	Results of Charpy V-Notch Impact Tests on Actual Carbon Steel Pressure Vessel Specimens	151
II.52.1	Chronological Outline	189
II.52.2	Targets Used in Flux Trap	191
II.52.3	Reactivity Effects Due to Changing Experimental Facilities	192
II.I.1	Extent of Reaction and Energy Releases as Functions of Initial Particle Diameter	215
II.J.1	Energy Release by a Nuclear Excursion and Aluminum-Water Reaction for Marginal Containment by the HFIR Pressure Vessel and Primary Coolant System	228
II.J.2	Properties of the HFIR Pressure Vessel and Primary Coolant System	229
II.J.3	Properties of the HFIR High-Pressure Coolant System	232

Table No.	Title	Page
II.J.4	Thermal Power of Al-H_2O Reaction	235
II.J.5	Consequences of a Nuclear Excursion and Prompt Al-H_2O Reaction in the HFIR and Initial Conditions for a Delayed Al-H_2O Reaction	236
II.J.6	Extent of Reaction and Energy Releases as Functions of Initial Particle Diameter	238
II.L.1	HFIR Analog Calculations	254

Part I. The High Flux Isotope Reactor — Accident Analysis

PREFACE

This analysis of the consequences of potential accidents to the High Flux Isotope Reactor is the second of two documents which constitute the safety analysis of that reactor. The first[1] of these presents a reasonably detailed description of the reactor and its ancillary facilities. The accident analysis, which deals primarily with potential environmental contamination and its attendant hazards to the general population, refers frequently to this description.

During the course of the accident analysis it became obvious that certain design changes were desirable in order to enhance the overall safety of the system. Where these are not reflected in ORNL-3572, they have been briefly described in footnotes herein or have been discussed in the text. A revision to ORNL-3572 was issued to AEC reviewers, incorporating these changes and bringing that document up to date as of March 1965.

---

[1]F. T. Binford and E. N. Cramer (eds.), *The High Flux Isotope Reactor — A Functional Description*, ORNL-3572 (May 1964).

1. INTRODUCTION

The High Flux Isotope Reactor (HFIR), which is described in detail elsewhere,[1] is being designed and built for the primary purpose of generating thermal neutron fluxes in excess of 10^{15} neutrons cm^{-2} sec^{-1} in order to produce relatively large quantities of the transplutonium elements. In general, the reactor design concepts fall within the confines of existing technology; and therefore, most of the safety problems associated with its operation have been dealt with before in connection with the design and operation of other ORNL reactors.

The design of the reactor and its auxiliaries has, to a very large extent, been influenced by two important requirements: (1) that the reactor be kept as free as possible from frequent or lengthy shutdowns other than those required for refueling and routine maintenance, and (2) that significant radioactive contamination of the environment from any cause whatsoever be prevented. The former is necessary to ensure the required continuity of operation. The latter is, of course, required of any reactor built and operated at ORNL; it is provided for by the control and safety systems[2] and by the operating procedures[3] and is guaranteed by the reactor containment features.[4]

In addition to the fuel cladding, the reactor is provided with two other types of containment. The first of these, which may be considered "primary containment," is the reactor pressure vessel and the primary coolant loop.[5] This system has been deliberately designed so that during normal power operation even a major release of fission products from the fuel[6] can be handled in a routine manner and only a relatively short time would be required before normal operation could be resumed. Virtually all the activity released from the fuel would remain trapped in the primary coolant loop and could be removed in an orderly fashion by decay and by the use of the primary coolant system demineralizers[7] and the hot off-gas (HOG) filters.[8]

---

[1] F. T. Binford and E. N. Cramer (eds.), *The High Flux Isotope Reactor – A Functional Description*, ORNL-3572 (May 1964) (hereafter referred to as ORNL-3572).

[2] ORNL-3572, chap. 8.

[3] ORNL-3572, sect. 12.5.

[4] ORNL-3572, chap. 4.

[5] ORNL-3572, sects. 5.4 and 6.2.

[6] ORNL-3572, sect. 9.4.

[7] ORNL-3572, sect. 6.2.2.

[8] ORNL-3572, sects. 4.6 and 4.7.

The second type of containment is furnished by the HFIR dynamic containment or "confinement" system.[9] Air is constantly exhausted from the special building hot exhaust system (SBHE).[10] This system, designed to remove a total of ~28,600 cfm of air, directs the exhaust through appropriate filters to the 250-ft HFIR stack, with the stack discharge orifice at elevation 1085 ft. It provides constant inleakage of air to the potentially contaminated areas, thus preventing the outleakage of air- or vapor-borne fission products from the building at ground level. The effluent air, in passing through the SBHE filters, deposits therein, with the exception of the noble gases, virtually all the airborne activity. Of the 28,600 cfm exhausted from the building, approximately 5000 cfm is exhausted through inlet registers located under the plastic pool cover.[11] Thus, for those cases where the pool cover remains in place following a fission product release from the fuel, a third line of containment is operative. The pool cover, however, is primarily for the protection of personnel in the building, and its presence will prevent or greatly reduce the release of activity into the reactor bay itself.

The secondary, or building, containment is required to provide protection only if the primary containment is inoperative. This may occur under the following conditions: (1) when a fission product release from the fuel occurs while the reactor vessel is open, (2) as a result of an accident to the fuel element or to the target while they are being handled or stored outside the reactor vessel, (3) because of an accident involving an experiment or other source of radioactive material not contained in the primary loop, or (4) in the extremely unlikely event of a primary coolant system rupture concurrent with a fission product release within the closed reactor vessel. Nevertheless, the secondary containment is a maximum reliability system which is capable of handling any credible accident and which will always be in operation whenever there is a possibility of any significant release of radioactivity. Administrative safeguards require that the secondary containment be in operation whenever the reactor is operating or when fuel is being handled. Normally, the system will only be shut down when this is required for maintenance or testing. During such periods, special procedural safeguards will be effective in preventing reactor startup and fuel handling.

Another type of environmental contamination involves the accidental introduction of contaminated water into White Oak Creek as a result of spillage and runoff or because of the failure or malfunction of the HFIR aqueous waste disposal system.[12] Such events are effectively prevented by the design of the system[13] and by operating procedures but in any event would be relatively minor in terms of hazard to the population. The activity level of the creek is constantly monitored,[14] and its rate of discharge to the Clinch River through White Oak Lake can be controlled. Moreover, the time lag between introduction of

---

[9]ORNL-3572, chap. 4.

[10]ORNL-3572, sects. 4.5 and 4.7.

[11]ORNL-3572, sect. 5.5.1.

[12]ORNL-3572, sect. 11.3.

[13]The only significant potential source of contaminated runoff from the primary coolant system is a leak in the pipe tunnel. This area is equipped with a curb of sufficient height to retain any leakage and direct it to the Process Waste Drainage (PWD), where it may be controlled.

[14]R. J. Morton (ed.), *Status Report No. 1, Clinch River Study*, ORNL-3119 (July 1961).

contaminated water into the watershed at the HFIR site and the appearance of activity at the mouth of the creek is between 12 and 24 hr.[15] This gives ample time to institute control measures or to spread the warning downstream should this become necessary.

2. METHOD OF ANALYSIS

The method which has been selected to pursue the investigation of the environmental consequences of an accident consists first of a detailed examination of the results of a "unit" release of activity and then the application of the results so obtained to releases of various magnitudes. The only credible cause for a massive release of fission products from the fuel is overheating to an extent sufficient to cause melting and destruction of the integrity of the fuel cladding. This can be brought about either by an increase in power beyond the capability of the heat removal mechanisms, a decrease in heat transfer, or a combination of both.

The consequences of such an occurrence will vary, depending upon whether or not the primary cooling system, which is also the primary containment, remains intact throughout the incident. There are three types of potential accidents in which the primary containment is definitely not in operation. These are as follows:

1. a core meltdown caused by a power excursion during low- or zero-power testing with the pressure vessel open,
2. melting of some portion of a spent fuel element in the reactor or storage pools due to loss of natural convection cooling shortly after removal from the reactor vessel,
3. a criticality accident in the pool as a result of the mishandling of new or slightly spent fuel elements.

Because of various considerations to be discussed subsequently all these potential accidents are relatively minor in terms of fission products released and environmental consequences.

There are two types of potential accidents to the fuel which could occur while the primary containment is operative. These are:

4. a meltdown during power operation due to a power excursion,
5. a meltdown during power operation because of flow blockage or other type of heat-transfer loss.

Although the magnitude of the release from the fuel in the latter two cases may be relatively large, few or none of the fission products would be released to the environment, but they would be retained within the primary containment.

Finally it is necessary to consider the case where the meltdown occurs during power operation and is either of sufficient violence to rupture the primary containment or occurs concurrent with a rupture of the primary containment. It will be seen that the energy required to cause a violent rupture of the primary system is so great that such an occurrence may be considered incredible. Moreover, only a relatively large rupture of the primary system can cause depressurization quickly enough to significantly damage the core. Nevertheless, a sixth case will be considered:

---

[15] W. H. McMaster, ORNL Health Physics Division, private communication (March 1964).

6. a meltdown during power operation due to a power excursion or heat-transfer loss concurrent with a rupture of the primary coolant system.

In addition to these six, all of which directly involve the fuel elements, there are three other types of potential accidents which, although they are in general much less severe, require consideration. These are:

7. an accident to the plutonium target[16] caused by mechanical damage or overheating,
8. an accident involving radioactive material other than that contained in the fuel or target, that is, contaminated waste, ion exchange resin, etc.,
9. an accident to an experiment other than the target.

Each of these types of accidents will be discussed, and those which may result in significant environmental contamination will be considered in detail.

3. CONSEQUENCES OF THE EMISSION OF FISSION PRODUCTS FROM THE HFIR STACK FOLLOWING AN ACCIDENTAL RELEASE

Calculation of the downwind radiation doses to be expected as a result of the emission of fission products from the HFIR stack have been made using the Gaussian plume formula.[17] The method, which takes into consideration decay, growth of daughter products, and the augmentation of the stack height due to emission velocity, is described in Appendix A. The data presented in this appendix are based upon release from the fuel of all the fission products present in 0.001% of the fuel (1 kw equivalent) immediately following 15 days' operation at 100 Mw. Aside from the exceptions noted therein, the results do not include any allowance for the effect of the SBHE and HOG filters, the demineralizers, or any other decontamination mechanism such as scrubbing action by the primary coolant and pool water or deposition on the building and duct walls.

The doses for the accident cases may be obtained by utilizing these results, in connection with the reactor power corresponding to the amount of fuel affected, together with an appropriate reduction to represent the decontamination factors expected.

Two cases have been considered: (1) the "worst average" case in which it is assumed that those meteorological conditions which maximize the dose persist independently for each point downwind throughout the incident, and (2) the "most representative" case in which the most probable meteorological conditions prevail.[18] Because it is extremely unlikely that "worst average" conditions will exist for any point during an accident and impossible that they exist for more than one point, and because the "most representative" conditions do not correspond to a lower bound, the mean value of these two cases is considered to be a conservative basis upon which to estimate the radiation doses and, therefore, has been selected for this purpose. It is worth noting that the results so obtained are considerably more pessimistic than those obtained under the conditions most commonly employed in

---

[16] ORNL-3572, sect. 5.2.1.

[17] F. A. Gifford, Jr., *Nucl. Safety* 1, 3 (March 1960); **2**, 2 (December 1960); **2**, 4 (June 1961).

[18] See Appendix A, sect. 4, for a more precise definition.

previous safety analyses, namely, moderately stable atmospheric conditions and a wind speed of 1 m/sec.[19,20] This is particularly the case within 5 km of the stack.

In order to facilitate the application of the decontamination factors the fission products have been divided into five groups according to their release characteristics and the type of radiation doses which they deliver.

1. Fission products important with respect to internal dose are
   a) iodines,
   b) bone seekers,
   c) all others.
2. Fission products important with respect to external or submersion dose are
   a) noble gases,
   b) all others.

The internal and external doses to be expected following a unit release of fission products from the fuel are given as a function of distance downwind in Figs. I.3.1–I.3.6. No credit for filtration or

[19] E. N. Cramer (ed.), *A Critical Discussion of 23 US Power Reactor Hazard Reports*, to be published.

[20] J. J. DiNunno *et al.*, *Calculations of Distance Factors for Power and Test Reactor Sites*, TID-14844 (March 1963).

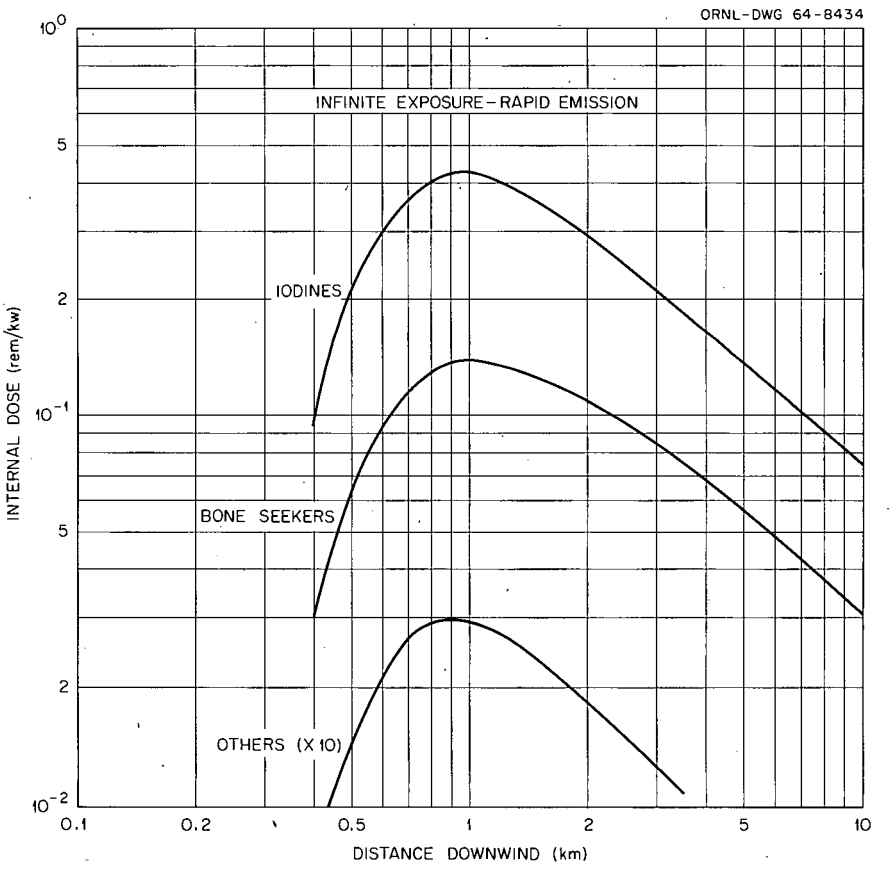

Fig. I.3.1. Internal Doses Resulting from an Unfiltered Fission Product Release from HFIR – Infinite Exposure and Rapid Emission.

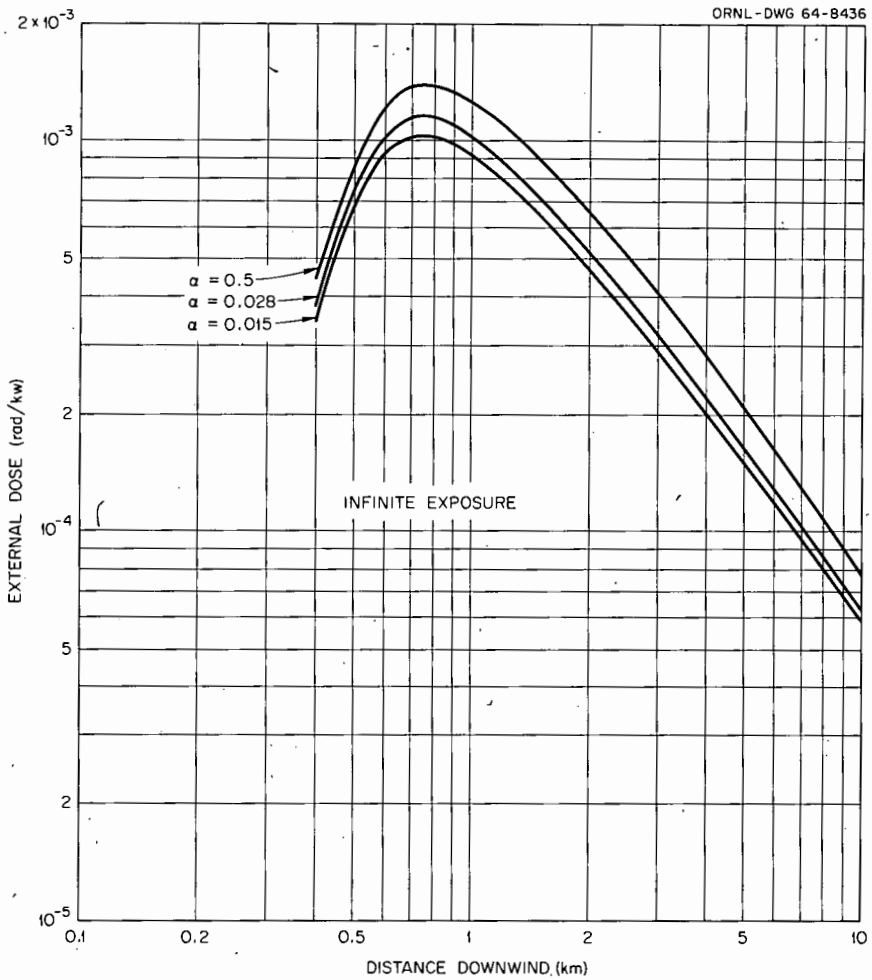

Fig. I.3.2. External γ Dose from Noble Gases Following a Fission Product Release from HFIR – Infinite Exposure.

other means of decontamination is included in these curves, and it is assumed that all the fission products in the affected fuel reach the stack. Decontamination effects will be included separately. With the exception of the noble gases, all doses are based on rapid emission from the building and an infinite exposure time.

In the actual cases, it is assumed that following a meltdown 50% of the iodines, 100% of the noble gases, and 2% of the other fission products will escape from the immediate vicinity of the affected portion of the fuel. These fractions are in agreement with current practice and appear to represent reasonably realistic estimates, although the fraction chosen for the solids is somewhat higher than that usually recommended.[21]

---

[21] G. W. Parker, *Trans. Am. Nucl. Soc.* 6(1), 120 (June 1963).

The design criteria specify that the filter media in both the SBHE and the HOG[22] systems be capable of retaining 99.95% of all particulate matter having a diameter greater than 3 μ and 99.99% of the (reactive) iodine. Laboratory-scale investigations with filter systems using these media indicate that overall decontamination factors up to 3000 for iodine can be achieved.[23] A full-size filter system similar to, but somewhat less elaborate than, that of the HFIR has been tested in the Oak Ridge Research Reactor, and in these tests a decontamination factor of approximately 600 (ref. 24) was demonstrated. Because in any such accident the iodine is released under water and must be conveyed first through the water and then through either the SBHE or CHOG ducts before reaching the filters, it is

[22]ORNL-3572, sects. 4.7.1 and 4.7.2.

[23]*Nucl. Safety Program Semiann. Progr. Rept. Dec. 31, 1963,* ORNL-3547.

[24]Letter from R. E. Adams and T. M. Sims to F. T. Binford, June 16, 1964.

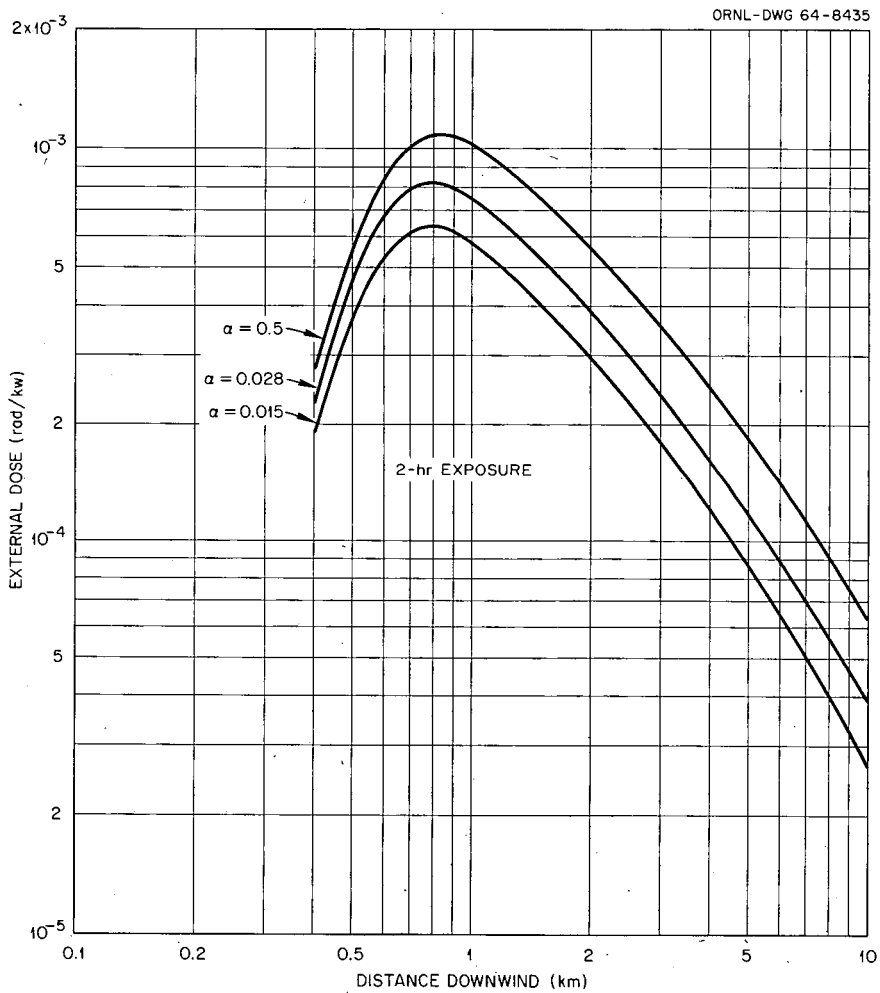

Fig. I.3.3. External γ Dose from Noble Gases Following a Fission Product Release from HFIR – 2-hr Exposure.

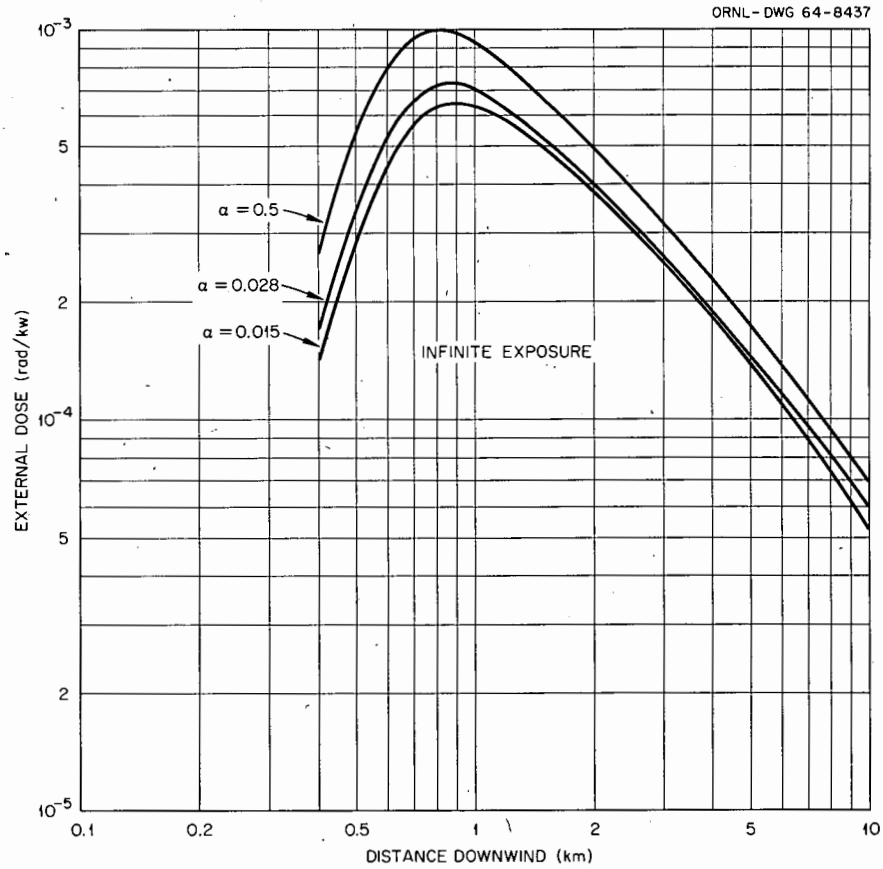

Fig. I.3.4. External β Dose from Noble Gases Following a Fission Product Release from HFIR – Infinite Exposure.

estimated that the amount of iodine actually reaching the filters will be reduced by a factor of between 3 and 10. Thus it would appear conservative to assume an overall decontamination factor for iodine of 2000. This, as will be shown later, is higher by a factor of 100 than that necessary to satisfy the limits established by 10 CFR 100, under MCA conditions.

There appears to be no obvious decontamination mechanism which will readily remove the noble gases from the effluent stream. They are, however, released under water and do have finite solubility. Nevertheless it will be assumed that 100% of the noble gases are released from the affected portion of the fuel, and that these pass through the system and are discharged from the stack.

Experience has shown that the mobility of the nonvolatile fission products is less than that of the iodines, that the filters will be more effective in removing them, and that they will be more effectively retained in the water and on the various surfaces. It is conservative to assume that both filtration and retention in the building will each be at least 50% more effective in the case of the nonvolatile fission products than in the case of the iodines. Consequently an overall decontamination factor of 4500 is assumed for the nonvolatile fission products.

The assumptions made regarding decontamination are summarized in Table I.3.1.

It will become obvious that the controlling doses will be the external, or submersion, dose due to the noble gases and the thyroid dose due to the inhalation of iodine. The internal and submersion doses due to all other fission products are several orders of magnitude less than those and will not be considered further here.

Table I.3.1. HFIR Decontamination Factors

	Fraction Released from Fuel	Fraction Escaping Deposition	Fraction Escaping Filter	Decontamination Factor
Iodines	0.5	0.333	0.0015	2000
Noble gases	1.0	1.0	1.0	1
Nonvolatiles	0.02	0.222	0.001	4500

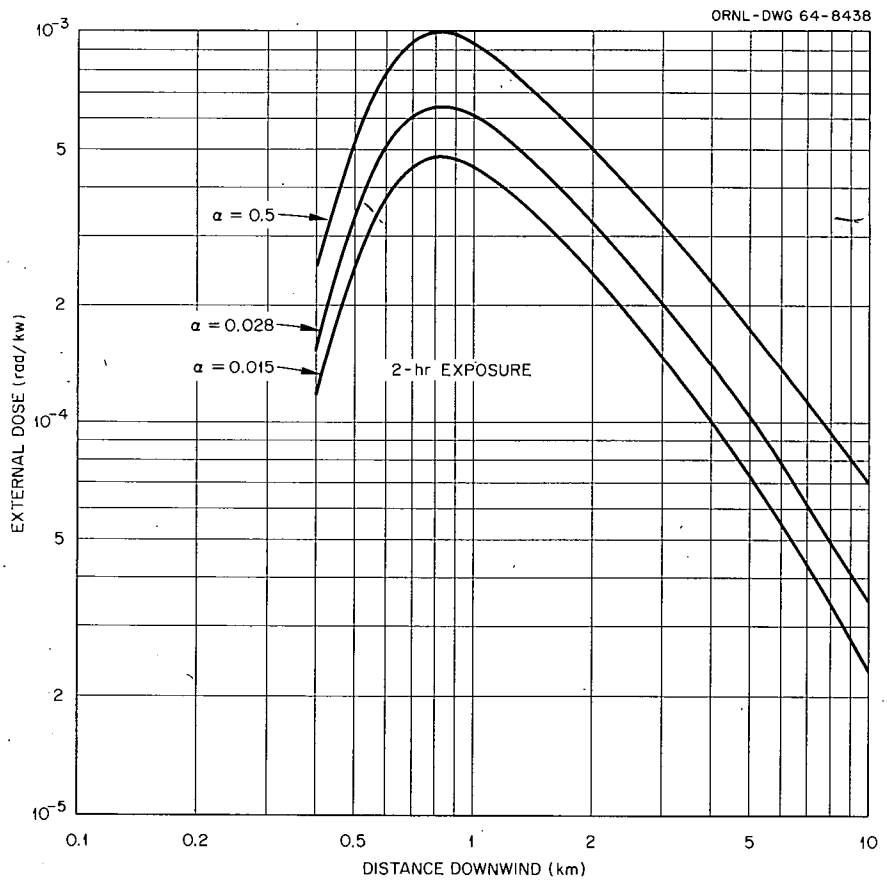

Fig. I.3.5. External β Dose from Noble Gases Following a Fission Product Release from HFIR – 2-hr Exposure.

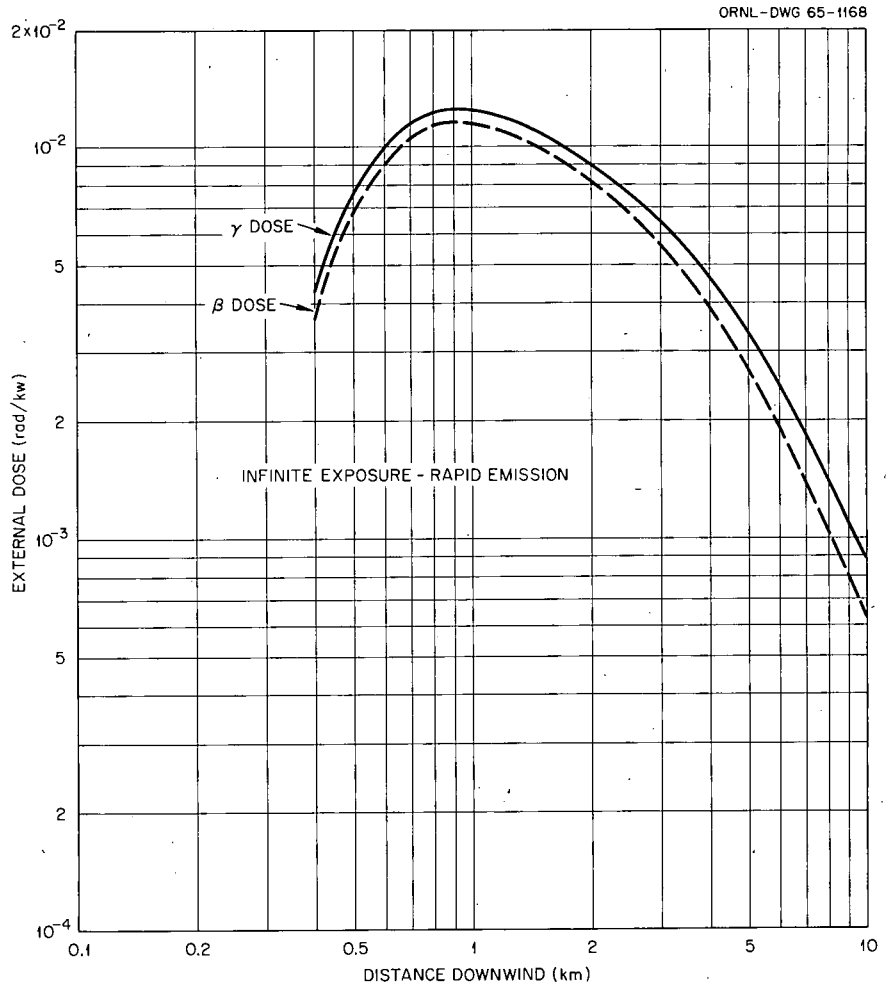

Fig. I.3.6. External Dose Due to Fission Products Other than Noble Gases Following a Fission Product Release from HFIR – Infinite Exposure and Rapid Emission.

4. INTEGRITY OF THE CONTAINMENT SYSTEM

The foregoing results hold only provided that the containment systems function as designed. A schematic diagram of these systems is presented in Fig. I.4.1, and reference to this diagram will facilitate the subsequent discussion. In the case of accidents which occur within the primary coolant system and do not involve breaching of that system, any escaping fission products must pass not only through the CHOG filters but also through the SBHE filters as well. Moreover, because the automatic block valves (see p. 15) will close when a high radiation level is detected in the primary coolant system, very little activity will actually reach these filters. For all other types of accidents where there is a possibility of a significant fission product release into the building itself, the activity must be removed by the SBHE system. Both the SBHE and the off-gas systems are designed for maximum reliability, and their failure concurrent with a fission product release is not considered to be credible.

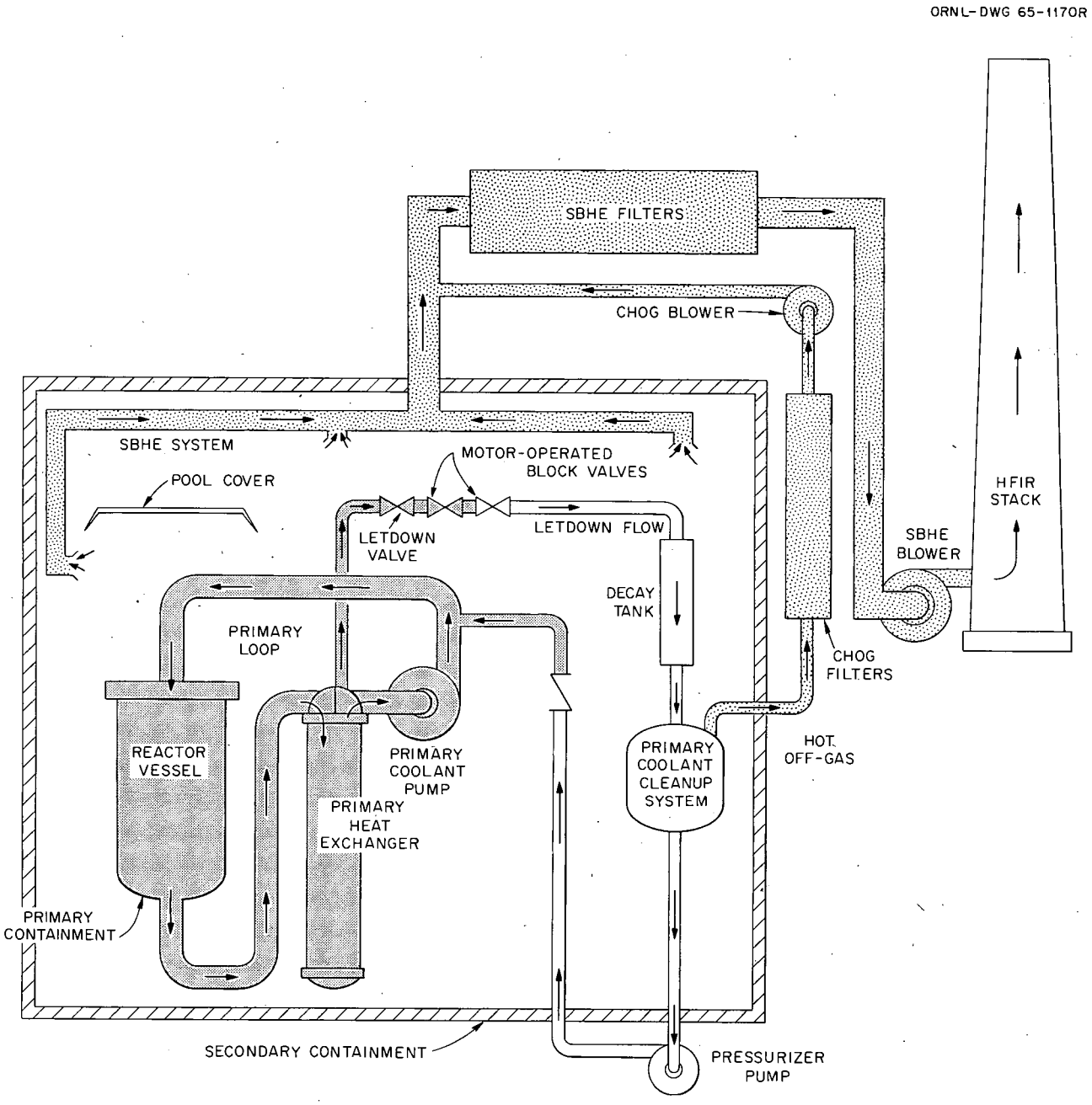

Fig. 1.4.1. Schematic Diagram of HFIR Containment Systems.

Nevertheless, four types of failures could be postulated and it is necessary to examine them. They are: (1) failure of the SBHE or CHOG fans, (2) failure of the SBHE or CHOG filters, (3) failure of the automatic block valves, and (4) an accident of sufficient violence to tear a large hole in the building. These will be discussed below; however, it should first be pointed out that the secondary containment alone is always adequate to contain any accident provided that the building remains intact and the SBHE system is in operation. Moreover, in many cases – those in which the primary coolant system remains closed – the primary containment alone is adequate.

Failure of the SBHE or CHOG Fans. – Failure of the SBHE fans would have two results: (1) the building forced draft would be cut off and (2) the effective stack height would be reduced to 76.2 m, the actual stack height. Neither of these results is of any consequence provided it does not occur concurrently with a fission product release into the building itself. This is because any fission product release from the primary coolant system is routed through the CHOG filters and blower to the SBHE filters. Moreover, if the release in the primary system is of major proportions, the block valves will close automatically and thus isolate the fission products in the primary containment loop. Reduction of the effective stack height to the actual stack height would increase the maximum downwind doses, which occur at a distance of about 1 km from the stack, by a factor of about 1.5, and would have little effect at greater distances.

The SBHE fans* are installed in duplicate.[25] One fan is in continuous operation while the other is on standby. The standby fan will come on the line upon an indication of significant loss of air flow. The fans receive their power, respectively, from one of the two normal-emergency power supplies.[26] Normal power is supplied from the preferred TVA feeder. Upon failure of the preferred feeder, the buses are automatically switched to the alternate TVA feeder. Should this also fail, both emergency generators start automatically and power is fed to the preferred fan. Should emergency power to this fan fail, the second emergency generator will start the standby fan. Failure of the preferred fan or motor will cause a loss of air flow which will actuate automatic startup of the standby fan.[27] It is believed that this system is sufficiently reliable to rule out the credibility of an SBHE fan failure concurrent with a fission product release from the fuel.

Failure of the CHOG fans concurrent with a fission product release into the primary coolant system would merely result in a decrease in the rate at which gaseous and vapor-borne activity would reach the SBHE filters. Because of the automatic isolation by the block valves, only relatively small or controlled amounts of activity will reach these filters. Failure of the CHOG fans following a release into the building would be of no consequence from an environmental point of view. The CHOG fans are installed in duplicate and are connected to their power supplies in a manner quite similar to the SBHE fans. Their failure concurrent with a fission product release is not considered likely enough to be credible.

---

*Answer 53 describes the addition of a third SBHE fan in parallel with the original fans.

[25]ORNL-3572, sect. 4.7.1.

[26]ORNL-3572, sect. 10.1.

[27]ORNL-3572, sect. 4.9.1.

Failure of the SBHE or CHOG Filters. – Because the SBHE and CHOG filters[28] constitute the final barriers which prevent fission products from entering the atmosphere, it is important that their efficiency be maintained. As has been pointed out in Sect. 3, it is expected that each of these banks of filters will achieve a decontamination factor of about 700 for iodines and over 1000 for solid fission products. As will be seen in Sect. 6, these factors are considerably greater than is actually required to prevent intolerably high environmental contamination of the atmosphere. As a practical matter, every effort will be made to achieve the highest decontamination factors consistent with safety and economy. The filters will be tested following installation and periodically thereafter.

As originally designed, each bank of filters contains in series a Fiberglas prefilter, an absolute filter, two charcoal absorbers, and a final absolute filter. In each system a standby filter bank is provided. Once installed and tested, the only obvious cause of gross filter failure is fire. Moreover, because in each bank two charcoal absorbers are installed in series, failure of one absorber section alone will not result in complete failure of the system.

The Fiberglas is fireproof, and the absolute filters are fire resistant; however, the charcoal is flammable. While it is possible to postulate various ways in which the charcoal could be ignited, the only credible mechanism for supplying large amounts of heat to the charcoal is the absorption of energy from the decay of fission products trapped thereon. A conservative estimate[29] of the average temperature rise in the CHOG filters, should the iodine inventory available from the HFIR MCA be trapped within the first 0.2 in. of charcoal on the first filter, is about 50°F. A similar calculation indicates a 3°F average temperature rise in the SBHE filters. It is desired to prevent the temperature from increasing above 300°F, which is well below the reported ignition temperature of 550°F. In view of the automatic isolation of the primary coolant loop in the event of a major fission product release and the small average temperature rise in the filters which could result from deposition of the iodine inventory, it appears impossible to achieve the ignition temperature of charcoal. Nevertheless, precautions are being taken to guard against such an "incredible" fire.

These precautions have taken the form of a design change in which the exhaust from the CHOG filters is routed through the SBHE filters rather than directly to the HFIR stack. This imposes a second set of filters between the CHOG system and the atmosphere and reduces the number of parallel paths by which activity can reach the atmosphere.

In addition, silver-plated copper mesh filters will be installed between the absolute filter and first charcoal absorber in both the CHOG and SBHE filter pits. These will reduce the temperature rise in the charcoal by carrying some of the iodine load and will also serve as flame arresters should a fire occur at a point upstream of the metal filters.

With these changes, it is believed that the failure of the filter system concurrent with a reactor accident can be considered incredible.

---

[28] ORNL-3572, sect. 4.7.

[29] F. T. Binford, January 1965 (unpublished).

Failure of the Automatic Block Valves. – As a result of the safety analysis, it became apparent that for many of the postulated accidents the results could be minimized by taking advantage of the block valves[30] in the pressure letdown lines. Each of these four lines contains three valves in series. One of these provides for normal pressure regulation and the other two are block valves, both of which are equipped with pneumatic operators. The normal function of the block valves is to close upon reduction in system pressure below normal and thus prevent the flow of primary coolant system water to the primary coolant cleanup system.

In addition to this normal function, the operation of the block valves has been modified so that upon the detection of high radiation in the primary coolant system, a signal is transmitted to the safety system which causes automatic closing of both block valves in all the pressure letdown lines. The detectors and associated electronics have safety system reliability (two out of three coincidence circuits which may be tested). The same signal which closes these block valves also initiates a reactor scram. The exact radiation level at which this action will be initiated has not yet been determined but will be set at the lowest level consistent with orderly operation.

While failure of the block valves will not increase the consequences of the maximum credible accident, their proper operation will greatly reduce the consequences of fission product releases within the primary coolant system. Moreover, because of the redundance incorporated in the design, their failure is considered extremely unlikely.

Failure of the Reactor Building.* – The HFIR containment building[31] is constructed of reinforced concrete, and, as will be shown in Sect. 4.2, it does not appear that any credible accident to the reactor could develop sufficient violence to grossly rupture the primary coolant system, much less the reactor building. Perhaps the only circumstances which could cause gross damage to the building would be a violent earthquake, virtually unknown in the East Tennessee region,[32] or armed attack. On the other hand, the building is penetrated by a number of doors[33] for both personnel and vehicles, and large glass windows are located between the observation gallery adjacent to the control room and the contained portion of the building. Two of the personnel doors in the reactor bay – one leading to the personnel decontamination room and the other to the outside – are of the air-lock type, as is the vehicle entrance. The two remaining personnel doors, both of which open into the corridor between the water wing and the reactor bay, are of the ordinary type. They are equipped with automatic door closers but will be kept locked during operations which require containment. Doors are equipped with panic bars so that in an emergency they may be opened from the reactor bay side. It is conceivable that one or more of the doors may remain open during a release into the building; however, with the possible exception of the vehicle air lock in the reactor bay, such an occurrence would not materially affect the ability of the SBHE system to provide containment. It is possible that the windows in the observation

---

[30]ORNL-3572, sect. 8.6.4.

*Further discussed in answer 59 and Appendix K.

[31]ORNL-3572, sect. 3.3.

[32]ORNL-3572, sect. 2.3.3.

[33]ORNL-3572, sect. 3.3.1.

gallery might be broken as a result of an accident which also releases fission products into the building, but this is unlikely because of their location. Moreover, the observation gallery is maintained at a higher pressure than the reactor bay. Because none of the credible accidents involve an increase in pressure in the reactor bay, the leakage would be inward.

4.1 Integrity of the Primary Coolant System*

As has been pointed out previously, the primary containment is effective whenever the reactor is operating routinely. It consists of the high-pressure portion of the primary coolant loop,[34] which is designed to operate at a maximum pressure of 1000 psi. Studies of the integrity of this system during an accident involving the rapid release of large amounts of energy have been made by W. R. Wise, Jr., and his findings are presented in Appendix B. These are also shown in Fig. I.4.2. This curve gives the highest defensible energy excursion which would not result in gross failure of the reactor vessel under the conditions to be expected during the release. The magnitude of the allowable energy release is plotted against the duration of the release, which is here taken to be linear. These data hold provided the pressure vessel and the high-pressure piping satisfy the strength requirements specified.[35] It can be seen that for very fast excursions – total energy release times of the order of 3 msec – the system can withstand 220 Mwsec of energy or the equivalent of the detonation of 110 lb of TNT. For slower releases – times of the order of 100 msec – the system can withstand 360 Mwsec, and for still slower excursions the value approaches 500 Mwsec. The results found by Wise are reinforced by independent calculations performed by R. E. Shappel,[36] who found that at least 270 Mwsec are required to rupture the pressure vessel.

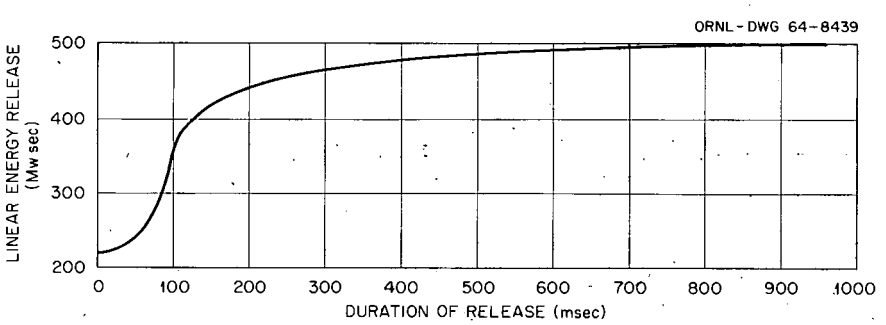

Fig. I.4.2. Upper Bound Containment Potential of HFIR Under Normal Operating Conditions.

*Further discussed in answer 56 and Appendix J.

[34]ORNL-3572, sect. 6.2.1.

[35]The vessel was designed, fabricated, and inspected to meet the requirements of the ASME Boiler and Pressure Vessel Code, sect. VIII, 1959 ed., and Nuclear Code Case 1273N. Additional tests were performed to corroborate specific design assumptions and to assure material integrity and adequacy under expected operating conditions of radiation and pressure and temperature cycling. Further control over vessel integrity will be exerted by the use of surveillance specimens within the vessel at critical locations, which will be periodically tested to determine the changes in material properties due to radiation dosage.

[36]R. E. Shappel to J. R. McWherter, letter dated Oct. 30, 1963.

4.2 Sources and Magnitudes of Energy Releases

There are only two potential sources which could conceivably supply sufficient energy to approach the bounds indicated in the previous section. The first of these is a power excursion caused by the rapid introduction of excess reactivity. The second is the release of a large quantity of energy as the result of extensive exothermic chemical reactions. Such chemical reactions are initiated only at very high temperatures and can occur only under abnormal conditions which permit the fuel temperature to reach the melting point or higher. The only obvious ways in which such temperatures can be developed are as follows: (1) by a power excursion, (2) by a failure of both the control and safety systems coupled with an operating error which permits the power level to grossly exceed the heat-removal capacity of the system, (3) by a flow blockage due to the presence of foreign material in the cooling system or due to mechanical failure of a fuel element, or (4) loss of primary coolant system pressure resulting in steam formation in the core and blanketing of the fuel plates. Of these, the second – concurrent failure of the control and safety systems – is considered highly improbable because of the strong redundance incorporated in both systems and because of the large number of independent failures required to bring it about.[37]

It has been determined that the maximum damage from an uncontrolled reactivity addition is that which would occur should an optimum void be swept into the target region while the reactor is at full power and at a time near the end of the fuel cycle. Under full-flow conditions, the void would represent a total increase of about 1.3% in reactivity and would be introduced over a period of about 30 msec. The consequences of this and other types of reactivity additions have been studied by means of analog techniques and are summarized in Appendix C. The calculations indicate that introduction of this optimum void could result in a maximum energy release of about 52 Mwsec, a peak power level of ~1250 Mw, and the possibility of some localized melting at the hot spots.

Subsequent analyses, also included in Appendix C, which involve extrapolation of SPERT data and calculation of the SPERT experimental cases employing the same analog techniques used for the HFIR lead to the conclusion that all the low-power computations (for which experimental data are available for comparison) are conservative; and it appears that the high-power results are also conservative. This, together with the conservative procedures employed in the hot-spot analysis,[38] makes it appear likely that little or no melting would actually occur.

The only other potentially large source of energy is one or both of the two theoretically possible exothermic chemical reactions, both of which can only be initiated by excessive fuel temperatures. These are the reaction of U_3O_8 with aluminum and the well-known Al-H_2O reaction.* The former has been

---

[37]ORNL-3572, sects. 8.3 and 8.4.

[38]ORNL-3572, sect. 7.5.4.

*Further discussed in answer 23 and Appendix I.

studied by Fleming and Johnson[39,40] and the latter by Epstein.[41,42] Based upon the work of Fleming and Johnson, it is estimated that the maximum energy release due to the U_3O_8-Al reaction would be ~0.65 Mwsec per kilogram of U_3O_8-Al mixture reacted for the case of the fuel in the inner annulus and ~0.75 Mwsec per kilogram of mixture reacted for the fuel in the outer annulus. Since these annuli contain ~9.4 and 21.6 kg of U_3O_8-Al mixture, respectively, the maximum energy potentially available from the reaction cannot exceed 22.4 Mwsec. On the other hand, the energy release from the Al-H_2O reaction is ~4.2 kcal per gram of aluminum reacted[43] or 17.6 Mwsec per kilogram of aluminum (or water) reacted. Consequently, since the total aluminum inventory in the fuel plates is ~88 kg, the maximum potential energy from this source is ~1550 Mwsec. As will be seen, it is not credible to suppose that either of these reactions can occur to any appreciable extent in the HFIR.

There is considerable doubt as to whether U_3O_8 mixtures containing the high percentage of aluminum found in the HFIR fuel will react violently; moreover, the primary concern is not the energy release per se, but rather the additional heat available from the reaction, which on the average amounts to about 109 Btu per pound of aluminum and might increase the probability of the Al-H_2O reaction.

The U_3O_8 reaction is thought to be possible only at temperatures in excess of 1200°F, and only a small amount will react rapidly at temperatures below 1400°F. The Al-H_2O reaction requires an initiating temperature of at least 2140°F and, in addition, usually requires that the aluminum be finely dispersed in water. Moreover, 1 kg of water is required to react with each kilogram of aluminum.

Use of the foregoing information makes it possible to estimate the maximum energy release in the case of each of the three credible accidents listed above.

Reactor Power Excursion. – Reference to Appendix C reveals that under the worst power excursion, which would release 52 Mwsec of nuclear energy, the average peak fuel element temperature will not exceed 800°F, which is far below that required to initiate either reaction. Moreover, it would be necessary to heat a portion of the core to greater than 1600°F before the additional heat associated with a complete U_3O_8-Al reaction could, even if absorbed adiabatically, raise the aluminum temperature sufficiently high to initiate the Al-H_2O reaction. This is ~400°F above the melting point of aluminum.

On the other hand, the peak hot-spot area is shown by the calculations to reach sufficiently high temperature to initiate both reactions. As has been pointed out, these values are thought to be extremely conservative and even here there is doubt that melting will occur. Nevertheless, it is necessary to concede that some chemical energy may be released at the hot spots as a result of the maximum credible reactivity insertion. Based on conservative assumptions, the hot-spot regions have been found to be confined to not more than 5% of the total fuel-plate area. Thus, the maximum chemical energy release

---

[39] J. D. Fleming and J. W. Johnson, *Trans. Am. Nucl. Soc.* **6**(1), 158 (June 1963).

[40] *Final Report, Project No. B-153, Task II, Reactions in Al–35 Weight Percent U_3O_8 Dispersion,* Georgia Institute of Technology, Engineering Experiment Station.

[41] L. F. Epstein, *Metal Water Reactions VII, Reactor Safety Aspects of Metal Water Reactions,* GEAP-3335 (January 1960).

[42] L. F. Epstein, *Nucl. Sci. Eng.* **10**, 247–53 (July 1961).

[43] R. C. Limatainen *et al.*, "Studies of Metal Water Reactions at High Temperatures II," *TREAT Experiments Status Report on Results with Aluminum, Stainless Steel-304, Uranium, and Zircaloy-2,* ANL-6250, p. 13, Table 1.

could not exceed ~88 Mwsec and the total energy release would be ~140 Mwsec, which is far below that necessary to rupture the primary coolant system.

There has been a great deal of speculation regarding the possibility of autocatalytic propagation of the Al-H_2O reaction and eventual involvement of a large portion of the core. On the basis of experience, this does not appear to occur, probably because water is required in order to permit the reaction to proceed; and at the temperatures required for the reaction, very little water is present. This is supported by the results of the SL-1 accident, in which a 130-Mwsec nuclear excursion released ~24 Mwsec of chemical energy, and the SPERT-1 destructive test, in which a 31-Mwsec nuclear excursion released 3 to 4 Mwsec of chemical energy.[44] It is interesting to note that by linear interpolation of these two cases, a 52-Mwsec HFIR excursion corresponds to an 8-Mwsec chemical energy release.

Flow Blockage. – A second method of overheating, which is probably more likely than a nuclear excursion, involves blockage of flow to some portion of the core during power operation. This could occur because of the presence of foreign material in the cooling system or because of the mechanical failure of one or more fuel plates. In this case, a significant fraction of the core may be deprived of adequate cooling for an appreciable time during which the reactor continues to operate at full power. This situation has been analyzed in Appendix D. It is shown that even under very pessimistic assumptions at most 24% of the fuel plates will suffer melting and that the total energy release will not exceed 182 Mwsec. This is less than the minimum of 210 Mwsec required to rupture the pressure vessel. Moreover, because the energy release from the chemical reaction would be expected to proceed at a much slower rate than a TNT explosion, the containment potential of the vessel would be somewhat higher than the 210 Mwsec minimum.*

Loss of Primary Coolant Pressure.** – Finally, it is necessary to consider the case where pressure is suddenly lost to the primary coolant system. It has been shown[45] that leaks in the primary coolant system equivalent to an open 3-in. valve or less can be handled by the system without damage. If, however, a considerably larger leak developed, the system would depressurize rapidly and some overheating might occur in the core. Reactor shutdown would be simultaneous with the pressure loss due to both safety-system action and because of loss of moderator due to steam formation. Because only about 50 gal of water is required to pressurize the primary coolant system, and because of the configuration of the piping and the location of the reactor vessel in a pool of water,[46] it does not seem possible that such an incident would lower the water to an extent sufficient to uncover the core. Consequently, the amount of melting to be expected would be small compared with that caused by a flow blockage; and no substantial energy release is anticipated.

---

[44] *Argonne National Laboratory Chemical Engineering Division Summary Report April–June 1963*, ANL-6725, p. 220.

*Further discussed in Appendix J.

**Further discussed in answers 23 and 43.

[45] ORNL-3572, sect. 8.8.5.

[46] ORNL-3572, sect. 6.2.1.

As a consequence of the foregoing discussion, it appears safe to consider that a massive rupture of the primary coolant system is incredible. It is credible, however, to postulate an accident releasing fission products from the core, some of which escape from the reactor vessel through leaking flanges, broken beam tubes, etc.

5. ACCIDENTS INVOLVING THE REACTOR FUEL

As has been pointed out in Sect. 2, it is possible to identify six types of potential accidents which may be accompanied by damage to the reactor fuel. Of these six, the first three occur when the fuel is outside the primary containment. The fourth and fifth, which would in general have less severe environmental consequences, can occur only under conditions of double containment. The sixth case, which includes an accident of sufficient violence to severely damage the core and also to cause some leakage of fission gases or contaminated water from the primary containment, is a combination of the other two types. It is an accident of this type which is considered to be the maximum credible accident.

5.1 Accidents Involving Fuel Within the Primary Containment

The two types of fuel meltdown accidents which can occur when the primary coolant system is closed up differ only in initial cause and, to some extent, in magnitude. Both are the result of overheating brought about in the one instance by a power excursion and in the other by a coolant flow blockage. Of these, probably the most likely is a flow blockage caused by foreign material inadvertently introduced into the system. A reactor excursion of sufficient magnitude to grossly damage the fuel is effectively prevented by the safety system,[47] and operation at an excessive power level would require simultaneous failure of both the safety and control instrumentation and in most instances an operator error as well. Inspection procedures for the fuel have been developed to ensure correct loading of the fissile material and poison. Initially, 100% examination of the plates by x-ray scanning techniques is specified.

Regardless of the initial cause of overheating, the results will be similar and will differ only in degree. They may range from little or no damage to the fuel to the actual meltdown of a substantial fraction of the core accompanied by significant damage to the reactor internals and to the reactor vessel itself. Nevertheless, in view of the analysis presented in Sect. 4 and the estimated strength of the reactor vessel, it is clear that the primary containment will remain essentially intact. Thus, even in the most extreme cases there will be only a minor release of fission products from the primary coolant system. This is because of the automatic closure of the block valves upon detection of high radiation in the primary coolant system. Even should this automatic feature fail, manual closure of the block valves would trap over 90% of the released activity in the primary system should this action be taken within 5 min of the release. If the block valves are not closed at all, the activity would be discharged to the atmosphere through the CHOG and SBHE filters. The consequences of this are somewhat less than that postulated for the maximum credible accident discussed subsequently.

---

[47] ORNL-3572, sect. 8.4.

5.2 Accidents Involving Fuel Outside the Primary Containment

As in the case of the potential accidents discussed in the previous section, those which may occur when the reactor vessel is open or when the fuel is outside the reactor, and which present an environmental hazard, are all the result of overheating the fuel. The main difference between these accidents and those discussed previously is that in these cases the fission products are not retained in the primary coolant loop but escape into the pool water and are disposed of through the SBHE system.[48]

When the vessel is open the reactor cannot be operated at any substantial power level, although it is possible to have some forced convection cooling under these conditions. Therefore, there is little possibility of a meltdown due to loss of flow. The possibility of a power excursion exists; but, as pointed out in Appendix C, there is little likelihood that any credible reactivity addition could cause significant damage.

One other safety problem encountered in the operation of the HFIR is that of protection against afterheat because of the high power density associated with the fission product decay following shutdown. It has been found[49] that 1 sec after shutdown following 15 days' operation at 100 Mw, the maximum fuel plate heat flux will be ~42,000 Btu ft^{-2} hr^{-1} [75,200*]. This falls to ~6200 Btu ft^{-2} hr^{-1} [11,000*] 1 hr after shutdown, as shown in Fig. I.5.1. Immediately after shutdown, the fuel element, which is still generating in excess of 7 Mw of heat, is protected by continuing the forced convection cooling either by the use of the primary coolant pump motors or by the battery-driven pony motors,[50] any one of which is sufficient. The fuel will be retained in the reactor under forced convection cooling for a period of about 1 hr, after which it may be removed from the reactor vessel. At this time, the total power will be ~1.1 Mw [1.4*]. It has been experimentally determined[51] that, when in an upright position and situated to provide a good free convection loop, the natural convection burnout heat flux will be in excess of 47,000 Btu ft^{-2} hr^{-1}. Thus, the fuel elements can easily be cooled after removal from the reactor following this delay.

The only problem which arises in this connection relates to the temperature distribution to be expected in the fuel element should it be placed in a horizontal position, thus destroying the efficiency of the natural convection cooling. Experiments and analysis by Gambill[52] indicate that under these conditions a heat flux of 1250 Btu ft^{-2} hr^{-1} might result in a hot spot surface temperature as high as 1000°F. Consequently, the handling tools and the operating procedures are specifically designed to effectively prevent spent fuel from being oriented at any appreciable angle from the vertical.

Critical experiments using the initial version of the HFIR core indicate that two new fuel annuli assembled and immersed in water will be only slightly subcritical. A series of critical tests using the

---

[48] ORNL-3572, sect. 4.5.

[49] N. Hilvety, *Gamma and Beta Heat Generation in HFIR Cores*, ORNL-CF-60-4-110 (April 1960).

*Later calculations by T. G. Chapman, *Revised HFIR Shutdown Heat Rates*, ORNL-CF-65-9-7.

[50] ORNL-3572, sects. 6.5 and 10.1.4.

[51] Letter from W. R. Gambill and D. R. Bundy to C. E. Winters, Dec. 2, 1959. More details of the general experimental program can be found in ORNL-3026, *Burnout Heat Fluxes for Low Pressure Water in Natural Circulation* (Dec. 20, 1960).

[52] W. R. Gambill, *HFIR Natural-Circulation Heat-Removal Limits*, May 18, 1964 (unpublished).

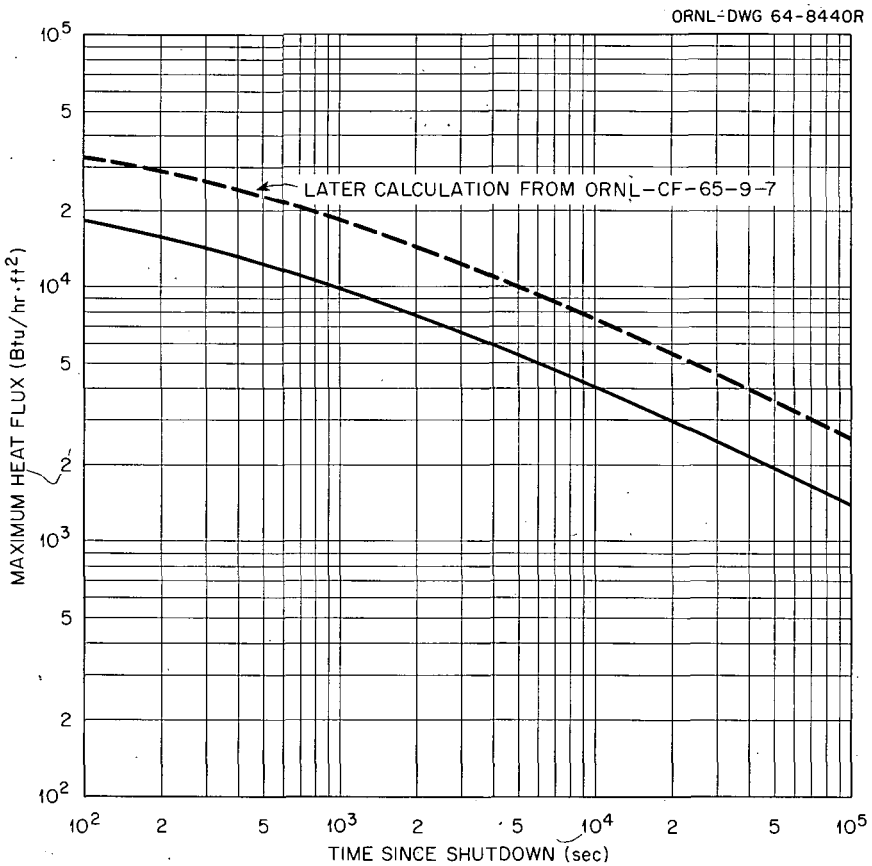

Fig. 1.5.1. Maximum Fuel Plate Heat Flux of HFIR Fuel Following 15-Day Operation at 100 Mw.

current core is expected to give additional information concerning criticality problems which may arise in connection with fuel handling and storage. While it is not expected that a pair of assembled new fuel elements in water will be critical, they will be treated as if this is the case, and fuel elements will always be handled separately.

Spent fuel cores will be stored assembled on racks arranged in an "always safe" array. Each rack contains a central "poison post"[53] containing sufficient cadmium to ensure that the stored fuel is well below critical. Although the shutdown margin of a depleted core is far greater than that of a new core, the poison post is adequate to handle either. This point has been verified by the critical experiment program now in progress. In the unlikely event that a pair of fuel elements become stuck together in the reactor and must be removed together, they will be locally poisoned before so doing.

Among the other precautions required to prevent inadvertent criticality is the usual one of ensuring that the control plates are inserted when a new core is being installed in the reactor and that of preventing introduction of the "optimum void" in the form of a hollow tool or other device during startup

[53]ORNL-3572, sect. 11.6.

in the test modes.[54] The former is provided for by the operating procedures and the latter by the design of the tools and by requiring that the target or a suitable substitute be in place whenever the reactor is brought critical. In addition, initially at least, each new fuel core will be tested in the ORNL criticality facility before being accepted for use in the reactor. It is expected that a more simple reactivity test will eventually be devised, and when this is done it will replace the presently planned criticality tests.

It is worth noting that in the most likely cases a criticality accident could involve only new or slightly depleted fuel, so that the fission product inventory would be considerably lower than would be the case for fuel which had been subjected to a full power cycle.

6. THE MAXIMUM CREDIBLE ACCIDENT

Despite the arguments presented above to show that the potential accidents are either very unlikely or have been recognized and precautions taken to prevent them, there still exists the finite probability that a fission product release may occur. Such an incident may be the result of minor damage to the fuel with insignificant results or may consist of an extensive meltdown of the core accompanied by the release of a substantial fraction of the volatile fission products. Paradoxically, the accidents which are most likely to result in extensive damage to the reactor internals and cause large fission product release from the fuel can occur only under conditions of double containment, and if the primary containment remains intact, there will be little or no release of fission products to the atmosphere. On the other hand, fission product releases which occur when the primary containment is inoperative will be of lesser magnitude, but will be discharged through the SBHE system and cause some environmental contamination.

The potentially worst case would involve extensive meltdown of the core concurrent with failure of the primary containment. This is considered highly improbable, because of the strength of the primary system discussed in Sect. 4.1, and because a depressurization accident caused by rupture of the primary coolant system would not result in extensive melting. Nevertheless, to cover any such possibility, the maximum credible accident is postulated to be an extensive meltdown of the reactor core concurrent with a failure of the primary containment sufficiently severe to allow some of the fission products to escape directly into the building, but not violent enough to grossly rupture the reactor vessel or the high-pressure piping.

In order to obtain a realistic estimate of the consequences of the maximum credible accident, it is first necessary to establish the amount of fuel which could sensibly be considered to be involved. In the worst accident heretofore, the SL-1 accident, ~32% of the core was melted with ~50% of the fuel reaching melting temperature. In the SPERT-I destructive test about 35% of the core was melted.[55] In the calculation presented in Appendix D, it is estimated that at worst 24% of the HFIR core could

---

[54] ORNL-3572, sect. 8.3.2.

[55] *Argonne National Laboratory Chemical Engineering Division Summary Report April–June 1963*, ANL-6725, p. 220.

melt. It seems reasonable, therefore, to postulate that the maximum credible accident in the HFIR would involve the melting of not more than 50% of the reactor fuel.

The extent of the release of fission products from the melted fuel has been discussed in Sect. 3. It will be assumed that 100% of the noble gases, 50% of the iodines, and 2% of the other fission products eventually leave the vicinity of the fuel.

While some of the fission products will escape into the building quite rapidly because of the postulated leakage from the primary containment, the remainder will diffuse more slowly from the water, either through the leaks or through the CHOG system. To account for this it will be assumed that 25% of the released fission products escape from the primary containment and are rapidly removed from the region over the pool by the SBHE system. The other 75% are assumed to be removed more slowly at a rate comparable to that achieved by the CHOG system. The released fission products are assumed to pass through the SBHE or CHOG system and to be discharged from the stack following filtration.

The downwind doses from the maximum credible accident have been calculated under the foregoing assumptions using the unit values given in Figs. I.3.1–I.3.6 and the decontamination factors listed in Table I.3.1. The results are presented in Fig. I.6.1. For convenience these results have been tabulated in Table I.6.1 for a number of points of interest including the exclusion area boundary, boundary of the low-population zone, and population center distance as defined in 10 CFR Part 100. For this purpose the exclusion area distance is taken to be the nearest distance to private land (non-government-controlled) from the HFIR – 2.82 km southeast. The population center distance is taken to be the shortest distance to residential Oak Ridge – 7.62 km north, and the low-population-zone boundary is 5.72 km from the HFIR.

It is clear from Table I.6.1 that the controlling factor is indeed the whole-body dose from noble gases, and this is acceptably low at the reference points specified in 10 CFR 100. The iodine doses, which are given in each instance for infinite exposure and rapid emission, are quite low. This is because of the overall decontamination factor of 2000 which has been applied. It can be seen that an overall decontamination factor of only 19 for iodine would be required to produce a 300-rem thyroid dose at the exclusion area boundary. Hence, this value would not be exceeded if the filters provide an iodine decontamination factor of about 7 provided the other assumptions remain valid.

The internal doses due to fission products other than iodines are quite low and have not been included in the table. At the point where they are a maximum the dose due to bone seekers would not exceed 20 mr and for the other fission products it would be an order of magnitude lower. The submersion dose due to fission products other than noble gases is also of this order. This, of course, is under the assumption that the total decontamination factor for these fission products is 4500 as previously discussed.

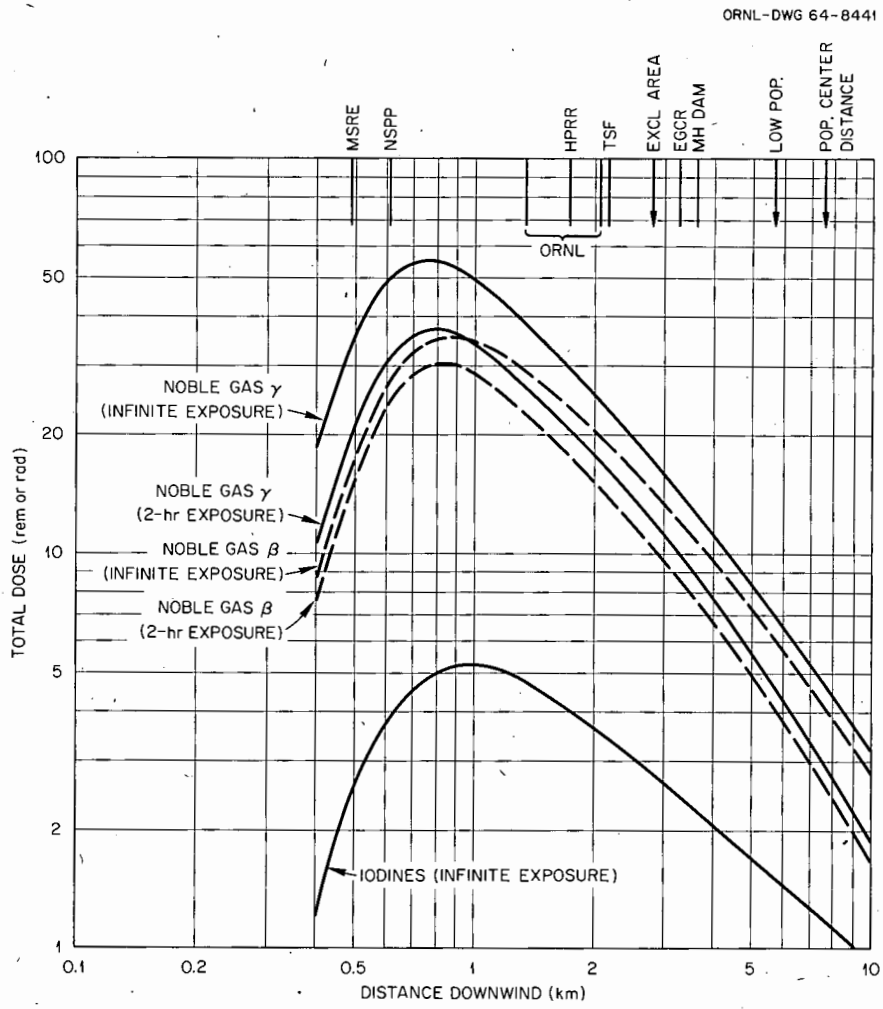

Fig. 1.6.1. Doses to be Expected Downwind Following the HFIR MCA.

6.1 Local Consequences of the Maximum Credible Accident

Aside from the cost incurred to repair any damage resulting from a massive energy release in the reactor vessel, the local effect of a major fission product release in the primary coolant system would be confined to the hazards incurred during the cleanup of the system. The primary coolant system shielding has been designed to accommodate a meltdown. The original shield design was based upon a dose rate not to exceed 1 rem/hr 24 hr after a major[56] core meltdown. Extrapolation of these results to the maximum credible accident discussed above indicates that local radiation levels up to 150 rems/hr may occur initially in the vicinity of the primary coolant cleanup system shielding. Since immediate access to these regions is not required, this would not present a serious problem.

---

[56]The word "major" is used here in the sense defined in ORNL-3572, sect. 9.4.

Table I.6.1. Downwind Doses Following the Maximum Credible Accident at Various Locations

Facility	Location	Thyroid* Dose (rems)	Whole-Body Dose (rads)		Percentage of Time Wind Blows in Specified Direction
			Gamma	Beta	
MSRE	0.49 km NNW	2.5	20[a]	15	0.86
NSPP	0.61 km WNW	3.9	32[a]	25	0.91
ORNL	1.34-2.06 km NNW-WNW	3.5–4.8	17–26	15–23	3.1
HPRR	1.73 km ESE	4.0	21	18	4.7
TSF	2.13 km S	3.4	16	14	2.0
Excl. Area	2.82 km SE**	2.8	13**	11	3.0
EGCR	3.26 km NE	2.5	15	13	12.1
MH Dam	3.65 km S	2.2	13	11	2.0
Low Pop.	5.72 km	1.5	7.2	6.2	
Pop. Center	7.62 km N	1.2	4.8	4.2	3.4

Note: Whole-body doses for locations including and within the exclusion boundary are given for 2-hr exposure. All others are calculated for infinite exposure time.

[a]These are probably underestimated because of proximity to the stack.

The radiation dose rate which might occur in the building as a result of a release would depend upon what fraction of the fission products actually reached the occupied areas. Because of the existence of the pool cover and the location of the SBHE intake registers in the pool walls,[57] only a small fraction of the activity would be expected to escape into the reactor bay itself. Moreover, the local variations in concentrations, together with the positions of the persons who happen to be within the building, would have an important effect on the radiation dose sustained.

To get some idea of the magnitude of the radiation doses to be expected, they have been estimated under the assumption that the iodines and noble gases are distributed uniformly throughout the reactor bay. The calculations are presented in Appendix F.

The external gamma dose rate at the windows in the visitors' gallery would be initially 0.8 r/hr per kilowatt and would fall to half that value in about 25 min. In the center of the reactor bay, the initial dose rate would be ~1.2 r/hr per kilowatt. Thus if, as postulated in the maximum credible accident, 25% of the fission gases escaped from the primary coolant system, and if half of this escaped from under the pool cover and entered the reactor bay, the dose rate at the windows could be as high as 85 r/min. It is likely, however, that the control-room personnel could escape if they acted promptly.

On the other hand, persons in the reactor bay at the time of such an incident are almost sure to become casualties because of the extremely large internal iodine dose rate. This is estimated to be

[57]ORNL-3572, sect. 4.5.

*Revised in answer 30 to include methyl iodide and subsequent charcoal filter optimization.

**Calculated in answer 45 to be 29.6 rads in fumigation conditions with a different wind direction.

about 61 rems/min per kilowatt of fuel affected. Thus, under the conditions outlined above the initial internal dose rate could be as high as 380,000 rems/min.[58]

The direct dose immediately outside the building will, because of the 8-in.-thick concrete walls, be lower than that at the observation gallery windows by at least a factor of 10, or about 500 r/hr under the stated conditions. The integrated dose received by a person standing just outside the building wall for 10 min immediately following the accident would be about 70 r. Consequently, a dangerous exposure can be avoided by prompt evacuation of the area near the reactor building. Plans for emergency action in such cases are included in the Operating Procedure Manual.

7. ACCIDENTS OTHER THAN TO THE FUEL

Aside from the accidents discussed above, all of which include damage due to overheating of the reactor fuel, there are three other types of accidents which could conceivably occur, but which involve radioactive material other than that in the fuel. Of these, probably the most important from an economic standpoint is damage to the plutonium target. Associated with this is the personnel hazard from the alpha-emitting components which could be incurred during cleanup and recovery operations following such an accident. In addition to the central facility designed to accommodate the target, the HFIR is provided with a number of experimental facilities; and it is possible that malfunction of an experiment could result in the release of radioactivity. Finally there is always the possibility that contamination may occur because of leakage or other inadvertent release of radioactive material during handling of waste materials. Perhaps most concern in this connection is with reference to the handling of waste materials, including spent fuel, contaminated aqueous waste, contaminated filters, and spent demineralizer resin.

7.1 Accidents to the Target

The HFIR target[59] consists of thirty-one 3/8-in.-OD aluminum capsules containing initially ^{242}Pu in the form of PuO_2 and aluminum. The PuO_2 charge is specified to be 10 g per target capsule, or a total of 310 g of PuO_2.

Basically there are two types of accidents which are possible. These include: (1) a small leak in one of the target capsules as a result of mishandling, improper fabrication, or mechanical damage; and (2) gross failure of one or more target capsules as a result of severe overheating, waterlogging, or mechanical damage. Of these two, the former could occur either in the reactor or during handling in the pools. Should it occur within the reactor, no serious result would follow; and because of the fission products present in the target material, it would be detected by the primary coolant activity monitors.[60] Once a leak is discovered it would become necessary to determine if the leak requires an immediate

---

[58]See footnote 4, Appendix A.
[59]ORNL-3572, sect. 5.2.1.
[60]ORNL-3572, sect. 8.7.5.

shutdown or whether operation may continue until the end of the cycle. Should the leak occur or be detected when the reactor vessel is open or after the target has been removed from the reactor core, there would very probably be a minor release of fission gases into the SBHE system. It has been estimated[61] that the entire iodine and noble-gas inventory of a single target capsule would, at the time when these gases are most abundant, be approximately equivalent to a 20-kw release from the reactor core.

The second type of accident could occur either as a consequence of a major energy release in the reactor such as that discussed in Sect. 4.2 or because of gross flow blockage of the target cooling channels. If caused by an energy release, the damage could occur either from overheating or as a result of mechanical forces and if by a flow blockage, from overheating.

Although the target material would almost certainly remain within the primary cooling system, its emission would not add anything significant to the results of the maximum credible accident. The fission products present at the time of their greatest abundance could increase the consequences of the MCA at most 1.25%. The bone-seeking alpha emitters could increase the internal dose to the bone by an order of magnitude,[62] but since this is already quite low – 20 mr – the increase is not particularly significant. Hence, no serious off-area consequences are anticipated as the result of an accident to the target.

The primary concerns with respect to damage to the target are the monetary value of the target and the product and the hazards associated with cleanup and recovery. The latter arise because of the extremely low permissible body burdens of the various alpha emitters present. These have been computed for all the heavy isotopes of interest and are reproduced in Table I.E.1, Appendix E. It can be seen from this table that, in many cases, the permissible air concentrations are nearly two orders of magnitude lower than that for ^{90}Sr. For this reason, emergency procedures for dealing with contamination by transplutonium elements will be established in advance.

Under normal operating conditions, the average heat flux at the surface of the target capsules will be $\sim 5.8 \times 10^5$ Btu ft^{-2} hr^{-1}; and the hot-spot heat flux is estimated to be $\sim 1.0 \times 10^6$ Btu ft^{-2} hr^{-1}. This is at least a factor of 3 less than the burnout heat flux;[63] and therefore it appears that the target can survive, without damage, a considerably higher power level than that which would cause damage to the reactor fuel. These high heat fluxes persist for only relatively short periods of time.[64]

At this time, the target design is being tested in a hydraulic mockup to verify its adequacy from a mechanical and hydraulic standpoint. Experiments, including the operation of similar capsules in the Engineering Test Reactor, are in progress to obtain more information concerning the thermal conductivity of the target material, to determine the degree of gas release, and to investigate the dimensional stability of the target material. In addition, the irradiation of 18 target capsules is in progress at Savannah River in flux conditions approaching those encountered in HFIR.

---

[61] O. O. Wyrick, ORNL Chemical Technology Division, private communication (April 1964).

[62] See Appendix F.

[63] T. G. Chapman, *HFIR Target Design Study*, ORNL-TM-1084.

[64] ORNL-3572, sect. 5.2.1.

7.2 Accidents to Experiments*

While the exact nature of the investigations which will be performed in the HFIR experiment facilities is yet to be determined, it is probable that initially they will consist of beam-type experiments and static irradiations. There is, however, no intention of restricting the use of the reactor to these kinds of experiments.

All experiments in ORNL reactors are required to meet two basic criteria: (1) they must not present an unacceptable hazard to personnel, and (2) they must not interfere with the orderly operation of the reactor. To ensure that these criteria are satisfied, all experiments must undergo an internal safety review[65] before they are installed. In many cases, this review also extends throughout the design period. Initially, the review is carried out by the Technical Assistance Department of the ORNL Operations Division. It is attempted at this level to resolve any problems regarding safety and to produce a design which meets the necessary requirements. Once agreement has been reached, the experiment may be approved for insertion in the reactor by the Technical Assistance Department. If any significant hazard existed, even though it has been corrected by the design, the experiment is submitted with appropriate recommendations to the Experiment Review Committee for further review. When this committee concurs that the experiment is safe, it may be inserted in the reactor. The committee also periodically reviews the operation of all experiments to make sure that its recommendations are being carried out.

In general, accidents to experiments consist of leaking capsules, broken off-gas lines, etc., and do not contribute any significant environmental contamination. Great care is taken to ensure that no malfunction of an experiment can initiate a serious reactor accident.

7.3 Miscellaneous Accidents

Of the various other accidents involving radioactive material which may occur, the most interesting from an environmental point of view are those which involve the introduction into nearby Melton Branch of a significant amount of radioactive contamination. This could occur as a result of misoperation of the liquid waste system[66] in such a manner that activity impounded in the retention ponds is discharged directly to Melton Branch or as a result of a ground spill and subsequent runoff to the creek. The location of the reactor with respect to the watershed is shown in Fig. I.7.1.

Under normal operating conditions, neither of the retention ponds will contain a large quantity of activity. The only circumstances under which any substantial quantity of concentrated waste solution might be present in these ponds are those which could occur following a fission product release concurrent with a primary coolant system rupture and failure of the process waste drain system.[67] This could put contaminated primary coolant into the process waste drains in the pipe tunnel or heat exchanger

---

*Further discussed in answers 11, 32, and 44.

[65]ORNL-3572, sect. 12.7.

[66]ORNL-3572, sect. 11.3.

[67]ORNL-3572, sect. 11.3.1.

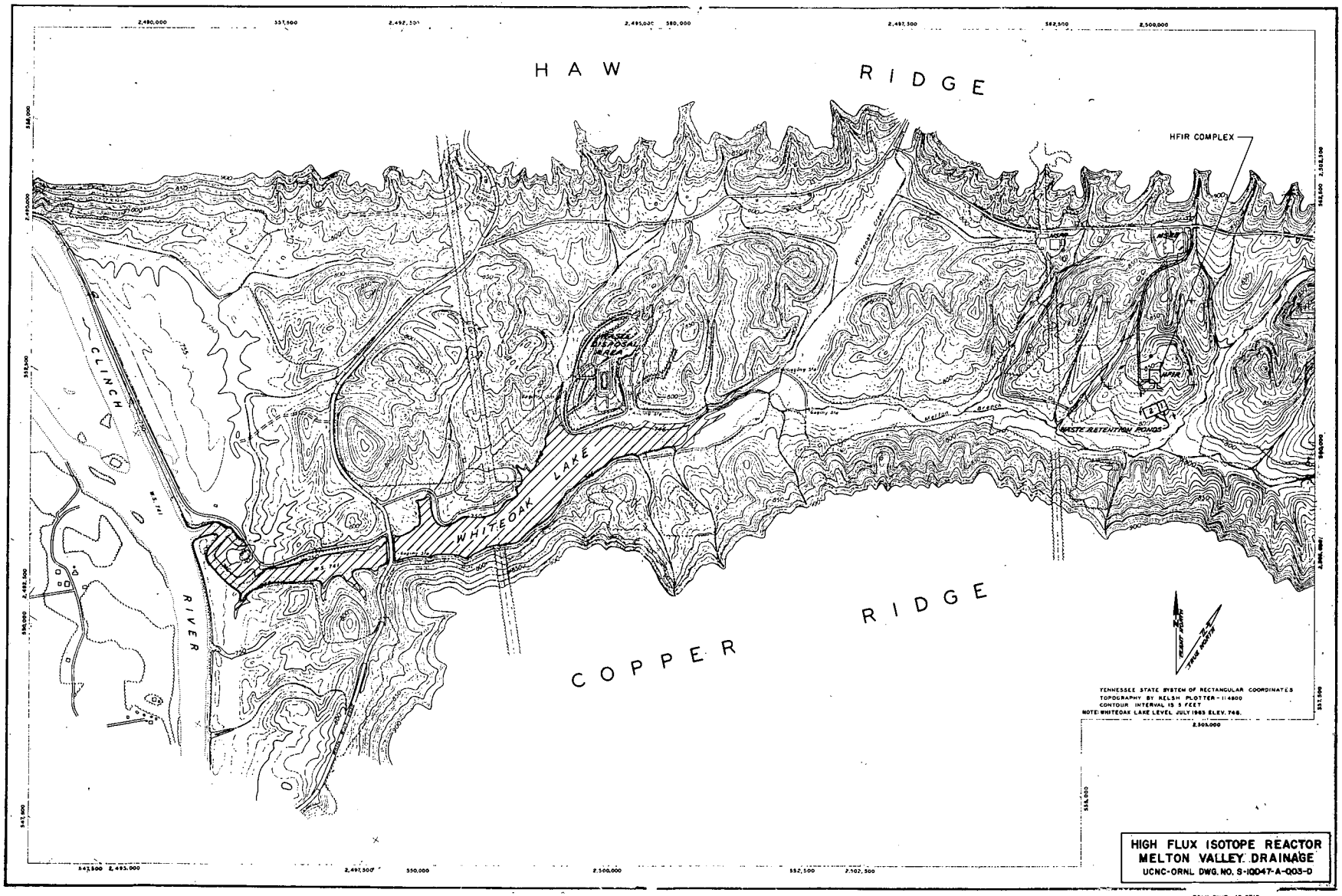

Fig. I.7.1. High Flux Isotope Reactor Melton Valley Drainage.

cells. The entire high-pressure portion of the primary system contains only 13,800 gal, and there appears to be no mechanism by which more than a small fraction of this could be discharged.

Contaminated water resulting from any other type of release would be cleaned up by use of the system demineralizers so that any activity present would be rapidly collected thereon. The contaminated effluent from demineralizer regeneration is collected in the 13,000-gal intermediate level waste storage tank[68] before being sent to the ORNL waste disposal system[69] for treatment and final disposition.

The fission products of most significance with respect to contamination of the watershed are the long-lived isotopes ^{90}Sr, ^{106}Ru, ^{137}Cs, and ^{144}Ce. These, together with their characteristics, are listed in Table I.7.1. Clearly the controlling factor here is ^{90}Sr; and as can be seen from Appendix E, which lists the occupational MPC's for the transplutonium isotopes, the nonoccupational values – one-tenth of the occupational – are all higher than that for ^{90}Sr and, in most cases, higher by a factor of 10, despite the fact that they are lower for air.

In a study of the ORNL waste disposal pits undertaken in 1960,[70] it was found that, with the exception of ^{106}Ru, virtually 100% of the long-lived activity is removed from solution by sorption as contaminated water percolates through soil of the type found in the vicinity of the HFIR site. The ^{106}Ru is removed to the extent of about 93%. This, coupled with the fact that (based upon the release fractions postulated in Sect. 6) not more than 1% of the inventory listed in Table I.7.1 would escape from the fuel, makes it appear unlikely that any sizable release to the watershed can occur.

Should the release postulated in Sect. 6 occur, and should the entire quantity of long-lived isotopes released reach the river, the computational procedures in the referenced report indicate that the result could be equivalent to the discharge of about 200 curies of ^{90}Sr into the Clinch River. Under the assumptions that the average flow rate of the river is 5000 cfs and that there is little or no reduction in the concentration due to dispersion or settling but only by dilution, the integrated dose received at

Table I.7.1. Characteristics of the Long-Lived Fission Products

Isotope	Half-Life	MPC[a] ($\mu c/cm^3$)	Critical Organ	HFIR Inventory[b] (curies)
^{90}Sr-^{90}Y	28 years	1×10^{-7}	Bone	5.1×10^3
^{106}Ru-^{106}Rh	1 year	1×10^{-5}	Kidney	9.0×10^3
^{137}Cs	26.6 years	2×10^{-5}	Muscle	5.2×10^3
^{144}Ce-^{144}Pr	290 days	1×10^{-5}	Bone	1.9×10^5

[a]Nonoccupational MPC for water. (See *Report of Committee II on Permissible Dose for Internal Radiation*, Pergamon, New York, 1959.)

[b]After 15 days at 100 Mw.

[68]ORNL-3572, sect. 11.3.2.

[69]J. F. Manneschmidt and E. J. Witkowski, *The Disposal of Radioactive Liquid and Gaseous Waste at ORNL*, ORNL-TM-282 (August 1962).

[70]F. T. Binford, *An Analysis of the Potential Hazards Associated with the Disposal of Radioactive Waste in Open Pits at ORNL*, ORNL-CF-60-5-63 (May 1960).

the Oak Ridge Gaseous Diffusion Plant located ~7.4 miles downstream is equivalent to that received from ~3 weeks at continuous nonoccupational tolerance. At locations farther downstream, the integrated dose would be considerably less because of additional dilution and dispersion in the Watts Bar reservoir.

8. ROUTINE RELEASE OF ACTIVITY

The HFIR operation will, like all other operations of this nature, from time to time inadvertently release small quantities of fission products to the environment. From the standpoint of atmospheric contamination, the most important of these is ^{131}I. Based upon the recently established 168-hr-week MPC in air for ^{131}I of 1×10^{-10} $\mu c/cm^3$ (ref. 71) and the concentrations given in Fig. I.A.14 of Appendix A, it is easy to deduce that the continuous release of 0.75 mc of ^{131}I per minute from the HFIR stack would not, on the average, exceed the nonoccupational MPC at any point even if the wind direction were constant over a long period of time. Upon taking into consideration the fact that the wind blows in one direction at most 12.5% of the time, this figure can safely be increased to 6 mc/min or 8.6 curies per day.

Upon incorporating into this calculation the overall decontamination factor for iodine of 2000 developed in Sect. 3, the discharge of 6 mc/min of ^{131}I would represent the continual release within the containment system of the iodine production at 100 Mw from about 8.3% of the core. It seems clear that no difficulty should be encountered in meeting this requirement.

On the other hand, it has recently been suggested that where dairy operations are involved, the MPC for ^{131}I should be reduced by a factor of about 700 to 1.4×10^{-13} $\mu c/cm^3$ in order to compensate for reconcentration in milk.[72] The nearest area of actual or potential dairy farming in the direction of the prevailing winds is ~3.6 km southwest of the HFIR site. Thus use of Fig. I.A.14 in Appendix A, and the fact that the wind blows in this direction 12.5% of the time, yields an acceptable average discharge rate of 0.042 mc/min or 60 mc/day. On the same basis as before, this represents the ^{131}I production from about 0.06% of the core or ~5.5 g of ^{235}U. This can be compared to the allowable uranium contamination of the new fuel plates of 5 $\mu g/ft^2$ or a total of about 0.0022 g of uranium. There should also be little difficulty in meeting this requirement, although this may well depend upon the actual decontamination factors obtained by the containment system, particularly during operation following a meltdown. Should this occur, special equipment such as additional iodine traps would be incorporated into the system if necessary. The foregoing estimates are presented, not for the purpose of establishing criteria, but rather to give some idea of the scope of the problem and to demonstrate the ability of the containment system to handle it. Further study is under way, particularly with respect to the second case discussed above and its relationship to all ORNL facilities.

---

[71] *Background Material for the Development of Radiation Protection Standards,* Federal Radiation Council Staff Report No. 2 (September 1961).

[72] H. M. Roth to J. A. Swartout, letter, Mar. 25, 1964, citing information contained in *Health Phys.* 9(12) (December 1963).

Contaminated aqueous waste will be handled through the normal ORNL waste disposal system. It is combined with other wastes from the Laboratory and disposed of in a manner which will ensure that the concentration of radioactive material in the Clinch River is kept well below the maximum permissible.[69]

9. RELATIONSHIP OF HFIR TO OTHER FACILITIES

The HFIR is located within the ORNL complex in the southwest corner of the AEC reservation at Oak Ridge, Tennessee.[73] Among other Laboratory facilities located nearby are the Oak Ridge Research Reactor (ORR), the Low-Intensity Test Reactor (LITR), the Bulk Shielding Reactor (BSR), and the Pool Critical Facility (PCF), all of which are located at the main site of the Laboratory and are ~1.7 km northwest of the HFIR site. Other nearby facilities include the Molten-Salt Reactor Experiment (MSRE), ~0.49 km northwest, the Tower Shielding Facility (TSF), which is ~2.13 km south, the Health Physics Research Reactor (HPRR), ~1.73 km east-southeast, and the Experimental Gas-Cooled Reactor (EGCR),* which is ~3.26 km northeast. In addition to these, the Transuranium Processing Plant (TRU) is being constructed adjacent to and north of the HFIR; and the Nuclear Safety Pilot Plant (NSPP) is located ~0.61 km west-northwest of the HFIR site. The locations of these and other ORNL facilities are shown in Fig. I.9.1 and listed in Table I.6.1, together with the MCA doses.

It is clear from the discussion in Sect. 6 that it would be necessary to evacuate the HFIR and desirable to evacuate the nearby facilities** in the event that a major fission product release should occur at the site. This would include the TRU facility, the MSRE, and the NSPP. All these facilities as well as the HFIR can be shut down and evacuated on very short notice without any damage other than lost time being incurred.

Evacuation of the HPRR would probably be in order, but would not be necessary unless the wind were from the general direction of the northwest, which occurs only about 3% of the time. Evacuation of the TSF would also only be necessary if the wind were blowing toward this facility from the direction of the HFIR. As can be seen from Fig. I.6.1, the whole body gamma dose at the EGCR due to noble gases from the HFIR MCA would not exceed 10 rads for a 2-hr period and the iodine dose would not exceed 2.5 rems. Both of these would be considerably decreased if personnel at the EGCR site remained indoors during the incident. Since the wind speeds required to produce doses of this magnitude are quite small, the plume would require at least an hour to reach the EGCR site so that there is ample time for warning.

Evacuation of the HFIR site would normally be along the access road to Melton Valley Drive (see Fig. I.9.1) and then east or west along this road depending upon the wind direction. If at the time of the accident the wind were blowing from a southerly direction, it would be necessary to evacuate the site via an alternate route to the south.

---

[73]ORNL-3572, chap. 2.

*This project later abandoned for other reasons.

**Further discussed in answers 33 and 48.

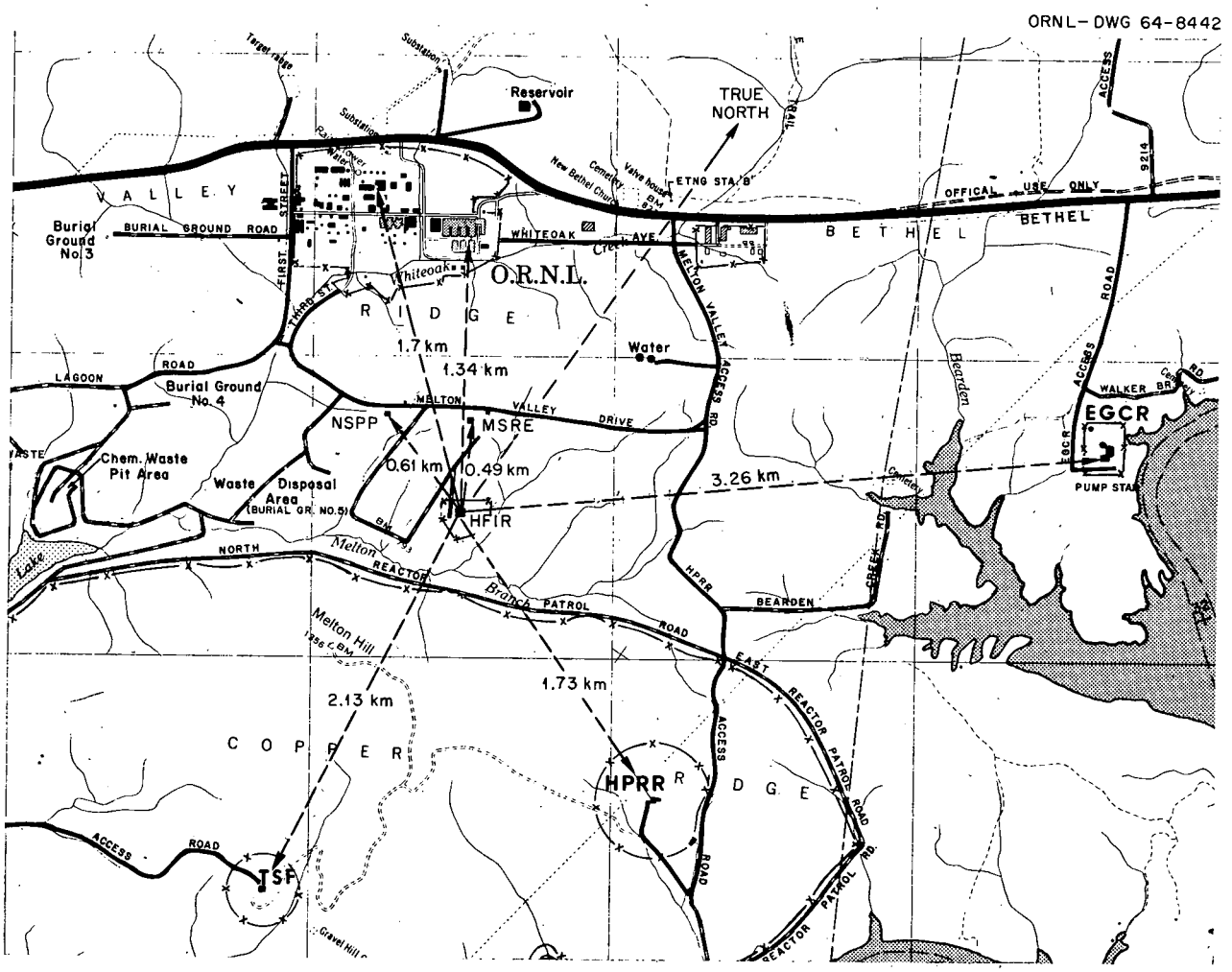

Fig. I.9.1. Location of ORNL Facilities with Respect to HFIR.

The only densely populated site which might require evacuation is the main ORNL complex, which is located 1.34 to 2.06 km northwest of the HFIR site. The doses which could be delivered at this location are of sufficient magnitude to make evacuation of the Laboratory necessary should the wind be from the southeast at the time of a major fission product release at the HFIR. The time required for the plume to arrive at the nearest populated portion of ORNL will, of course, depend upon the wind speed. Fortunately, the higher the wind speed, the lower will be the dose delivered. For the case of worst average conditions the plume will arrive at ORNL approximately 1 hr and 45 min after the release in the building, whereas for the case of most representative conditions the time required is only about 15 min; however, in the latter case, the dose is lower by a factor of nearly 3.

Unannounced practice evacuations have demonstrated that ORNL can be evacuated in about 10 min, and it is daily demonstrated that the ORNL parking lot can be evacuated in about 15 min. Any abnormal release of radioactive material from the HFIR will activate monitoring devices which transmit a signal

to the ORNL Emergency Control Center,[74] and evacuation of the Laboratory would be ordered from this point using emergency procedures already in existence.

9.1 Interrelationship with Other Facilities

The HFIR shares several utilities, namely 250-psi steam, 13.8-kv electrical power, and 70-psi potable water with other facilities. Loss of any or all of these utilities due to causes originating at other facilities will not result in the initiation of an accident at the HFIR. Loss of any of these would, if extended for any length of time, require that the reactor be shut down; however, there is sufficient time to permit this to be accomplished in an orderly fashion.

Loss of normal electrical power has been anticipated and provided for by means of the normal-emergency power system.[75] Such a loss would cause a setback in reactor power to 10 Mw if of short duration and would force a reactor shutdown if extended.

9.2 Effect of Accidents in Other Facilities

The effect on HFIR operation of accidents involving atmospheric contamination from the nearby facilities has not yet been fully assessed. Of these facilities, those in which accidents are most likely to result in contamination at the HFIR site are the EGCR, the MSRE, and the TRU facilities. While a serious accident at the MSRE or the TRU facility could conceivably damage steam lines leading to the HFIR, they are far enough from the HFIR building so that no other mechanical damage is likely. Under the worst conditions, accidents in these facilities could make an emergency shutdown and evacuation of the HFIR necessary. Such action will be provided for in the operation procedures and does not constitute a likely means of initiating an accident in the HFIR itself, which can be shut down by actuating a single switch, or which, in emergency, does not need to be attended at all.

10. SUMMARY AND CONCLUSIONS

The foregoing analysis makes clear that certain aspects of the HFIR operation present safety problems which, although they differ little in kind from those encountered in other operations, are perhaps somewhat more severe. These problems arise because of the very high power density required and because of the large quantity of fuel contained in a single fuel element.

The problems have been recognized by the designers and operators of the reactor, and every effort has been made to eliminate the possibility of an accident by appropriate design and by the establishment of sound operating procedures. Because the reactor cannot sustain large power excursions or serious coolant failure without the likelihood of some damage occurring, extreme measures have been taken in the design to prevent such occurrences. In fact, the HFIR can almost be said to have two three-channel

---

[74] ORNL-3572, sect. 8.7.1.

[75] ORNL-3572, sect. 10.1.

safety systems, because the automatic control system itself has many of the features normally found in a safety system.

The quality control procedures utilized to ensure that the reactor fuel satisfies the requirements of the specifications and the procedures which prescribe the method of handling are designed to guarantee against inadvertent criticality or failure of the fuel during operation. Fabrication and handling of the target are also rigidly controlled; and, where necessary, pilot experiments will be performed in order to obtain information concerning various parameters related to safety.

Nevertheless, the possibility of a major accident must be admitted, and it has been shown that such accidents can be satisfactorily contained by the HFIR containment system. Because of the fact that most of the potential causes for accidents have been recognized and preventive measures taken, it is not considered that an accident to the HFIR is more likely than is the case at any of the other ORNL reactors. The HFIR has been designed specifically to contain a considerable core failure without serious disruption of operations.

The general conclusion which can be drawn is that, while there are a number of potential causes for accidents to the HFIR, these have been recognized and eliminated by design and operating procedures; that the containment of the HFIR is superior to that of other research reactors at ORNL; that even in the event of a major accident the consequences are not particularly serious from an environmental point of view; and that the reactor can be operated in a safe and orderly fashion.

APPENDIX A

CONSEQUENCES OF THE RELEASE TO THE ATMOSPHERE OF FISSION PRODUCTS FROM THE HIGH FLUX ISOTOPE REACTOR

1. Introduction

This analysis is designed to furnish basic information concerning the magnitude of the downwind radiation doses to be expected as a consequence of the emission of radioactive effluent from the 250-ft HFIR stack following a release of fission products within the HFIR building. Although the primary purpose is to obtain information concerning the HFIR, the analysis is developed in such a way that it may be readily applied to other ORNL facilities.

Two general cases are considered: the "most representative conditions," in which average meteorological conditions are assumed to persist throughout the incident, and "worst average conditions," in which very pessimistic meteorological conditions obtain. A precise definition of these terms is deferred until later and may be found on p. 46.

While chiefly concerned with accident situations in which the release takes place over a relatively short time, the analysis has been extended to cover the case of uniform emission over extended periods of time.

All the calculations have been performed on a unit basis; that is, per fission product equivalent of unit power after 15 days operation for the accident situations, or per curie emitted per unit time for the case of uniform emission. Unless otherwise stated, no credit is taken for the effect of filters or other modes of decontamination following release in the building. The effects of the various decontamination mechanisms may, in most cases, be accounted for quite apart from the methods herein described. To permit this, the fission products have been divided into groups, the members of which behave in a similar manner with respect to decontamination.

Every attempt has been made to assure conservative results. For the most part, the doses are computed under the assumption that the receptor remains directly downwind of the point of emission for the entire duration of the incident rather than for the 2-hr period suggested in 10 CFR Part 100. As a practical matter, there is little difference between the 2-hr dose and the infinite dose for the points of greatest interest unless the emission rate is quite low. In those cases where there is a significant difference, both results have been obtained.

The computations have been programmed for machine calculation, and the results, presented in the form of graphs, may be used in conjunction with known decontamination factors to estimate the consequences of accidents as well as the results of various operating conditions.

2. Atmospheric Concentrations Downwind Due to Accidental Releases

The downwind atmosphere concentrations resulting from emission from a stack are obtained through the use of the "Gaussian plume formula" in the form proposed by Gifford,[1] but with appropriate modifications of the source term to account for the effects of dilution within the building prior to emission, and also for decay both before and after emission from the stack. The basic equation for the activity concentration χ at a point x meters downwind, y meters crosswind, and at an elevation z meters with respect to a source of constant strength Q curies/min is

$$\chi(x, y, z, u) = \frac{Q}{2\pi u \sigma_y \sigma_z} \exp\left(-\frac{y^2}{2\sigma_y^2} - \frac{z^2}{2\sigma_z^2}\right), \tag{1}$$

where χ (x, y, z, u) is expressed in curies/m^3 if u is the average wind speed in meters per minute and σ_y, σ_z are the horizontal and vertical dispersion parameters, respectively, expressed in meters. These dispersion parameters are functions of x, the distance downwind, and also depend upon the prevailing atmospheric stability conditions. Their values for various stability conditions are given in graphic form in Figs. I.A.1 and I.A.2.

The source term Q in Eq. (1) is constant. Consider, however, the case where a quantity q (curies) of a radioisotope having decay constant λ (min^{-1}) is released into a building of volume V (m^3). Let α (min^{-1}) be the (constant) fraction of the building volume which is passed up the stack each minute, with this loss of air being constantly replaced by inleakage. Then, if mixing is assumed to be uniform

[1] F. A. Gifford, Jr., *Nucl. Safety* **1**, 3 (March 1960); **2**, 2 (December 1960); **2**, 4 (June 1961).

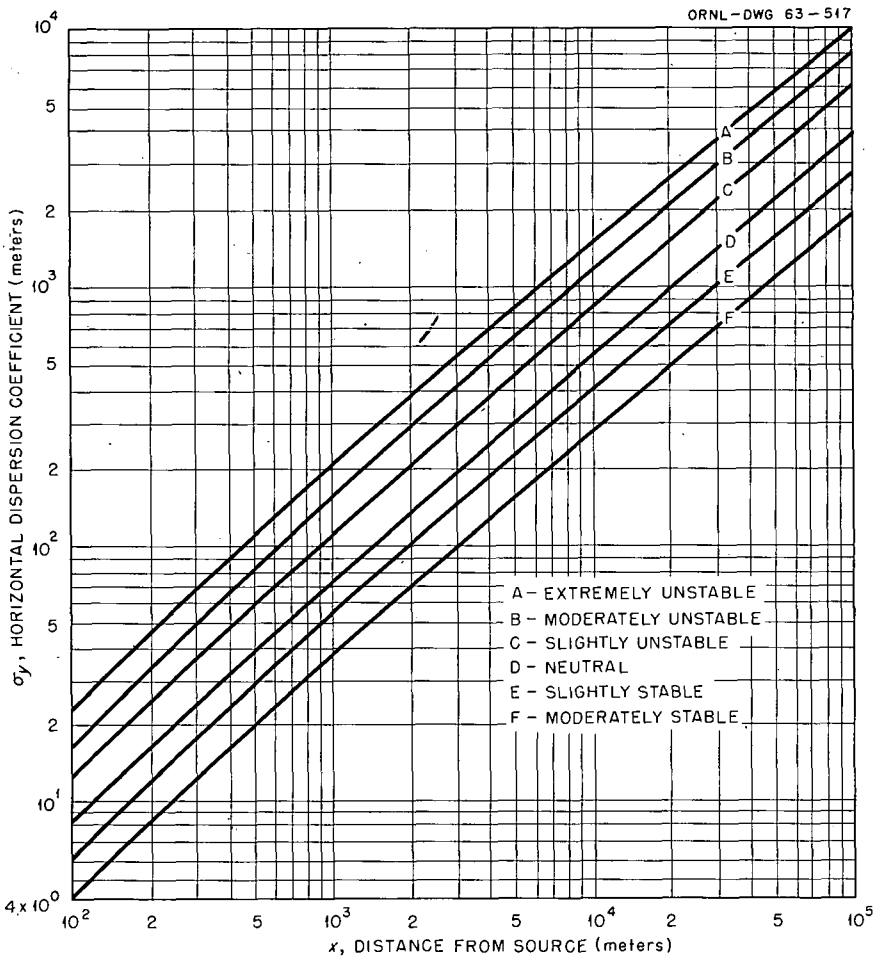

Fig. I.A.1. Horizontal Dispersion Parameters.

and instantaneous, the initial concentration $\zeta(0)$ (curies/m^3) of the radioisotope in the building at time $t = 0$ (min) will be $\zeta(0) = q/V$; and the rate of change of concentration is given by

$$\dot{\zeta}(t) = -(\lambda + \alpha)\,\zeta(t) .$$

Whence, at time t, the concentration in the building is simply

$$\zeta(t) = \frac{q}{V}\,e^{-(\lambda+\alpha)t} .$$

Since a volume αV of this mixture is being emitted from the stack each minute, the emission rate from the stack, denoted by $\epsilon(t)$, is[2]

$$\epsilon(t) = \alpha V\,\zeta(t) = \alpha q e^{-(\lambda+\alpha)t} . \qquad (2)$$

[2]Despite the physical situation used to derive the emission equation, it also holds for other situations, that is, if α is the fractional rate of outgassing from the primary coolant system.

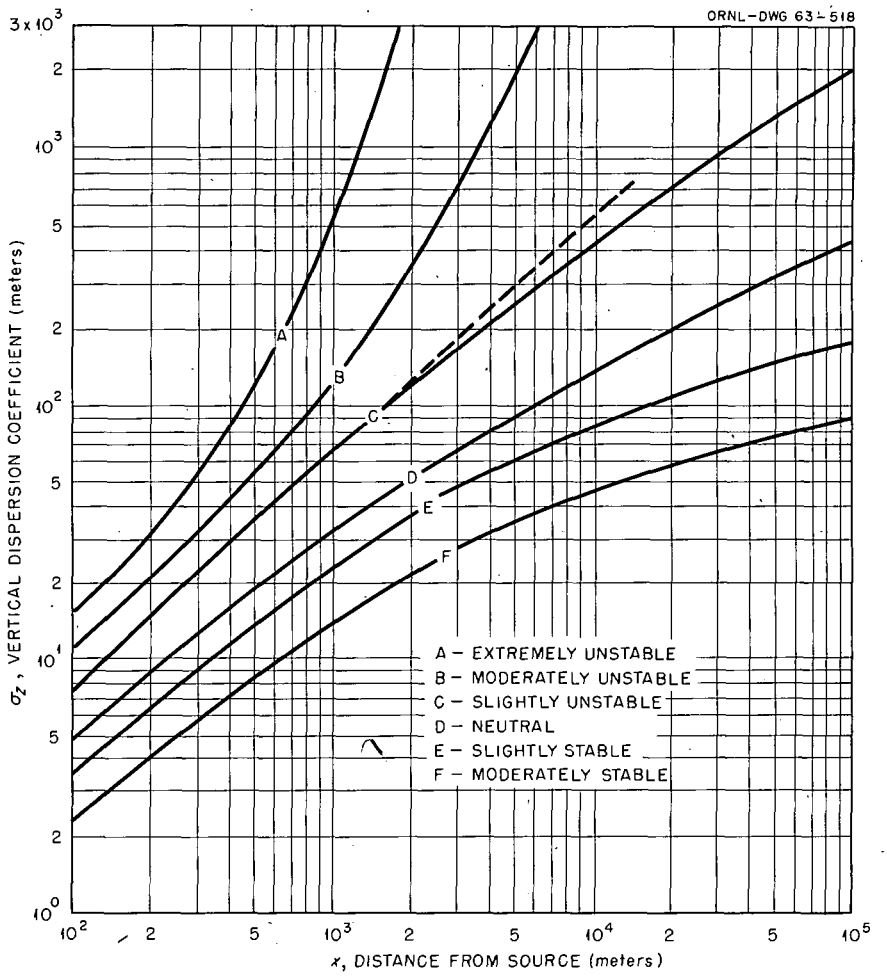

Fig. I.A.2. Vertical Dispersion Parameters.

If decay during passage downwind is neglected, this becomes the source term for Eq. (1). To include the effects of decay during the time required for the activity to travel a distance x at a speed u, it is necessary to multiply the emission rate by the factor $e^{-\lambda x/u}$. Thus, the effective source term associated with the concentration at the point (x, y, z) becomes

$$Q = Q(t, x) = \alpha q \exp\left[-(\lambda x/u) - (\lambda + \alpha)t\right] .$$

It is convenient to set $t + x/u = \tau$, so that

$$Q(\tau, x) = \alpha q \exp\left[(\alpha x/u) - (\lambda + \alpha)\tau\right] . \tag{3}$$

Then $Q(\tau, x)$ is the effective source term corresponding to the point (x, y, z) at a time τ after the initial fission product release in the building. Because for values of τ less than x/u the emitted activity has not yet arrived a distance x downwind, it is clear that $Q(x, \tau) = 0$ when $\tau < x/u$. Upon substituting Eq. (3) into Eq. (1), the concentration at the point (x, y, z, τ) is found to be

$$\chi(x, y, z, \tau, u) = \frac{\alpha q}{2\pi u \sigma_y \sigma_z} \exp\left[\frac{\alpha x}{u} - (\lambda + \alpha)\tau - \frac{y^2}{2\sigma_y^2} - \frac{z^2}{2\sigma_z^2}\right], \qquad \tau > x/u . \tag{4}$$

The concentration χ is expressed in curies per cubic meter, and it is worth noting that these units are numerically equal to those of concentration expressed in microcuries per cubic centimeter. For convenience, the dimensions of the other parameters are listed in Table I.A.1. These units will be used throughout unless otherwise indicated.

Table I.A.1. Dimensions of the Parameters Which Appear in the Concentration Equation

$[\alpha] = \text{min}^{-1}$	$[u] = \text{meters/min}$	$[x],[y],[z] = \text{meters}$
$[q] = \text{curies}$	$[\sigma_y],[\sigma_z] = \text{meters}$	$[\lambda] = \text{min}^{-1}$
$[\tau] = \text{min}$	$[\chi(x, y, z, u, \tau)] = \text{curies/m}^3 \text{ or } \mu\text{c/cm}^3$	

Let h be the stack height in meters. Then at ground level the value of z in Eq. (4) becomes $z = -h$. To account for reflection of the plume at ground level, the factor 2 is dropped from the denominator. Moreover, since the highest concentrations obviously occur directly downwind, the crosswind distance y is set equal to zero. The concentration equation therefore becomes

$$\chi(x, h, u, \tau) = \frac{\alpha q e^{-h^2/2\sigma_z^2}}{\pi u \sigma_y \sigma_z} \cdot e^{\alpha x/u} \cdot e^{-(\lambda+\alpha)\tau} \, \mu\text{c/cm}^3 , \tag{5}$$

and this holds for $\tau > x/u$. The factor

$$\frac{e^{-h^2/2\sigma_z^2}}{\pi u \sigma_y \sigma_z}$$

represents the effect of atmospheric dilution following emission from the stack. It will hereafter be referred to as the "stack factor" and be designated by

$$S(x, u) \equiv \frac{e^{-h^2/2\sigma_z^2}}{\pi u \sigma_y \sigma_z} . \tag{6}$$

Now the stack height, h, is not fixed but is a function of the exit velocity, the stack orifice diameter, the wind speed, and the rate at which heat is being added to the effluent. There is little agreement among meteorologists concerning the best method of estimating the effective stack height; however, Holland[3] has proposed a relation which appears to agree with observation in the Oak Ridge area:

$$h = h_0 + \frac{1.5\, vd + 3 \times 10^{-4} s}{u} ,$$

where u, the wind speed, and v, the exit velocity, are expressed in miles per hour; d, the orifice diameter, is in feet; s is the heat input in calories per second; and h, h_0 are, respectively, the effective and actual stack heights given in feet. For the present purpose, the heat input is neglected and the effective stack height taken to be

$$h = h(u) = h_0 + \frac{1.5\, vd}{u} , \tag{7}$$

[3] *Meterology and Atomic Energy*, AECU-3066, p. 72, USAEC Publication (1955).

with h and h_0 both expressed in meters, provided that d is given in meters and v and u are expressed in the same units. The values of these parameters for the HFIR stack are

$$h_0 = 76.2 \text{ m}; \; v = 465 \text{ m/min}; \; d = 1.524 \text{ m};$$

so that

$$h(u) = 76.2 + \frac{1063}{u} \text{ meters}$$

for the HFIR.

2.1 Concentration of Daughter Products

Equations (4) and (5) have been derived under the tacit assumption that the radioisotope under consideration decays to a product which is of no interest. This is not always true.

Let q_p^0 be the number of curies of a parent isotope originally released in the building. Then, if λ_p is the decay constant of the parent, the total number of curies of the parent which remain at time τ is

$$q_p(\tau) = q_p^0 e^{-\lambda_p \tau}$$

and the total number of curies $q_d(\tau)$ of the daughter isotope which have resulted from decay of the parent will, at time τ, be

$$q_d(\tau) = \frac{\lambda_d q_p^0}{\lambda_d - \lambda_p} \left(e^{-\lambda_p \tau} - e^{-\lambda_d \tau}\right),$$

where, here, λ_d is the decay constant of the daughter.

If the emission process is assumed to involve no physical separation of the two species, then the ratio $q_d(\tau)/q_p(\tau)$ will, for any given value of τ, be everywhere the same, in particular at the point $(x, 0, -h)$ downwind. Consequently, the ground-level concentration of the daughter can be written

$$\chi_d(x, u, \tau) = \alpha q_p^0 \, S(x, u) \cdot \frac{\lambda_d}{\lambda_d - \lambda_p} e^{\alpha x/u} \left[e^{-(\lambda_p + \alpha)\tau} - e^{-(\lambda_d + \alpha)\tau}\right]. \tag{8}$$

Now in many cases, notably the noble gases, the parent is volatile while the daughter is a solid. Thus, if the stack is equipped with some decontamination mechanism, such as a filter or a charcoal absorber, the parent may be stripped of the daughter isotope which was formed by decay following release into the building but prior to emission from the stack. If the removal is complete, the amount by which the concentration of the daughter at a point $(x, 0, -h)$ is reduced is given by

$$\Delta\chi_d(x, u, t) = \alpha q_p^0 \, S(x, u) \, e^{-(\lambda_p + \alpha)t} \cdot \frac{\lambda_d}{\lambda_d - \lambda_p} \left[1 - e^{-(\lambda_d - \lambda_p)t}\right] e^{-\lambda_d x/u},$$

where t, it will be recalled, is the time between initial release and emission. Upon utilizing the relation

$\tau = t + x/u$ and subtracting this increment from Eq. (8), the corrected daughter concentration is found to be

$$\chi_d'(x, u, t) = \alpha q_p^0 S(x, u) \frac{\lambda_d e^{\alpha x/u}}{\lambda_d - \lambda_p} \left[1 - e^{-(\lambda_d - \lambda_p)x/u}\right] e^{-(\lambda_p + \alpha)\tau} . \tag{9}$$

In some cases (the iodines) the parent is effectively removed by the filter system; but the daughter is volatile and is, therefore, emitted from the filter at approximately the same rate at which it is formed. The downwind concentration due to such a reemitted daughter is estimated under the assumptions (1) that all of the parent is trapped on the filter, and (2) that the daughter is emitted as fast as it is formed.

The rate at which the parent is being deposited in the filter is numerically equal to the emission rate given in Eq. (2), and the rate at which it is being lost is just its decay rate. Hence

$$\dot{q}_p(t) = \alpha q_p^0 e^{-(\lambda_p + \alpha)t} - \lambda_p q_p(t) , \qquad q_p(0) = 0 ,$$

so that at a time t after the initial release, the filter contains

$$q_p(t) = q_p^0 e^{-\lambda_p t} (1 - e^{-\alpha t}) \text{ curies}$$

of the parent. Thus it is, under assumption (2), emitting $2.22 \times 10^{12}\ q_p(t)$ atoms or $q_p(t)\lambda_d$ curies of daughter isotope per minute. This decays by an amount $e^{-\lambda_d x/u}$ during its passage downwind. Hence, again letting $\tau = t + x/u$, the appropriate source term for the Gaussian plume formula becomes

$$Q(x, \tau) = q_p^0 \lambda_d e^{-(\lambda_d - \lambda_p)x/u} \left[e^{-\lambda_p \tau} - e^{-(\lambda_p + \alpha)\tau} \cdot e^{\alpha x/u}\right] ,$$

so that the concentration at the point $(x, 0, -h)$ due to the emission of the daughter from the filter becomes

$$\chi_d''(x, u, \tau) = q_p^0 \lambda_d S(x, u) e^{-(\lambda_d - \lambda_p)x/u} \left[e^{-\lambda_p \tau} - e^{-(\lambda_p + \alpha)\tau} \cdot e^{\alpha x/u}\right]. \tag{10}$$

Of some interest in connection with Eq. (10) is the case in which α is very large; that is the case in which the parent is entirely deposited on the filter almost immediately after the release. Since $\tau > x/u$, Eq. (10) simplifies under this condition to

$$\chi_d''(x, u, \tau) \cong q_p^0 \lambda_d S(x, u) e^{-\lambda_d x/u} \cdot e^{-\lambda_p(\tau - x/u)} . \tag{10'}$$

For convenience, the four equations for the ground-level concentration directly downwind are repeated below:

$$\chi_p(x, u, \tau) = \frac{\alpha q_p^0}{\pi u \sigma_y \sigma_z} e^{-h^2(u)/2\sigma_z^2} \cdot e^{\alpha x/u} \cdot e^{-(\lambda_p + \alpha)\tau} \tag{11}$$

for the case of the parent,

$$\chi_d(x, u, \tau) = \frac{\alpha q_p^0 e^{-h^2(u)/2\sigma_z^2}}{\pi u \sigma_y \sigma_z} \cdot \frac{\lambda_d e^{\alpha x/u}}{\lambda_d - \lambda_p} \cdot \left[e^{-(\lambda_p + \alpha)\tau} - e^{-(\lambda_d + \alpha)\tau}\right] \tag{12}$$

for the case of the unseparated daughter,

$$\chi_d'(x, u, \tau) = \frac{\alpha q_p^0 e^{-h^2(u)/2\sigma_z^2}}{\pi u \sigma_y \sigma_z} \cdot \frac{\lambda_d e^{\alpha x/u}}{\lambda_d - \lambda_p} \left[1 - e^{-(\lambda_d - \lambda_p)x/u}\right] e^{-(\lambda_p + \alpha)\tau} \tag{13}$$

for the case of a daughter which is removed prior to emission, and

$$\chi_d''(x, u, \tau) = \frac{q_p^0 e^{-h^2(u)/2\sigma_z^2}}{\pi u \sigma_y \sigma_z} \cdot \lambda_d e^{-(\lambda_d - \lambda_p)x/u} \left[e^{-\lambda_p \tau} - e^{-(\lambda_p + \alpha)\tau} \cdot e^{\alpha x/u}\right] \tag{14}$$

for the case of the volatile daughter of a parent which is removed prior to emission. In each case, $h(u)$ is given by Eq. (7).

3. Ground-Level Doses

The ground-level dose rates may be computed from the ground-level concentrations if it is assumed that they are proportional to these concentrations. This is a valid assumption for the case of the internal doses received as a result of inhalation of contaminated air and is approximately true in the region of interest for external doses received as a result of submersion in the contaminated cloud. The derivation of the appropriate constants of proportionality will be considered in this section.

As a practical matter, there are three groups of fission products which are usually controlling in determining the total dose received and these will be given most attention. They are the iodines, which affect primarily the thyroid gland; a group of mixed fission products, mainly bone seekers, which also contribute to the internal dose; and the noble gases, which are the chief contributors to the external dose.

3.1 Calculation of Internal Doses

The internal dose rate for a single fission product may be computed directly from a knowledge of the ground-level concentration at the point under consideration, the rate of inhalation of the contaminated air, and the dose delivered per unit of radioactive material inhaled. Thus, if β is the rate of inhalation, or breathing rate, in cubic centimeters per minute, and κ is the dose delivered in rems per inhaled microcurie, then the rate at which the internal dose D_{int} (rems) is being received is[4]

$$\frac{dD_{\text{int}}}{d\tau} = \beta\kappa\, \chi(\tau) \text{ rems/min.} \tag{15}$$

The dose per inhaled microcurie is usually related to some critical organ; and, in general, there will be more than one radioisotope which affects that organ. Therefore, the total dose rate to a given organ will be a sum of terms similar to the right-hand side of Eq. (15). For example, if there are N fission products present for which the bone is the critical organ, the total dose rate to the bone will be

[4]Note that κ is not an instantaneous dose per microcurie, but represents the total dose which will be delivered by the inhaled activity during its entire residence in the body. Hence $dD_{\text{int}}/d\tau$ really represents the rate at which the "eventual" dose is being delivered.

$$\frac{dD_{\text{int}}}{d\tau} = \beta \sum_{j=1}^{N} \kappa_j \chi_j(\tau) \text{ rems/min} ; \tag{16}$$

The appropriate form of each of the χ_j's may be selected from Eqs. (11–14), depending upon the particular circumstances under consideration.

The total internal dose delivered by the N isotopes at the point $(x, 0, -h)$ in a time t following the initial release is obtained by integrating Eq. (16) with respect to τ between x/u and $t > x/u$. Thus

$$D_{\text{int}}(t) = \beta \sum_{j=1}^{N} \kappa_j \int_{x/u}^{t} \chi_j(\tau)\, d\tau \text{ rems} \tag{17}$$

is the expression for the internal dose.

3.2 Calculation of External Doses

The external doses are estimated utilizing the assumption that for distances sufficiently far from the stack the energy release from the contaminated cloud is adiabatic; that is, exactly as much energy is absorbed in each unit volume of the cloud as is released there. This gives conservative (high) results at distances sufficiently far from the stack so that the concentration gradient is small, but gives results which are lower than the actual value within a few hundred meters of the stack, because it neglects the direct radiation contribution from the high concentration on the axis of the plume near the stack.

Let E^{γ} be the gamma energy (Mev) emitted per disintegration from a given radioisotope. Then, if the concentration at the point $(x, 0, -h)$ and at the time τ is $\chi(x, \tau)$ $\mu c/cm^3$, the gamma energy emission density at that point will be $3.7 \times 10^4\ E^{\gamma}\ \chi(x, \tau)$ Mev cm^{-3} sec^{-1}. Under the foregoing assumption, this is also the rate at which energy is being absorbed at that point. If the density of air is taken to be 1.25×10^{-3} g/cm^3, and it is recalled that 1 Mev is equivalent to 1.6021×10^{-6} erg, the energy absorption rate becomes

$$3.7 \times 10^4\ E^{\gamma}\ \chi(x, \tau) \times 1.6021 \times 10^{-6}/1.25 \times 10^{-3} = 47.42\ E^{\gamma}\ \chi(x, \tau)\ ,$$

or, since by definition the absorption of 100 ergs/g is equal to 1 rad, and there are 60 sec/min, the external gamma dose rate becomes

$$\frac{dD^{\gamma}_{\text{ext}}}{d\tau} = 28.4\ E^{\gamma}\ \chi(x, \tau) \text{ rads/min} .$$

A similar expression involving the average beta energy, E^{β}, emitted per disintegration may be written for the external beta dose rate.

As in the case of the internal doses, it is usually necessary to consider a sum of several terms each representing the contribution of a single isotope. Consequently, the external dose rates become

$$\frac{dD^{\gamma}_{\text{ext}}}{d\tau} = 28.4 \sum_{j=1}^{N} E_j^{\gamma}\ \chi_j(\tau) \text{ rads/min} \tag{18}$$

and

$$\frac{dD^{\beta}}{d\tau} = 28.4 \sum_{j=1}^{N} E_j^{\beta} \chi_j(\tau) \text{ rads/min} , \tag{19}$$

with the appropriate forms for the $\chi_j(\tau)$ being chosen from Eqs. (11–14).

The external doses which have been delivered at a time t following the initial fission product release in the building are, as before, obtained by integrating between x/u and t. Thus

$$D_{\text{ext}}^{\gamma}(t) = 28.4 \sum_{j=1}^{N} E_j^{\gamma} \int_{x/u}^{t} \chi_j(\tau)\, d\tau \text{ rads} , \tag{20}$$

and

$$D_{\text{ext}}^{\beta}(t) = 28.4 \sum_{j=1}^{N} E_j^{\beta} \int_{x/u}^{t} \chi_j(\tau)\, d\tau \text{ rads} . \tag{21}$$

The procedure outlined above is satisfactory provided the number of individual fission products is small. However, when N is large, in particular when N includes the entire fission product spectrum, the use of Eqs. (20) and (21) would require that the explicit equations for the growth and decay of the fission products be written down. This can be avoided, and an upper bound to the external dose can be obtained by using data published by Perkins and King[5] which give the total energy release from the fission products of ^{235}U as a function of both irradiation and decay time.

The Perkins and King data, which are given in terms of Mev per second per watt of reactor power, may be converted for use with the foregoing equations as follows.

In general, the expression for the external dose rate has the form

$$\frac{dD_{\text{ext}}}{d\tau} = 28.4\, S(x, u)\, \alpha e^{\alpha x/u} \sum_{j=1}^{N} E_j b_j e^{-(\lambda_j + \alpha)\tau} ,$$

where the b_j are constants having curies as their units and which depend upon the quantity of each fission product initially present per kilowatt of reactor power and upon their individual decay schemes. The total dose delivered cannot exceed that obtained by integrating between x/u and ∞. Hence

$$D_{\text{ext}} \leq 28.4\, S(x, u) \sum_{j=1}^{N} \frac{\alpha}{\lambda_j + \alpha} E_j b_j e^{-\lambda_j x/u} .$$

The factor $\alpha/(\lambda_j + \alpha)$ is always less than 1; and, since α represents the fractional rate of emission of the released fission products from the building, a large value of α signifies that there has been little time for decay in the building, so that the decay time is essentially x/u. Therefore

$$D_{\text{ext}} < 28.4\, S(x, u) \sum_{j=1}^{N} E_j b_j e^{-\lambda_j x/u} \tag{22}$$

---

[5] J. F. Perkins and R. W. King, *Nucl. Sci. Eng.* **3**, pp. 726–46 (1958).

and the total rate of energy release is $3.7 \times 10^{10} \sum_{j=1}^{N} E_j b_j e^{-\lambda_j x/u}$ Mev/kwsec. Let $p(x/u)$ be the fission power in Mev per watt-second following operation at 1 w and at a time x/u following shutdown. The values of p have been plotted by Perkins and King[5] as a function of shutdown time for various operating times. Then clearly

$$3.7 \times 10^{10} \sum_{j=1}^{N} E_j b_j e^{-\lambda_j x/u} = 10^3 \, p(x/u) \, ,$$

whence

$$\sum_{j=1}^{N} E_j b_j e^{-\lambda_j x/u} = 2.703 \times 10^{-8} \, p(x/u)$$

and

$$D_{\text{ext}} < \frac{7.676 \times 10^{-7} \, p(x/u) \, e^{-h^2(u)/2\sigma_z^2}}{\pi u \sigma_y \sigma_z} \, . \tag{23}$$

The values of p are given for both gamma and beta energies in the reference cited.

4. Numerical Results for the Accident Cases

As a practical matter, there are only a relatively few of the fission products which contribute significantly to the consequences of a reactor accident; and it will be convenient to consider these fission products in groups according to their characteristics with respect to the likelihood of release, ease of decontamination, and type of dose delivered.

Also of interest are the effects of the magnitudes of certain parameters which enter into the dose equations. These include the exhaust rate α, the wind speed u, the atmospheric stability condition, and the time of exposure. An extensive parameter study has not been attempted; however, the effect of variation of some of the parameters has been examined in those cases where it is relevant to the HFIR situation.

In order to obtain a fair estimate of the consequences of a reactor accident, two different sets of assumptions have been employed regarding the meteorological conditions which prevail at the time of the accident. In the first of these, it is assumed that the most frequently occurring stability condition, namely a slightly unstable or "C" condition, persists throughout the incident, and that the average wind speed is 100 m/min (~4 mph). These are called the "most representative conditions."

The second set of assumptions represents extremely pessimistic meteorological conditions. It can be seen from the dose equations that for any given stability condition, there exists, for each value of x, a value of the wind speed u which maximizes the dose at that point. These maximum values of the dose have been computed and plotted as a function of x for each of the stability conditions.[6] The envelope of these curves then represents the dose received at each point under the assumption that these maximizing

[6]Since the "A" (extremely unstable) condition is unknown in the Oak Ridge area, it has been omitted.

conditions exist at each point throughout the incident. These are called the "worst average conditions." It should be noted that the curve obtained under these conditions does not represent a series of simultaneous doses; for, if the worst average conditions exist at $x = 2$ km, for example, then they obviously do not exist simultaneously at $x = 4$ km.

4.1 Internal Doses

The internal doses have been computed for fast exhaust rates and infinite exposure. Because the isotopes involved are effectively removed from the effluent air by the filters, these results, when applied to the actual accident case, will be sufficiently low so that it is unnecessary to estimate the lower and more realistic values which would be found using slower exhaust rates and finite exposure times.

4.1.1 Internal Doses Due to Iodines. – There are five fission product iodines which are significant contributors to the internal dose. Because, in each case, the critical organ is the thyroid, the expression for the total iodine dose will be the sum of five terms. None of the daughters of iodine are significant contributors to the internal dose; therefore, the appropriate form of the expression for concentration is that given in Eq. (11) and the expression for the total internal iodine dose delivered in time t is from (16)

$$D_{\text{int}}(x, t) = \frac{\alpha\beta e^{-h^2(u)/2\sigma_z^2}}{\pi u \sigma_y \sigma_z} \sum_{j=1}^{5} q_j \kappa_j \left[\frac{e^{-\lambda_j x/u} - e^{-\lambda_j t} \cdot e^{-\alpha(t-x/u)}}{\lambda_j + \alpha} \right] \text{rems/kw} . \tag{24}$$

The value of β, the breathing rate, is taken to be that of "standard man" during a working day – 2.08×10^4 cm^3/min (ref. 7). The parameters associated with 1 kw equivalent of fission iodine are listed in Table I.A.2.

It is worth noting that as $t \to \infty$ and if $\alpha >> \lambda_j$, then Eq. (24) takes the simpler form

$$D_{\text{int}} \leq \frac{\beta e^{-h^2(u)/2\sigma_z^2}}{\pi u \sigma_y \sigma_z} \sum_{j=1}^{5} q_j \kappa_j e^{-\lambda_j x/u} . \tag{25}$$

Table I.A.2. Parameters Used for Iodine Dose Calculations

Isotope	Half-Life	λ_j (min^{-1})	j (rems/μc)[a]	q_j (curies/kw)
^{131}I	8.05 days	5.98×10^{-5}	1.484	16.20
^{132}I	2.4 hr	4.81×10^{-3}	0.054	37.11
^{133}I	20.8 hr	5.55×10^{-4}	0.399	54.83
^{134}I	52.5 min	1.32×10^{-2}	0.025	64.11
^{135}I	6.68 hr	1.73×10^{-3}	0.123	49.77

[a]Data from Burnett (ref. 8).

[7]*Report of Committee II on Permissible Dose for Internal Radiation*, Pergamon, New York, 1959.

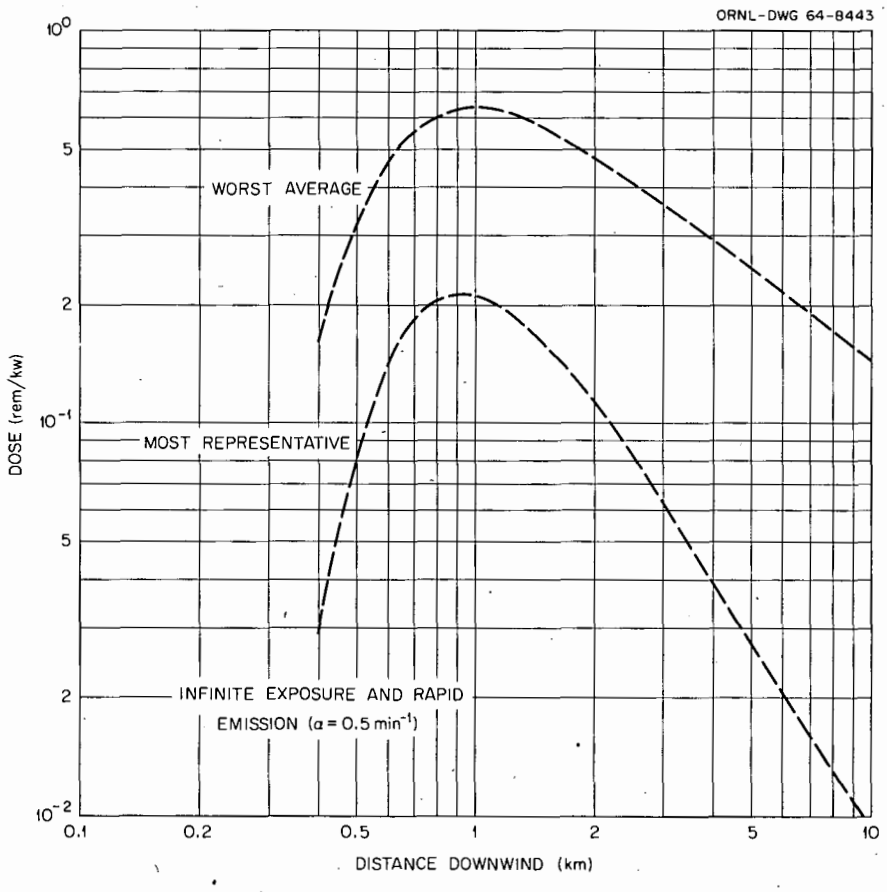

Fig. I.A.3. Internal Dose Due to Iodines – Infinite Exposure and Rapid Emission.

Because the internal dose is not particularly significant in the case of an accident to the HFIR, the iodine dose has been evaluated in the form of Eq. (25). The results are given in Fig. I.A.3 for both the most representative and the worst average cases. Somewhat lower results are obtained if the more accurate equation is used.

4.1.2 Internal Doses Due to Other Fission Products. – Other than the iodines, there are 26 fission products and fission product pairs which are listed by Burnett[8] as being controlling with respect to the inhalation dose. Of these, seven are either so short lived or present in such small quantities that they may be neglected with respect to the others. The fission products considered, together with the appropriate parameters, are listed in Table I.A.3.

The contribution of the daughters of these fission products has been taken into consideration by adjusting the values of κ_j. Consequently, the appropriate equations for the doses are, except for the number

[8]T. H. J. Burnett, *Nucl. Sci. Eng.* **2**, p. 382 (May 1957).

Table I.A.3. Parameters Used to Compute Internal Dose Due to Fission Products Other than Iodine

Isotope	λ_j (min^{-1})	κ_j (rems/μc)	q_j (curies/kw)
	Bone Seekers[a]		
^{89}Sr	8.88×10^{-6}	0.416	6.94
^{90}Sr-^{90}Y	4.71×10^{-8}	44.3	0.05
^{91}Y	8.28×10^{-6}	0.337	8.16
^{95}Zr	7.62×10^{-6}	0.062	8.21
^{97}Zr-^{97}Nb	6.78×10^{-4}	0.004	52.30
^{95}Nb	1.37×10^{-5}	0.012	13.87
^{140}Ba-^{140}La	3.76×10^{-5}	0.090	30.95
^{141}Ce	1.51×10^{-5}	0.019	14.04
^{143}Pr	3.51×10^{-5}	0.023	27.79
^{144}Ce-^{144}Pr	1.66×10^{-6}	1.200	1.78
^{147}Nd	4.26×10^{-5}	0.189	13.21
	Others[b]		
^{103}Ru-^{103m}Rh	1.18×10^{-5}	0.007	5.49
^{105}Rh	3.16×10^{-3}	0.0014	7.59
^{106}Ru-^{106}Rh	1.32×10^{-6}	0.065	0.09
^{127m}Te-^{127}Te	5.30×10^{-6}	0.018	0.23
^{129m}Te-^{129}Te	1.46×10^{-5}	0.046	2.27
^{131m}Te-^{131}Te	3.85×10^{-3}	0.0077	22.46
^{132}Te	1.50×10^{-4}	0.0015	35.65
^{137}Cs-^{137}Ba	4.96×10^{-8}	0.0086	0.05

[a] κ_j values computed by H. Heacker.

[b] κ_j values computed by T. H. J. Burnett.

of terms, identical to Eq. (24). Again, the simplified form – Eq. (25) – is used. The results are given in Figs. I.A.4 and I.A.5.

4.2 External or Submersion Dose

The external dose from an accident in the HFIR is due almost entirely to the noble gases. This is because the HFIR ventilation system, which is designed to remove the halogens and nonvolatile fission products from the effluent air, is incapable of removing the noble gases. Moreover, they are known to be released quite readily from leaking or molten fuel. For this reason they will be considered in some detail.

It is convenient to divide the noble gas doses into three categories according to their origin. These are: (1) the dose due to the direct emission of the noble gases present at the time of the accident; (2)

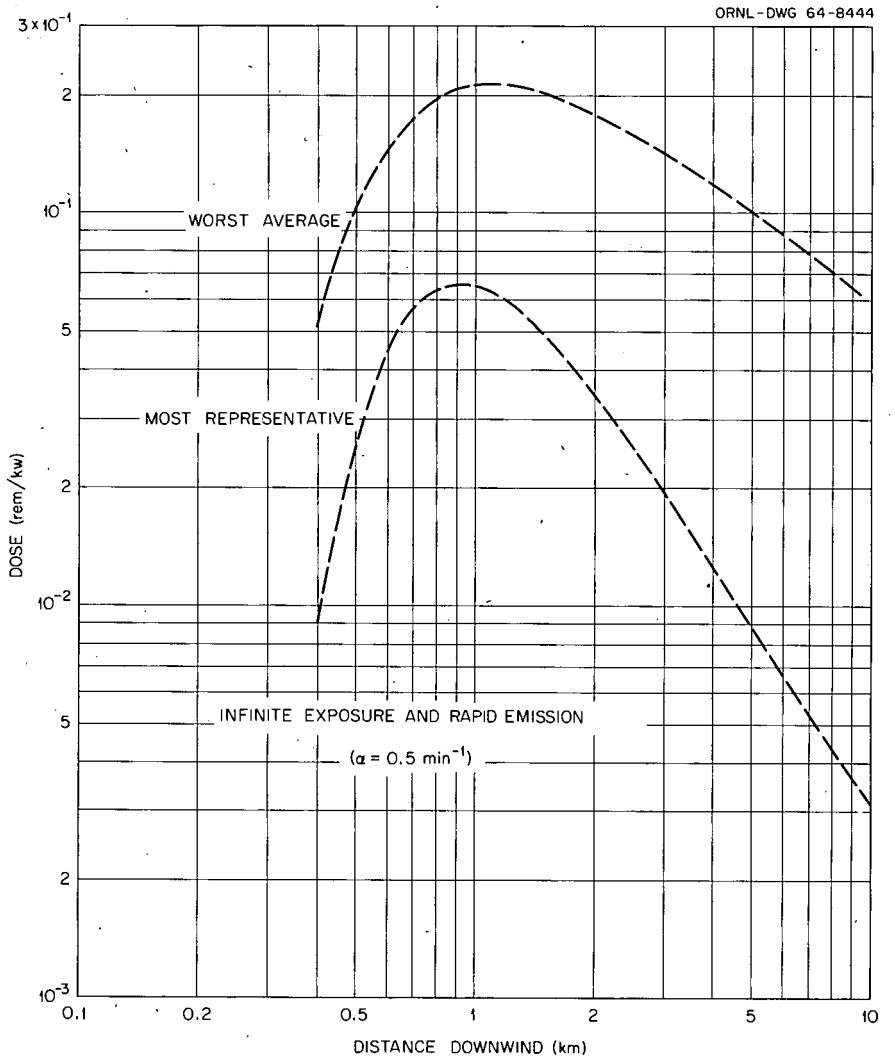

Fig. I.A.4. Internal Dose Due to Bone Seekers – Infinite Exposure and Rapid Emission.

the dose due to the daughters of the noble gases which are formed following emission from the stack (those formed prior to emission from the stack are, since they are solids, assumed to remain on the filters); and (3) the noble gases formed by the decay of iodine which has been deposited on the filters.

There are ten noble gas isotopes which are of significance so far as direct emission is concerned. Of these, three – namely ^{88}Kr, ^{89}Kr, and ^{138}Xe – decay into daughters which also contribute significantly. Of these, ^{88}Rb and ^{138}Cs are the most important. Two of the iodines, ^{133}I and ^{135}I, decay to radioactive xenons, the most important of which is ^{135m}Xe. The equation for the dose utilizes the expressions for concentration given in Eqs. (11), (13), and (14) and the external dose equations (20) and (21):

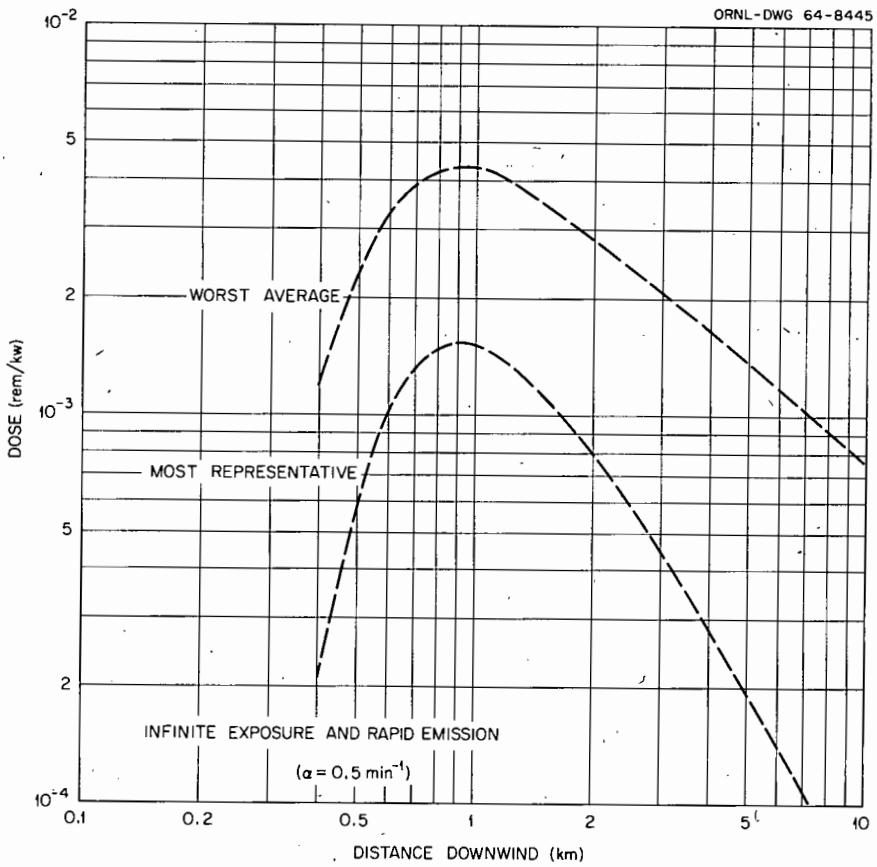

Fig. I.A.5. Internal Dose Due to Fission Products Other than Iodines and Bone Seekers – Infinite Exposure and Rapid Emission.

$$D_{ext}(t) = 28.4 \left[\sum_{j=1}^{10} E_{p_j} \int_{x/u}^{t} \chi_p(\tau)\, d\tau + \sum_{j=1}^{3} E_{d_j} \int_{x/u}^{t} \chi'_{d_j}(\tau)\, d\tau + \sum_{j=1}^{3} E_{d_j} \chi''_j(\tau)\, d\tau \right] . \quad (26)$$

Here, the subscripts p and d refer to the parent and daughter, respectively, and the E_j's are chosen according to whether it is the gamma or beta dose which is sought. The parameters for use with Eq. (26) are listed in Table I.A.4.

Because the noble gas doses are quite sensitive to the exhaust rate and the time of exposure, they have been computed not only for a high exhaust rate (α = 0.5) but also for exhaust rates corresponding to the maximum rate of removal through the HFIR primary coolant cleanup system (α = 0.015) and the rate of emission from the reactor bay assuming normal SBHE air flow and uniform dispersion (α = 0.028). The doses have been computed for both infinite and 2-hr exposure and are given in Figs. I.A.6–I.A.11.

4.2.1 External Doses from Fission Products Other than Noble Gases. – An upper limit to the external dose from all the fission products may be estimated from Eq. (23). The values of $p(x, u)$ are taken from

Table I.A.4. Parameters Used to Compute[a] External Dose from Noble Gases

Direct Emission

Isotope	λ_{p_j} (min^{-1})	q_{p_j} (curies/kw)	$E^{\gamma}_{p_j}$ (Mev/dis)	$E^{\beta}_{p_j}$ (Mev/dis)
^{83m}Kr	6.06×10^{-3}	4.05	0.415	0
^{85m}Kr	2.646×10^{-3}	12.65	0.181	0.233
^{87}Kr	8.88×10^{-3}	22.77	0.56	1.01
^{88}Kr	4.17×10^{-3}	31.21	2.07	0.331
^{89}Kr	2.178×10^{-1}	38.80	0	1.3
^{133m}Xe	2.094×10^{-4}	1.32	0.237[b]	0
^{133}Xe	9.120×10^{-5}	47.18	0.081	0.115
^{135m}Xe	4.44×10^{-2}	15.18	0.528[b]	0
^{135}Xe	1.266×10^{-3}	1.60	0.268	0.302
^{138}Xe	4.074×10^{-2}	46.39	0	1.0

Daughters

Isotope	λ_{p_j} (min^{-1})	λ_{d_j} (min^{-1})	q_{p_j} (curies/kw)	$E^{\gamma}_{d_j}$ (Mev/dis)	$E^{\beta}_{d_j}$ (Mev/dis)
^{88}Rb	4.17×10^{-3}	3.894×10^{-2}	31.21	0.47	1.61
^{89}Rb	2.178×10^{-1}	4.50×10^{-2}	38.80	0	1.5
^{138}Cs	4.074×10^{-2}	2.172×10^{-2}	46.39	2.01	1.08

Reemission

Isotope	χ_{p_j} (min^{-1})	λ_{d_j} (min^{-1})	q_{p_j} (curies/kw)	$E^{\gamma}_{d_j}$ (Mev/dis)	$E^{\beta}_{d_j}$ (Mev/dis)
^{133}Xe	5.55×10^{-4}	9.120×10^{-5}	54.83	0.081	0.115
^{135m}Xe	1.78×10^{-3}	4.44×10^{-2}	4.86	0.528	0
^{135}Xe	1.78×10^{-3}	1.266×10^{-3}	11.34	0.268	0.802

[a]Data from Blomeke and Todd, ORNL-2127.
[b]Includes daughters.

the Perkins and King data[5] for 1000-hr operation.[9] The stack factor $S(x, u) = e^{-h^2(u)/2\sigma_z^2}/\pi u \sigma_y \sigma_z$ is given for both "most representative" and "worst average" conditions in Fig. I.A.12. The value of u used for the "most representative" case is 100 m/min, and the values used to compute the "worst average" case are those which maximize $S(x, u)$, namely,

$$u_{max} = 27.90/(\sqrt{1 + \sigma_z^2/1452} - 1) .$$

[9]Perkins and King give curves of Mev per watt-second for 10-, 100-, and 1000-hr operation. The nominal HFIR operating time is expected to be 360 hr; hence, use of 1000 hr is an overestimate.

The noble gas doses are subtracted from the result, thus giving the external doses to be expected from all the fission products other than noble gases. These data are obtained under the assumption of high exhaust rate and infinite exposure and are given in Fig. I.A.13.

5. Continuous Release of Activity

Equation (1) can be utilized to obtain an estimate of the results of a continuous release of the volatile fission products from the stack. Because "worst average" conditions cannot be expected to prevail over long periods of time, the "most representative" conditions ("C" stability, $u = 100$ m/min) have been utilized. Therefore, if decay during passage downwind is neglected, the concentration in microcuries per cubic centimeter at ground level at a point x meters downwind and y meters crosswind from the stack due to the continuous emission of 1 curie/min is given by

$$\chi(x, y) = \frac{e^{-h^2(u)/2\sigma_z^2}}{\pi u \sigma_y \sigma_z} \cdot e^{-y^2/2\sigma_y^2} \ \mu c \ cm^{-3} \ curie^{-1} \ min \ , \tag{27}$$

where again the factor 2 in the denominator of Eq. (1) is dropped to account for reflection and z has been set equal to $-h$, the effective stack height.

Because it is the consequences under average conditions which are sought, and because the wind directions are given in terms of the sixteen 22.5° sectors which represent the cardinal compass points, Eq. (27) is averaged with respect to y over the base of an isosceles triangle having altitude x and vertex angle $\pi/8$. Thus

$$\overline{\chi}(x) = \frac{e^{-h^2(u)/2\sigma_z^2}}{\pi u \sigma_y \sigma_z} \cdot \frac{1}{x \tan \pi/16} \int_0^{x \tan \pi/16} e^{-y^2/2\sigma_y^2} \, dy = \frac{e^{-h^2(u)/2\sigma_z^2}}{\sqrt{2\pi} \, u \sigma_y \sigma_z} \cdot \frac{\sigma_y}{x \tan \pi/16} \operatorname{erf}\left(\frac{x \tan \pi/16}{\sigma_y \sqrt{2}}\right) .$$

For the values of interest,

$$0.9 < \operatorname{erf}\left(\frac{x \tan \pi/16}{\sigma_y \sqrt{2}}\right) < 1 \ ;$$

hence

$$\overline{\chi}(x) \cong \frac{e^{-h^2(u)/2\sigma_z^2}}{\pi u \sigma_y \sigma_z} \cdot \sqrt{\frac{\pi}{2}} \frac{\sigma_y}{x \tan \pi/16} = \frac{6.301 \, \sigma_y}{x} S(x, u) \ . \tag{28}$$

The results for the "most representative" case are given in Fig. I.A.14. These can be corrected for simple decay by multiplying the values given in the curve by the quantity $e^{-0.01\lambda x}$, where λ is the decay constant in min^{-1} and x is the downwind distance in meters.

Again, because the results of average conditions are sought, the distribution of the wind direction must be considered. The average values for the ORNL area are given in Table I.A.5. Hence, the values found from Fig. I.A.14 should be reduced by the fraction corresponding to the direction under consideration.

ACKNOWLEDGMENT

The author wishes to acknowledge the very extensive contribution to this work of J. Barish, of the Central Data Processing Facility, who programmed and performed the calculations.

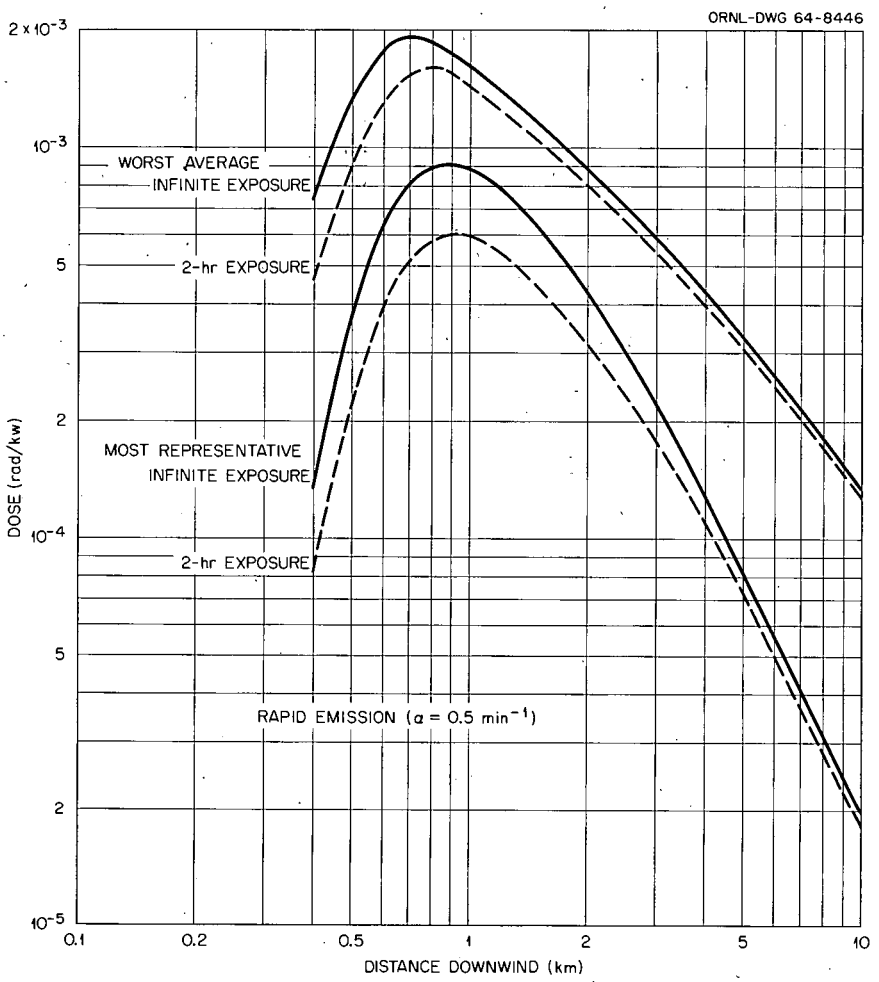

Fig. I.A.6. External γ Dose Due to Noble Gases – Rapid Emission.

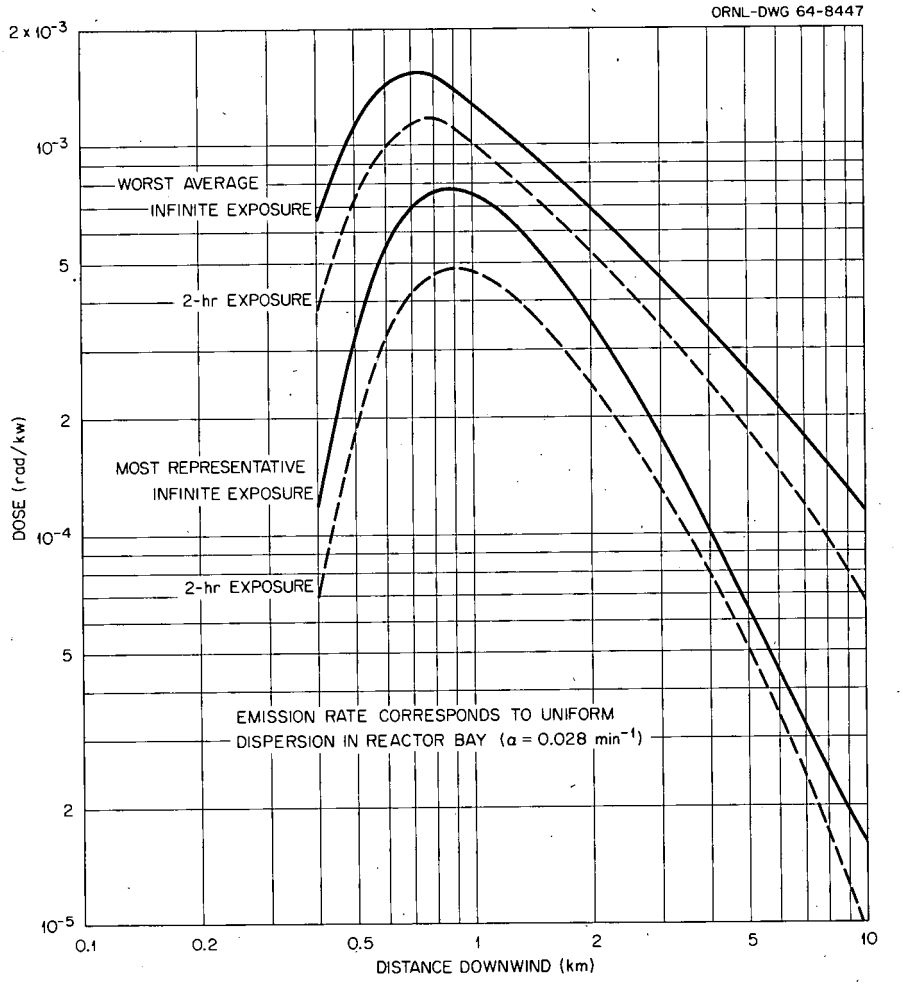

Fig. I.A.7. External γ Dose Due to Noble Gases – Emission Through Reactor Bay.

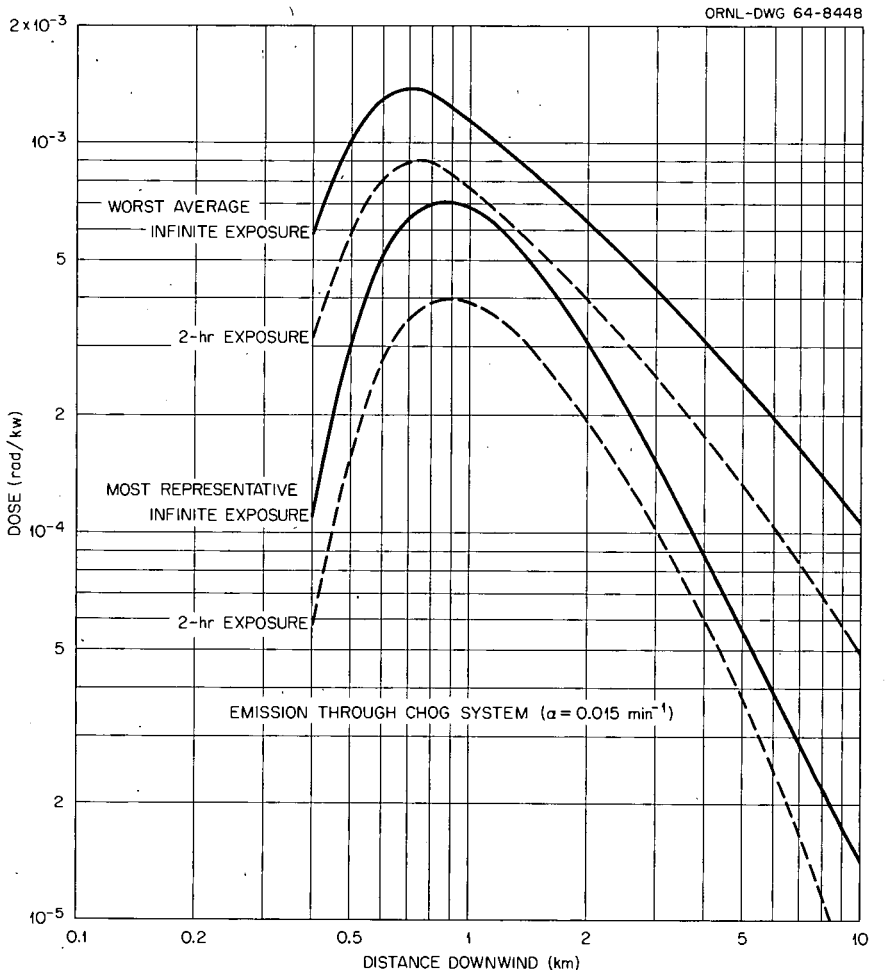

Fig. I.A.8. External γ Dose Due to Noble Gases – Emission Through CHOG System.

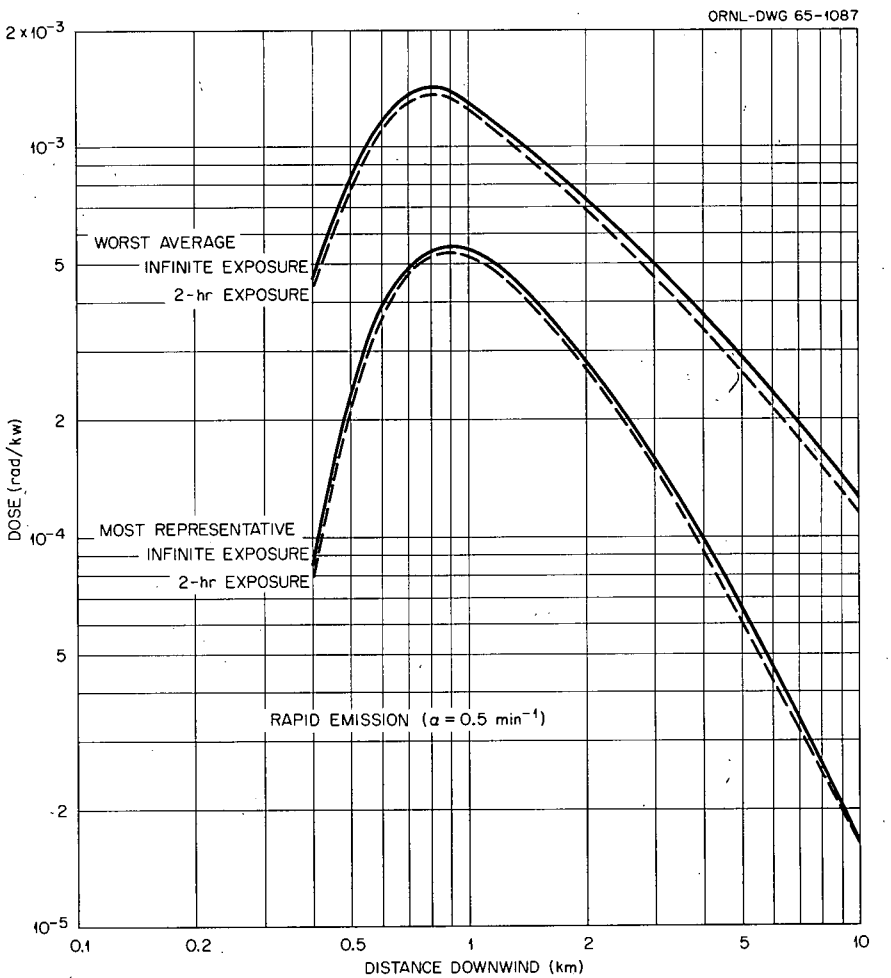

Fig. 1.A.9. External β Dose Due to Noble Gases – Rapid Emission.

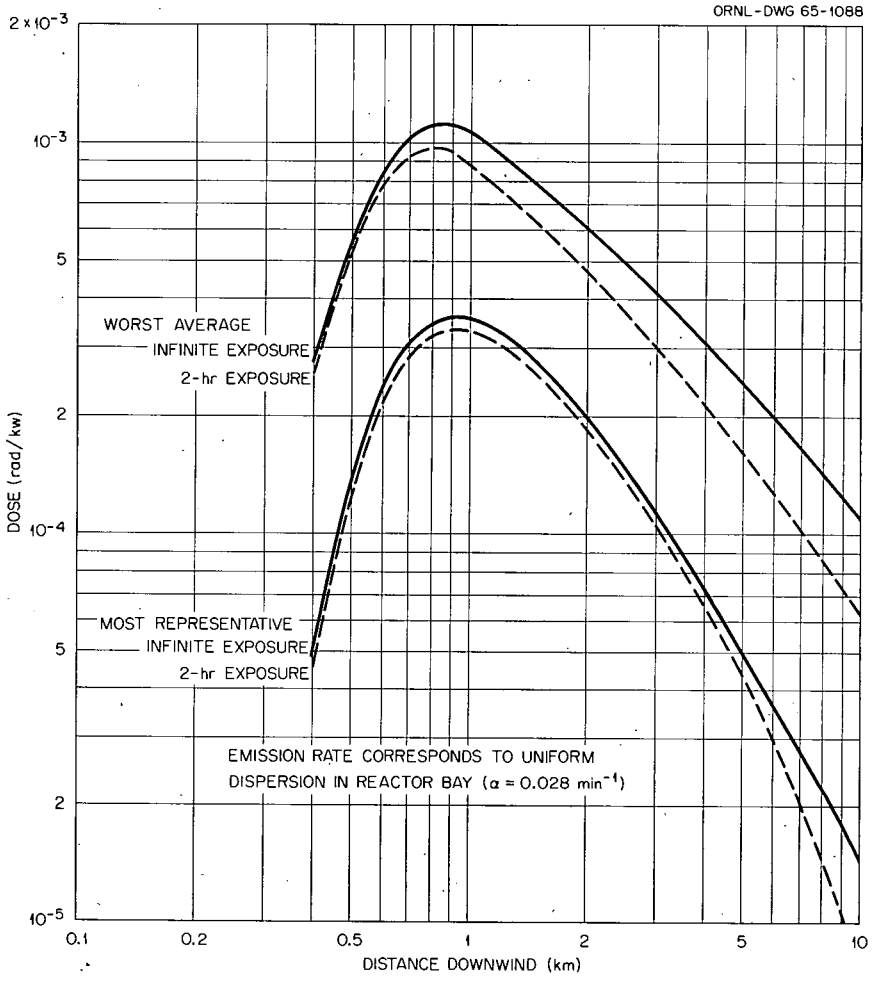

Fig. I.A.10. External β Dose Due to Noble Gases – Emission Through Reactor Bay.

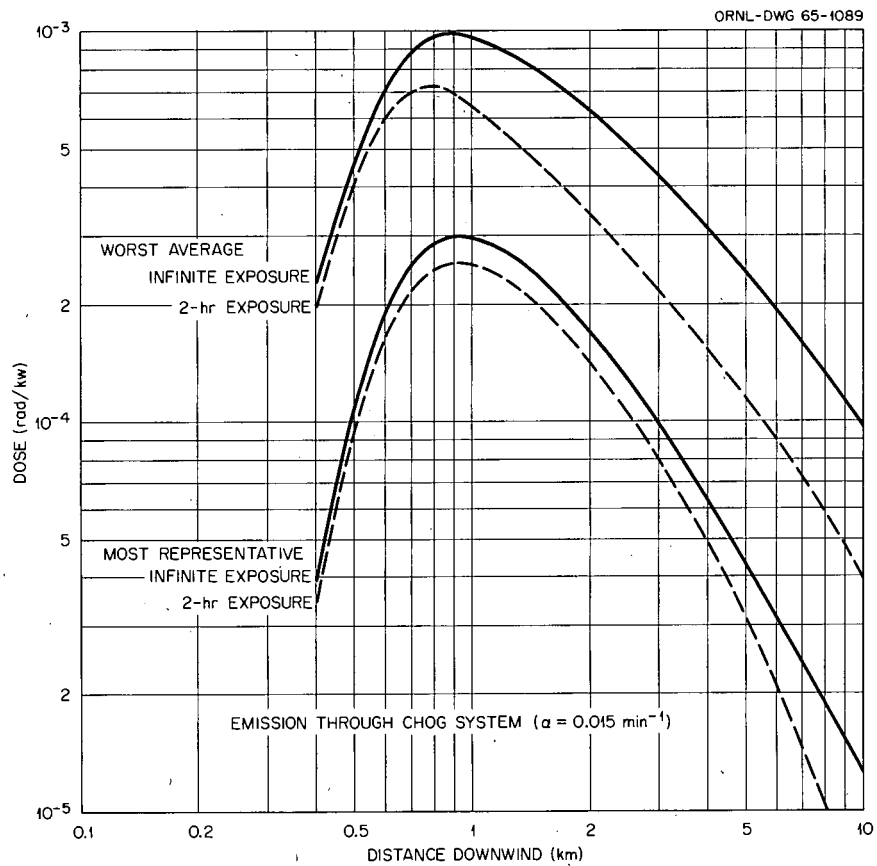

Fig. I.A.11. External β Dose Due to Noble Gases – Emission Through CHOG System.

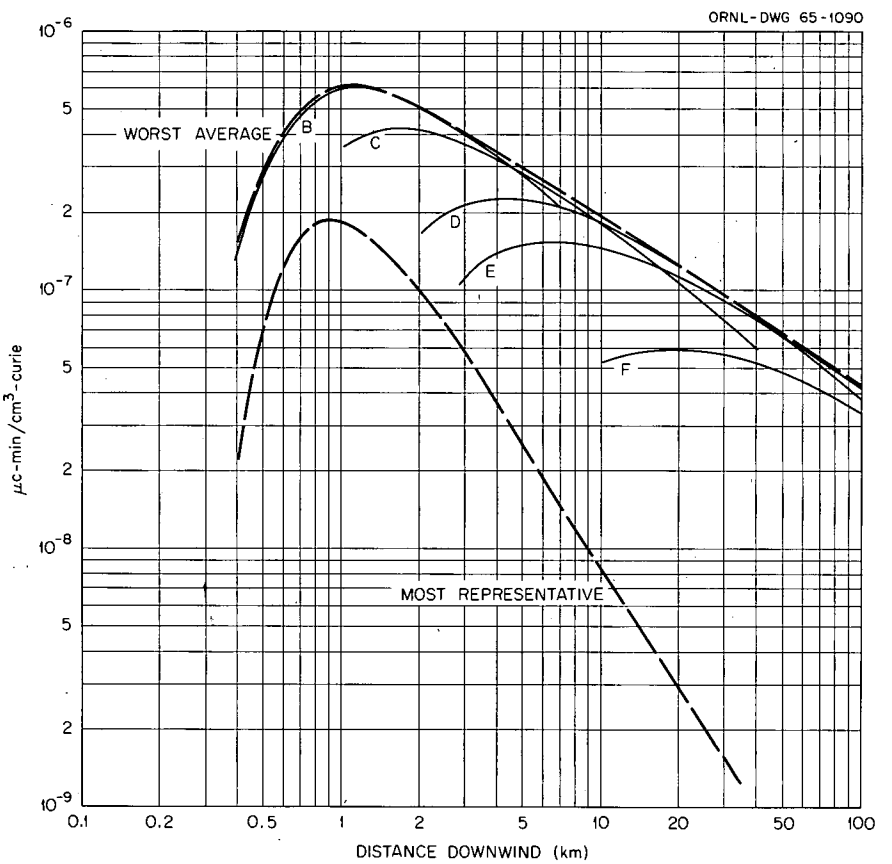

Fig. I.A.12. HFIR Stack Factor.

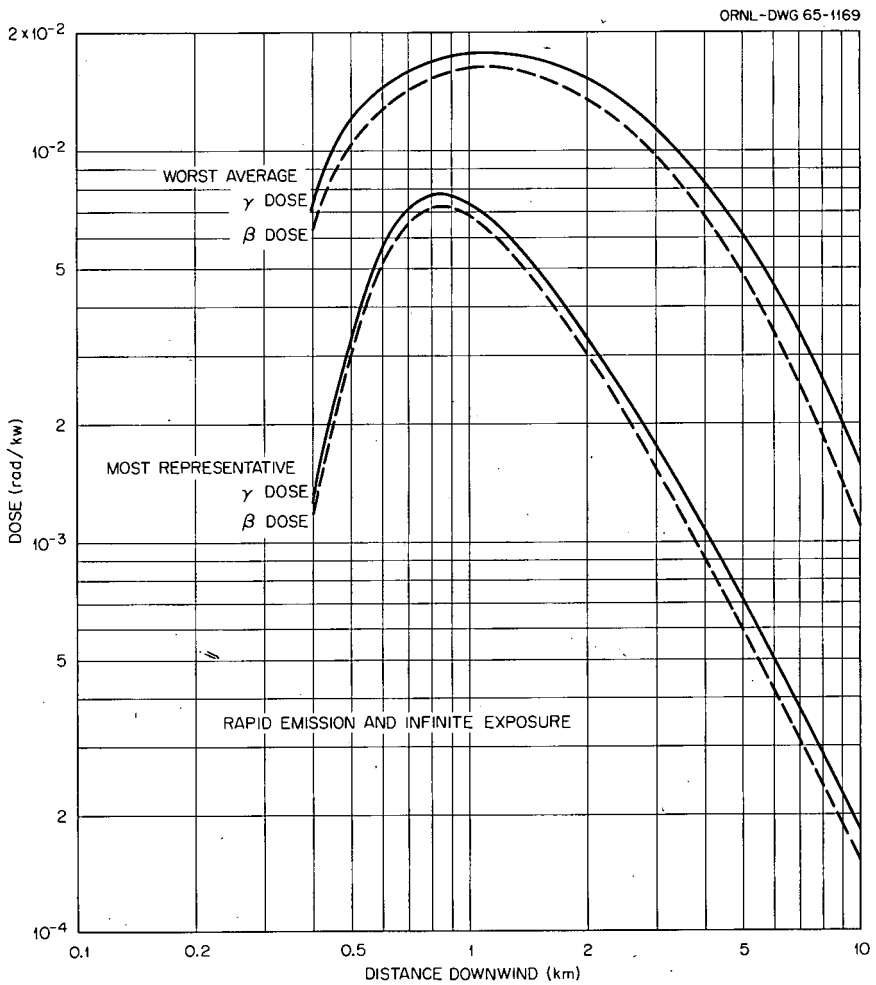

Fig. I.A.13. External Doses Due to Fission Products Other than Noble Gases – Infinite Exposure and Rapid Emission.

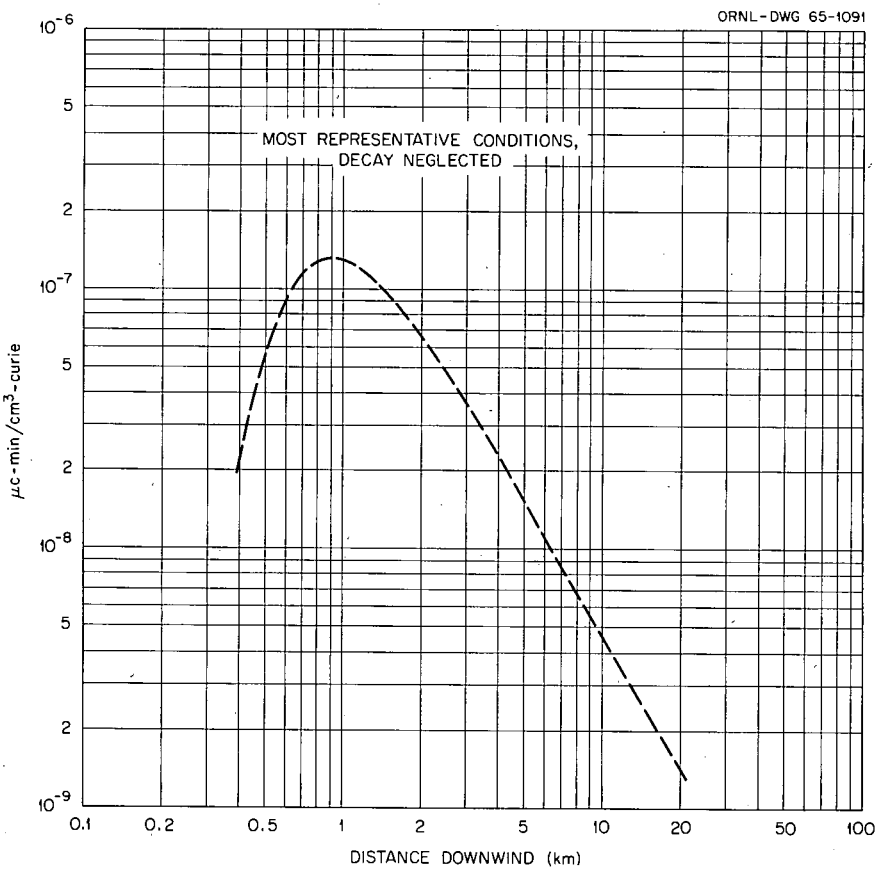

Fig. I.A.14. Average Downwind Fission Product Concentration Due to Continuous Release of One Curie per Minute.

Table I.A.5. Frequency of Wind Direction at ORNL[a]

Direction Toward Which Wind Blows	Percent of Total Time
N	3.389
NNE	7.259
NE	12.076
ENE	8.160
E	7.009
ESE	4.742
SE	3.023
SSE	1.348
S	1.978
SSW	3.200
SW	12.501
WSW	8.985
W	4.047
WNW	0.914
NW	1.327
NNW	0.857
Calm	19.185

[a]W. M. Culkowski, U.S. Weather Bureau, private communication, January 1964.

APPENDIX B

HFIR EXCURSION CONTAINMENT POTENTIAL*

Letter Report of 15 March 1964

Prepared for
Reactor Division
Oak Ridge National Laboratory
By
Walter R. Wise, Jr., Ph.D.
Excursion Containment Consultant

1. Foreword

The Reactor Vessel Containment Program, currently nearing completion at the U.S. Naval Ordnance Laboratory, White Oak, is addressed to characterizing the excursion containment potential of nuclear facilities, and particularly reactor pressure vessels. This program, sponsored by the Atomic Energy Commission at a cost of $1,400,000 over a period of eight years, is the Commission's most fundamental and comprehensive research effort directed to the excursion containment potential of reactor vessels per se. The extensive experimental phase, including tests in model vessels made of A212B steel, has been completed; the major portion of the theoretical work is virtually complete; and final summary reports** now in preparation are scheduled for publication in the first half of 1964. These reports will constitute the most extensive and authoritative reactor vessel excursion containment information published in the United States. The basic rationale and data of these reports, through the writer as their principal author, were employed to characterize the excursion containment potential of the HFIR.

2. Introduction

In this report, upper bounds in terms of TNT will be placed upon the excursion containment potential of the HFIR.[1] The rationale for employing TNT to simulate and provide useful upper bounds on nuclear accidents can be readily expressed: Nuclear excursions cannot be micro scaled; TNT explosions can, and furthermore, many of their scaling properties are well known. This makes available a very important tool that is often the sine qua non for complex multiparameter problems: experiments in small models. Although the flux and character of the energy released during a postulated MCA may not be identical to those of the TNT explosion, they are often sufficiently alike to permit use of the TNT model as a reasonable and defensible upper-bound simulant. This is true for the HFIR.

---

*Updated in question 56 and Appendix K.

**NOLTR 63-140 (Aug. 16, 1965).

[1]HFIR design specifications employed in this report were supplied to the author by the Reactor Division, Oak Ridge National Laboratory.

3. Tentatively Postulated MCA's[2]

It is understood from information provided by the Reactor Division, Oak Ridge National Laboratory, that the following accidents have been entertained or tentatively postulated by the Division as probable MCA's for the HFIR:

1. The linear release of 50 Mwsec in 3 msec.
2. The linear release of 100 to 200 Mwsec in 100 to 1000 msec.

Now, a nominal value for the heat of detonation of TNT is 1050 cal/g. At this energy density, 200 Mwsec, for example, would be closely equivalent to the energy released by the detonation of 100 lb of TNT.

4. Characteristics of Marginally Contained TNT Accident

The HFIR pressure vessel is fabricated of A212B steel with the properties: $\sigma_y = 38{,}000$ psi; $\sigma_u = 70{,}000$ psi; ϵ (elongation) = 22%. It is interesting, in the beginning at least, to consider an *idealized* HFIR pressure vessel for which the material is homogeneous and isotropic and the end closures and all nozzles remain sound during gross plastic deformation of the vessel wall. Additionally, assume that all water is drained from the reactor pool. Under these circumstances, we entertain the detonation of a center-initiated, compact charge of TNT at the core location, which would occupy a volume of the same order as that of the uranium core; its temperature and pressure would be 77°F and atmospheric. Upon detonation, the solid explosive would be transformed almost discontinuously in time to a gaseous fireball at virtually the same volume with temperatures and pressures of the order of 5000°F and 2,500,000 psi behind the detonation front. As a consequence of this immense energy flux, two destructive mechanisms would be produced: the shock wave and the internal-blast pressure, that is, the quasi-static (or equilibrium) pressure generated by the gases released from the explosive charge. About half the energy is released in the shock wave and the remainder in the internal-blast pressure.

The shock wave, a microsecond mechanism, would propagate through the media surrounding the core and strike the wall of the reactor vessel. In response to the impulse, the wall would be given a virtually instantaneous velocity. Portions of the wall nearest the core would be given the greatest velocity and undergo the greatest deformation. The inertia and tensile strength of the vessel would resist the impulsive force during acceleration of the wall. Subsequently, the tensile constraint would attempt to bring the wall to rest.

In general, shock-wave attenuation in elastic media is less than in inelastic, plastic, or relatively compressible media. For the case at hand, attenuation of the shock would be greater in water than in steel, and in air or similar gases the attenuation would be considerably greater than in water or steel. Thus, it is seen that if water were lost from the reactor vessel immediately prior to the accident, the shock-attenuation potential of the system would be increased, and the shock strength at the composite

---

[2]Editors' note: The term MCA as used here by Dr. Wise differs in connotation from that used in the safety analysis itself. The energy releases suggested to Dr. Wise by ORNL were for the purpose of defining the scope of the problem.

wall would be decreased with a consequent decrease in deformation. Clearly then, the deformation volume of the reactor vessel is a function of water content: the largest deformation is associated with the case of no loss of water from the vessel and conversely for the full loss of water.

Following the shock wave would be the explosion gases, and assuming containment, these gases would be confined in the reactor vessel. The resulting quasi-static pressure, of milliseconds duration as opposed to microseconds for the shock pressure, is a significant function of two variables: the volume into which the explosion gases flow and the capacity (quality and quantity) of the heat sinks available to these gases. If a major portion of the water is retained in the vessel, the water constitutes a significant heat sink. If a major portion or all of the water is lost from the vessel, the complex metal structures surrounding the core become an important heat sink. In any event, these sinks significantly enhance the containment potential of the HFIR vessel for energy releases occurring in hundreds of milliseconds.

The internal-blast pressure (of the order of hundreds of psi) is less than the shock pressure (of the order of thousands of psi), but it tends to persist for hundreds of milliseconds as opposed to microseconds for the shock pressure. Distortion of the vessel wall from the shock pressure precedes arrival of the internal-blast pressure, so that the expansion volume immediately available to the explosion gases would be the initial expansion volume plus whatever deformation volume is produced by the shock pressure. The magnitude of the internal-blast pressure is not sufficient to further distort the wall.

5. Excursion Containment Bounds

From the most authoritative information available, bounds on the excursion containment potential of the HFIR are entertained and estimated as follows:

1. The marginal TNT containment potential of the *idealized* HFIR pressure vessel for the case of no water in the reactor pool and no loss of water from the vessel immediately prior to the accident is estimated to be 180 lb of TNT (360 Mwsec). If any portion of the vessel water were lost immediately prior to the accident, the containment potential would be greater than 180 lb of TNT. If all the vessel water were lost immediately prior to the accident, the containment potential would exceed 360 lb of TNT (720 Mwsec). These estimates are predicated upon the *unrealistic* assumption that parts of the vessel wall nearest the charge would elongate as much as 22% and that all closures, nozzles, and weldments in the vessel wall, particularly those nearest the charge, would remain sound.
2. Since the HFIR reactor vessel is fitted with numerous and complex closures, nozzles, and weldments, the maximum permissible elongation of the vessel wall should be restricted to one-third of the specified 22% minimum, say $\epsilon = 7\%$. Imposing the 7% restriction, we now consider an accident that the HFIR vessel could be *realistically* expected to contain. Again it is assumed that the reactor vessel is full of water, but there is no water in the reactor pool. Under these conditions, the containment potential of the HFIR is estimated to be 55 lb of TNT (110 Mwsec). If any portion of the vessel water were lost immediately prior to the accident, the potential would be greater than 55 lb of TNT. If all the vessel water were lost, the potential would exceed 110 lb of TNT (220 Mwsec).

3. If all reactor pool water were retained – and this is understood to be the most likely condition in the remote event of an accidental excursion – the inertia of the reactor pool water would increase the containment potential of the reactor vessel to more than 110 lb of TNT (220 Mwsec), irrespective of whether the vessel water be lost or retained in any quantity. If a loss of reactor pool water were suffered, but a head of at least 8 ft above the top of the reactor vessel were retained, the containment potential of the vessel would remain in excess of 110 lb of TNT (220 Mwsec) irrespective of the loss or retainment of vessel water in any quantity.
4. The detonation of TNT (in microseconds) is a more efficient violence mechanism than linear releases occurring in milliseconds and significantly more efficient than those occurring over hundreds of milliseconds. It is estimated that either of the following accidents:

   a) the linear release of 110 Mwsec in 3 msec,

   b) the linear release of 330 Mwsec in 100 to 1000 msec,

   would be contained within the HFIR pressure vessel and its nozzle complex, irrespective of whether the water in the vessel and/or reactor pool be lost or retained in any quantity.

6. Containment Qualifications

To avoid ambiguity in defining the excursions considered above, it is specified that, irrespective of the compounding of nuclear or other events that may occur in the reactor, the upper bound on the resultant total accident (the energy released) is in each case relative to the normal operating energy level of the reactor as a base. Furthermore, for accidents with release rates slower than that of TNT, an important requirement must be satisfied: the release of gas products per unit energy for the slower reactant must not exceed that for TNT. Upon some reflection, it is seen that the limitations on compounding and gas products are both practicable and necessary for the determination of upper-bound containment potentials. This rationale applies not only to the HFIR, but to reactors generally.

The specified containment bounds will be valid only if the following requirements are satisfied:

1. The vessel wall, weldments, closures, and nozzles must possess everywhere the chemical, mechanical, and physical properties specified in the design of the reactor, and
2. These properties, as they relate to containment, must not be negated in time by inclusions, NDT considerations, radiation effects, stress concentrations, high temperatures, cycling, etc.

All the realistic accidents entertained might grossly deform such reactor internals as the core assembly, the beam tubes, and the control rods that extend through the lower portion of the reactor vessel into the sub-pile room. In consequence, minor breaching of correlative nozzles and closures could result, but rupture of the reactor vessel per se would not occur. Also, the accidents could produce a small permanent set in some of the studs or bolts that make the various flanged joints of the reactor vessel. This could be particularly characteristic of the studs that make the top-head joint. In consequence, breaching could occur in the form of leakage at these joints; but again, the gross containment integrity of the reactor vessel would not be violated, and gross failure of the vessel nozzle and piping complex external to the vessel should not occur.

7. Summary Conclusions

Basic rationale on the bounds and qualifications of reactor containment was discussed in the previous paragraphs. A detailed summary of upper bounds upon the realistic excursion containment potential of the HFIR (ϵ = 7% max) is now given for various conditions and accidents. The limitations, qualifications, and restrictions discussed above apply in each case as appropriate.

1. Complete loss of reactor pool water; TNT energy flux.
   - *a*) Retainment of all reactor vessel water: containment potential = 55 lb of TNT (110 Mwsec)
   - *b*) Partial loss of reactor vessel water: containment potential > 55 lb of TNT (>110 Mwsec).
   - c) Complete loss of reactor vessel water: containment potential > 110 lb of TNT (>220 Mwsec).

2. Complete loss of reactor pool water; energy release rates slower than TNT rate.
   - *a*) Full retainment or partial loss of reactor vessel water; 3 msec linear release: containment potential > 110 Mwsec.
   - *b*) Complete loss of reactor vessel water; 3 msec linear release: containment potential > 220 Mwsec.
   - c) Retainment of at least $\frac{2}{3}$ of reactor vessel water; 100 to 1000 msec linear release: containment potential > 360 Mwsec.
   - *d*) Complete loss of reactor vessel water; 100 to 1000 msec linear release: containment potential > 330 Mwsec.

3. Retainment of head of pool water at least 8 ft above top of reactor vessel for retainment or loss of reactor vessel water in any quantity.
   - *a*) TNT energy flux: containment potential > 110 lb of TNT (>220 Mwsec).
   - *b*) Linear release in 3 msec: containment potential > 220 Mwsec.
   - c) Linear release in 100 to 1000 msec: containment potential would not be appreciably affected by inertial constraint of pool water.

4. The reactor pool and vessel are full of water under normal operating conditions – the conditions deemed most likely to exist in the event of an accidental excursion. Fortuitously, these are the very conditions that yield the greatest containment potential of the HFIR vessel (Fig. I.B.1). Since Fig. I.B.1 characterizes the containment case of greatest general interest, we shall be specific as to its meaning: the energy flux defined therein constitutes the highest defensible upper bound upon the excursion containment potential of the HFIR vessel and its nozzle complex. Large losses of vessel and pool water would adversely affect the containment potential; but, if at least two-thirds of the vessel water and 8 ft of pool water above the vessel were retained, the containment potential given in Fig. I.B.1 would remain valid.

5. In all the accidents discussed thus far, the release of gas products per unit energy was that correlative with the detonation of TNT. It should be noted that for essentially thermal releases (virtually no gas products) occurring in hundreds of milliseconds the excursion containment potential of the HFIR and its nozzle complex would be greatly enhanced.

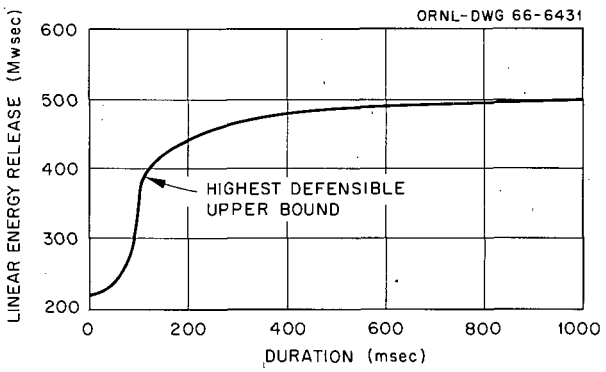

Fig. I.B.1. Upper Bound Containment Potential of HFIR Under Normal Operating Conditions.

The summary provided in the paragraphs above constitutes reasonable and highly defensible upper bounds upon the excursion containment potential of the HFIR pressure vessel and nozzle complex. The conclusions, based upon known theory and replicable experimental results, are drawn from the writer's background and experience in producing the most extensive and authoritative reactor vessel excursion containment information known to be available.

Walter R. Wise, Jr.

Walter R. Wise, Jr., Ph.D.[3]
Excursion Containment Consultant

APPENDIX C

REACTIVITY CONSIDERATIONS*

As is the case with all reactors, there are numerous ways of adding varying amounts of reactivity to the nominal HFIR core. Some of these, of course, are associated with normal operation of the reactor, while others constitute "accidents." The latter reactivity additions may or may not be credible, but all, by definition, are possible. From a practical point of view, it is desirable to select for analytical consideration only those accidents which are physically reasonable from the standpoint of available mechanisms for producing the accident. If all the selected accidents can be tolerated within the various degrees of acceptable core damage associated with each accident, then the question of credibility can be

[3]The writer was Director and Principal Investigator of the NOL Reactor Vessel Containment Program from its inception in January 1956 to August 1963. He has continued to oversee the program in a consulting capacity and will do so until the final reports (the writer is principal author) are published in mid-1964.

*Further discussed in answers 11, 12, 20, 22, 26, 38, 51, 54, and 55 and Appendices H and L.

avoided altogether. In this report, the "reasonable" HFIR reactivity accidents and associated mechanisms are discussed; on the basis of analog transient analyses, which included comparisons of the HFIR and selected SPERT cores, it is concluded that no serious core damage will result from any of these accidental reactivity additions. Some melting of localized hot-spot areas is predicted for a few extreme cases; however, because of the small fraction of core volume involved and the anticipated low frequency of occurrence, such accidents are not considered to constitute serious monetary or hazards problems.

Closely associated with the problem of reactivity accidents is the steady-state reactivity shutdown margin. Criteria pertaining to shutdown margins, a summary of shutdown margins, and a reactivity accountability are included as a part of this analysis.

1. Transient Behavior

1.1 Method of Analysis

Two methods of analysis have been used to examine the behavior of the HFIR when subjected to various reactivity additions. The method used most extensively was a mathematical analysis, using an analog model of the HFIR; the other method involved the extrapolation of SPERT experimental data to HFIR conditions. This latter analysis is discussed in greater detail at the end of this section.

The reactor model selected for the analog studies was based on the usual set of heat removal and reactor kinetics equations. Wherever practical to do so, the constants and assumptions used were selected on a conservative basis. In the following paragraphs an effort is made to explain in a qualitative way the extent of the conservatism. A completely quantitative analysis of the degree of conservatism has not been possible because of a lack of appropriate experimental data.

The analog calculations were performed in such a way that the average HFIR core and very localized hot-channel, hot-streak, and hot-spot portions of the average core were considered simultaneously. However, in so doing it was assumed that the transient behavior of the reactor was dependent only on average conditions, local net deviations from the average being neglected insofar as feedback is concerned. This means that no advantage was taken of negative reactivity feedback associated with strongly weighted moderator density changes in the high-power-density regions.

Variations in reactivity resulting from temperature changes throughout the average core were accounted for by dividing the core into four regions: flux-trap target, water annulus between target and fuel, fuel, and reflector-control. Each of these regions had individual reactivity coefficients and heating and heat removal rates. Reactivity variations resulting from possible void formation in the fuel region coolant were not included because of the uncertainty associated with the worth and quantity of the voids. The degree of conservatism associated with this simplification is greater for low-power operation and for short-period reactivity accidents. In several of the calculated cases the nominal maximum plate surface temperatures exceeded the saturation temperature before the peak power occurred. This means that voids would occur in the fuel region and would contribute to the negative reactivity feedback in time to reduce the peak power and temperature.

Reactivity temperature coefficient data used in the calculations were obtained in large part from HFIR critical experiments.[1] In these experiments, the temperature coefficients for the island and for the fuel region were determined as a function of moderator temperature up to the normal full-power moderator temperature for the reactor. Coefficients for the other less important regions were obtained from normalized calculations. Since it was not possible to obtain experimental coefficients for the end-of-core-life conditions, calculations were also used to predict the ratio of beginning-of-cycle to end-of-cycle coefficients for the fuel region, the only region for which this ratio is significant. The end-of-cycle coefficient for the fuel region was calculated to be one-half that at the beginning of the cycle.

The fuel region temperature coefficient was found to be somewhat sensitive to the moderator temperature. The coefficient becomes more negative as the moderator temperature increases. This effect was included in some of the calculations, while in others an average coefficient was used. From the standpoint of establishing the peak power and temperatures during a fast transient the variation in temperature coefficient with temperature was not really important; for all cases of interest the increase in average bulk moderator temperature up to peak power was less than 30°F.

A fuel plate expansion coefficient of reactivity was also included in the analog calculation. Its value was determined from the fuel region void coefficients measured in the HFIR critical experiments.[1] When the coolant flow rate (and thus the water-film heat transfer coefficient) is low, the fuel plate expansion coefficient is equally as important as the moderator temperature coefficient in terminating an excursion.

Reactivity control by means of control plates was characterized by a power-level or rate-trip signal, a delay between signal and plate release, a linearly decreasing safety plate acceleration (to 1*g* at the end of the first 6 in. of travel), and a control plate differential worth that was a function of plate position.

The heat-transfer mechanism simulated in the analog model was that associated with a flat-fuel-plate, rectangular-coolant-channel geometry. Heat transfer from the plates to the coolant was assumed to take place by conduction and convection and by direct deposition of gamma and neutron energy in the coolant.

Resistance to the flow of heat from the plates to the water was provided by the aluminum fuel plate, an aluminum oxide film between the plate and water, and the fluid film; the latter two resistances were assumed to have negligible heat capacity. The inlet temperature of the coolant water was assumed to be constant during the transient because of the short duration of the transient relative to the primary coolant cycle time.

Fuel region afterheat was included in the analysis and was assumed to have a maximum value of 7% of the steady-state power.

The kinetic equations used in the analog studies to describe the transient behavior of the HFIR core in a manner consistent with the above approximations and assumptions are as follows; the nomenclature is set forth in Table I.C.1.

Nuclear equations:

$$\frac{dP}{dt} = \frac{(1-\beta)k-1}{l^*} P + \sum_{i=1}^{i=5} \lambda_i C_i \tag{1}$$

[1]D. W. Magnuson, *High Flux Isotope Reactor Critical Experiment No. 2*, ORNL-CF-61-9-52 (Sept. 27, 1961).

Table I.C.1. Nomenclature

a	Ratio of power produced in fuel plates to total power
A	Heat transfer surface area
b	Ratio of power produced in coolant to total power
C_F	Total heat capacity of metal, Btu/°F
C_w	Total heat capacity of coolant, Btu/°F
C_i	Delayed neutron precursor for ith group [units and normalization consistent with use of power instead of neutron density in Eqs. (1) and (2)]
$F(t)$	Control plate and accident reactivity variations with time, Δk
g	Acceleration due to gravity, in./sec^2
h	Heat transfer coefficient, Btu hr^{-1} ft^{-2} (°F)$^{-1}$
k	Effective neutron multiplication factor
k_0	Effective neutron multiplication factor at time zero
l^*	Prompt neutron lifetime, sec
P	Total reactor power, Btu/sec
S	Distance control plate moves after release, in.
t	Time, sec
T_1	Oxide-metal interface temperature
T_2	Oxide-water interface temperature
$\overline{T}_F$	Average metal temperature over region
t_i	Average bulk water temperature at core inlet
$\overline{T}_j$	Average bulk water temperature throughout jth region
$\overline{T}_j(0)$	Average bulk water temperature throughout jth region during steady state
T_o	Average bulk water temperature at region outlet
T_w	Average bulk water temperature throughout region
α_j	Temperature coefficient of reactivity for jth region of core, Δk/°F
β_i	Delayed neutron fraction for ith group
λ_i	Decay rate of ith delayed neutron precursor
λ_1	Rate at which heat is transferred out of metal, Btu sec^{-1} (°F)$^{-1}$ (determined from steady-state conditions)
λ_2	Ratio of heat transfer rate per unit temperature drop across oxide film to λ_1 (determined from steady-state conditions)
τ	One-half residence time of coolant in region

$$\frac{dC_i}{dt} = -\lambda_i C_i + \frac{\beta_i kP}{l^*} \tag{2}$$

$$k = k_0 + F(t) + \sum_{j=1}^{n} \alpha_j [\bar{T}_j - \bar{T}_j(0)] \tag{3}$$

Heat removal equations:

$$C_F \frac{d\bar{T}_F}{dt} + \lambda_1(\bar{T}_F - T_1) = aP \tag{4}$$

$$\bar{T}_F - T_1 = \lambda_2(T_1 - T_2) \tag{5}$$

$$C_w \frac{d\bar{T}_{H_2O}}{dt} - \frac{C_w}{\tau}(T_i - \bar{T}_w) - hA(T_2 - \bar{T}_w) - bP = 0 \tag{6}$$

$$C_w \frac{dT_o}{dt} - \frac{C_w}{\tau}(\bar{T}_w - T_o) - hA(T_2 - \bar{T}_w) - bP = 0 \tag{7}$$

Control plate movement equations:

$$\frac{d^2S}{dt^2} = 4g - \frac{1}{2} gS \text{ in.}^{-1} \qquad (0 \leq S \leq 6 \text{ in.}) \tag{8}$$

$$\frac{d^2S}{dt^2} = g \qquad (S > 6 \text{ in.}) \tag{9}$$

In Eqs. (6) and (7) the quantity h is the heat transfer coefficient of the coolant film. During a transient, in which the flow rate remained constant, the h value was maintained constant for heat fluxes less than the steady-state burnout heat flux.[2] When the latter heat flux was reached, the h value associated with that location was set equal to zero and was presumed to remain at zero until the power level was reduced to about one-half of the power level that corresponded to the steady-state burnout heat flux. The absolute value of the average-core heat transfer coefficient prior to the film blanketing condition was taken as the minimum predicted by the applicable steady-state correlation.[3] This was conservative since the use of a low h value resulted in less negative reactivity feedback associated with moderator expansion. At the hot spot a nominal h value, corresponding to steady-state hot-spot conditions,[4] was used.

---

[2]In the analog analysis, incipient boiling heat fluxes were used in lieu of burnout heat fluxes for modes 1 and 2 because adequate correlations for the latter were not available. This approach is not considered unduly conservative, because at high power a narrowing of the coolant channel tends to make the incipient boiling point and the burnout point nearly equal. For very low power and with no forced flow (mode 3) there is a significant separation of the incipient boiling point and burnout point; for this mode adequate burnout data were available.

[3]W. R. Gambill and R. D. Bundy, *HFIR Heat Transfer Studies of Turbulent Water Flow in Thin Rectangular Channels*, ORNL-3079 (June 5, 1961).

[4]N. Hilvety and T. G. Chapman, *Summary of HFIR Hot Spot Studies*, ORNL-CF-62-1-52 (Jan. 30, 1962).

When the h value at the hot spot is set equal to zero, the ratio of hot-spot temperature to surrounding plate temperature increases, and thus the radial heat transfer away from the hot spot ($\frac{5}{64}$ in. diameter) should increase. In the analog analysis no increase in radial transfer was permitted after the h value was set equal to zero. Therefore, in this respect the calculated hot-spot plate temperatures are higher than would actually be expected.

The hot-spot conditions used in the analog model were the same as those used in the steady-state analysis of the core;[4] that is, all conceivable tolerances and abnormalities (blisters, fuel segregation, etc.) within specifications were considered to exist in a consistent manner at the same time and place. Although much factual statistical data on the distribution of abnormalities in the fuel plates is still not available, it appears that the probability of existence of the worst combination of heat removal conditions is very small. This needs to be kept in mind when using the calculated results to evaluate core damage and the ability of the HFIR to handle reactivity accidents.

An accurate evaluation of the calculational results in terms of core damage becomes quite questionable when the predicted plate temperatures approach and exceed the melting temperature of the fuel plates. There are, however, some SPERT data which indicate that for calculated temperatures well in excess of the melting point no actual melting or even plate warpage will occur. For this reason, it appeared conservative to assume, for purposes of evaluating the calculated results, that no melting would occur until in the calculation the melting temperature was reached and enough additional heat was added (heat of fusion) to actually melt the aluminum. In the calculation the heat of fusion was represented by an increase in plate temperature equal to the heat of fusion divided by the specific heat. Therefore, the calculated melting point temperature was equal to

$$1950°\text{F} = 1210°\text{F (melting temperature)} + \frac{167 \text{ Btu/lb}}{0.226 \text{ Btu lb}^{-1} \text{ °F}^{-1}} = 1210°\text{F} + 740°\text{F} .$$

Calculated temperatures above 1210°F should be interpreted accordingly.

From an operating point of view, the occurrence of a very small fission product leak is probably not the most serious type of core damage resulting from a transient. A permanent buckling of the fuel plates could significantly reduce the coolant velocity adjacent to a plate containing hot spots. Theoretically, this would reduce the burnout power level margin for normal full power operation. This might mean that the particular core, after experiencing a severe transient, would have to be operated at reduced power or discarded. Calculations indicate that for peak transient hot-spot heat fluxes less than the steady-state burnout heat flux, excessive permanent buckling of the fuel plates should not occur. Furthermore, the occurrence of accidents that would produce heat fluxes in excess of the above are considered to be so infrequent that the rejection of a core upon such an occasion would be of little concern.

1.2 Modes of Operation

Three general modes of operation have been provided for the HFIR.[5] For purposes of the safety analysis they can be briefly outlined as follows. Mode 1 (normal operating mode) is for pressurized op-

[5] *The High Flux Isotope Reactor, a Functional Description,* ORNL-3572, vol. 1 (May 1964).

eration (~600 psi) at full coolant flow and also at 10% full flow. At full flow the power can range from zero to 100 Mw (normal full power operation). The power level at 10% flow can range from zero to 10 Mw (power outage condition). Mode 2 provides for low-power operation at 10% flow and low pressure (vessel head open). The maximum power level under these conditions is about 2.5 Mw. Mode 3 permits very low-power operation with no flow and low pressure (vessel head open). For this case, maximum power level is about 100 kw.

All three modes of operation were considered in the analog analysis. For each mode the appropriate sets of accidental reactivity additions, flow rates, initial power levels, burnout heat fluxes, and safety system characteristics were used. The safety system level and rate trips selected for the three modes of operation are shown in Table I.C.2.

Table I.C.2. Safety System Level and Rate Trips

	Mode of Operation		
	1	2	3
Level trip (Mw)	13–130	3.25	0.130
Rate trip (Mw/sec)	20	0.50	0.020
Minimum change in power to actuate rate trip (Mw)	5	0.125	0.005

For mode 1 operation the level trip is proportional to the coolant flow rate, but all other level trips and all rate trips are fixed. The level and rate trips selected for mode 1 are as low as appears practical for flexibility in operation and for freedom from false scrams due to instrument noise. The level and rate trips for mode 2 operation were set so as to accommodate rather wide variations in the ratio of maximum to average power density resulting from asymmetric operation of the control rods. For mode 3 operation the trip points were set in a manner consistent with that used for mode 1.

In the analog analysis it was necessary for some cases to use a level trip to simulate a rate trip as a result of computer background noise. This was done by using the "minimum change in power to actuate rate trip" or a multiple thereof as a level trip. This substitution was considered equivalent and adequate provided the rate of rise in power level was fast compared to the rate trip being evaluated. For cases where the rate of rise was not adequately fast for the simulated rate trip to be accurate, an actual rate trip or the power level trip appropriate for the mode under investigation was used.

It was also necessary to consider the changing characteristics of the core as a function of time in the fuel cycle. At the beginning of the fuel cycle, when the control plates effectively separate most of the Be-H_2O reflector from the fuel region, the neutron lifetime is just one-half of the neutron lifetime at the end of the fuel cycle. However, the advantages of the longer neutron lifetime at the end of the fuel

cycle are negated to some extent by the existence of a low thermal conductivity aluminum oxide film at the hot spot, greater fuel plate deflection, and, generally speaking, a lower safety-plate differential reactivity worth. In many cases the end-of-cycle conditions result in higher hot-spot plate temperatures than beginning-of-cycle conditions. Therefore, both extreme conditions were considered for all three modes of operation, although the end-of-cycle conditions should only be applicable to mode 1.

Additional pertinent characteristics associated with the HFIR analog model and the three modes of operation are listed in Table I.C.3.

1.3 Reactivity Addition Accidents

1.3.1 Introduction. – Four general types of reactivity accidents, categorized according to their mechanisms for occurrence, were considered. They are as follows:

1. reactivity additions associated with the control elements,
2. reactivity additions associated with "voids" in the central target region,
3. reactivity additions associated with cold water insertion,
4. reactivity additions associated with experiments, primarily the plutonium target in the island.

A summary of the more pertinent analog calculations and results pertaining to accidental reactivity additions is presented in Table I.C.4. It should be emphasized that the results in this table are strictly calculational results that have not been normalized in accordance with experimental data. All evidence available indicates that the calculations are quite conservative; that is, they predict higher temperatures, power, and energy releases than would actually be expected. The entire "Reactivity Addition Accidents" section deals only with calculations. A later section reevaluates the calculated results on the basis of experimental data.

Typical calculated transient characteristics of the HFIR when subjected to a ramp reactivity addition during high-power, mode 1 operation are shown in Fig. I.C.1. These curves illustrate how the fluid film heat transfer coefficient is set equal to zero when the hot-spot heat flux reaches the steady-state burnout heat flux. As indicated by the dashed curve, the coefficient is presumed to return to its original value after the power is substantially reduced. The particular curves shown represent case 4, Table I.C.4.

Several of the cases listed in Table I.C.4 are not discussed in detail herein. These cases were calculated for the purpose of investigating the sensitivity of pertinent temperatures and energy releases to anticipated variations in parameters such as reactivity insertion rate, control element differential worth, initial power level, etc. No strong sensitivities were observed that might tend to alter the conclusions arrived at after analyzing the specific cases discussed in the following paragraphs.

1.3.2 Control Plate Accidents. – Two types of control plate removal accidents were considered. One is the runaway case in which the five shim elements (inner shim-regulating cylinder and four shim-safety plates) are driven out of the reactor with the maximum speed of the shim drives, or the shim-regulating cylinder is driven out with the faster regulating drive. It is also possible to add the velocity of the latter to that of the former, for a maximum shim-regulating cylinder movement of about 1 in., to obtain the worst condition.

Table I.C.3. Characteristics of the HFIR Analog Model

Mode I, Full-Power, Full-Flow, Steady-State Conditions

	Target Region	Target Annulus Region	Fuel Region: Start of Cycle, Nominal	Fuel Region: Start of Cycle, Hot Streak	Fuel Region: Start of Cycle, Hot Spot	Fuel Region: End of Cycle, Nominal	Fuel Region: End of Cycle, Hot Streak	Fuel Region: End of Cycle, Hot Spot	Control Region
Metal heat capacity, C_F, Btu/°F	1.49	0	35.7	35.7	41.4	35.7	35.7	41.4	13.1
Metal heat generation, aP_i, Btu/sec	853	0	92,400	132,500	242,300	92,400	132,500	242,300	627
Mean metal temperature, $\overline{T}_f$, °F	365	125	230	349	428	238	469	627	152
Metal-oxide interface temperature, T_1, °F	199	125	222	337	407	230	457	606	150
Oxide-water interface temperature, T_2, °F	199	125	222	337	407	222	344	417	150
Water inlet temperature, T_i, °F	120	120	120	121	121	120	121	121	120
Water outlet temperature, T_o, °F	136	130	189	257	257	189	255	255	128
Water heat generation, bP_i, Btu/sec	144	264	2721	2775	2775	2721	2775	2775	283
Water transit time, 2τ, sec	0.0417	0.2514	0.0397	0.0403	0.0403	0.0397	0.0418	0.0418	0.0901
$\lambda_1 = aP_i/(\overline{T}_f - T_1)$	5.203	∞	11,555	11,326	11,377	11,555	11,326	11,377	241
$\lambda_2 = (\overline{T}_f - T_1)/(T_1 - T_2)$	∞	−1	∞	∞	∞	1.333	0.1034	0.1131	∞
Temperature coefficient, α_j, (Δk/°F) ($\times 10^{-5}$)	+3.2	+2.7	−9.7[a] −1.0[b]			−4.8[a] −0.5[b]			+1.1

Reflector flow rate, gpm	840
Reflector power level, Mw	3
Primary system flow rate, gpm	15,000
Prompt neutron lifetime, l^*, μsec	
Beginning of cycle	35
End of cycle	70
Effective delayed neutron fraction, β_{eff}	
Beginning of cycle	0.0070
End of cycle	0.0071
Steady-state burnout heat flux,[c] Btu hr^{-1} ft^{-2} (°F)$^{-1}$	2.47×10^6
Fuel region water film heat transfer coefficient, h, Btu hr^{-1} ft^{-2} (°F)$^{-1}$	
Average core	12,000
Hot spot	15,000

Table I.C.3 (continued)

Mode 1, Low Power, Full Flow

Temperatures and heat generation rates reduced to be consistent with initial steady-state power

Temperature coefficients different, depending on initial temperatures

If initial bulk water temperature less than 120°F, burnout heat flux[c] will be $> 2.47 \times 10^6$; assumed $= 2.47 \times 10^6$

Heat transfer coefficients assumed the same

Mode 1, Low Power, 10% Flow

Temperatures and heat generations appropriate

Temperature coefficients appropriate

Burnout heat flux[c] $= 4.70 \times 10^5$

Fuel region water film heat transfer coefficient, h, Btu hr^{-1} ft^{-2} $(°F)^{-1}$

Average core	1970
Hot spot	2460

Mode 2, Low Power, Low Pressure, 10% Flow

Burnout heat flux[c] $= 1.57 \times 10^5$

Heat transfer coefficients same as mode 1, 10% flow

Mode 3, Low Power, Low Pressure, No Forced Flow

Burnout heat flux = 5400

Heat transfer coefficient $\cong$ 300 Btu hr^{-1} ft^{-2} $(°F)^{-1}$

Note: Mode 3 analog calculations did not include heat transfer and associated reactivity feedback. Only nuclear portion, including control plates, was simulated.

Control System Characteristics (also see Table I.C.1)

Initial acceleration was 4g for all calculations discussed in this report

Safety system delay time: 10 msec for modes 1 and 2; 15 msec for mode 3

Scram signal: Rate and level; values dependent on mode of operation

[a]Water.

[b]Fuel plates.

[c]Burnout heat fluxes tabulated for modes 1 and 2 are actually calculated steady-state incipient-boiling heat fluxes. Actual burnout heat fluxes are somewhat greater.

The shim drive speed is 5.75 in./min (0.096 in./sec), and the regulating drive speed is 15 in./min (0.25 in./sec). With the control elements initially at the clean core, symmetrical, critical position, the differential worth of the shim-regulating cylinder and of the set of four shim-safety plates is about 0.01 $\Delta k/k$ per inch. For this initial control element position and for the maximum drive speed condition with all five control elements being withdrawn, the reactivity addition rate would be 0.0044 $\Delta k/k$ per second for the first inch of travel and 0.0019 $\Delta k/k$ per second for about the next 2 in., after which it decreases.

Table I.C.4. Summary of Pertinent Analog Results for Reactivity Addition Accidents. Part 1

Case No.	Mode of Operation	Time in Cycle (days)	Fuel Coolant Velocity (fps)	Initial Steady-State Power (Mw)	Safety System: Initial Differential Worth ($\Delta k/k$ per in.)	Safety System: Scram* Signal (rate or level)	Reactivity Accident: Reactivity ($\Delta k/k$)	Reactivity Accident: Ramp (msec)	Peak Power (Mw)	Heat Flux Peak Hot Spot (Btu hr^{-1} ft^{-2})	Plate[a] Temperature Peak Hot Spot (°F)	Plate Temperature Peak Average (°F)	Bulk Water Temperature Peak Average (°F)	Time-Integrated[b] Power for Transient (Mwsec)	Plate Surface[c] Temperature Nominal Max at Peak Power (°F)
1	1	0	42.0	100.0	0.00058	20 Mw/sec	0.013	30.0	1175	$>2.47 \times 10^6$	2100	590	250	34	598
2	1	0	42.0	100.0	0.00058	20 Mw/sec	0.013	60.0	550	$>2.47 \times 10^6$	1800	450	220	30	
3	1	0	42.0	100.0	0.00058	20 Mw/sec	0.015	75.0	500	$>2.47 \times 10^6$	1900	440	215	30	
4	1	0	42.0	100.0	0.0035	20 Mw/sec	0.013	30.0	1075	$>2.47 \times 10^6$	1850	550	235	28	
5	1	0	42.0	100.0	0.0035	20 Mw/sec	0.015	40.0	1040	$>2.47 \times 10^6$	1875	560	240	28	
6	1	0	42.0	<0.1	0.0035	20 Mw/sec	0.013	0.0	900	$>2.47 \times 10^6$	1150	400	160	21	
7	1	0	42.0	<0.1	No safety		0.013	0.0	1250	$>2.47 \times 10^6$	1600	530	190	30	
8	1	~15	42.0	100.0	0.00059	20 Mw/sec	0.013	30.0	1250	$>2.47 \times 10^6$	3200	800	300	52	693
9	1	~15	42.0	100.0	0.00059	20 Mw/sec	0.01	30.0	775	$>2.47 \times 10^6$	2600	590	245	37	
10	1	~15	42.0	100.0	0.00059	20 Mw/sec	0.008	30.0	475	$>2.47 \times 10^6$	2000	445	210	27	427
11	1	~15	42.0	100.0	0.0035	20 Mw/sec	0.013	30.0	1075	$>2.47 \times 10^6$	2600	670	260	38	623
12	1	~15	42.0	100.0	0.0035	20 Mw/sec	0.011	30.0	675	$>2.47 \times 10^6$	2000	510	220	28	499
13	1	~15	42.0	100.0	0.0035	20 Mw/sec	0.01	30.0	525	$>2.47 \times 10^6$	1750	440	205	22	
14	1	~15	42.0	<0.1	0.00059	20 Mw/sec	0.013	0.0	1030	$>2.47 \times 10^6$	2250	640	250	38	
15	1	~15	42.0	<0.1	0.0035	20 Mw/sec	0.013	0.0	420	$>2.47 \times 10^6$	900	340	170	15	
16	1	0	42.0	100.0	0.00058	20 Mw/sec	0.05/sec		125	2.4×10^6	450	250	160	~11	
17	1	0	42.0	5×10^{-8}	No safety		0.005/sec		170	1.9×10^6				<10	
18	1	0	4.2	<0.1	0.0035	20 Mw/sec	0.013	0.0	900	$>4.7 \times 10^5$	1250	540	200	22	
19	1	0	4.2	<0.1	No safety		0.013	0.0	1250	$>4.7 \times 10^5$	1900	790	280	35	629
20	1	0	4.2	<0.1	No safety		0.015	0.0	1500	$>4.7 \times 10^5$	2050	910	315	40	
21	1	0	4.2	<0.1	0.0035	20 Mw/sec	0.015	0.0	1400	$>4.7 \times 10^5$	1700	770	265	32	
22	1 and 2	0	4.2	5×10^{-8}	0.0035	20 Mw/sec	0.005/sec		32	2×10^5					
23	2	0	4.2	<0.1	0.0035	20 Mw/sec	0.013	0.0	900	$>1.57 \times 10^5$	1300	540	200	22	
24	2	0	4.2	<0.1	No safety		0.013	0.0	1250	$>1.57 \times 10^5$	1900	790	280	35	
25	2	~15	4.2	<0.1	0.00059	20 Mw/sec	0.013	0.0	800	$>1.57 \times 10^5$	2050	780	320	32	
26	2	~15	4.2	<0.1	0.00059	5 Mw/sec	0.013	0.0	720	$>1.57 \times 10^5$	1900	740	310	30	
27	2	~15	4.2	<0.1	0.00059	6 Mw	0.013	0.0	740		1800	700	290	29	
28	2	~15	4.2	<0.1	0.0035	20 Mw/sec	0.013	0.0	300	$>1.57 \times 10^5$	850	370	195	10	

*The effect of a level scram at 130 Mw instead of a rate scram was discussed in answer 19. The 0.013 $\Delta k/k$ 30-msec ramp accident was reevaluated without control rod action in answer 54 and Appendix L.

[a]Plate temperatures above 1950°F indicate melting of the hot spot; actual temperature of molten metal is less by (1950 – 1210) = 740°F. Indicated temperatures between 1210 and 1950°F should be 1210°F. See discussion, p. 73.

[b]Integrated power includes *all* energy generated during transient. In a typical initial 100-Mw case (case No. 1), the duration of the transient is ~75 msec. The energy generated in this time at 100 Mw is 75×10^{-3} sec × 100 Mw = 7.5 Mwsec.

[c]This is the maximum nominal oxide-water interface temperature at the core horizontal midplane at the time the power peaks (does not include hot spot effects). Corresponding saturation temperatures are as follows:

Mode 1 (600 psi): 486°F
Modes 2 and 3 (10 psi): 240°F

Table I.C.4. Summary of Pertinent Analog Results for Reactivity Addition Accidents. Part 2

Case No.	Mode of Operation	Initial Neutron Multiplication Factor (k)	Safety System: Initial Differential Worth ($\Delta k/k$ per in.)	Safety System: Level Trip (kw)	Safety System: Delay Time (msec)	Reactivity Accident ($\Delta k/k$ per sec)	Peak Power (Mw)	Approximate Time-Integrated Power for Transient (Mwsec)	Estimated[a] Plate Temperature, Peak Hot Spot (°F)
29	2	0.95	0.00058	250	10	0.01	12.6	0.6	160
30	2	0.95	0.0035	250	10	0.01	2.0	0.1	120
31	2	0.95	0.00058	500	10	0.01	28.0	1.0	240
32	2	0.95	0.0035	500	10	0.01	5.0	0.2	140
33	3	0.95	0.00058	5	15	0.03	28.0	1.0	240
34	3	0.95	0.0035	5	15	0.03	0.63	0.03	120
35	3	0.95	0.00058	10	15	0.03	80.0	4.0	620
36	3	0.95	0.0035	10	15	0.03	1.8	0.1	120

[a]It was assumed that the coolant average temperature was 120°F and that the control rods were asymmetrical to the extent that the ratio of maximum to average power density was twice the usual value.

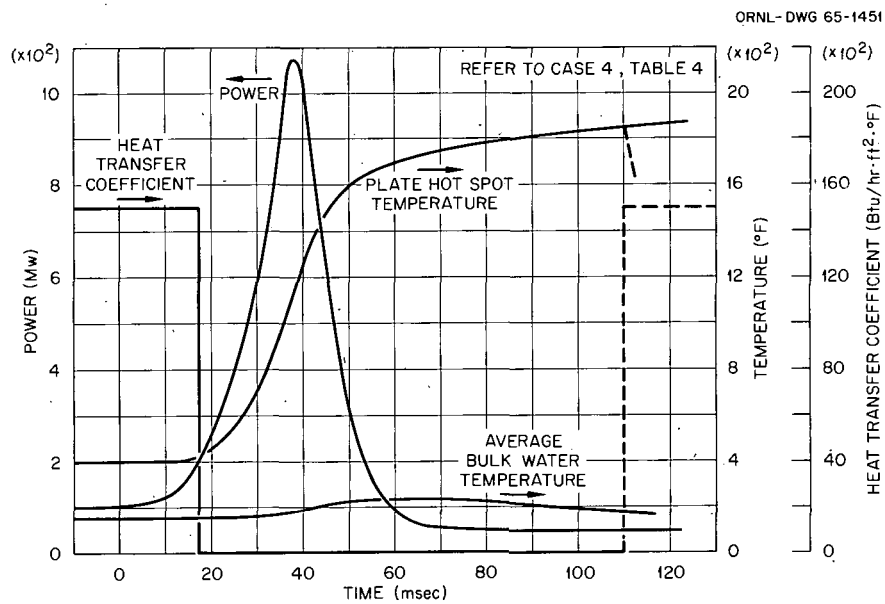

Fig. I.C.1. Typical Transient Curves for a Ramp Reactivity Accident.

If the control elements are in an extreme asymmetrical, critical position (shim-safety plates withdrawn), as they might be during mode 2 and 3 operation, the *initial* differential worth of the safety plates would be reduced to about 0.0008 $\Delta k/k$ per inch, and the reactivity addition rate corresponding to the maximum withdrawal speed would be 0.0032 $\Delta k/k$ per second.

Near the end of the fuel cycle, the maximum reactivity addition rate would be much smaller, and the initial differential worth of the safety plates still would be about 0.0008 $\Delta k/k$ per inch.

The other case in which the control elements can add reactivity accidentally is associated with the structural integrity of the shim-regulating cylinder drive mechanism. The use of a control element that must be inserted against gravitational and hydraulic forces introduces a possible problem in connection with failure of the supporting or drive mechanisms; such a failure would result in withdrawal of the control element and thus in a positive reactivity addition. In the event of a mechanical failure of the drive mechanism, a hydraulic cylinder on the lower end of the drive rod will act as a shock absorber (normally used to balance the downward forces of gravity and pressure on the shim-regulating cylinder drive mechanism) and will limit the shim-regulating cylinder maximum withdrawal speed to 39 in./min (0.65 in./sec), even if the force-balancing feature is depressurized. The corresponding maximum reactivity addition rate would be about 0.0065 $\Delta k/k$ per second.

The results from the analog calculations made in connection with the control element reactivity accidents indicate that for beginning-of-cycle mode 1 operation at full flow and full power and with the safety plates in the least sensitive position (normally should not be in this position) 0.050 $\Delta k/k$ per second can be inserted continuously without the hot-spot heat flux exceeding the burnout heat flux [16].[6] The hot-

[6]Bracketed numbers refer to corresponding cases in Table I.C.4.

spot peak plate temperature calculated for this case was only 450°F, and the total energy release during the brief transient was about 11 Mwsec (this includes *all* energy generated during the transient).

Starting from low power (<100 kw) and full flow (mode 1), the self-shutdown mechanisms alone limited the peak heat flux to less than the burnout heat flux, when reactivity was added at the rate of 0.005 $\Delta k/k$ per second [17]. The peak power in this case was only 170 Mw, and the total energy release was less than 10 Mwsec.

For mode 2 operation the transients resulting from the introduction of 0.010 $\Delta k/k$ per second starting at source level were studied for the two safety plate initial worths and two safety system trip conditions [29–32]. Case [31] is an extreme case wherein the initial safety plate differential worth of 0.00058 $\Delta k/k$ per inch was used with a level trip of 500 kw (corresponds to a rate trip of 2 Mw/sec, which is four times that specified for the mode 2 operation). This case resulted in an increase in hot-spot plate temperature of approximately 120°F; the other three cases [29,30,32] resulted in even lower hot-spot temperature increases.

For mode 3 operation, the calculations were performed with the safety system level trip set at 5 kw and 10 kw (corresponds to rate trips of 20 kw/sec and 40 kw/sec, which are respectively equal to that specified and twice that specified for this mode); the above reactivity insertions resulted in trivial excursions [33–36].

It was concluded from this analysis that reactivity additions resulting from runaway control elements would result in no serious core damage and particularly no melting of the hot spots.

1.3.3 Voids in the Central Target Region. – The existence of a water-moderated flux trap in the HFIR introduces the possibility of reactivity additions resulting from displacement of some of the flux trap water. Just how much reactivity can be added by this means depends upon what stationary objects happen to be in the flux trap at the time the water density is changed. With nothing but water initially in the flux trap, the maximum change in reactivity is about 0.032 $\Delta k/k$; with a typical 300-g plutonium target in the island, the maximum change in reactivity is about 0.015 $\Delta k/k$. The optimum void fractions[7] associated with these changes are 0.70 and 0.42 respectively.

There are several ways in which voids might possibly be added to the flux trap during normal operation with the plutonium target in place. These include (1) the formation of a vortex, in which case the void could be maintained in the island for a significant period of time; (2) the sweeping in of bubbles with the coolant flow, in which case the void could be maintained only if enough bubbles were available; and (3) the blockage of flow to the target and subsequent steam formation in the flux trap. Cases 1 and 2 appear to be the most serious because the voids can enter more rapidly. Assuming that the voids are swept into the high-coolant-velocity region of the target first, the effective ramp at full flow for a 0.42 void fraction is about 0.03 sec. The associated maximum change in reactivity is only 0.013 instead of 0.015 $\Delta k/k$, because there is not enough space for the optimum void fraction in the high-velocity region. The coolant velocity in the low-velocity region of the target is low enough that voids associated with it can be ignored when considering this particular accident. At 10% flow (modes 1 and 2), the corresponding

[7]These fractions are defined as void volume divided by total flux trap volume.

ramp time is 0.3 sec. For mode 3 (zero flow) the effective ramp associated with the free-bubble velocity is about 0.6 sec, and since this velocity is essentially the same for both the "low" and "high" velocity regions of the target the associated reactivity is 0.015 $\Delta k/k$.

In the analog analysis it was assumed that the voids entered on the above ramps and remained in the flux trap. The results indicate that for mode 1, full-power operation, typical safety plate worth, and clean core condition [4], the temperature at the hot spot will exceed the melting temperature, but not enough heat will be added to result in incipient melting of the localized spot. The peak average plate temperature was about 550°F, and the total energy release was 28 Mwsec. For the end-of-cycle conditions [8], the calculations indicated that the hot spot melted, achieving a temperature of about 1250°F in excess of the melting temperature of the aluminum plates; the corresponding average plate temperature and total energy release were about 800°F and 52 Mwsec respectively.

Within about two days from the end of the fuel cycle, the safety rod differential worth is significantly greater than at the end of the cycle. Under these conditions [11], the hot spot melted and the calculated temperature exceeded the melting temperature by 650°F. The corresponding average plate temperature was 670°F, and the total energy release was 38 Mwsec.

The amount of reactivity that can be inserted on a 30-msec ramp and just produce melting at the hot spot for the above operating conditions was calculated to be 0.011 $\Delta k/k$ [12] for no less than two days from the end of the cycle and 0.008 $\Delta k/k$ [10] at the end of the cycle.

For low-power (<100 kw), full-flow mode 1 operation, a 0.013 $\Delta k/k$ step insertion (used to approximate a 30-msec ramp) for a clean core [6,7] results in no melting either with or without safety action, but at the end of the fuel cycle [14] the calculation indicates melting of the hot spot; the calculated temperature exceeds the melting temperature by 300°F. For more than about two days from the end of the cycle [15], no melting occurred.

Reducing the mode 1 flow rate to 10% [18–22] did not change the above low-power results significantly.

Under mode 2 and mode 3 conditions, a 0.013 $\Delta k/k$ step at low power [26] resulted in no melting at either the beginning or end of the cycle with the safety system rate trip at 5 Mw/sec or less. As shown in Table I.C.2, the selected rate trip for mode 2 is 0.5 Mw/sec and for mode 3 it is 0.02 Mw/sec.

It is interesting to note that in the cases for which melting was predicted, plate surface temperatures well in excess of the saturation temperature were obtained prior to the peak in power. This means that negative feedback from voids would result in lower peak powers and temperatures than indicated.

Considering the degree of conservatism incorporated in the analog model and the expected low frequency of occurrence of void accidents involving more than 0.008 $\Delta k/k$, it is not expected that this type of accident would constitute a serious monetary loss or a significant hazard as a result of possible fission product release.

Void accidents involving appreciably more than 0.013 $\Delta k/k$, such as might be achieved without the target in the flux trap, have not been analyzed in detail because adequate precautions are being taken to ensure against them; the necessity for this is obvious. At the present time it is specified that the reactor will not be operated without the target or its equivalent in the flux trap. Thus it is only neces-

sary to provide the necessary shutdown margin to accommodate the accidental addition of 0.032 $\Delta k/k$ during shutdown with all safety plates in, and this has been done as will be set forth in Sect. 2.

1.3.4 Reactivities Associated with Experiments. – The insertion of an all-aluminum target in the flux trap adds reactivity because of the flux trap positive void coefficient and the low absorption cross section of the aluminum. However, when the target contains about 300 g of ^{242}Pu and has been irradiated for about 0.1 year, the absorption cross section is sufficient to result in essentially no net negative reactivity change. For purposes of the safety analysis, an uncertainty of about 0.01 $\Delta k/k$ was considered. Therefore, if the target were to fall out of the flux trap (such an accident can really be classified as "unreasonable"), 0.01 $\Delta k/k$ would be added at a maximum rate that is consistent with the maximum flow rate through the target. Comparing this case with the void accident cases shows that no core damage would result.

The other experimental facilities in the HFIR are located sufficiently far from the core to prevent any significant reactivity changes. Even flooding of the beam holes did not produce a detectable change in reactivity in the HFIR critical experiments.

1.3.5 Cold-Water Accidents. – The worst cold-water accident would, in principle, occur when the coolant in the core is hot, because the temperature coefficients are greatest and because there is a greater temperature difference available. For a given difference in water temperatures, the greatest increase in reactivity would occur if the cold water entered only the fuel region. A change in fuel region temperature from 155°F (average fuel region coolant temperature at 100 Mw) to 32°F would add something less than 0.013 $\Delta k/k$. For a more probable case, in which the cold water enters all parallel regions of the reactor, the same change in temperature, making allowances for the different coolant velocities, would add approximately 0.008 $\Delta k/k$.

One way in which the above temperature changes might possibly take place is associated with mode 3 operation of the reactor. With no flow through the primary system, it is possible that the water in the heat exchangers could be at a rather low temperature and the water in the reactor vessel at a relatively high temperature while running low-power experiments. If suddenly one or more of the three main circulating pumps were turned on,[8] cold water would be injected into the core. The rate at which the temperature would change in the core is dependent upon how quickly the pumps attain full speed, how much mixing takes place between the pump and core, and on what type of temperature gradients existed just prior to the accident. Assuming that all three pumps are turned on simultaneously (contrary to normal pump startup procedure), the shortest effective ramp conceivable for the above reactivity additions is about 60 msec. The minimum rate, assuming instantaneous starting of the pumps and no mixing, is about 30 msec. Analog calculations [26] indicate that 0.013 $\Delta k/k$ can be stepped in without hot-spot melting. Therefore, there appears to be no serious problem with a cold-water accident for mode 3 operation.

---

[8]As mentioned previously, it is not desirable in these studies to discuss the question of credibility. However, to avoid implying that there are not operating procedures and instrumentation that normally guard against inappropriate operation of the cooling system which might result in cold-water accidents, the reader is referred to detailed discussions on the subject in ORNL-3572.

During mode 1 and mode 2 operation, similar types of cold-water accidents would be less serious than the one described for mode 3, because the water would already be circulating, and therefore the change in temperature would be less. The biggest temperature differences for modes 1 and 2 would occur with the flow rate initially at 10% full flow. Calculations [18,26] indicate that for significantly worse conditions no fuel plate melting would occur.

1.4 Significance of SPERT Data

In attempting to make use of SPERT data for partially analyzing the transient behavior of the HFIR, two approaches were taken. The first was to use the HFIR analog model, with appropriate SPERT input data, to calculate specific SPERT cases. The purpose in doing this was to determine whether or not the HFIR model was conservative. Since the applicable SPERT tests had relatively low coolant flow rates, were unpressurized, had only self-shutdown mechanisms, and started at essentially zero power level, a direct comparison with the HFIR at power could not be made.

The results of the comparison with the available SPERT data indicated that the HFIR model was quite conservative for the low-power conditions. Furthermore, there were indications that the absence of voids in the analog model was responsible for a significant portion of the conservatism. Judging from a comparison of calculated water film temperatures for the low- and high-power cases, it was concluded that voids would also be present in similar transients at high power; thus it was further concluded that the model should be conservative for the corresponding initial-high-power cases. Since the degree of conservatism is not known, one cannot really take advantage of it in a quantitative sense. However, an indication of conservatism provides additional confidence in an analytical method that would have been used unhesitantly in the absence of the experimental data.

The SPERT core and test calculated was that identified as SPERT IV DU-12/25;[9] physical characteristics of this core and the HFIR core are compared in Table I.C.5.

The particular SPERT experiments were conducted at atmospheric pressure, using effective step changes in reactivity of approximately 0.00973 and 0.0126 $\Delta k/k$. Calculations were made with these same step changes, but no void coefficients were included. In order to compare the "experimental" results with the calculated results, the SPERT data were extrapolated to a pressure of 2500 psi to obviate the necessity for including voids in the calculation; the result was a 30% increase in peak power, a 100% increase in energy release, and about a 60% increase in plate temperatures.[10] These data are compared with the calculations in Table I.C.6. Also included in Table I.C.6 are the low-pressure experimental data.

As indicated by the comparison of results in Table I.C.6, the calculation is conservative by a considerable amount. In the actual experiments, there was no evidence of core damage. The calculations, however, indicate melting for both cases, even though hot-spot factors were not included.

---

[9] *Quarterly Technical Report, SPERT Project, January, February, March, 1963*, IDO-16893 (May 20, 1963).

[10] F. Schroeder (ed.), *Quarterly Technical Report, SPERT Project, October, November, December, 1960*, IDO-16687 (June 1, 1961).

Table I.C.5. Characteristics of SPERT (DU-12/25) and HFIR Cores

	SPERT, DU-12/25	HFIR
Core geometry	Square parallelepiped	Cylindrical flux trap
Type of fuel element	Aluminum-clad plates, U-Al alloy meat	Aluminum-clad plates, U_3O_8-Al dispersion meat
Fuel loading, kg	3.8	9.4
Core dimensions, cm		
Outside diameter		44.0
Inside diameter		14.0
Length of side	38.0	
Height (active)	61.0	50.8
Effective core volume, liters	62.2	50.8
Fuel plate surface area, cm^2	2.05×10^5	3.99×10^5
Surface-area-to-volume ratio, cm^{-1}	3.3	7.85
Fuel plate thickness, cm	0.152	0.127
Coolant channel thickness, cm	0.455	0.127
Metal-to-water ratio (based on fuel plates only)	0.335	1.0
Overall metal-to-water ratio	0.66	1.0
Fuel plate heat capacity, Btu/°F	23.2	35.7
Prompt neutron lifetime, μsec	57.0	35.0[a]
Moderator temperature coefficient in fuel region, $\Delta k/°F$	-8.33×10^{-5}	-5.8×10^{-5}[b] -8.7×10^{-5}[c]
Fuel plate temperature coefficient, $\Delta k/°F$	-0.33×10^{-5}	-1.0×10^{-5}[b] -1.6×10^{-5}[c]
Void coefficient, fuel region average, $\Delta k/\%\rho$	0.0024	0.0029
Effective delayed neutron fraction	0.007	0.0071
Power density ratio, nominal maximum-to-average	2.4	1.45

[a]Clean core condition.
[b]Clean core, 68°F moderator temperature.
[c]Clean core, 155°F moderator temperature.

Table I.C.6. Comparison of Experimental and Calculated SPERT (DU-12/25) Results

Reactivity Step Insertion ($\Delta k/k$)	Experimental Stable Period (msec)	Peak Power (Mw)			Total Energy Release During Transient (Mwsec)			Maximum Plate Temperatures (°F)[a] At Peak Power			Maximum		
		Experimental		Calculated	Experimental		Calculated	Experimental		Calculated	Experimental		Calculated
		10 psi	2500 psi		10 psi	2500 psi		10 psi	2500 psi		10 psi	2500 psi	
0.00973	20.7	169	220	440	9.6	19.1	38	300	435	1340	307	450	1960
0.0126	10.1	505	657	1625	12.2	24.4	66	364	540	3000	378	560	4440

[a]Does not include hot-spot conditions. Calculated values do not consider heat of fusion; temperatures above 1210°F should be corrected for this fact; see p. 73.

Part of this conservatism probably results from the use of a water film heat transfer coefficient (h) that is too small and/or a percentage heat generation rate in the coolant (b) that is too small. Increasing the values of these two parameters would reduce the plate temperatures, peak power, and total energy release, because of less heat generation in the plate, a smaller resistance to heat transfer out of the plate, and because there would be greater negative feedback.

Evidence of low h and b values is obtained by comparing plate temperatures at the peak power and at the peak temperature. The experimental data show a small percentage difference between these two temperatures, while the calculated percentage difference is relatively large.

The h and b values used in all the HFIR calculations have purposely been low so as to result in conservative plate temperatures. However, in previous HFIR analog studies[11] and also during the SPERT-HFIR studies, the effect of varying h was investigated. The results indicated that a 40% increase in h reduces the peak power by only 3% and the maximum plate surface temperature by only 14%. Furthermore, increasing b from 2.5% to a reasonable upper limit of about 6% does not make a very significant difference in the lack of agreement between experiment and calculation. Thus, at least for the high-pressure cases, it appears that there is an additional feedback mechanism that is not being accounted for in the calculation. It is interesting to note, however, that for the high-pressure comparison the "experimental" temperatures were not above the saturation temperature. Therefore, if one discounts the possibility of significant void formation in hot-spot regions that were not instrumented, and if the method used for extrapolating from low pressure to 2500 psi was reasonably correct, he must conclude that at least at high pressure there was a shutdown mechanism not associated with void formation in the usual sense. Whether or not the same or another unaccounted for feedback mechanism exists at higher power ($\sim$100 Mw) can only be speculated upon. If the mechanism is associated with voids, it probably exists at higher power levels also.

The other approach used in trying to make use of SPERT data involved a direct analytical comparison of the SPERT and HFIR transients resulting from the same reactivity additions. A comparison of the physical characteristics of the two cores indicated that the HFIR, with no safety system other than the self-shutdown mechanisms, should experience a less severe transient than the particular SPERT core of interest, when both cores are subjected to the same reactivity addition. The reason for this is that the HFIR, while having about the same void and temperature coefficients, has almost 2.5 times the surface-area-to-volume ratio and just a little over one-half the water-to-core volume ratio as the SPERT core. This means that for a given increase in fuel plate temperature the increase in moderator temperature and thus the negative reactivity feedback are considerably greater for the HFIR. This assumes of course that the greater flow resistance associated with the narrower HFIR coolant channels will not impede the density change to the extent that the potential improvement will be negated.

Another feedback mechanism which favors the HFIR is the fuel plate expansion reactivity coefficient. This coefficient for the HFIR is about three times that for the particular SPERT core. Since the plate

---

[11] N. Hilvety, R. D. Cheverton, and O. W. Burke, *Preliminary Analysis of HFIR Transients Resulting from Ramp Reactivity Additions*, ORNL-CF-63-5-45 (May 9, 1963).

coefficient is really a moderator expulsion coefficient, the above comment relating to the increased flow resistance of the narrower HFIR channel applies here, too.

The particular SPERT core being compared with the HFIR has one clear advantage: it has a longer prompt neutron lifetime when compared to the HFIR clean core condition (57 compared to 35 μsec). For the end-of-cycle condition, the neutron lifetime for the HFIR is about 70 μsec.

Results from the SPERT-HFIR comparison calculations are shown in Table I.C.7. When evaluating the comparison, several things need to be kept in mind. The calculations did not include any hot-spot factors but did include the nominal maximum-to-average power density ratios (2.4 for SPERT and 1.45 for the HFIR). (Plate temperatures for these "maximum" power density spots and for the average core are tabulated.) Neglecting the possible effect of power distribution on reactivity feedback, a comparison of the average plate temperatures is probably more indicative of the differences to be expected from the different SPERT and HFIR core characteristics.

In the above calculations all reactivity feedback was based on average core conditions. The inclusion of feedback from properly weighted "hot" areas of the cores, where the reactivity importance might be greater, should decrease the extent of the transient. However, because the SPERT core has a greater maximum-to-average nominal power density ratio than that for the HFIR, it is possible that inclusion of such a factor would show that on a relative basis, SPERT transient temperatures and power densities would not be so much higher than those for the HFIR.

Two other simplifications used in these HFIR-SPERT calculations involved the use of a constant h value, and the heat of fusion of the fuel plates was not accounted for. Had h been reduced to essentially zero when the burnout heat flux was reached, the corresponding calculated temperatures would have been relatively higher for SPERT. To account for the heat of fusion, all plate temperatures between 1210 and 1950°F should be 1210°F, and all temperatures above 1950°F should be reduced by 740°F.

The application of the above "normalizing" conditions and second-order corrections does not alter the conclusion that plate temperatures and heat fluxes for the HFIR would actually be significantly lower than in the particular SPERT core, when subjected to the same reactivity addition. Since the SPERT core suffered no apparent damage when subjected to a 0.0126 $\Delta k/k$ step change, it is further concluded that the HFIR would not be damaged by the same reactivity addition, which is about as large as would be considered "reasonable." This latter conclusion is, of course, applicable to the initial-low-power, low-flow-rate condition only. However, there is no apparent reason why the conclusion would not also be applicable for higher powers and flow rates. Even so, since there is insufficient high-power SPERT data to compare with, one can at best conclude that the method for analyzing the high-power cases is conservative.

In view of the physical differences in the SPERT and HFIR cores, a further evaluation of the calculated results is of interest. It is observed in Table I.C.7 that the peak average power density calculated for the HFIR was about 1.7 times that calculated for SPERT, indicating that the negative feedback per unit power density was less for the HFIR in spite of its lower water volume and greater heat transfer surface area per unit core volume. The reasons for this are that the HFIR has about 2.0 times as much aluminum (fuel plate) per unit core volume to store heat in during a transient, and the HFIR power rise

Table I.C.7. Comparison of SPERT and HFIR Calculated Transient Characteristics

Reactivity Step Insertion ($\Delta k/k$)	Coolant Velocity (fps)	h [Btu hr^{-1} ft^{-2} ($^{\circ}$F)$^{-1}$]	Peak Power (Mw)	Peak Average Power Density (Mw/liter)	Energy Release Per Unit Core Volume at Time of Peak Power (Mwsec/liter)	Total Energy Release Per Unit Core Volume (Mwsec/liter)	Peak Maximum[a] Plate Temperature[b] ($^{\circ}$F)	Peak Average Plate Temperature[b] ($^{\circ}$F)	Peak Maximum[a] Heat Flux[c] (Btu hr^{-1} ft^{-2})
					SPERT				
0.00973	12	3.5×10^3	440	7.1	0.29	0.61	1960	890	6.4×10^6
0.0126	12	3.5×10^3	1625	26.1	0.56	1.06	4440	1980	15.0×10^6
0.0126	12	4.93×10^3	1575	25.3	0.53	0.98	3800	1700	17.7×10^6
					HFIR				
0.00973	5	2.1×10^3	420	8.3	0.20	0.39	950	450	1.6×10^6
0.00973	12	4.4×10^3	410	8.1	0.20	0.35	760	380	2.6×10^6
0.00973	20	6.4×10^3	410	8.1	0.20	0.37	660	340	3.3×10^6
0.00973	42	10.5×10^3	420	8.3	0.20	0.39	560	310	4.5×10^6
0.00973	42	2.1×10^3	480	9.4	0.22	0.47	1100	510	2.0×10^6
0.0126	5	2.1×10^3	1600	31.5	0.39	0.73	2000	890	3.8×10^6
0.0126	12	4.4×10^3	1550	30.5	0.35	0.67	1650	760	6.2×10^6
0.0126	20	6.4×10^3	1540	30.3	0.33	0.65	1450	690	8.0×10^6
0.0126	42	10.5×10^3	1510	29.7	0.33	0.63	1225	610	10.8×10^6

[a]Includes only nominal maximum-to-average power density ratio; does not include hot-spot effects.

[b]Calculated values do not consider heat of fusion, and temperatures above 1210°F should be corrected for this fact.

[c]Assumes constant h value.

is quicker because of the shorter neutron lifetime. The effect of the latter can be factored out to some extent by comparing total energy release per unit volume at the time the transient is turned around. As indicated in Table I.C.7, the total energy release for the HFIR is about 30% less than for SPERT. Of course the peak power density and the total energy density, per se, are of little consequence, since plate temperatures are more indicative of core damage.

2. Shutdown Margin

2.1 Introduction

The discussion of shutdown margin in the HFIR requires that the following factors be recognized as significant:

1. The fixed geometry of the core precludes the removal or rearrangement of the fuel as a means of adjusting reactivity.
2. The same economic considerations which dictated the fixed geometry can impose an economic penalty on an excessive shutdown margin.
3. Variations in core worth will occur as a result of unplanned variations in manufacture and as may be planned for increased utilization. Variations will also occur as a result of changes in the reflector and target.
4. Control plate worth will diminish with time until ultimately replacement will be required in order that an adequate shutdown margin may be maintained.

2.2 Shutdown Margin Criteria

It shall be possible to shut down the reactor and maintain a shutdown condition at all times, even when any two of the following independent events occur simultaneously.

2.2.1 Occurrence of an Optimum Void in the Trap Region. – This can result in a $\Delta k/k$ increase of about 0.015 if the target is installed and about 0.032 if the target is not in place.

2.2.2 Removal of the Target. – Except for the short time required to effect the change, the target or its equivalent will remain in place at all times. The shutdown margin must be sufficient to keep the reactor subcritical in the event a void occurs simultaneously with the removal of the target. The removal of the target will cause a change in reactivity which varies from a maximum of $+0.006\ \Delta k/k$ to a minimum of $-0.008\ \Delta k/k$ depending on the irradiation history. Introduction of the optimum void without a target will increase k by about 0.032.

Control plate withdrawal without the target or its equivalent in place is to be prohibited. Operating procedures will require all control elements to be fully inserted and mechanically locked during fuel loading operations. The occurrence of a void with the target removed and with the control elements withdrawn therefore requires the simultaneous occurrence of three independent events or failures and is not to be included in the requirements for shutdown margin. As in all reactors, manual manipulation of the fuel and control elements must be controlled administratively, and a succession of errors can lead to unwanted criticality. In this respect, manipulation of the target is no different.

2.2.3 Complete Withdrawal of Any One Control Element. – This situation will occur during testing periods. Should an optimum void occur simultaneously with complete withdrawal of one control element, the reactor must be maintained subcritical by the four remaining elements. The optimum void can increase reactivity by 0.015 $\Delta k/k$, and withdrawal of the shim-regulating cylinder, which is worth more than any one of the others, can increase reactivity by approximately 0.014. The total increase in reactivity resulting from a void and complete withdrawal of a control plate is about 0.029.

2.2.4 One Control Plate Fails to Scram. – Inasmuch as the shim-regulating cylinder does not scram in the sense of providing a rapid insertion, the shutdown, if required as a result of the occurrence of an optimum void, must be accomplished, with the two elements immobilized, by the remaining three safety plates. Introduction of a void can increase reactivity by 0.015 $\Delta k/k$, and movement of the shim-regulating cylinder and one of the shim-safety plates from the inserted position to the position where the reactor would normally be critical with all rods symmetrical increases reactivity by about 0.01. The total increase in reactivity for this case would be about 0.025.

2.2.5 Occurrence of a Startup Accident. – A catastrophic failure of the control system in which all control elements are being withdrawn at maximum speed requires safety release in order to stop the withdrawal of the four shim-safety plates and to immobilize the shim-regulating cylinder.

If one safety plate fails to scram and continues to move to the fully withdrawn position, we would have a case similar to the condition discussed under event 2.2.4 above, except that one plate would be fully withdrawn with the shim-regulating cylinder at the critical position. This condition would increase the reactivity above that of the shutdown reactor by about 0.04 $\Delta k/k$.

The simultaneous occurrence of a startup accident and an optimum void would require a shutdown margin no greater than the one discussed above (see discussion under event 2.2.4).

Combination of the above events can be summarized into four significant cases, in each of which it is required that the reactor be subcritical. This is shown in Table I.C.8.*

Certain mechanical failures can be anticipated, such as the jamming of a control plate during testing prior to startup (see event 2.2.3 above), which might require undue reduction of the shutdown margin in order to remove the target and fuel elements. Because of the fixed geometry of the core, the usual research and test reactor procedures of removal of individual fuel elements would not be possible. If such a situation occurs, it may be necessary to employ temporary poisons** to ensure an adequate margin during the removal of the target and the fuel. If necessary, this can be accomplished by the insertion of poison strips in the fuel elements or by the addition of poison to the reactor water. The insertion of poison strips appears most desirable as it does not require cleaning up the coolant after use; techniques necessary for insertion of the strips are being developed and will be demonstrated during the preneutron tests on the assembly.

---

*Further discussed in answer 20.

**Further discussed in answer 22A.

Table I.C.8. Cases for Which Core Must Be Subcritical

Case	Events	Control Plate Position	Flux Trap Condition
I	2.2.1 and 2.2.2	All plates fully inserted	Optimum void, no target
II	2.2.1 and 2.2.3	Four plates inserted, any one plate fully withdrawn	Optimum void, with target
III	2.2.1 and 2.2.4	Three out of four scram from critical	Optimum void, with target
IV	2.2.5	Three out of four scram from critical, one shim safety fully withdrawn	No void, with target

2.3 Measurement of Shutdown Margin

In order for the criteria for shutdown margin to have significance in terms of reactor operation, it is necessary to have a high degree of confidence that the criteria are being met. The details of the tests which will be applied to ensure that the criteria are being met have not been worked out at the present time; however, it will be required that the tests be conducted in such a way as to not unduly decrease the safety of the reactor during the tests.

2.4 Critical Experiment Results

Experimental data associated with HFIR control plate worth and shutdown margin were obtained from a series of critical experiments (HFIRCE-2 and -3). The most recent experiments (HFIRCE-3) were conducted on a core that is identical to the first production cores with the exception of the burnable poison loading and a diametral dimension. The difference in the latter is insignificant, but the ^{10}B loading in the first several production cores is greater than in the HFIRCE-3 core. The control plates used most recently in the critical experiment are identical to those that will be used in the HFIR. They contain an Eu_2O_3 black region, a tantalum gray region, and an aluminum follower. The worth of these rods is expected to be slightly different in the HFIR than in the HFIRCE-3 experiments because of a slightly different water content in the control region.

The target used in the HFIRCE-3 is a mockup of the present design of the reactor target and simulates its most reactive condition. The feed material for the reactor target consists of 310 g of PuO_2 with 1% ^{239}Pu, 1% ^{241}Pu, and the rest ^{242}Pu. In the critical experiment target these materials and appropriate daughter products were simulated with Ag, ^{235}U, and ^{238}U. In both targets, the ratio of metal (aluminum) to water is 0.75.

Table I.C.9 summarizes the criticality measurements made with the Eu_2O_3-Ta-Al plates and the estimated maximum criticality conditions for the HFIRCE-3 core and the first and second production cores in the HFIR. These measurements and estimates were made with the control plate and void conditions noted in Table I.C.8, and therefore the values set forth as the amount of $\Delta k/k$ subcritical may be regarded as the excess shutdown margin.

Table I.C.9. Excess Shutdown Margin at 20°C for Cases I Through IV of Table I.C.8

Case	Excess Shutdown Margin, $-\Delta k/k$			
	HFIRCE-3[a]	HFIRCE-3[b]	First Production Core[c]	Second Production Core[d]
I	0.0513	0.0513	0.0538	0.0408
II	0.0363	0.0226	0.0251	0.0121
III	0.0235	0.0167	0.0192	0.0062
IV	0.0167	0.0099	0.0124	~0.0

[a]HFIRCE-3 fuel elements in HFIRCE-3 facility.
[b]HFIRCE-3 fuel elements in HFIR facility.
[c]Fuel elements being fabricated by ORNL, installed in HFIR facility.
[d]Fuel elements being fabricated by vendor, installed in HFIR facility.

The first several production cores will contain the same amount of fuel (9.40 kg of ^{235}U) but more burnable poison (^{10}B) than the HFIRCE-3 core. The ^{10}B loading of the inner element of the first production core was increased from the specified 2.12 g for HFIRCE-3 to 3.6 g. The ^{10}B loading for the second and subsequent production cores has been set at 2.80 g. These changes were made to accommodate a change in the control region water content and to accommodate possible differences in fuel and burnable poison loadings. The poison loading for the first production core was based on the worth of a set of Ag-Ni-Al control elements, while the loading for the second and subsequent cores was based on the worth of the Eu_2O_3-Ta-Al elements, which were not available for the early tests. In arriving at the amount of boron to add to the production cores, it was assumed that the HFIRCE-3 core had the least reactive combination of fuel and poison loadings permitted within specifications and that the production cores would have the most reactive combination permitted within specifications. For this very unlikely combination of circumstances, the minimum shutdown margin at room temperature is calculated by extrapolation of HFIRCE-3 results to be essentially zero (column headed "Second Production Core[d]" in Table I.C.9).

2.5 Reactivity Accountability

A summary of reactivity accountability for a core loading built to the second production core specifications is given in Table I.C.10. The target referred to in Table I.C.10 is the target that was used in the HFIR critical experiments. It contains 8.35 g of ^{235}U, 127.9 g of ^{238}U, and 107.6 g of Ag; the metal-to-water ratio (by volume) is 0.75 over the active length of the target. Considering the most recent set of heavy-element cross sections, this target corresponds to an initial ^{242}Pu loading of 300 to 480 g, the larger value being the most probable, and the smaller value being the most conservative insofar as positive reactivity and heat removal are concerned. At approximately 0.4 year of irradiation the Pu target will have its maximum concentration of ^{245}Cm and thus its maximum positive reactivity effect on the core.

Table I.C.10. Summary of Reactivity Accountability for the Second Production Core

Parameter	Reactivity (Δk) Time in Cycle (days) 0	2	14
Fuel worth with following core conditions: no boron burnable poison; no target; no Be poisoning; zero power at 70°F	0.135[a]		
Boron burnable poison	−0.050[a]	−0.037	−0.009
Temperature deficit (evaluated with the HFIRCE-3 target,[b] zero power at 70°F to 100 Mw)	−0.004		
Simulated plutonium target, based on HFIRCE-3 target[b]			
Maximum (time zero and again at 0.4 year)	+0.008[a]		
Minimum (0.1 year)	−0.001		
$^{135}Xe + {}^{149}Sm$ (at power)	0	−0.049	−0.053
All fission products	0	−0.053	−0.086
Be poison ($^{6}Li + {}^{3}He$)			
Time zero	0[a]		
0.2 year	−0.013		
5 years	−0.016		
Beam tube flooding	~0		
Fuel loading tolerance (±1%)	±0.0015		
Boron loading tolerance (±10%)	±0.0038		
Fuel distribution tolerance (±10%)	±0.0054		
Boron distribution tolerance (±35%)	±0.0023		
Minimum $k_{eff}-1$ (clean core, 100 Mw)	0.054		
Typical nominal $k_{eff}-1$ (clean core, 70°F)	0.093		
Maximum $k_{eff}-1$ (clean core, 70°F)	0.106		

[a]These reactivities used for "typical nominal" case.
[b]See text for description of target.

If the initial target loading contains 3 g of ^{239}Pu and 3 g of ^{241}Pu in addition to the ^{242}Pu, the reactivity effect of the clean target will be the same as the above 0.4-year target.

The use of a burnable poison in the HFIR introduces the possibility of achieving a higher neutron multiplication factor in a partially burned core than in a clean core because of burnable poison burnup. Such a case might exist, depending on how much reactivity is initially controlled by the burnable poison, if the partially burned core is set aside for decay of the xenon. For the present HFIR design the burnable poison loading is small enough so that for all conditions the maximum neutron multiplication factor exists at the beginning of the fuel cycle.

Another time-dependent variable that affects the reactivity of the core is the poison (^6Li, ^3He) concentration in the beryllium reflector. As indicated by Table I.C.10, most of the poison buildup takes place in the first two or three months. If the innermost portion of the beryllium reflector (removable reflector) is used without replacement for more than about three months, the poison will result in a very significant decrease in core lifetime compared to that achievable with "clean" beryllium. The reason for this is that the beryllium poison does not contribute significantly to the shutdown margin since it is located outside of the already "black" control region. At the end of the fuel cycle the beryllium poison will, of course, capture neutrons that otherwise would be reflected to the core. Thus, it is not possible to tailor either the fuel or burnable poison loadings separately to compensate significantly for the beryllium poison buildup; this must be done by replacing the removable beryllium reflector periodically or by adding both fuel and burnable poison.

The amount of reactivity permitted in a particular core assembly will depend upon the worth of the Eu_2O_3-Ta-Al control plates, and the minimum permissible plate worth will depend upon the economics associated with the decreasing core life as the control plate worth decreases. It is estimated that at least 50 Mwyr of operation will be required to significantly reduce the integral worth. After that time the change from successive core loadings will be very small and readily checked with the standard control plates and core[12] or by other means.

APPENDIX D

MAXIMUM ENERGY RELEASE FROM CORE FLOW BLOCKAGE IN THE HFIR*

1. Introduction

The flow blockage accident for the HFIR core has been analyzed for the maximum energy release which could reasonably result. This accident is defined, for the purposes of analysis, as the instantaneous cessation of flow and the corresponding convection cooling of some or all of the fuel element plates in the HFIR core. For a conservative result, all instrumented shutdown and power setback mechanisms such as a decreased flow signal or high fission product activity are assumed not to operate; and shutdown reactivity must therefore originate from a self-shutdown mechanism. The latter assumption is made not because the operation of such power-limiting mechanisms is doubtful, but in order to circumvent the questions of whether or not such mechanisms have "safety system" reliability and the time response of such mechanisms after a flow blockage.

The possible consequences of any flow blockage in the HFIR core include meltdown and distortion of fuel plates within about a second because of the high power density at full 100 Mw (thermal) power

---

[12]The core and Eu_2O_3-Ta-Al control plates used in the HFIRCE-3 experiments, and which will be used to attain initial criticality in the HFIR, will not be operated at a high power and will be preserved as "standards" for use in future tests to help determine the sources of changes in reactivity observed in the reactor.

*Appendix I and question 55 further consider energy releases from the aluminum-water reaction.

level. The main concern is for a flow blockage of a small portion of the core such that the negative reactivity effects may not prevent sufficient energy accumulation that the Al-H_2O reaction could occur to a significant extent. The exact sequence of events leading up to a mechanism terminating the full power generation for such a situation cannot be stated with certainty. However, SPERT transient tests with aluminum-clad, plate-type fuel element cores provide information on the dominant self-shutdown mechanisms for such cores. Also, the SPERT I destructive test series gives valuable insight to the character of the energy release and consequent core damage as the rate and amount of energy generation are increased.

Results of in-pile and out-of-pile research on metal-water reaction propagation provides a basis for estimating the maximum credible energy release from aluminum-water reaction following a flow blockage. Using conservative estimates of the self-shutdown mechanisms of the HFIR core coupled with unrealistically high energy release values per fuel plate, the maximum credible energy accumulation which could dynamically load the HFIR pressure vessel is determined.

2. Energy Sources

Potential sources of energy causing heating in blocked regions of the core are fission heat and chemical energy both from the reaction between aluminum and U_3O_8 inside the fuel element, and between the aluminum cladding and H_2O coolant.[1] Minimum temperatures at which a significant chemical reaction is believed to occur are 1500°F[2] and 2138°F (1170°C)[3] for the Al-U_3O_8 and Al-H_2O reactions respectively. The Al-H_2O reaction also usually requires molten aluminum to be dispersed as small droplets or vaporized metal into steam or water for the reaction to proceed to a significant extent.[3] A temperature of 1750°C (3128°) is required for essentially complete reaction.[4]

Potential energy release values calculated for an average power fuel element plate are shown in Table I.D.1. The "fission" source was based on the heat capacity of a plate between 230°F (110°C) and 2138°F (1170°C) or 3128°F (1750°C) assuming the plates were all aluminum. The 230°F temperature is a mean fuel temperature for an average power location.[5] The "fission" energies listed are therefore the energy accumulations required in an average fuel element plate before any or complete Al-H_2O reaction can occur.

The Al-U_3O_8 reaction energy was obtained from the maximum credible energy release vs weight percent aluminum in ref. 2, using the fuel element "meat" compositions of 65 and 60 weight percent aluminum for the inner and outer fuel elements. Using just the aluminum in the "meat" is the most realistic

---

[1]Hydrogen generated by any Al-H_2O reaction is also a potential energy source if it would react with oxygen. However, no mechanism exists whereby any hydrogen thus formed could contact oxygen; therefore no energy from hydrogen reaction was considered in the following analysis of the pressure vessel integrity.

[2]J. D. Fleming and J. W. Johnson, *Exothermic Reactions in Al-U_3O_8 Composites*, Georgia Institute of Technology.

[3]L. J. Epstein, *VII: Reactor Safety Aspects of Metal-Water Reactions*, GEAP-3335.

[4]R. O. Ivins, I. J. Testa, and P. Krause, "Studies of the Aluminum-Water Reaction in TREAT," *Chemical Engineering Division Summary Report, October, November, December, 1962*, ANL-6648, p. 201 (1963).

[5]N. Hilvety, R. D. Cheverton, and O. W. Burke, *Preliminary Analysis of HFIR Transients Resulting from Ramp Reactivity Additions*, CF-63-5-45 (May 9, 1963).

Table I.D.1. Potential Energy Releases Following HFIR Flow Blockage Accident for One Fuel Element Plate

Source	Energy (Mwsec)		Comments
	Inner Fuel Element	Outer Fuel Element	
Fission heat to allow any Al-H_2O reaction	0.268	0.244	Based on total enthalpy change from 230 to 2138°F of 659 Btu per pound of Al; plate assumed to be all aluminum
Fission heat to allow complete Al-H_2O reaction at 1750°C (3182°F)	0.384	0.350	Based on enthalpy change from 230 to 3182°F of 944 Btu per pound of Al; plate assumed to be all aluminum
Al-U_3O_8 reaction	0.0358	0.0438	Based on Al-U_3O_8 composition in the "meat"
Al-H_2O reaction	1.116	1.016	Based on 4.2 kcal per gram of Al heat of reaction, and reaction limited by amount of H_2O available in one coolant channel

case and also gives the highest energy release since the energy release decreases with increasing aluminum weight percent in the region of interest.[2] The energy values in Table I.D.1 show that the potential energy release from the Al-U_3O_8 reaction is small compared with the fission heat required.

The Al-H_2O reaction has a heat of reaction of 4.2 kcal per gram of aluminum and proceeds according to

$$2Al + 3H_2O \longrightarrow Al_2O_3 + 3H_2 .$$

This highly exothermic reaction has rapid energy release capabilities (in the multimillisecond range) when a significant fraction (>30%) of the available aluminum reacts.[4,6] Investigation of the amounts of water in a coolant channel and aluminum as cladding showed that ~75% of the cladding could be reacted by water in an adjacent coolant channel. Since some of the water would be removed by vaporization if cladding temperature exceeds 1170°C, a conservative (high) estimate of the potential energy release per plate was based on the amount of water available in a coolant channel. From Table I.D.1, the Al-H_2O reaction potential energy release of about 1.1 Mwsec per plate is the dominant energy source.

3. Determination of the Maximum Credible Energy Release

In this section, the rationale for and determination of the maximum credible energy release, that is, a release obviously conservative on a realistic basis, are presented. The maximum credible energy release is determined by the maximum credible fraction of the core that could contribute maximum credible energy release. In determining the maximum credible energy release per plate, the main question is the extent of Al-H_2O reaction to be included. In order to appreciate the development of a maximum credible

[6] R. O. Ivins, I. J. Testa, and P. Krause, "Studies of the Aluminum-Water Reaction in TREAT," *Chemical Engineering Division Summary Report, January, February, March, 1963*, ANL-6687, p. 179.

energy release, it is important to understand the difference between a flow blockage of a very small fraction of the core (several plates) and a blockage of a large fraction of the core.

3.1 Small Flow Blockage

A small enough blockage will not initially develop sufficient shutdown reactivity to reduce the reactor power. The fuel plate temperature will then continue to increase beyond the melting point and will reach temperatures (>1170°C) where Al-H_2O reaction could occur. Appreciable Al-H_2O reaction requires small molten droplets or vaporized metal to be dispersed into water or steam, as shown by TREAT experiments with SPERT I[4] and SL-1[6] fuel plates.

A nonexplosive type of reaction involving a small fraction of the molten aluminum would result if the molten aluminum were not dispersed into small (<200-mil-diam) particles, or no reaction as in the case of the WTR fuel meltdown incident.[7] The upper limit on a plate's energy release from the Al-H_2O reaction for this situation would be about 1.1 Mwsec per plate (see Table I.D.1) since some of the water in adjacent coolant channels will certainly have vaporized if the cladding temperature approaches 1170°C.

The termination of a small flow blockage incident would probably be through operator action based on increased fission product activity in the primary coolant water, the unusual reactivity changes occurring, or changes in other variables reflecting the core operating condition. In any event, such an incident would probably cause flow blockage in at least the several adjacent coolant channels due to plate distortion and melting and pressure from steam formation. Spreading of flow blockage could generate sufficient negative reactivity to override the maximum reactivity addition available to the servo-control (i.e., one dollar) and terminate full-power operation. An estimate of the fraction of the core involved in overheating is based on overriding a one-dollar reactivity addition and is shown in Table I.D.2. The negative reactivity change is estimated by assuming a fuel temperature increase from 230 to 2138°F and water temperature increase from 180 to 470°F (for 525 psia pressure); no steam void formation is assumed. The resulting 9.6% of the core, equivalent to about 52 fuel plates, is therefore a reasonable estimate of the highest fraction of the core which could generate significant Al-H_2O reaction energy. The maximum energy release per plate for this case is obtained from the fission heat to reach 3182°F (1750°C) and the Al-H_2O and Al-U_3O_8 reaction energy release in Table I.D.1 for a total of approximately 1.5 Mwsec per plate. The maximum energy release, therefore, for the small flow blockage case is 52 plates × 1.5 Mwsec per plate, or 78 Mwsec.

3.2 Large Flow Blockage

The previous section dealt with flow blockage which did not result in self-shutdown from full-power operation before some Al-H_2O reaction could have occurred. A large flow blockage, on the other hand, shall be considered to initially involve a sufficient fraction of the core that *no* Al-H_2O reaction occurs, that is, plate temperatures are limited to a maximum of 1170°C. The initial flow blockage will probably spread, as in the small blockage case, to at least the adjacent coolant channels.

---

[7] "Westinghouse Testing Reactor Incident," *Nucl. Safety* 2(2), 70–73 (December 1960).

Table I.D.2. Computation of Fraction of Core Required to Override One-Dollar Reactivity Addition from Servo-Control Action Following Small Flow Blockage

Fraction of core involved to produce $\delta k = -0.7\%$ is $0.7\%/7.3\% \cong 0.096$ of core
Number of fuel plates involved = 540 plates × $0.096 \cong 52$ plates

Condition	Fuel Plate	Coolant	Comments
Temperature change	230 to 2138°F	180 to 470°F	See text
Reactivity coefficient	$-10^{-5}/°F$	$-10^{-4}/°F$ at 170°F	Coolant coefficient increases with temperature as a function of water density change with temperature[a]
Change in criticality (% δk)	2.0	5.3	

[a]J. G. Crocker *et al.*, *Nuclear Startup of the SPERT IV Reactor*, IDO-16905, p. 32 (July 24, 1963).

The estimation of the maximum credible fraction of the core releasing the maximum credible energy per fuel plate is shown in Table I.D.3. This fraction has been made ultraconservative, and hence a maximum credible value, by using only negative reactivity from the coolant and ignoring the negative reactivity contribution from the fuel. Coolant temperature rise is assumed to 525 psia saturation temperature (470°F), and a conservative value for the reactivity coefficient of the water is also used. No steam void effects are assumed. Local pressure in the HFIR core will always be above 525 psia during 100-Mw operation; so the coolant temperature rise before boiling begins will be higher than 470°F. Also the assumption that no boiling will occur adjacent to fuel plates at temperatures up to 1170°C is obviously conservative with respect to the negative reactivity generated. About 24% of the core involving 130 fuel plates results as the maximum credible fraction of the core blocked with self-shutdown preventing any Al-H_2O reaction.

Table I.D.3. Computation of Fraction of Core Required to Override One-Dollar Reactivity Addition from Servo-Control Action Following Large Flow Blockage

Fraction of core involved to produce $\delta k = -0.7\%$ is $0.7/2.9 \cong 0.24$ of core

Number of fuel plates involved = 540 plates × 0.24 = 130 plates

Condition	Coolant	Comments
Temperature change	180 to 470°F	Negative reactivity contribution from fuel ignored
Reactivity coefficient	$-10^{-4}/°F$	
Change in criticality, % δk	2.9	

The final step in determining the maximum credible energy release for a flow blockage is to determine the maximum credible energy release per plate when combined with the 130 plates from Table I.D.3. The energy release per plate of about 1.4 Mwsec from Table I.D.1 for a temperature limited to 2138°F is obviously conservative since it includes all the Al-H_2O reaction energy for a situation where this reaction could not contribute to the energy release. Therefore the combination of 130 plates, each releasing 1.4 Mwsec, yields a maximum credible energy release of 182 Mwsec.

3.3 Energy Release Time Scale

The time scale of the energy release would be in the millisecond range for the Al-H_2O reaction or a steam explosion. Microsecond release times similar to TNT explosions are not possible; however, much slower release times are very likely for limited Al-H_2O reaction. The heat release from afterheat of melted fuel plates would not contribute to the energy in a millisecond pressure wave because of the large heat removal available in the core coolant flow once the power is reduced. Therefore the shortest release time, which results in the most damaging pressure wave, from a core flow blockage would be in the millisecond time range.

4. Summary

The preceding analysis has been presented to establish a maximum credible energy release following a flow blockage of the HFIR core. As discussed earlier in this report, the "maximum credible" terminology does not connote a realistic or credible value or circumstance. The maximum credible energy release determined in this report is therefore incredibly high since it is based on an incredibly high fraction of the core releasing all the available Al-H_2O energy. The fraction of the core involved in the maximum credible energy release of 182 Mwsec is 24%.

APPENDIX E

MAXIMUM PERMISSIBLE CONCENTRATIONS OF THE TRANSURANIC ISOTOPES

The data presented in Table I.E.1 have been taken from the *Transuranium Quarterly Progress Report for Period Ending February 28, 1962,* ORNL-3290, and are occupational tolerances listed for a 40-hr week.

Table I.E.1. Maximum Permissible Concentrations

Nuclide	Water		Air		Body Burden		Specific Activity (curies/g)
	Critical Organ	MPC_w ($\mu c/cm^3$)	Critical Organ	MPC_a ($\mu c/cm^3$)	Critical Organ	Value (μc)	
^{238}Pu	Bone	1.53×10^{-4}	Bone	2.02×10^{-12}	Bone	0.046	17.4
^{239}Pu	Bone	1.35×10^{-4}	Bone	1.79×10^{-12}	Bone	0.045	0.061
^{240}Pu	Bone	1.35×10^{-4}	Bone	1.79×10^{-12}	Bone	0.045	0.227
^{241}Pu	Bone	7.14×10^{-3}	Bone	9.42×10^{-11}	Bone	0.990	112
^{242}Pu	Bone	1.42×10^{-4}	Bone	1.88×10^{-12}	Bone	0.048	3.90×10^{-3}
^{243}Pu	GI tract	1.21×10^{-2}	GI tract	2.14×10^{-6}	Bone	7.23	2.59×10^{6}
^{244}Pu	Bone	1.27×10^{-4}	Bone	1.68×10^{-12}	Bone	0.043	1.93×10^{-5}
^{245}Pu	GI tract	1.35×10^{-3}	GI tract	2.39×10^{-7}	Bone	3.04	1.21×10^{6}
^{241}Am	Bone	1.27×10^{-4}	Bone	5.57×10^{-12}	Bone	0.054	3.24
^{242m}Am	Bone	1.27×10^{-4}	Bone	5.57×10^{-12}	Bone	0.067	9.73
^{242}Am	GI tract	2.73×10^{-3}	Liver	3.93×10^{-8}	Liver	0.064	8.10×10^{5}
^{243}Am	Bone	1.26×10^{-4}	Bone	5.56×10^{-12}	Bone	0.044	0.192
^{244m}Am	GI tract	5.08×10^{-2}	Bone	3.99×10^{-6}	Bone	0.179	2.97×10^{7}
^{244}Am	GI tract	9.10×10^{-3}	Bone	1.73×10^{-7}	Bone	0.180	1.27×10^{6}
^{245}Am	GI tract	1.67×10^{-2}	GI tract	2.96×10^{-6}	Liver	11.6	6.40×10^{6}
^{242}Cm	GI tract	7.05×10^{-4}	Liver	1.19×10^{-10}	Liver	0.047	3.32×10^{3}
^{243}Cm	Bone	1.57×10^{-4}	Bone	6.88×10^{-12}	Bone	0.092	52.6
^{244}Cm	Bone	2.14×10^{-4}	Bone	9.40×10^{-12}	Bone	0.104	83.3
^{245}Cm	Bone	1.02×10^{-4}	Bone	4.50×10^{-12}	Bone	0.043	0.157
^{246}Cm	Bone	1.02×10^{-4}	Bone	4.49×10^{-12}	Bone	0.043	0.265
^{247}Cm	Bone	1.07×10^{-4}	Bone	4.71×10^{-12}	Bone	0.044	3.62×10^{-5}
^{248}Cm	Bone	1.32×10^{-5}	Bone	5.81×10^{-13}	Bone	0.005	3.07×10^{-3}
^{249}Cm	GI tract	8.25×10^{-2}	Liver	7.51×10^{-6}	Liver	0.827	1.18×10^{7}
^{249}Bk	GI tract	0.140	Bone	7.76×10^{-10}	Bone	0.600	1.67×10^{3}
^{250}Bk	GI tract	9.62×10^{-3}	Bone	1.37×10^{-7}	Bone	0.045	3.89×10^{6}
^{249}Cf	Bone	1.24×10^{-4}	Bone	1.64×10^{-12}	Bone	0.041	3.59
^{250}Cf	Bone	3.53×10^{-4}	Bone	4.66×10^{-12}	Bone	0.041	1.31×10^{2}
^{251}Cf	Bone	1.17×10^{-4}	Bone	1.55×10^{-12}	Bone	0.039	1.78
^{252}Cf	GI tract	2.53×10^{-4}	Bone	6.83×10^{-12}	Bone	0.015	5.57×10^{2}
^{253}Cf	GI tract	4.14×10^{-3}	Bone	8.24×10^{-10}	Bone	0.036	2.87×10^{4}
^{254}Cf	GI tract	1.22×10^{-5}	Bone	5.42×10^{-12}	Bone	0.00075	9.19×10^{3}
^{253}Es	GI tract	6.35×10^{-4}	Bone	7.44×10^{-10}	Bone	0.0368	2.58×10^{4}
^{254m}Es	GI tract	5.40×10^{-4}	Bone	4.87×10^{-9}	Bone	0.0196	3.17×10^{5}
^{254}Es	GI tract	6.70×10^{-4}	Bone	1.84×10^{-11}	Bone	0.0217	1.07×10^{3}
^{255}Es	GI tract	6.91×10^{-4}	Bone	6.07×10^{-10}	Bone	0.0361	2.14×10^{4}
^{254}Fm	GI tract	1.70×10^{-4}	Bone	6.03×10^{-8}	Bone	0.0202	3.81×10^{6}
^{255}Fm	GI tract	7.72×10^{-4}	Bone	1.63×10^{-8}	Bone	0.0362	5.72×10^{5}
^{256}Fm	GI tract	1.25×10^{-5}	GI tract	2.21×10^{-9}	Bone	0.00076	4.59×10^{6}

APPENDIX F

MISCELLANEOUS CALCULATIONS

1. Calculation of the Initial Iodine Dose Rate Within the Building

The initial thyroid dose rate per kilowatt equivalent of core melted is estimated under the assumption that the iodine is uniformly distributed within the reactor bay, which has a total volume of 446,000 ft^3 or 12,630 m^3.

Let q_j be the number of curies of the jth iodine isotope released per kilowatt; let κ_j be the dose delivered in rems per inhaled microcurie, β be the breathing rate, and V be the building volume in cubic meters. Then the dose rate[1] from the release of 1 kw equivalent of the five iodine isotopes will be

$$\frac{dD}{dt} = \frac{\beta}{V} \sum_{j=1}^{5} \kappa_j q_j \ .$$

For this calculation β is taken to be 3×10^4 cm^3/min, which is somewhat higher than that for standard man, but has been selected to compensate for the possible effects of excitement and heightened activity during the incident. The values of κ_j and q_j are those given in Table I.A.2 of Appendix A. Thus the iodine dose rate becomes

$$\frac{dD}{dt} = 132.4 \text{ rems kw}^{-1} \text{ min}^{-1} \ .$$

Because only 50% of the iodine is released from the melted fuel, this may be reduced to 61.2 rems kw^{-1} min^{-1}.

2. Calculation of the External Dose Rate Within the Building

For this purpose the reactor bay is considered to be a cylinder having the same length (33.5 m) as the reactor bay, but twice the volume. The volume source term is obtained by dividing the actual building volume into the total number of curies of iodine and noble gas released per kilowatt and multiplying the result by 3.7×10^{10} dis $curie^{-1}$ sec^{-1}.

The dose rates are then found on the axis of this cylinder and reduced by a factor of 2 in order to approximate the dose rates expected near the floor or near the roof of the building.

Let q_j be the number of curies of the jth isotope released initially into the building; let V be the actual building volume in cubic centimeters, L be the length of the building in centimeters, and R be the radius (cm) corresponding to twice the actual building volume. The radiation flux at ground level at one end of the building is given approximately by

---

[1]See ref. 4, Appendix A.

$$\psi_E = \frac{3.7 \times 10^{10}}{8V} \sum_j q_j \int_0^L \int_0^R \frac{2r\,dr\,dx}{r^2 + (L-x)^2} = 0.366 \sum_j q_j \left[L \ln\left(\frac{R^2 + L^2}{L^2}\right) + 2R \tan^{-1}\frac{L}{R} \right],$$

and at the center of the building by

$$\psi_C = \frac{3.7 \times 10^{10}}{4V} \sum_j q_j \int_0^{L/2} \int_0^R \frac{2r\,dr\,dx}{r^2 + (L-x)^2} = 0.732 \sum_j q_j \left[\frac{L}{2} \ln\left(\frac{R^2 + L^2/4}{L^2/4}\right) + 2R \tan^{-1}\frac{L}{2R} \right].$$

In these computations $L = 3350$ cm and $R = 1550$ cm. Consequently the radiation fluxes become

$$\psi_E = 1.8 \times 10^3 \sum_j q_j, \qquad \psi_C = 2.63 \times 10^3 \sum_j q_j .$$

The value of $\sum_j q_j$ is obtained by taking one-half the sum of the iodines and the sum of all the gamma-emitting noble gases, because only 50% of the iodines are considered to leave the affected part of the fuel. Thus, using the data in Appendix A the value of $\sum_j q_j$ becomes 247 curies, so that

$$\psi_E = 4.45 \times 10^5 \text{ photons cm}^{-2}\text{ sec}^{-1}, \qquad \psi_C = 6.50 \times 10^5 \text{ photons cm}^{-2}\text{ sec}^{-1} .$$

In order to obtain the dose rate, it is necessary to estimate the average gamma energy. This is done by dividing $\sum q_j$ into $\sum q_j E_j$, where E_j is the total energy of the jth isotope.[2] The resulting average energy is about 0.95 Mev. Now a flux of 1 photon cm^{-2} sec^{-1} having this energy corresponds to a dose rate of approximately 1.85×10^{-6} r/hr. Hence the dose rate at the end of the building is initially about 0.8 r kw^{-1} hr^{-1}, and at the center of the building it is about 1.2 r kw^{-1} hr^{-1}.

3. Estimate of the Bone Dose from the Target

The dose delivered by the contents of the HFIR target under accident conditions can be estimated by comparing it to the quantity of bone-seeking fission products in the core. The 11 bone-seeking fission products listed in Table I.A.3, Appendix A, can be expressed in terms of equivalent curies of ^{90}Sr by dividing $\sum \kappa_j q_j$ by 44.3, the value of κ_j for ^{90}Sr. It is found in this way that the bone seekers present in the HFIR following 15 days' operation at 100 Mw are equivalent to 38,750 curies of ^{90}Sr.

Now at its worst, the potential bone dose from the target is due almost entirely to the presence of ^{244}Cm, which reaches a maximum after about 5 months' irradiation and thereafter rapidly declines. At this time[3] a target containing originally 300 g of ^{242}Pu will contain approximately 11,700 curies of ^{244}Cm. Since the MPC for ^{244}Cm is 31.9 times less than that for ^{90}Sr, this is equivalent to 373,000 curies of ^{90}Sr. Thus the potential bone-seeking dose from the target is about an order of magnitude greater than that from the fission products contained in the reactor fuel.

---

[2]It is realized that this procedure is quite crude, but it suffices for the purpose at hand.

[3]H. C. Claiborne and M. P. Lietzke, *Californium Production in the High Flux Isotope Reactor*, ORNL-CF-59-8-125 (August 1959).

Part IIa. Safety Review Questions and Answers 1—41

ABSTRACT

Review by the USAEC of the HFIR Safety Analysis, ORNL-3572 and *draft* ORNL-3573, resulted in two sets of questions. The first set was developed by the Division of Reactor Licensing and was forwarded informally in early June 1965. These questions were answered verbally by the HFIR staff during meetings with DRL and a subcommittee of the Advisory Committee on Reactor Safeguards in June 1965. Following a July meeting with the ACRS, a request for additional information was made to ORNL by the USAEC. Forty-one questions were listed, with questions 1 through 20 being duplicates of the set discussed with DRL and the ACRS. The table of contents comprises a list of the questions, with answers given in the body of the report.

Originally published as ORNL-CF-65-11-29 (Nov. 12, 1965).

CONTENTS

1A. It appears that the meteorological models applied to evaluation of the consequences of the MCA assume flat terrain. Describe the applicability of these models to the topographic conditions in the area of the site including the "channeling effect" of the valley with restriction in lateral effluent spread, effect of impingement of the effluent plumes on the neighboring hillsides, and the consequences of an MCA during fumigation conditions. 109

B. Evaluate the consequences of the MCA associated with leakage from the reactor building during high wind speed conditions. 111

C. What is the estimated dose to the operators from the MCA? 111

2A. Provide, if available, the joint frequency data for wind speed and direction associated with the various stability types (A, B, C, D, E, F, and G). 111

B. What are the atmospheric dilution factors used for estimating stack release rates for routine operations and for accident situations utilizing the joint frequency data? 111

C. State the wind speeds and associated effective stack heights that were used to calculate the "worst average" dilution factors. 113

3A. Recent studies at Oak Ridge have shown that a relatively large portion of the iodine evolving from a fuel meltdown is in an organic form and is poorly removed by washout, by silvered-copper mesh, or by charcoal filters. Is the removal factor of 2000 claimed in the accident analysis consistent with these studies? 114

B. How and with what frequency will these filters be tested? 115

4A. What experience is available on the manufacture of involute plates, particularly with regard to maintaining tolerances, proper curvature, and channel spacing? 115

B. What tests will be run to detect unbonding blisters and fuel inhomogeneities in the fuel plates? 115

5A. What is the calculated coolant velocity to cause collapse of the involute fuel plate? 116

B. What is the maximum anticipated velocity in a fuel channel under the most adverse combination of tolerances, flow maldistribution, etc.? 116

6A. Discuss the integrity of the fuel plates with respect to fission gas buildup and burnup of the burnable poison. 116

B. Could plate growth due to fuel burnup cause excessive deflections and stresses? 117

C. Could this cause binding of the outer fuel element and the control cylinder? 117

7. Provide design details of the attachment between the drive tubes and the shim-safety elements. What are the design and expected stresses at this point? 117

8. Provide details on the design of the hydraulic cylinder which limits the maximum reactivity rate associated with any shim-plate failure to 0.0065 per second 119

9. Describe the test program for the inner and outer control elements and their drives to ensure proper operation and to verify that no interference or binding can occur between the inner control cylinder and the outer shim-safety plates. 120

10. Quantitatively, how are the reactivity coefficients for the core expected to vary during the operating cycle? 122

11. What are the limits for reactivity which can be added by experiments in the target hole? 122

12. Discuss the possibility and consequences of a large reactivity overshoot with the control plates being withdrawn past their critical position during xenon burnout in a scram recovery. 122

13A. What is the maximum total delay time (including detector delay time) between the onset of an unsafe condition and the initiation of rod drop during startup and full-power operation? 123

B. Has the total system been tested or will it be tested to measure this time with all three and with only two of the coincident circuits tripping? 123

14. How was the time response of the neutron flux amplifier determined? What was the magnitude of the input steps? 124

15. What is the accuracy of the heat-power calculator and what are the error contributions of the temperature and flow inputs? 124

16. What control problems are anticipated from the photoneutrons from the beryllium reflector? How will they affect startup immediately after scram? What magnitude flux is expected at the detector positions from the photoneutrons after shutdown? 124

17A. What consideration has been given to the use of scram or setback actions initiated by a loss of power to the facility or to the pumps? 125

B. Provide curves showing primary coolant flow vs time following loss of pumping power and reactor power level vs time due to the associated cutback. 125

18. What is the relieving capacity of the high-pressure relief valves, and what was the basis, or criterion, which determined this capacity? 125

19. What peak power and plate temperatures would result if scram action is initiated by the 130-Mw overpower scram instead of the rate scram for an addition of 0.013 $\Delta k/k$ (Table I.C.4)? 127

20. In Table I.C.8 in Appendix C, was only the "no void" condition considered in Case IV? 128

21. Would any fuel melting occur if an irradiated core were to fall to the bottom of the pool? 128

22A. Discuss the reasons that a backup system for reactivity control has not been incorporated into the design of the HFIR. 129

B. What are the consequences of two or three quadrants of the control system sticking in the full-out position under various accident or abnormal conditions? 130

C. Could a pressure surge in the core damage all control elements sufficiently to prevent their motion? If so, what are the possible sources of such pulses? What kind of reactivity transients could lead to this event? 130

D. Under what circumstances would a slower-acting backup control system be of real value? 131

23. Provide information regarding the following aspects of the adequacy of the core cooling system:

A. A discussion of the reason that a core spray system or other emergency cooling system is undesirable or unnecessary. 131

B. An analysis of the thermal effects on the core resulting from a rapid depressurization of the primary system or a complete loss of coolant flow. 131

C. An analysis of the extent and consequences of metal-water reactions which might occur as a result of a loss of flow, a loss of coolant, a rapid primary system depressurization, or other credible accidents. 131

24A. Discuss the adequacy of the beam-tube design. 135

B. In particular, discuss the desirability and feasibility of incorporating an additional closure or seal at the outer ends of the beam tubes to limit loss of coolant from the main coolant system should the beam tubes fail at a point within the reactor pressure vessel. 136

C. Discuss the course of accidents involving various modes of beam tube failure. 137

D. Could modifications of the provisions for emergency cooling help minimize the consequences of any of these? 137

E. Discuss the extent of knowledge of long-term irradiation effects on the beam tubes, the adequacy of the surveillance program, and the probability of beam tube failure with the proposed procedures. 138

25. State the evacuation alarm set point and indicate what action is to be taken if it is reached. Also indicate the approximate radiation levels which will require evacuation of the facility by the reactor operators, and discuss the need for radiation shielding at the reactor control room. 138

26. Provide an analysis of the reactivity effects resulting from possible fuel movement (e.g., effects of fuel melting and transport during an accident or relative movement of the two elements). Analyze appropriate accidents which could involve significant reactivity insertions or insertion rates from this source. 139

27. Discuss the possible effects of a fire in the control room. 139

28A. Furnish further information regarding the reliability and fail-safe characteristics of the reactor control and instrumentation system. 140

B. Indicate how the system has functioned in testing to date. 141

C. What are the most crucial segments of the instrumentation system? 141

D. What are possible modes of failure and their consequences? 142

E. What could result from failure to detect fuel element failure promptly? 142

F. Discuss accidents in which the instrumentation reacts improperly, or fails to function as intended, including that time when reactivity is being inserted at its maximum design rate. 142

G. Discuss this choice of maximum reactivity insertion rate. 143

29A. Discuss alternate ways of limiting any irradiation of the public or of personnel at the Oak Ridge National Laboratory in the unlikely event of a serious accident, such as by isolation of the building and recirculation of building air through filters rather than by releasing of radioactivity through the facility stack. 144

B. Also discuss the need for additional radiation monitoring instrumentation for the stack exhaust in order to provide information regarding the rate and quantity of radioactivity released during potential accidents. 149

30. Provide the latest information available relative to the effectiveness of the installed filters to remove radioactive iodine from the exhaust in the event of a fission product release accident. 150

31A. State the NDT of the pressure-vessel material and indicate how this is expected to vary during the reactor lifetime. 150

B. How well is the flux known? 152

C. Are there other important reactor structural members subject to considerable neutron irradiation? If so, what are the consequences of their failure? 152

32. State the criteria to be used in evaluating experiments which may be performed in or near the reactor. 153

33. Indicate whether nearby facilities can be safely shut down and evacuated in the event of a severe accident at the HFIR. 153

34A. Describe how the design of future HFIR core loadings may vary from the initial core design. 154

B. By what criteria will changes in core design or operating conditions be measured for safety? 154

C. When will regulatory review be deemed appropriate? 154

D. Discuss steps taken in operating new core designs (including first) which will minimize the chance of fuel failure. 154

35. Discuss the possibility that thermal expansion or damage to the beryllium reflector could affect control rod motion. 155

36A. Provide information as to the maximum value of the overpower scram set point and the reason that this value was chosen. 155

B. Provide analyses of accidents in which this setting plays an important role. 156

37. Present a description and analysis of the hazards associated with the type of targets which may be used which are not described in the documents submitted. 156

38A. Provide results of analyses of reactivity transients considerably more severe than those previously treated, considering possible sources of such transients as control system failure, larger than expected reactivity effects associated with a central void, unexpected locally positive void effects in the core, fuel movement, etc. 156

B. What role do metal-water reactions play herein? 157

C. What is the latest information on chemical reactions involving this fuel? 158

D. Is xenon burnout ever important in any possible accidents? Can the boron in the fuel ever contribute adversely to an accident? 159

E. Please document the spatial distribution of local void effects and provide estimates of uncertainties therein. 159

F. Have reactivity accident studies allowed for the possibility of the return of water to the core? 160

39. What procedures will be followed if a normal removal of irradiated fuel is impossible due to fuel damage or sticking? 160

40. Discuss the reliability of the emergency air supply to the control rod drives. 161

41A. Are there possibilities of shielding the control room so that the probability of evacuation of reactor operators can be reduced? 161

B. Are there any significant safety advantages that could be achieved with an alternate emergency control area? 161

APPENDIX G. Use of Tensile Specimens 162

QUESTIONS AND INFORMATION REQUESTS ON THE HFIR

1A. It appears that the meteorological models applied to evaluation of the consequences of the MCA assume flat terrain. Describe the applicability of these models to the topographic conditions in the area of the site including the "channeling effect" of the valley with restriction in lateral effluent spread, effect of impingement of the effluent plumes on the neighboring hillsides, and the consequences of an MCA during fumigation conditions.

The meteorological model used to evaluate the consequences of the HFIR MCA does tacitly include the assumption of flat terrain. The validity of the model has been discussed with personnel of the U.S. Weather Bureau,[1] and they concur in the conclusion that, because of the low hill profiles and the broad valleys (~90 m from valley floor to hilltops – valley width ~1500 m), the only significant effect is the marked channeling of winds up and down the valleys, which run in the northeast-southwest direction. This effect, which can be observed by referring to Table I.A.5 in Appendix A, is actually beneficial because the distances from the HFIR site to populated areas are greatest in these prevailing wind directions.

The doses on the hilltops are, in general, lower than the ground-level center-line doses except in cases where the wind is blowing across the hills. This latter situation occurs infrequently and is generally the result of some external meteorological disturbance which also results in better dispersion conditions and higher winds than those utilized in computing the consequences of the MCA. In any case, the hilltops so affected are unoccupied and are within the AEC-controlled area. Consequently, no additional hazard is involved.

The so-called "fumigation" condition frequently occurs for short periods of time (15 to 30 min) in the morning at the HFIR site. This condition is brought about by the breakup of an early-morning inversion and is accompanied by freshening winds and good dispersion. Observations taken at ORNL during the past year indicate that during these periods there is, on the average, an increase in wind speed by a factor of 6.5.

The doses under fumigation conditions have been computed as follows. It is assumed that a ground-based inversion of height just slightly greater than the stack height (76.2 m) exists, and that this condition is accompanied by F-type stability (moderately stable). The dose at each point at ground level downwind is then computed using Pasquill's method with the source term modified as described in Appendix A, but, in this case, subject to the constraints that the effective stack height, h, remains constant at 76.2 m and that the value of σ_z becomes constant when $\sigma_z = h/2 = 38.1$ m. The dose equation has the usual form:

$$D_i = \frac{e^{-h^2/2\sigma_{zi}^2}}{\pi u_i \sigma_{yi} \sigma_{zi}} \Sigma A_j e^{-\lambda_j x/u_i} .$$

[1]F. A. Gifford, Jr., U.S. Weather Bureau, personal communication to F. T. Binford, Oak Ridge National Laboratory.

Here the summation represents the source term, and the other factor represents the dilution due to atmospheric dispersion. The subscript i refers to the inversion condition, that is, low wind speed and F stability.

As the inversion breaks up the wind speed increases and the dispersion conditions improve – type C stability (slightly unstable) has been chosen as representative. It has been shown[2] that under fumigation conditions the dilution factor can be appropriately expressed in the form

$$\frac{1}{(2\pi)^{1/2}\sigma_{yf}u_f h},$$

where the subscript f is used to designate fumigation conditions, that is, moderate wind speeds and C-type stability. The source term, however, depends upon the previous history of the plume and remains essentially unchanged. Consequently, the ground-level dose under fumigation conditions becomes

$$D_f = \frac{\sum A_j e^{-\lambda_j x/u_i}}{(2\pi)^{1/2}\sigma_{yf}u_f h}.$$

The dose under fumigation conditions can be conveniently expressed in terms of the previously calculated dose under inversion conditions, and the changes which take place in the dispersion parameters and the wind speed:

$$\frac{D_f}{D_i} = \sqrt{\frac{\pi}{2}}\,\frac{u_i\sigma_{yi}\sigma_{zi}}{u_f\sigma_{yf}h}\,e^{+h^2/2\sigma_{zi}^2}.$$

A perusal of Fig. I.A.1 indicates that $\sigma_{yi}/\sigma_{yf} \cong 0.33$. The wind-speed ratio u_i/u_f has previously been found to be 1/6.5, and $h = 76.2$. Therefore

$$D_f/D_i = 8.35 \times 10^{-4}\sigma_{zi} \exp\left[+2903.22/\sigma_{zi}^2\right].$$

Values of D_f following unit release have been plotted for the noble gas gamma dose and the internal iodine dose, respectively, in Figs. II.1.1 and II.1.2. For comparison, the "worst average," "most representative," and "mean" values previously computed and set forth in Part I have also been included. In all cases, the computations were performed for infinite exposure and rapid emission.

It is clear from these curves that the fumigation case produces essentially the same results as the mean value at distances greater than the exclusion area boundary, but that the fumigation doses are somewhat higher near the stack. Because of the high decontamination efficiency of the filters, this is of little or no concern with respect to the internal iodine dose; however, in the highly unlikely event of a south or southwest wind, the noble gas doses at the main portion of ORNL might be increased by a factor of as much as 1.2. Whole-body doses near the stack base would, of course, be much higher. However, it is worth noting that, based upon the frequency of inversions in the ORNL area and the duration of the fumigation conditions, the probability per unit time of a fission gas release occurring during a period of fumigation is about two orders of magnitude less than the probability of such a release under some other set of conditions.

---

[2] F. A. Gifford, Jr., *Nucl. Safety* 2(4), 47–51 (1961).

B. Evaluate the consequences of the MCA associated with leakage from the reactor building during high wind speed conditions.

Experience with the ORR containment system leads to the conclusion that the HFIR containment is adequate to prevent leakage from the HFIR building even during periods of high wind.

The ORR is a mill-type structure and has a volume of approximately 800,000 ft^3. The exhaust rate from this building is approximately 6000 cfm under containment conditions, and all of this flow is due to leakage at the negative pressure of about 0.3 in. of H_2O. In over a year of constant monitoring of the differential pressure at various points on the building walls, no wind-induced decrease of external pressure below the internal pressure has ever been observed except when the containment system was not in operation.

The HFIR is a concrete structure much tighter than the ORR. The reactor bay contains approximately 450,000 ft^3, and the exhaust rate is approximately 12,500 cfm. Most of this flow enters the reactor bay through the filtered fresh-air intake units, which regulate the flow so as to maintain a nominal -0.3 in. H_2O in the reactor bay. It may be inferred, therefore, that the probability of any significant leakage concurrent with a massive fission product release is nil.

C. What is the estimated dose to the operators from the MCA?

The dose to the operators following the HFIR MCA will, of course, depend upon their location and actions during and immediately following the accident. The dose rates to be expected at the observation gallery windows, at the center of the reactor bay, and just outside the reactor building, have been estimated and may be found on pp. 26 and 27.

Prompt evacuation of the control room in the event of a major release of fission products to the reactor bay should require no more than 15 sec. The dose rate at the control-room windows is estimated to be about 85 r/min for the maximum credible accident. This would lead to a dose of about 25 r if the operator were exposed for 15 sec. The dose rate should be at least a factor of 10 below this once the operator leaves the control room, and it should not take him more than 15 sec more to leave the building by either of two routes.

2A. Provide, if available, the joint frequency data for wind speed and direction associated with the various stability types (A, B, C, D, E, F, and G).

Joint frequency data for the wind speeds and directions associated with the various stability conditions are not available.

B. What are the atmospheric dilution factors used for estimating stack release rates for routine operations and for accident situations utilizing the joint frequency data?

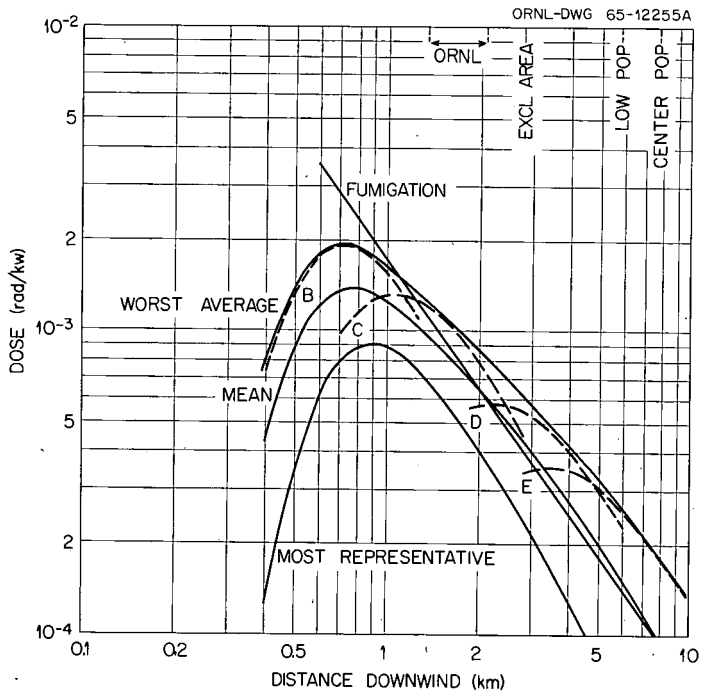

Fig. II.1.1. Noble Gas Gamma Dose. Infinite exposure, rapid emission ($\alpha = 0.5$).

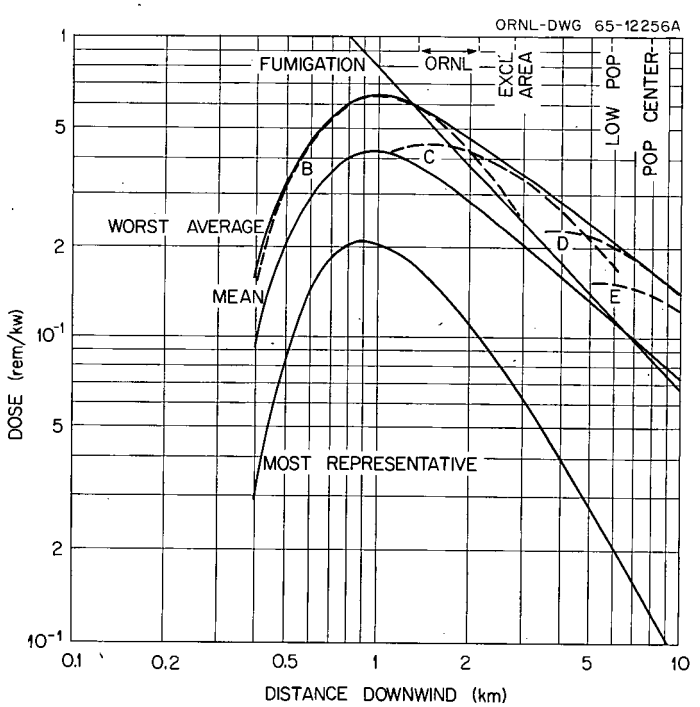

Fig. II.1.2. Internal Iodine Dose. Infinite exposure, rapid emission ($\alpha = 0.5$).

As stated in A, the joint frequency data are not available. However, the "worst average" conditions include the assumption that the most unfavorable wind speeds associated with each stability condition occur at each point and that the wind direction is toward the receptor for the entire duration of the incident. Incorporation of weighting factors based on the joint frequencies would result in more realistic but less conservative values of the doses than those presented.

C. State the wind speeds and associated effective stack heights that were used to calculate the "worst average" dilution factors.

As clearly set forth in Appendix A, p. 46, the "worst average conditions" are computed at each point downwind, for each stability condition, and for each group of isotopes using that unique value of the wind speed which maximizes the dose for that point, that stability condition, and that group of isotopes under consideration. Thus, in general, for each point x and each group of isotopes, five different wind speeds were used – one for each stability condition. Moreover, the wind speeds used for the computation of the 2-hr exposures were different from those used to compute the infinite exposures. The numerical value of these wind speeds is obtained by setting the partial derivative with respect to u of the dose equation

$$D = \frac{e^{-h^2(u)/2\sigma_z^2}}{\pi u \sigma_y \sigma_z} \sum_j A_j e^{-\lambda_j x/u}$$

equal to zero and solving for u. The values of u so obtained were then used to compute D. In the actual computations, over 500 different wind speeds were used for each stability condition. To give some idea of the wind speeds used, the values of u which maximize the noble gas gamma dose for infinite exposure and rapid emission are plotted in Fig. II.2.1.

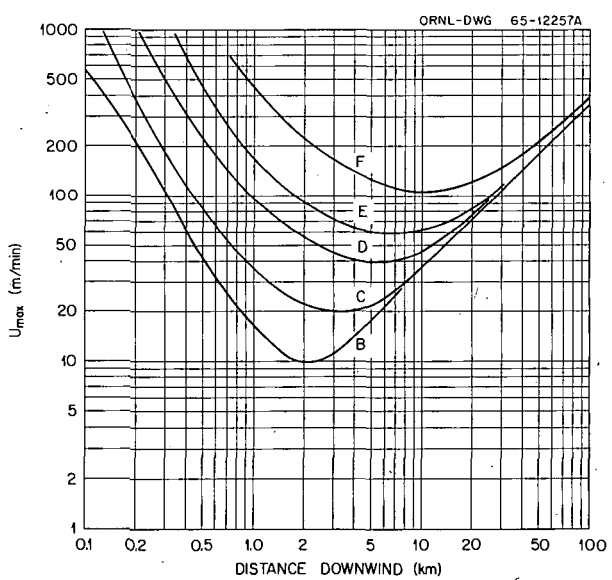

Fig. II.2.1. Wind Speeds Used to Compute "Worst Average" Noble Gas Gamma Dose. Infinite exposure.

The effective stack height corresponding to each wind speed is obtained as set forth in Appendix A, p. 40. It is

$$h(u) = 76.2 + 1063/u ,$$

where u is the wind speed obtained as described above.

3A. Recent studies at Oak Ridge have shown that a relatively large portion of the iodine evolving from a fuel meltdown is in an organic form and is poorly removed by washout, by silvered-copper mesh, or by charcoal filters. Is the removal factor of 2000 claimed in the accident analysis consistent with these studies?*

There have been no studies at Oak Ridge, recent or otherwise, which show that a relatively large portion of the iodine evolving from the meltdown of HFIR fuel is in organic form. What has been observed is that in some cases small fractions of the iodine released from the meltdown of some types of fuel have been found in an organic form tentatively identified as methyl iodide. It is thought that the organic iodide may form during or immediately after its release due to reaction with contaminants in or near the fuel or may form as a result of contact with organic contaminants while it is adsorbed on the walls of the containment building. In the latter case, there appears to be a direct relation between the time permitted for reaction and the amount of organic iodide formed.

The decontamination factor claimed for iodine is composed of two factors: (1) a decontamination factor of 3 for washout as the iodine escapes through the pool and reactor water, and (2) a decontamination factor of 666 due to the removal of iodine by the charcoal filters. It is believed that the formation of methyl iodide during the actual release will be quite small and that its presence will not affect the very conservative factor of 3. The subsequent formation of methyl iodide in the building would likewise have no effect on this factor. These conclusions are reinforced by the results of tests made following the ORR fuel meltdown of July 1, 1963. In this incident, fission gases were released into the ORR pool water. The tests revealed the presence of the daughters of noble gases on various building surfaces, but in no case was any iodine detected. This indicates that virtually all of the iodine indeed remained in the water.

Because of the fact that both the SBHE and CHOG systems are designed to rapidly remove any iodine released from the primary containment, there is little time for methyl iodide to form in the building. It has been estimated that, at most, 5% of the iodine reaching the filters would be in the form of methyl iodide. Thus, if the decontamination factor for CH_3I were only 10** and the decontamination factor for molecular iodine were only 100, the total filter factor would be

$$\left(\frac{0.95}{100} + \frac{0.05}{10}\right)^{-1} = 69 ,$$

so that the overall decontamination factor would be $69 \times 3 = 207$. Despite the fact that this is lower

*Further information is in answers 30 and 46.

**This result was derived prior to the investigation of CH_3I described in ORNL-TM-1291. Later, more realistic results are given in the answer to Question 30.

than that normally expected by a factor of 10, it is still higher by a factor of 10 than that required to satisfy the guidelines of 10 CFR 100.

B. How and with what frequency will these filters be tested?

The filters will be tested following each installation and semiannually thereafter unless some unforseen circumstances make more frequent or special testing desirable. The present technique is to add iodine traced with radioactive iodine to the duct upstream of the filters and by sampling before and after the filters to measure the efficiency for removal of the iodine. Methods for measuring the decontamination factor for organic iodides are being investigated, and when such a technique becomes available it will be used.

The ORR has a similar filter system which has been in operation for about two years, and therefore a considerable lead time is available in terms of information on filter performance as a function of time.

4A. What experience is available on the manufacture of involute plates, particularly with regard to maintaining tolerances, proper curvature, and channel spacing?

No experience is yet available from the actual fuel element fabricator as to what tolerances will be achieved. He has just started his plate production and is in the final phase of the assembly and welding qualification. The elements are being fabricated under a cost-plus-type contract using procedures developed by ORNL.

Considerable data are available, however, from the elements fabricated at ORNL during the development period. Data on channel spacing from four elements are given in Table II.4.1. The variation in channel spacing is a function of variations in both plate forming and assembly. These data show that it was possible to achieve channel spacing control well within the specified tolerances.

In addition, plates also were fabricated and formed for use in the critical experiment. These plates showed comparable control in plate forming to the other two but were not welded into assemblies, so plate spacing data are not available.

It is expected that once a smooth, uniform production operation is established, improved uniformity should be realized.

B. What tests will be run to detect unbonding blisters and fuel inhomogeneities in the fuel plates?

The presence of any nonbonds or blisters in fuel plates will be revealed by two inspection techniques. The first will be the technique normally used by industry for determining nonbonds in aluminum plates, which is an anneal of the finished plates at 500°C and a complete visual examination. In our procedures, the plates are annealed and inspected twice: once before cold working and again after the long anneal to put them in the "O" condition.

As a second and more sophisticated check, every plate will be completely examined using an ultrasonic technique which has a demonstrated sensitivity for determining $^1/_{16}$-in.-diam nonbonds.

Table II.4.1. Summary of Plate Spacing Measurements on HFIR Fuel Assemblies

	Development Fuel Assembly		First Reactor Fuel Assembly		Design Requirements
	Inner	Outer	Inner	Outer	
Number of measurements obtained	5643	12177	5643	12177	
Maximum measurements, mils	57	55	56	52	50 + 10
Minimum measurements, mils	46	44	44	44	50 − 10
Average channel thickness, mils[a]	51.0	48.8	49.9	48.4	50
Maximum average channel cross section, mils	53	52	52	51	50 + 6
Minimum average channel cross section, mils	48	47	47	46	50 − 6

[a]The average thickness of the channels was calculated at each of the 11 axial measuring positions for every channel.

A special instrument which measures changes in x-ray attenuation of a very small ($^5/_{64}$-in. diam) area has been developed by the HFIR Project for demonstrating that the uranium homogeneity of every plate meets the specified tolerances. Every fuel plate will be scanned in its entirety, using one of these instruments. The effectiveness of these instruments has been confirmed by removing small analytical samples.

5A. What is the calculated coolant velocity to cause collapse of the involute fuel plate?

The calculated velocity is greater than 200 fps.

B. What is the maximum anticipated velocity in a fuel channel under the most adverse combination of tolerances, flow maldistribution, etc.?

The maximum anticipated velocity is approximately 100 fps. This high velocity could occur only in a localized region.

6A. Discuss the integrity of the fuel plates with respect to fission gas buildup and burnup of the burnable poison.

In a joint HFIR-ATR irradiation program, miniature U_3O_8-Al dispersion fuel-plate samples with and without boron burnable poison were irradiated in a special loop in the ETR. The range of variables

covered included tests in which the maximum burnup and temperature values were in excess of those expected in the HFIR. No blistering or other indication of failure was encountered with any of these samples, although earlier tests indicated difficulty in terms of blistering. The temperatures in the earlier tests were not well known, and it is believed that they were operated at inordinately high temperatures. The tests in which satisfactory results were obtained were carefully monitored for temperature.

B. Could plate growth due to fuel burnup cause excessive deflections and stresses?

Measurements on the fuel-plate sample indicated no significant change in length or width; however, an increase in thickness of as much as 3% was measured. On the basis of this information, no significant problem from this source is expected in terms of excessive deflections and stresses. As stated in the answer to question 34D, there is, of course, no way to completely ensure that a new element design is satisfactory without operating the element at design conditions.

C. Could this cause binding of the outer fuel element and the control cylinder?

The answer to question B indicated that no significant plate growth is anticipated; however, should it occur, it is very unlikely that it could cause binding of the outer fuel element and the control cylinder. The outer fuel plates are contained between two cylinders, one of which is free to rotate. Growth of the fuel-plate width would simply cause a small rotation and a slight departure from the involute shape. Growth in the length would increase the plate buckling but would not significantly affect the dimensions of the outer cylindrical "side plate" of the element.

7. Provide design details of the attachment between the drive tubes and the shim-safety elements. What are the design and expected stresses at this point?

The general arrangement of one of the shim-safety elements is shown in Fig. II.7.1. The attachment member is located at the lower end of the control element. Each shim-safety element is coupled to its drive tube through an adapter fabricated of 6061 aluminum. The adapter is bolted to the control element and is in contact with the control element over its full width to a depth of $3\frac{1}{4}$ in. Two rows of $\frac{1}{4}$-in.-diam machine screws serve as fasteners. These screws are staked in place to prevent loosening. A 4-in.-diam ring is welded to the adapter and serves as the connecting link to the drive tube. As can be seen in the figure, two gusset plates are incorporated to provide additional strength.

The design of this attachment must be such that the attachment is sufficiently strong to withstand repeated scramming of the rod in addition to the loads normally applied during steady-state operation. The normal load is made up of the weight of the control element, approximately 35 lb, plus the hydraulic load, which is approximately the same. The maximum acceleration at the beginning of the scram stroke is less than 6.5*g*, and the maximum deceleration observed during tests was 7*g*; this value was reached only for scrams of very short travel wherein the shock absorber had only limited stroke.

Y-12 PHOTO 116117

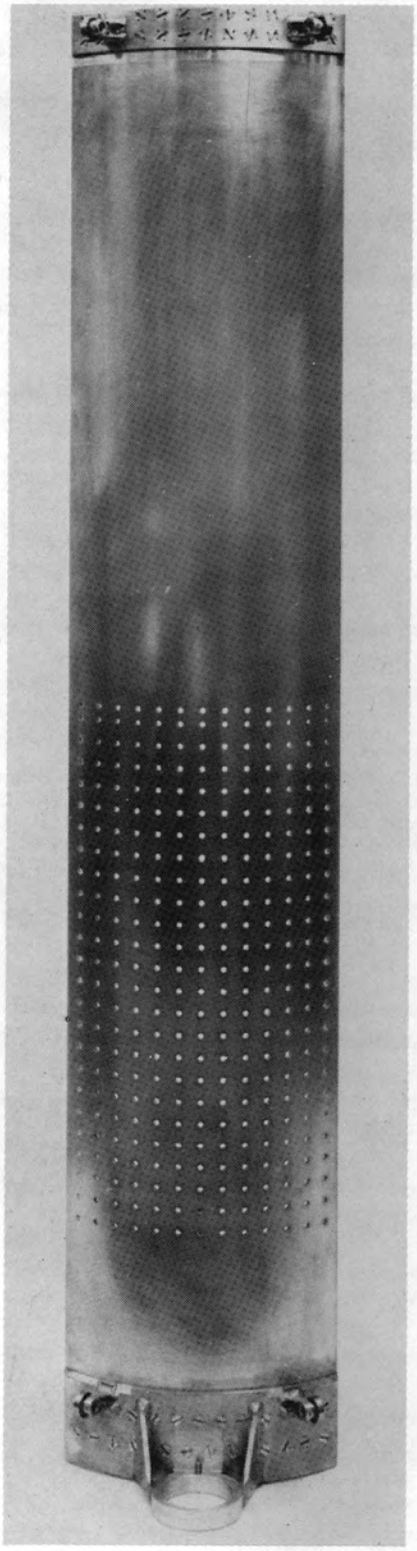

Fig. II.7.1. HFIR Shim-Safety Element.

The highest shear stress occurs in the welds connecting the ring to the adapter. The highest bending stress is in the cantilevered portion of the ring. The maximum shear stress during steady-state operation is approximately 80 psi. The maximum bending stress during normal operation is 700 psi. During a scram the stresses undergo a reversal as the control element is first accelerated and then decelerated. The maximum shear stress under these conditions is about 400 psi. The maximum bending stress under these same conditions is calculated to be about 7000 psi, even if it is assumed that all of the load is applied to the outer end of the cantilevered portion of the ring. This is conservative, as any bending of the ring would relieve the bending stress and the joint would revert to the load being carried in shear.

The attachment is a weldment that received a stabilizing heat treatment following welding. This heat treatment should produce a minimum tensile strength in the weldment of 18,000 psi.

8. Provide details on the design of the hydraulic cylinder which limits the maximum reactivity rate associated with any shim-plate failure to 0.0065 per second.

As described in ORNL-3572,[3] Sect. 8.2.3, and Appendix C, Sect. 1.3.2, the hydraulic cylinder is provided only on the shim-regulating cylinder drive. This velocity-limiting feature is provided for several reasons as set forth in the referenced material; however, the most significant feature from a safety standpoint is the protection it offers against failure of the regulating and/or shim drive gearing. Inasmuch as the shim-regulating cylinder moves downward to increase reactivity, the forces of gravity, water flow, and the reactor pressure acting on the area of the drive rod as it passes through the seal in the lower head of the reactor vessel, all combine to apply force in such a direction as to increase reactivity should the gearing fail in such a manner as to allow the drive rod to move downward. For this reason, plus the several others mentioned in the referenced material, it seemed advisable to provide force-balancing and velocity-limiting features.

The drive rod which extends through the bottom head of the reactor is coupled to the Acme lead screw of the shim drive. This lead screw extends through the rotating nut of the shim drive and is coupled to the upper end of the piston rod of the hydraulic cylinder. Due to this method of attachment, the piston rod and piston of the hydraulic cylinder move on a one-to-one basis with the shim-regulating cylinder, with no backlash or loss of motion between the two units. The hydraulic cylinder is filled with oil and is sealed at the bottom end. The piston rod passes through a seal at the top end to prevent leakage of oil from the cylinder. An oil supply line is also connected to the top end of the cylinder. The piston does not have piston or seal rings but is designed to provide a diametral clearance of about 0.004 in. with the cylinder wall. In addition to this clearance, the piston has an orifice connecting its upper and lower faces. The orifice is 0.084 in. in diameter and 0.042 in. long. Because of these interconnections between the top and bottom of the piston, there is no pressure differential across the piston when the shim-regulating drive is not moving.

The oil supply line to the top of the cylinder is supplied from bladder-type hydraulic accumulators which act as buffers between the reactor primary coolant system and the oil-hydraulic cylinder system. This type of interconnection pressurizes the hydraulic system to reactor pressure. In order to provide

[3] F. T. Binford and E. N. Cramer, *The High Flux Isotope Reactor: A Functional Description, Volume I*, ORNL-3572 (May 1964; Rev. Mar. 1, 1965).

complete buffering between the hydraulic and reactor water systems, two accumulators are used with a buffer water zone between the accumulators. An accumulator leak will therefore not contaminate the reactor system with oil or the hydraulic system with reactor water. Means are provided for routinely sampling the buffer region for detection of contamination from reactor water or from hydraulic oil.

The fact that the hydraulic cylinder has an internal pressure equal to that in the reactor system provides for the force-balance feature due to the action of the pressure on the piston rod. As mentioned previously, the area of the piston rod was selected to be slightly smaller than that of the drive rod entering the vessel. This was done in order to assure a small net downward force which will load the gears and tend to remove backlash, thus resulting in better servo performance.

The force-balancing feature also reduces the load on the gearing and thus reduces the probability of failure and assures longer life. It should be noted that the gearing is all designed for continuous duty on the basis that the force-balance feature is not present.

If the gearing should fail so as to release the rod for downward motion, the net force is very little in excess of friction, and the resulting velocity would only be about 12 in./min, that is, less than regulating rod speed. If, in addition, it were assumed that the force-balance feature were also lost, such as by failure of the oil supply line, the pressure in the cylinder would be atmospheric and the net downward force would be about 10 times that available with force balance. The resulting velocity would be limited to something less than 39 in./min. This maximum velocity is equivalent to about 0.0065 $\Delta k/k$ per second.

Design Data – Pressure Balance Cylinder

Manufacturer's designation	Hannifin hydraulic cylinder, model F2H18
Rating	3000 lb/in.^{2} operating pressure
Size	4-in.-ID cylinder × 32-in. stroke
Modifications	Piston rings removed and an 0.084-in.-diam × 0.042-in.-thick orifice installed in piston.

9. Describe the test program for the inner and outer control elements and their drives to ensure proper operation and to verify that no interference or binding can occur between the inner control cylinder and the outer shim-safety plates.

The control rod and control rod drive test facilities include a full-scale high-pressure test stand. The test stand is of sufficient size to accept a mockup of one complete quadrant of the reactor control region and is capable of 0 to 1000 psi pressure, 0 to 200°F temperature, and 0 to 500 gpm flow.

Although the test stand was originally fabricated primarily for control rod drive tests, it was modified to include six strain-gage bridges on the bearing mounting brackets at each corner of the outer control rod and on the two preload bearing mounting brackets, three differential transformers to measure vibration and deflection on the outer control rod, and a total of 23 pressure taps to measure differential pressure between the various gaps, etc.

Data were taken with 0, 10, 100, and 130% full flow at numerous combinations of positions of the inner and outer rods, at various pressures, and at 60, 150, and 200°F temperature. The control rods

performed satisfactorily during these tests, as well as for approximately 1500 or more routine cycles and scrams during the control rod drive development and certification tests.

A number of preliminary tests of pressure drops along the rods, thermal deflection tests, load deflection tests, rivet and bolted joint tests, etc., were also made on the control rods but will not be discussed in detail.

In order to ensure that the proper gaps will be achieved between the inner and outer control rods and between the control rods and the fuel element and reflector, these gaps have been measured in the reactor for a number of combinations of the critical components. A total of approximately 1500 gap measurements have been taken and reported using two removable reflector assemblies, two sets of outer control rod track and bearing assemblies, and three complete sets of control rods. These gaps are within the anticipated tolerance for all combinations.

A prototype outer control rod drive assembly was thoroughly developed and tested in the high-pressure test stand under all conditions of flow, pressure, and temperature. In addition, separate test facilities were used to provide preliminary information and life tests on the magnet actuator and engagement mechanism assemblies, bearings, seals, and gear boxes.

After completion of fabrication of the reactor-grade assemblies and a number of preliminary tests to check performance, a complete set of certification tests were performed on each assembly in the high-pressure test stand. These tests included 112 scrams from various elevations, with and without flow, and at 0, 600, and 900 psi pressure. Measurements of release time, response time, time of flight, control rod displacement, velocity and acceleration as a function of time, magnet armature displacement as a function of time, and drop current were taken during these tests.

The complete inner control rod drive assembly was tested in a high-pressure autoclave. Both the shim and regulating drives were run more than 200 cycles over their complete stroke. The pressure-balance system was developed and thoroughly tested in this facility.

After the reactor assembly and during the initial hydraulic tests on the components, differential pressure taps were again used to measure flow and pressure drop through the control region. In addition, a differential transformer was installed to measure the deflection and vibration on each outer control rod. The inlet orifice to the control region was modified during these tests due to a flow streaming problem from the orifice. After this modification the test data on pressure drop, flow, vibration, and deflection were very similar to test-stand data and well within acceptable limits.

The control rods and control rod drives performed satisfactorily during all hydraulic tests. Over 200 scrams have been logged for each outer control rod drive assembly, with three sets of control rods having been installed and under various conditions of flow and pressure. Each control rod drive assembly has been completely disassembled and inspected twice during this period. No abnormal characteristics or wear have been discovered.

Over 50 complete cycles of the inner control rod shim drive have been logged in testing both the drive and the pressure-balance cylinder in the reactor. The inner control rod regulating drive has been run in the reactor under simulated servo control by means of a computer for several hours under various simulated reactor conditions and simulated safety signals. Satisfactory results were obtained.

The control plates and drives have been in use during the startup program, which has been in progress since Aug. 25, 1965, and over 75 startups have been logged to date. Each startup has been preceded by routine tests on the safety system and control element drives. The operation has been satisfactory at all times during normal use with the exception of the necessity to provide vents between the fast insertion air motors and the gear boxes and one loose electrical connection on a terminal strip supplying power to the air-motor control solenoids.

10. Quantitatively, how are the reactivity coefficients for the core expected to vary during the operating cycle?

The fuel region moderator density coefficients are affected by control rod position because the control rods, to a large extent, control the return leakage of neutrons from the reflector. When the rods are inserted, neutron leakage to the reflector has little chance of returning. With the rods out, the return leakage is greater. Therefore, the moderator density coefficients become less negative as the rods are withdrawn. Calculations indicate that the coefficients decrease by a factor of 2 from the clean core symmetrical rod position to the fully withdrawn rod position.

11. What are the limits for reactivity which can be added by experiments in the target hole?

The limits for reactivity which can be added by experiments in the target hole are presently established at those corresponding to the present design of target. The major concern and limitation are based on the amount and rate of addition of reactivity that could be added by introducing the optimum void into the target region with the target installed. The amount and rate of addition are discussed in Sect. 1.3.3 of Appendix C. The worst case is the addition of 0.013 $\Delta k/k$ on a 0.03-sec ramp plus about 0.002 $\Delta k/k$ on a 0.3-sec ramp.

Changes in target composition also affect reactivity as discussed in Sect. 7.3.5 of ORNL-3572 and in Sect. 2.5 of Appendix C. This variation is primarily of concern in regard to shutdown margin; however, the criteria set forth in Table I.C.8, Sect. 2.2.5, of Appendix C, apply regardless of whether the target adds or subtracts reactivity.

12. Discuss the possibility and consequences of a large reactivity overshoot with the control plates being withdrawn past their critical position during xenon burnout in a scram recovery.

The minimum rate at which the ganged safety rods or the regulating rod can change reactivity while the rod drive motors are running is 2×10^{-4} Δk/sec. At full power, xenon burns up at an equivalent rate of less than 1×10^{-4} Δk/sec. Therefore, the control system has no trouble keeping up with xenon transients.

The question of xenon burnout during a transient is treated in the answer to question 38D.*

*See also answer 42A.

13A. What is the maximum total delay time (including detector delay time) between the onset of an unsafe condition and the initiation of rod drop during startup and full-power operation?

The maximum total delay time is the sum of the individual component delays in the safety channel. Assuming that safety action is required from an increase in flux, the components in the channel and their respective total delay times are tabulated below:

Component	Delay Time
Ion chamber	300 μsec
Flux amplifier (mode 1)	100 μsec
Trip comparator	150 μsec
OR gate	10 μsec
Magnet control amplifier	100 μsec
Magnet	
(a) Two-out-of-three	4900 μsec
(b) Three-out-of-three	3200 μsec
Total (two-out-of-three)	5.56 msec
Total (three-out-of-three)	3.86 msec

A mechanical actuator time, which represents the relaxation time of the push rod, must be added to the above release times. The value of this delay time is approximately 3.5 msec for three-out-of-three, and approximately 5 msec for two-out-of-three.

Should the safety action be required from reduction in flow, the same total delay times as those tabulated above would apply with the following exceptions: (1) The ion chamber and flux amplifier response times would be subtracted, and (2) a response time of approximately 250 msec should be added for the flow sensing and transmitting system.

It is extremely difficult to measure all of the delays in a single test, or some of them at all. For example, the diffusion time of the neutrons from the core to the chamber location and the chamber collection time can only be measured under laboratory conditions. However, periodic checks of the time response of certain groups of the equipment will be made. The grouping will be made on the basis of practical considerations. The tests will overlap on the channel to assure complete coverage.

B. Has the total system been tested or will it be tested to measure this time with all three and with only two of the coincident circuits tripping?

The following tests have been run. A simulated step in ion-chamber current was injected at the chamber signal terminals. The time required for the test signal to reduce the magnet current to 10% of its original value was recorded. For mode 1 the time was approximately 300 μsec.

Routine tests involving more than one channel and including some of the components tested above are performed as follows. A scram test signal is applied to either two- or three-channel OR gates.

Application of the test signal starts three timers which record: (1) the time the latch push rod has moved 0.015 in., which is somewhat more distance than is required to start shim-rod motion, (2) push-rod time of flight, and (3) shim-rod time of flight. Typical numbers for these time increments are: 13, 29, and 328 msec respectively for two-out-of-three; and 9.6, 25.2, and 324 msec for three-out-of-three.

It should be noted that measurements obtained in the latter test are not intended to give precise absolute times, since the time increment is composed of electronic, magnetic, and mechanical delays. Therefore, part of the timing sequence is obtained from mechanical motion by a switch which has inherent delays. However, the actual times can be deduced from the timer data. More importantly, changes in the behavior of the release system can be quickly detected.

14. How was the time response of the neutron flux amplifier determined? What was the magnitude of the input steps?

The time response of the flux amplifier was measured by applying a step function in current to its input terminals and observing the output on an oscilloscope. The magnitude of the input step was approximately 20% above the trip level. The recorded time is the time required for the output to reach the trip level rather than the 63% value.

15. What is the accuracy of the heat-power calculator and what are the error contributions of the temperature and flow inputs?

There are six heat-power calculators as described in ORNL-3572, Sects. 8.6.2 and 8.6.3. Three of these are associated with the safety system and are electronic. The other three are associated with the servo control system and are pneumatic.

The accuracy of the heat-power calculators has been guaranteed to be $\pm 2\frac{1}{2}\%$ at full scale (full scale is 150 Mw). Calibrations of the equipment have shown that the accuracy is somewhat better than $2\frac{1}{2}\%$. The overall accuracy of both flow and differential temperature channels is approximately $\pm 1\%$. The full scale for flow is 17,000 gpm, and the full scale for ΔT is 72°F.

16. What control problems are anticipated from the photoneutrons from the beryllium reflector? How will they affect startup immediately after scram? What magnitude flux is expected at the detector positions from the photoneutrons after shutdown?

Photoneutrons from the beryllium reflector will create no control problems in the HFIR. During a startup immediately after scram, the beryllium photoneutrons will act as a very large source of neutrons to the core and very few directly to the fission chamber, a desirable situation. Of more concern are the D_2O photoneutrons. For example, 1 min after scram from 100 Mw the fission power will be about three decades down, or approximately 100 kw. When the fission counter is withdrawn from the core by 95 cm, which is the approximate position it would be in for this condition, the combination of neutrons leaking from the core and those produced by D_2O photoneutrons at the fission counter location will produce a flux of 5×10^5 neutrons cm^{-2} sec^{-1}, which is the flux necessary to provide the desired 10^4 counts/sec. At this time the ratio of D_2O neutrons to core neutrons is 0.30, that is, only 30% of the counts are from

the D_2O. This situation will improve with time since the chamber will be moved closer to the core to obtain 10^4 counts. Ten minutes later the D_2O contribution will be down to 15%.

The neutron current in the ion chamber locations due to beryllium photoneutrons is estimated to be approximately 3% of the total current at 100 Mw (a negligible 0.1% is due to D_2O photoneutrons). One minute after scram from 100 Mw, assuming equilibrium gamma in the core, the current produced by beryllium photoneutrons will be approximately 5×10^{-2} of the 100-Mw value or the equivalent of approximately 150 kw power level. Ten minutes after scram, the current due to beryllium photoneutrons will be equivalent to a power of approximately 30 kw. These photoneutron currents tend to bias the safety system in the direction of producing a scram before it would otherwise occur, but only a negligible amount.

17A. What consideration has been given to the use of scram or setback actions initiated by a loss of power to the facility or to the pumps?

Setback and/or scram action is taken on actual flow reduction as indicated by the flow sensors rather than loss of power, since flow reductions may occur from other causes than loss of power. As described in ORNL-3572, the control system is designed so as to attempt to avoid the necessity for a scram during a power outage in order to minimize the probability of losing a core due to xenon buildup. Most power outages in this area are only of a few seconds duration, and, therefore, if a scram can be avoided, the reactor can be taken back up to power almost immediately without the necessity for recovery from the scram with its attendant control and operational problems.

B. Provide curves showing primary coolant flow vs time following loss of pumping power and reactor power level vs time due to the associated cutback.

Figure II.17.1 shows the variation in flow as a function of time after loss of power to all pumps (curve *a*). Curve *b* shows a typical servo-controlled power reduction as a result of the flow reduction. Curve *c* shows the safety trip setting as a result of the flow reduction; this includes the time delays of the flow-measuring system.

As described in ORNL-3572, Sect. 8.3.2*a*, the regulating servo requires help from the shim rods in taking the reactor power level down so as to avoid a scram. The variations from a smooth curve which can be observed in curve *b*, starting a little below 50 Mw, are the result of the intermittent action of these motors.

The allowable power level based on calculations does not decrease linearly with flow although the safety-system trip setting is reduced on this basis. This situation leads to a larger margin at lower flows. The calculated power level for the onset of nucleate boiling is greater than 20 Mw at 10% flow, as can be seen in Fig. 8.1.1 of ORNL-3572.

18. What is the relieving capacity of the high-pressure relief valves, and what was the basis, or criterion, which determined this capacity?

The criterion for sizing of the primary system relief valves is that the "Code" be satisfied in terms of overpressure with the sole source of overpressure being the capacity of the pressurizer pumps.

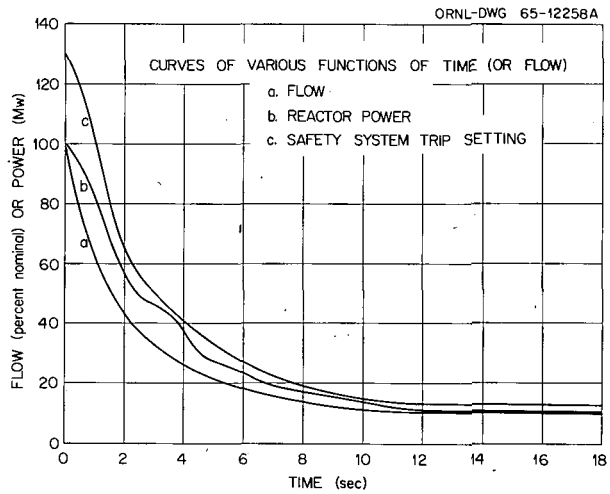

Fig. II.17.1. HFIR Flow Coastdown Studies.

Article 9 of Sect. III of the ASME Boiler and Pressure Vessel Code requires that the relieving devices installed to protect the system be of sufficient capacity to prevent a pressure rise in the system of greater than 10% above the design pressure. In addition, at least one valve must relieve at a pressure not greater than design pressure, while all others must relieve at pressures not greater than 105% of design pressure. For the primary system the limits are:

Maximum pressure	1100 psig
Maximum set pressure (one valve)	1000 psig
Maximum set pressure (remaining valves)	1050 psig

Other high-pressure relief valves are located at the discharge of the emergency pressurizer pump and must relieve the full capacity of that pump, and on the hot water injection system to relieve the primary side in the event of heating steam causing expansion of the water when the system is isolated by valving from the primary system.

The arrangement of primary system relief valves is as follows:

Valve No.	Set Pressure (psig)	Location	Orifice	Approximate Capacity at 10% Overpressure (gpm)
PSV 150	1025	Reactor vessel inlet pipe	H	>400
PSV 154	975		G	>200
PSV 155	900	Discharge of PU-11	G	>200
PSV 1125	1150	Hot water injection system	G	>200

Primary system tests have indicated that with the G orifice valve set at 975 psig and the H orifice valve set at 1025 psig, the pressure as measured at PT 127 did not exceed 1060 psig with circulating pumps PU-1A, -1B, and -1C and both main pressurizer pumps, PU-4A and -4B, in operation. It should

be noted that under these conditions 1100 psig is not exceeded anywhere in the primary system downstream of V-1198, which is the discharge check valve in the pressurizer pump line. It can be shown that the same is true for other combinations of primary pumps in operation. The piping, flanges, valves, etc., between V-1198 and the pressurizer pump will also be adequately protected since the shutoff head of the pressurizer pump is insufficient to cause a rise in pressure exceeding 110% of the maximum allowable pressure for this section.

A power outage test with the radiation letdown block valves closed indicated that PSV-155 set at 900 psig was adequate to carry the capacity of PU-11 and would limit system pressure to below the set point of PSV-154 when the primary circulating pumps were not in operation. This provided both adequate safety and adequate containment in the event of a simultaneous power failure and fuel-element cladding failure.

A question was asked at one of the HFIR review meetings regarding the effect on pressure in the primary system of temperature changes in the primary system such as might be caused by loss of secondary coolant to the heat exchangers, changes in reactor power level, etc. This situation was investigated early in the project, and it was found that the most conservative approach is to assume a step change in reactor power level, as this could be more nearly realized than any other change affecting the temperature. A step increase in power level of 100 Mw is equivalent to adding 200 gpm of water. The measured amount of water which must be added to the system to increase the pressure by 900 psi is approximately 50 gal. The addition of 200 gpm or the equivalent step change in power of 100 Mw would therefore change pressure at the rate of 3600 psi/min. If it is assumed that the pressure control system did not work, the pressure would rise until the pressure relief valve, PSV-154, opened. This valve alone can handle a flow greater than 200 gpm. Should this valve fail to open, PSV-150 would open at a slightly higher pressure and is capable of handling more than 400 gpm.

19. What peak power and plate temperatures would result if scram action is initiated by the 130-Mw overpower scram instead of the rate scram for an addition of 0.013 $\Delta k/k$ (Table I.C.4)?

As demonstrated in the transient analysis of the HFIR, the rate scram will terminate a fast transient sooner than the level scram will, and that is one of the reasons for incorporating a rate scram. Since the rate scram instrumentation has safety-system reliability, there is, in principle, no need to be concerned about the results that would be obtained if the rate scram were to fail. The question is even more of academic interest if considered in light of the discussion regarding the comparison between the SPERT core and the HFIR core, in which it is concluded that the HFIR core could quite probably stand a rapid insertion of 0.013 $\Delta k/k$ without damage even with the safety system being required only for shutdown of the reactor following the transient.

We do not have data to show the peak power and plate temperature calculated by the analog model for this set of conditions. However, it is possible to make several statements regarding the performance which would be observed under this condition. Test case No. 4 of Table I.C.4 is a typical full-power case in which 0.013 $\Delta k/k$ was ramped in on a 0.03-sec ramp. This case was run with

an initial safety rod worth of 0.0035 $\Delta k/k$ per inch of travel, which corresponds to about $1\frac{1}{2}$ days before the end of a fuel cycle. Figure I.C.1 shows the power and temperature behavior for this case.

Measurements made on the analog model indicate that the rate-trip actuation occurred at a power level of about 110 Mw. From the power curve of Fig. I.C.1, it can be seen that this corresponds to a time of about 6.3 msec after start of the reactivity ramp. The power level would reach the 130-Mw power trip at about 11 msec after start of the ramp. This time difference can be considered as an equivalent delay in start of control rod motion of 4.7 msec. Figure 8.8.2 of ORNL-3572 presents the results of analyses run to investigate the relationship between initial control element acceleration, safety-system delay time, and the amount of $\Delta k/k$ which could be inserted without exceeding a given criterion for fuel-plate hot-spot damage. The curves of interest are those labeled "damage criteria." "Damage criterion" is somewhat of a misnomer; however, it is defined as the point at which the hot spot reaches the melting temperature and also contains sufficient heat to overcome the heat of fusion. If we look at the curve labeled 6 *g* (typical of the measured HFIR response) and consider the $\Delta k/k$ inserted for safety-system delay times of 10 and 14.7 msec (10 + 4.7), we find an allowable insertion of 0.0147 $\Delta k/k$ on a 0.03-sec ramp for the first case and an allowable insertion of 0.0137 $\Delta k/k$ for the second case. The values taken from the 4 *g* curve are 0.0136 $\Delta k/k$ and 0.0128 $\Delta k/k$ for the rate and level trip respectively. The differences are indicative of the difference in performance to be expected between the rate trip and the level trip with a 0.03-sec ramp in reactivity starting at full power. If one considers the probable accuracy of such a calculation on an absolute basis, it could be said that there is no significant difference. The relative differences are probably real.

20. In Table I.C.8 in Appendix C, why was only the "no void" condition considered in Case IV?

The discussion of shutdown margin criteria (Sect. 2, Appendix C) is not sufficiently clear. It is not considered credible that two "accidents" will occur simultaneously, and in this sense the failure of one of the four safety rods to scram is not considered to be an accident. For all cases in which a scram takes place, it is assumed that only three of the safety rods scram. Thus, for case I the accident is the optimum void in the flux trap without the target. For cases II and III the accident is the optimum void in the flux trap with the target; and for case IV the accident is runaway control elements, that is, the "startup" accident.

21. Would any fuel melting occur if an irradiated core were to fall to the bottom of the pool?

The fuel elements are designed so that if one or both (assembled) elements are in an upright position in the pool a satisfactory return flow passage will be provided and no melting will occur. If the element should fall on its side, natural circulation in the channel would be impaired. A conservative calculation indicates that at least one day of cooling would be required after shutdown before the elements could be positioned horizontally without melting. Partially for this reason, the elements will be stored in the reactor pool for at least one day before being moved to the clean pool. Furthermore, the fuel element han-

dling tools have of course been designed so as to minimize the possibility of dropping a fuel element or positioning the element horizontally with the tool attached.

22A. Discuss the reasons that a backup system for reactivity control has not been incorporated into the design of the HFIR.*

Several situations have been considered in which a backup system for reactivity control would be desirable. One of these situations is set forth on page 22; another situation is described on page 89. The first situation mentioned, that of the two fuel elements sticking together, is associated with fuel handling and requires a method of reducing the reactivity of the fuel elements while removing them from the reactor to the storage racks. The second situation is that in which one or more of the control elements becomes stuck or jammed, and a method of reducing reactivity of the system is required in order not to violate the shutdown margin criteria while unloading the reactor. As noted on page 89, two auxiliary methods of reducing the reactivity were considered. The first method was that of inserting poison strips into the fuel element, the second was that of adding a poison to the reactor coolant water. The first method was chosen as it met the requirements for fuel handling as well as the situation involving stuck control elements. This technique was investigated during tests at the Critical Experiment Facility and in a mechanical mockup of the system. In addition, the program for investigation of the HFIR characteristics during the startup period includes demonstration of this technique, not only for the purpose of providing additional reactivity control, but also as a method of poisoning the core in order to measure control rod differential worth when desirable in the future.

The second method, that of poisoning the water, was decided against on the basis of the fact that experiments run in our Critical Experiment Facility and in the HFIR showed a considerable retention of the poison (boron solution) in the core region. These particular experiments were so designed that the poison solution was confined to the HFIR Critical Experiment No. 3 (HFIRCE-3) fuel element, and provisions were made for flushing of the element with acid and/or caustic to remove the retained poison. In the HFIR it would be necessary to poison the entire primary coolant system, and therefore it would appear that the target, control, and reflector regions would also retain some of the poison. Flushing of the entire coolant system with acids and caustic of adequate strength to remove the poison would be a highly undesirable technique due to the corrosion problem brought on by the action of the chemicals on the many dissimilar metal contact points. Inasmuch as a reduction of flux in the experiment facilities could seriously impair the ability of the facility to meet its objectives, it was decided that use of a "soluble" poison would not be acceptable. This situation is somewhat different from that in a power reactor, where the poison may be maintained or burned out while the reactor is producing power.

In addition to the poison-strip method provided for reducing reactivity, it should be recognized that insertion of either the shim-regulating cylinder or all four shim-safety plates is adequate to keep the

*Further discussed in answers 42 and 60.

reactor shut down. The shim-safety plates are provided with three different methods of insertion: scram insertion by gravity and spring force, electric motor insertion, and air motor insertion. The shim-regulating cylinder has only the electric motor for normal operation; however, provision has been made for slow insertion (approximately 30 min for full travel) by using a manually held unidirectional air motor, should difficulty be encountered with the electric motor drive.

It is believed that the above provisions, when considered together with the criteria for shutdown margin set forth in Table I.C.8, page 90, constitute an adequate system for ensuring that the reactivity can be reduced when necessary.

B. What are the consequences of two or three quadrants of the control system sticking in the full-out position under various accident or abnormal conditions?

Normally there are only three conditions during the lifetime of each fuel loading when a shim-safety quadrant is permitted to be fully withdrawn:

1. During checkout of the control and safety system, prior to startup with a new fuel loading, one control element at a time will be withdrawn to check for free motion and to measure the safety release time and the time of flight of the shim-safety elements. Operating procedures require that a target or its equivalent be in position during these tests in order to limit the increase in reactivity which would result from an optimum void insertion. If the control element being tested were to become stuck so that it could not be inserted, special operating procedures would be used to ensure safe removal of the target and fuel.

2. At the end of core life, all control elements would be fully withdrawn. The reactivity excursion analysis described in Appendix C included this case. The analysis for this case was based on a minimum initial safety rod worth of 0.00059 $\Delta k/k$ per inch, which corresponds to the end of control-element lifetime and assumes that only three of the four safety elements respond to the scram signal. The consequence of more than one of the safety elements failing to respond to the scram signal would be an increase in the calculated fuel-plate temperatures. Based on the comparison between the SPERT case and the HFIR case set forth in the above reference, it appears that the HFIR would not suffer serious damage from such an incident. At this time in core life, insertion of any one of the control elements would provide adequate reduction in reactivity to maintain the reactor shutdown. It does not appear reasonable to us to assume the coincidence of such a reactivity excursion concurrent with multiple failures of the safety system.

3. It is conceivable that all control elements might be almost fully withdrawn due to the buildup of xenon poisoning during recovery from a scheduled or unscheduled scram at some time other than at the end of core lifetime. The situation here would be similar to that described in the preceding paragraph B2.

C. Could a pressure surge in the core damage all control elements sufficiently to prevent their motion? If so, what are the possible sources of such pulses? What kind of reactivity transients could lead to this event?

The only mechanism which appears to have the capability of producing a pressure surge sufficiently large to give concern is that which was observed in the SPERT I destructive tests on the D-12/25 core for a rapid reactivity insertion of 0.024 $\Delta k/k$. No damage was observed in earlier tests at somewhat smaller reactivity additions. It appears from the information at hand that no pressure surge of sufficient magnitude to cause significant damage would occur in the HFIR for the reactivity accidents considered. Based on the comparison between the SPERT case and the HFIR, it would appear that a rapid reactivity transient larger than 0.024 $\Delta k/k$ would be required to initiate such a pressure surge.

D. Under what circumstances would a slower-acting backup control system be of real value?

As set forth in the answer to question 22A, there are several situations in which a backup control system is of some benefit. It should again be noted that insertion of either the shim-regulating cylinder or the four shim-safety quadrants is adequate to maintain the reactor in a shutdown condition.

23. Provide information regarding the following aspects of the adequacy of the core cooling system:

A. A discussion of the reason that a core spray system or other emergency cooling system is undesirable or unnecessary.

In order to prevent partial melting of nearly expired HFIR fuel elements immediately after shutdown from 100-Mw operation, it is necessary that the coolant flow rate be about 7% of normal full flow. The HFIR is equipped with a dc-powered emergency cooling system that will provide at least this much flow, provided that any one of the main circulation pumps is free from mechanical damage which would prevent its rotation by the integral dc motor. It is believed that this constitutes an adequate emergency cooling system. A description of this system is given in ORNL-3572.

As set forth above, it is not only necessary that the core be flooded but that circulation be maintained for about an hour following shutdown, and a core spray system would not in itself be adequate to prevent melting. In order to ensure that makeup water is available to keep the primary system full even in the event of failure of the diesel generators following a power outage, two interconnections are provided between the pool and the reactor system. One of the connections is through a check valve which automatically ensures that makeup water will be added if the reactor inlet pressure drops below pool pressure, and the other connection is through a manual valve.

B–C. An analysis of the thermal effects on the core resulting from a rapid depressurization of the primary system or a complete loss of coolant flow. An analysis of the extent and consequences of metal-water* reactions which might occur as a result of a loss of flow, a loss of coolant, a rapid primary system depressurization, or other credible accidents.

---

*Appendix I further considers energy releases from aluminum-water reactions.

A brief discussion of the depressurization accident was presented in Sect. 4.2, and in ORNL-3572, Sect. 8.8.5. However, in that analysis it was assumed that the pressure loss was due to a leak equivalent to an open 3-in. valve. Under those conditions, the reactor would continue to operate at full power for approximately ½ sec while the pressure fell to 300 psi, at which point the reactor would be shut down by a pressure scram. It was concluded that the temperature at the hot spots might exceed the burnout point for a short period of time (approximately ½ sec) starting about 2 sec after the initiation of the pressure loss. The present scram pressure setting is 375 psi, which would provide a small additional margin.

A quantitative analysis of a sudden or step decrease in pressure is difficult because of the virtual impossibility of predicting the exact sequence of events in the core following such an event. The number and magnitude of local hot spots and the physical behavior of the fuel in these regions could have a significant effect on the heat-removal characteristics of the rest of the core. For example, if the fuel melted and dripped out of the fuel plates, it might rearrange itself into a configuration better suited for removing heat. On the other hand, if several plates melted or buckled and came in close contact with one another, the heat-transfer mechanism could be inhibited to some extent.

Nevertheless, it is possible to take a semiquantitative look at the overall situation from an integral point of view and to draw some conclusions based upon this examination.

The model* utilized for this is as follows. It will be assumed that with the reactor operating at 100 Mw (9.48×10^4 Btu/sec), a step decrease in pressure occurs in which the pressure is instantly decreased from 40 atm to 1 atm. It is further assumed that, following this pressure reduction, the average rate of heat removal will be proportional to the difference between the fuel temperature and the temperature of the surroundings. The latter is assumed to remain unchanged during the pressure loss. In developing this model, the following nomenclature is used:

$G(t)$	Total heat-generation rate (Btu/sec)
$T(t)$	Fuel temperature minus temperature of surroundings (°F)
T_0	Initial value of $T(t)$ (°F)
T_w	Temperature of surroundings (°F)
$T_m(t)$	Fuel temperature (°F)
C	Specific heat of fuel (Btu lb^{-1} °F^{-1})
M	Total fuel weight (lb)
S	Heat-transfer area (ft^2)
t	Time (sec)
K	Heat-removal constant (Btu °F^{-1} sec^{-1})
h	Heat-transfer coefficient (Btu ft^{-2} hr^{-1} °F^{-1})
κ	Conductivity of steam (Btu ft^{-1} hr^{-1} °F^{-1})

The change in the value of $T(t)$ with time may then be expressed as

$$MC\,\dot{T}(t) = G(t) - K\,T(t),\ T(0) = T_0\ ,$$

*Answer 43 gives time sequence of events in case the assumed heat transfer did not take place.

whence

$$T(t) = e^{-\mu t}\left[T_0 + \int_0^t \frac{e^{\mu\tau} G(\tau)}{MC}\, d\tau\right],$$

so that

$$T_m(t) = T_w + e^{-\mu t}\left[T_0 + \int_0^t \frac{e^{\mu\tau} G(\tau)}{MC}\, d\tau\right],$$

where here

$$\mu \equiv K/MC .$$

The total heat-generation function $G(t)$ is obtained from analog studies of the system response following a loss of pressure. For convenience it is represented as a stairstep function having the form:

$$\begin{aligned}
G(t) &= 9.48 \times 10^4 \text{ Btu/sec}, & 0 < t < 0.05 \text{ sec}, \\
G(t) &= 6.21 \times 10^4 \text{ Btu/sec}, & 0.05 < t < 0.15 \text{ sec}, \\
G(t) &= 2.51 \times 10^4 \text{ Btu/sec}, & 0.15 < t < 0.25 \text{ sec}, \\
G(t) &= 1.42 \times 10^4 \text{ Btu/sec}, & 0.25 < t < 0.35 \text{ sec}, \\
G(t) &= 9.48 \times 10^3 \text{ Btu/sec}, & t > 0.35 \text{ sec}.
\end{aligned}$$

[Actually $G(t)$ decreases proportional to $t^{-0.2}$ after a few seconds but this is neglected here.]

Also, $M = 150$ lb, $S = 430$ ft^2, $C = 0.25$ Btu lb^{-1} °F^{-1}. Now K is an overall heat-removal constant such that $K = hS/3600$. The appropriate value of h is obtained by assuming that a film of steam 1.5 mils thick blankets the fuel. The conductivity, κ, of steam[4] increases almost linearly with temperature from 0.014 Btu ft^{-1} hr^{-1} °F^{-1} at 200°F to 0.051 Btu ft^{-1} hr^{-1} °F^{-1} at 1600°F. We have $h = 12\kappa/0.0015$ so that $K = 955.5\kappa$ Btu °F^{-1} sec^{-1}, $\mu = 25.5\kappa$ sec^{-1}. In the temperature equation both K and μ are taken to be constants; however, they are adjusted to appropriate average values for each of the temperature regimes.

Values of the average core temperature were found by using the average water temperature $T_w = 150$°F and the initial fuel temperature $T_m(0) = 202$°F. These are plotted in Fig. II.23.1. The equilibrium temperature of 648°F is well below the melting point.

The hot-spot fuel temperature was also estimated using a water temperature of 461°F and an initial metal temperature of 480°F. The power density may be as high as 2.5 times the average, and the values of $G(t)$ were adjusted accordingly. Under these assumptions, the hot spots would, as shown in Fig. II.23.1, reach a temperature of 1210°F, which is very close to the melting point. An additional 167 Btu/lb would be necessary to supply the required heat of fusion. Thus a complete reaction of the U_3O_8 fuel with aluminum, which could supply adiabatically a maximum of 109 Btu per pound of aluminum, would not be sufficient to cause melting. Hence there seems to be little possibility of a metal-water reaction, which requires an ignition temperature of 2140°F.

---

[4] A. W. Lemmon, Jr., *et al.*, *Empirical Evaluation of the Properties of Steam at Elevated Temperatures and Pressures*, BMI-858 (Aug. 25, 1963).

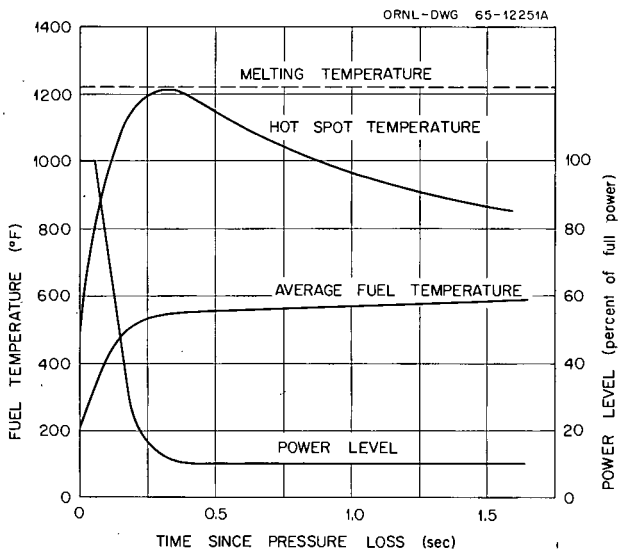

Fig. II.23.1. Variation of Reactor Power and Core Temperature with Time Following a Step Loss in Pressure.

It must be recognized that the validity of the heat-removal assumptions used above are open to question and that various physical occurrences in the core may alter them either for the better or for the worse. It is believed, however, that the temperatures deduced from this model are fairly realistic. This is reinforced by the fact that implicit in the hot-spot model is the assumption that only about 25% of the nuclear heat is removed during the transient immediately following the pressure loss, and that only 15% is removed in the average case. It seems reasonable to believe that at the temperatures involved, there is sufficient thermal driving force to accomplish this.

An analysis of the loss-of-coolant-flow accident is not quite so difficult as the sudden-depressurization accident, and it may be approached in several different ways. The results show that the core will start to melt at some time between 10 and 100 sec following the start of flow coastdown. The rate of temperature rise of the core, considered on the average, will fall between 75 and 40°F/sec at this time. Prediction of the sequence of events following melting is virtually impossible. The significant point is that the rate of temperature rise is not very rapid, and, therefore, if dispersal of the material occurs by dripping or running out of the core, it is probable that cooling will take place and little, if any, metal-water reaction would be expected. On the other hand, the material may stay together until the temperature is considerably in excess of the H_2O-Al reaction temperature and then be suddenly dispersed by a steam explosion, in which case there would almost certainly be some reaction.

The foregoing may not appear to be complete answers to the questions; however, it is our opinion that insufficient data exist for us to quantitatively answer these questions. It would serve little purpose for us to supply a sophisticated analysis for situations in which the basic assumptions would be guesses at best. If such information existed, it would certainly not be necessary to run tests such as the LOFT being undertaken at the NRTS.

It is our position that the design of the facility is adequate to reduce the probability of such failures to such a low level that they are not expected to occur during the life of the facility. If such an event should occur, despite our precautions, the containment features would be expected to be adequate to limit the exposure to a tolerable level.

24A. Discuss the adequacy of the beam-tube design.*

The HFIR horizontal beam tubes and experimental facility tubes which penetrate the reactor vessel have been designed for 1000 psig external pressure at 150°F with stress values not exceeding those permissible under Sect. VIII, Unfired Pressure Vessels, of the ASME Boiler and Pressure Vessel Code. The materials used in construction have a quality control in accordance with HFIR Procurement Notes SST-2 and AL-2 to ensure that the materials are of the highest quality commercially available and higher than specified in the ASME Code. Dimensional tolerances and welding have been maintained at a standard consistent with the high standards of the materials.

The design is based on a nominal lifetime of ten years. The actual life of the tubes will be determined by the corrosion rate and any detrimental effects of radiation damage as evidenced by surveillance specimens. The corrosion allowance is $\frac{1}{32}$ in. and is considered to be more than adequate for the ten-year lifetime, based on existing out-of-pile data.

All pieces of equipment exposed to reactor pressure have been hydrostatically tested to $1\frac{1}{2}$ times the design pressure. In addition, typical high-pressure bellows and beam-tube flanged joints have been tested to a hydrostatic pressure in excess of 4000 psig without failure. An investigation of the collapse resistance of the horizontal beam tubes was made by the Stress Analysis Laboratory of ORNL. The collapse predictions for the cylindrical portions of the tubes were obtained from the classical instability formula for cylindrical shells subjected to external pressure. For the instantaneous collapse predictions, the tangent modulus method was used in conjunction with the short-time stress-strain curve for the tube material. The creep collapse pressures were obtained by using the tangent modulus method in conjunction with the ten-year isochronous stress-strain curve for the tube material. The instantaneous collapse predictions obtained by the tangent modulus method agree well with experimental results. The creep collapse predictions are, however, only approximations that are probably conservative. The factors of safety against collapse at 1000 psig external pressure were calculated to be 6 and 3 for the instantaneous and ten-year creep conditions respectively.

Based on the above information and on the available information on the effects of radiation, which will be covered in a later section of this answer, we believe that the design of the horizontal beam and experimental facility tubes is adequate for the proposed service.

The horizontal beam tube extensions, which are welded to the beam tubes outside of the reactor pressure vessel and which extend through the concrete shielding, are designed to withstand an internal vacuum plus the head of water equal to the depth of the pool. They are also designed to withstand an internal pressure adequate to handle any normal pressure due to coolant which might be used either in the tube or

---

*Further discussed in answer 44.

in the shielding plugs. This is nominally 150 psig. As a practical matter, mechanical and fabrication considerations were overriding, and therefore the design is such that the weak point in the cylindrical extension tubes is the large-diameter (~7-in.-ID) outer end of the tube, which will meet Code requirements for a working pressure of about 500 psig. The outer ends of the horizontal beam tube extensions are provided with O-ring-sealed caps which are held in place by shear rings. The present design of the bolting for the end caps is adequate for a Code working pressure of 273 psig.

The outer end of each of the beam tubes is also provided with a rupture disk that discharges into the pool to relieve any overpressure which might result from small leaks from the reactor vessel, the plug coolant system, or from misoperation of the system provided for filling the beam tubes with dry air or helium.

The experimental facility tubes are designed to withstand 1000 psig internal pressure over their full length and are provided with a bolted flange outer closure which meets Code requirements for 1000-psig service.

B. In particular, discuss the desirability and feasibility of incorporating an additional closure or seal at the outer ends of the beam tubes to limit loss of coolant from the main coolant system should the beam tubes fail at a point within the reactor pressure vessel.

The present beam-tube design includes closures at the outer ends of the tubes. The two types of tubes, EF and HB, have different types of closures, however, due to differences in the intended use.

The EF tubes have been provided on the basis that they may be useful for irradiation-type experiments at some future time. In view of the fact that it is not intended to bring a beam out of these tubes, they are provided with a conventional flanged closure designed for 1000-psig service, and no further discussion of these tubes will be presented, as a failure inside the reactor vessel would not lead to any significant loss of water from the system.

The horizontal beam tube design incorporates an O-ring-sealed cap at the outer end. The bolting for the end cap is adequate to meet a Code working pressure of 273 psig for the present design. This pressure is well in excess of any anticipated pressure in the beam tubes. As stated previously, the outer ends of the beam tubes are connected into the pool via lines containing rupture disks set to relieve if the pressure exceeds that allowable.

In the event of a catastrophic failure of a horizontal beam tube inside the reactor vessel, the maximum pressure in the tube could rise to the maximum inlet pressure of the reactor. Although the nominal inlet pressure is presently 600 psi, the design will be discussed in terms of the 1000-psi design which applies to the primary coolant system. An evaluation of the present design was made in order to determine the limitations in regard to internal pressure. As set forth above, it was determined that the limiting factor is the bolting at one point on the outer cap. It was further determined that if these bolts were changed to high-strength bolts, the limitation would be shifted to the cylindrical outer section of the beam tube extension. As previously stated, this section has a Code allowable working pressure of about 500 psig. This allowable pressure is based on a Code allowable stress for the 6061 material of 5900 psi. This allowable stress is related to a minimum tensile stress set forth in the Code of 24,000 psi.

Tests made on welded joints of the actual beam tube material showed a tensile strength greater than 29,000 psi with failure occurring in the heat-affected zone. The maximum stress in the aluminum material at 1000 psig internal pressure in the beam tube would be about 12,000 psi. Although this is in excess of the Code allowable stress, it appears that the design is adequate to contain the reactor inlet pressure under this abnormal, once-in-a-lifetime, load application.

Several additional points may be considered relevant. The ~7-in.-ID section is surrounded by a close-fitting stainless steel shield, which would prevent rupture of this section even if it should yield. The next weakest link is the inner portion of the extension tube, which is adequate for a Code rating of about 600 psig. In view of the fact that the nominal inlet pressure is only 600 psig with a maximum of 1000 psig, it is believed that the design is adequate to prevent any significant loss of water from the system should the inner end of the tube rupture.

As a result of the review, it has been decided to change the present bolting to a higher-strength material which will give assurance that the beam tubes can contain the maximum design pressure of 1000 psig should the inner end fail catastrophically.

C. Discuss the course of accidents involving various modes of beam tube failure.

It appears that there are only three modes of failure which are of interest: (1) a small leak inside the reactor vessel; (2) a gross rupture inside the reactor vessel; and (3) failure of the flanged joint which connects the beam tube to the reactor vessel. Case 1 would result in a slow rise in pressure in the beam tube until the relief pressure of the rupture disk is reached. After operation of the rupture disk, the leakage water would leak into the pool. The installed rupture disk system can handle approximately 15 gpm with a pressure at the beam tube seal cap of 500 psig, which is the Code allowable pressure for the beam tube extension. The increase in radioactivity in the pool water would bring this situation to the operator's attention even if the experiment were not in operation. Case 2 was discussed in part B of this answer. Case 3 assumes complete failure of the flanged coupling between the beam tube and the reactor vessel. This coupling normally restrains the beam tube from outward movement in addition to preventing water from leaking from the reactor vessel to the surrounding pool. Failure of the flanged joint would result in a maximum outward movement of the beam tube of about $2\frac{1}{4}$ in. if the experimenter's barrel shutter were not in place. If the barrel shutter were in place, the movement would be limited to approximately $\frac{3}{8}$ in. The leakage from the reactor vessel through the failed flange coupling is calculated to not exceed 1930 gpm at 1000 psig for either case; leakage would be into the reactor pool. A leak of this magnitude would result in a shutdown of the reactor; however, this would be done in an orderly fashion by the low-pressure scram, with no damage resulting other than the mechanical damage already done to the beam tube and associated parts. This type of failure is not considered sufficiently probable as to constitute a significant hazard even if the consequences were significant.

D. Could modifications of the provisions for emergency cooling help minimize the consequences of any of these?

Inasmuch as the consequences of the accidents discussed in 24C are only such as to require repair of the mechanical damage, it is not seen how modifications to the provisions for emergency cooling would have any effect on such accidents.

E. Discuss the extent of knowledge of long-term irradiation effects on the beam tubes, the adequacy of the surveillance program, and the probability of beam tube failure with the proposed procedures.

There is very little quantitative information on long-term irradiation effects on this type of material. Some information was obtained from the ETR site in August 1963. One of their control rod guide tubes, which was fabricated from type 6061-T6 aluminum, had been exposed to an integrated fast-neutron (>1 Mev) dose of 2.6×10^{22} neutrons/cm^2. This occurred during ~15,000 hr at a calculated temperature of 153°F. Twelve hardness measurements were made after irradiation. The measurements ranged from R_B 69.5 to R_B 75.5 with an average hardness of R_B 72. This indicates that there was probably no significant change in the strength of the material. The fast-neutron (>0.8 Mev) dose in the HFIR beam tubes will be about 2.4×10^{22} in a ten-year exposure. Surveillance specimens in the HFIR will be exposed in a higher flux than the beam tubes, and these specimens will be evaluated periodically to determine if there is any significant change in mechanical properties.

In regard to the mechanical properties, we plan to use tensile specimens to demonstrate the absence of any adverse effects of irradiation. The use of tensile specimens was questioned by Mr. N. J. Palladino during a meeting of the HFIR staff and the ACRS Subcommittee on HFIR. A letter on this subject was prepared and forwarded to him; it is included in this report as Appendix G as a matter of record.

On the basis of the foregoing information, it is concluded that the probability of beam tube failure is sufficiently small.

25. State the evacuation alarm set point and indicate what action is to be taken if it is reached. Also indicate the approximate radiation levels which will require evacuation of the facility by the reactor operators, and discuss the need for radiation shielding at the reactor control room.

The radiation alarm set point for the general operating area is 23 mr/hr as monitored by selected monitrons. However, two of the selected monitrons must indicate simultaneously a radiation level $\geqq$23 mr/hr to automatically sound the evacuation alarm. A similar system is provided for monitoring particulate or gaseous activity in the general operating areas of the building. As is the case with the monitrons, two of the selected constant air monitors must indicate a level significantly above tolerance in order to automatically sound the evacuation alarm.

The control room is located outside the containment area, and a separate ventilation system is provided to minimize the probability of exposing the operator to particulate or gaseous activity; however, a monitron and constant air monitor are located in the control-room area for operator information. In addition, a wide-range, gamma-sensitive detector is located just outside the control room, in the high-bay reactor operating level. This instrument covers the range 0.1 to 10^5 r/hr on a logarithmic scale and provides a readout and alarm in the control room and in the HFIR Office and Maintenance Building,

which also has telephone, intercom, and public address system communication with the overall HFIR area. The reactor operators are required to evacuate the control room if the radiation level is in excess of 5 r/hr.

The HFIR control room is partially shielded by the 8-in.-thick concrete reactor building; however, this wall is penetrated by the observation gallery windows, which can be seen in Figs. 3.2.5 and 3.2.6 of ORNL-3572. There appears to be no significant advantage to having the operator remain in the control room following a serious accident, and it is not intended that he do so. For this reason it appears unnecessary to further shield the control room.

26. Provide an analysis of the reactivity effects resulting from possible fuel movement (e.g., effects of fuel melting and transport during an accident or relative movement of the two elements). Analyze appropriate accidents which could involve significant reactivity insertions or insertion rates from this source.

The HFIR core is undermoderated within the confines of the side plates but has positive void coefficients in the island and control region and nearly a zero coefficient between the two elements. As a result of the undermoderation within the fuel elements, removal of fuel plates (plus the associated fuel and burnable poison) increases reactivity. Calculations indicate that uniform removal of fuel plates from the core results in a maximum reactivity increase of 0.025 Δk; the corresponding fraction of fuel plate removal is about 30% (one experimental point at about 3% fuel plate removal checks the calculations satisfactorily). If a complete loss of flow and/or sudden loss of pressure accident were to occur in which fuel plate melting resulted, it is perhaps possible that there would be some increase in reactivity due to molten fuel plate material dripping out the bottom of the core. However, the safety rods, which would have scrammed as a result of the initiatory accident, would be capable of maintaining the reactor subcritical even if the full 0.025 Δk addition were achieved, which, of course, is very unlikely.

The amount of reactivity associated with longitudinal displacement of one fuel element relative to the other has not as yet been determined experimentally. However, since the water regions adjacent to the fuel elements already are overmoderated, or nearly so in the case of the water gap between the elements, it is not likely that longitudinal movement of one element relative to the other would increase reactivity. Experiments of this type will be conducted in the near future.

Relative movement of the two elements is normally prevented by the fact that the outer element is held in position by the inner shroud and the inner element is held in position by the target tower (see ORNL-3572, Figs. 5.1.2 and 5.1.4).

27. Discuss the possible effects of a fire in the control room.

The effects of a fire in the control room would depend upon many factors, such as the point of origin of the fire and its severity. The control room is not provided with a sprinkler system due to concern over a possible malfunction causing instrument damage; however, heat sensors are provided which sound local alarms as well as alarms at the fire department headquarters. Portable extinguishers are provided for use of the operating personnel.

The control room may not be left unattended while the reactor is in operation. This is an administrative rule which is strictly enforced. The operator has several means of shutting down the reactor from the control desk. Operation of a single switch is adequate to initiate a shutdown, and the system is so designed that the reactor requires no further attention once a shutdown is initiated.

In order to pursue this question further, it could be assumed that the fire originated with an explosion which disabled the operator. In this event the operator could not shut down the reactor, and the regulating system would continue to control the reactor until shimming of the control plates is required. At this time the regulating rod would be fully withdrawn, and the reactor power would start to decrease due to lack of ability to withdraw the control elements. Shutdown would follow almost immediately due to buildup of fission product poison. The safety system may be presumed to be operative during this sequence of events. The time required to reach the end of the regulating rod stroke will vary depending on the position at the time of the accident, but it would generally be a number of hours. Inasmuch as other personnel in the area, the fire department, and the emergency squad would arrive in a matter of minutes, the above discussion is somewhat academic.

If it is assumed that the operator is driven from the control room without shutting down the reactor, or if access cannot be gained to the control room, there are still many ways of shutting the reactor down. One of the easiest would be to open the manual breakers in the instrument battery room, which is located on the floor below, adjacent to the amplifier and relay room. This would remove the source of power for the instruments and safety plate magnets and would result in a scram. Removal of the power would result in a scram no matter whether the instruments were damaged or not. If access to the amplifier and relay room was also blocked, the shutdown could easily be initiated from the subpile room by unplugging the safety magnets. This action would also be independent of instrument condition. As noted in the answer to question 22, the shim-regulating cylinder could also be inserted from this location.

Even under conditions where the operator takes no action, selective failure would be required to bring about a dangerous condition. It would be necessary that the safety system be disabled first and that it fail in such a manner that it did not and could not shut the reactor down. Following failure of the safety system, it would be necessary to further postulate that the regulating system fails in such a manner that the regulating rod is withdrawn. Even in this case it would be necessary that the control system interlocks fail to produce a control element insertion (reverse). Note that in assuming failure of the safety system and the regulating system, two channels of each must fail.

28A. Furnish further information regarding the reliability and fail-safe characteristics of the reactor control and instrumentation system.

The safety system is maintained physically and functionally independent of the system of controls, interlocks, annunciators, startup instrumentation, and the like. In order to facilitate this separation between safety-related and non-safety-related equipment, the two systems have been referred to as safety and nonsafety systems.

The following steps have been taken to achieve the required reliability of the safety system:

1. Three independent safety channels are provided and arranged so that proper operation of any two will initiate a scram when required.

2. Built-in testing capabilities have been included so that each safety channel can be tested periodically on a schedule that makes the probability of the existence of two undetected random failures vanishingly small.
3. Where there exist credible mechanisms for nonrandom failures to disable more than one safety channel, fail-safe techniques have been used. The principal example of this is the continuity circuit which trips a channel when a vital module is removed from its drawer.
4. The safety channels have been clearly identified as to their safety functions, and strong administrative controls are exercised to prevent unauthorized modifications. The use of these channels for purposes other than protection is prohibited.

B. Indicate how the system has functioned in testing to date.

One channel of the safety system and one wide-range counting channel have been under continuous test in the ORR for approximately one year. During that time the systems have been subjected to extreme temperature cycling and high and low supply voltage variations as well as long-term routine operation. Two isolated electronic component failures occurred during this phase of the testing.

The systems in the HFIR have been largely operable for from three to six months. During the initial checkout phase, several failures occurred which were directly attributable to excessive handling. Since completion of initial checkout and calibration of the instrumentation, one transistor failure has occurred. The cause of this failure could not be established.

The performance of the instrumentation has been well within the design specifications and has been essentially noise and interference free. Those parts of the on-line testing system which are operable at low power all perform satisfactorily. The sensitivity and operability of the safety system have been checked by raising the reactor power level until safety action was initiated. All systems responded normally.

C. What are the most crucial segments of the instrumentation system?

The most crucial segment of the instrumentation system is that part which we refer to as the safety system. As described in ORNL-3572 and in part A of this question, the safety system is made up of three independent channels. Each of these channels receives information regarding various important parameters which reflect the status of the system. The function of this system is to prevent overheating of the reactor fuel due to any of these parameters getting outside their normal range. The arrangement of this system is described in ORNL-3572 in considerable detail. Any component in a channel which can prevent that channel from providing protection against improper values of any parameter is considered crucial for that channel. A built-in testing system is provided to detect such failures in any part of any of the three channels. Failure of any single channel does not prevent the safety system from providing protection. As is the case with all coincidence systems, common elements exist. In the case of the HFIR safety system these elements are the four safety release magnets, in which the magnetic circuit provides the meeting ground for the three safety channels. No attempt has been made to identify each component of a given safety channel which could prevent that channel from performing its function. As in any system, there are many such components which are equally important.

D. What are possible modes of failure and their consequences?

As set forth in part C of this question, there are many components in each safety channel which can fail in such a manner that the channel cannot perform its function. An undetected failure in one channel, if it be such as to block the entire channel rather than a single parameter in one channel, would require coincidence of the other two channels to initiate corrective action. If the failure is detected either at the time of the test or by observation of the instruments during operation, the operating procedures require that the defective channel be manually tripped so that either of the other two channels may take action should an unsafe condition arise.

If faults are detected in two of the safety channels, the reactor must be shut down. Undetected faults in two of the safety channels which are such as to block the entire channel would render the safety system inoperative. The test interval has been chosen such that the probability of occurrence of the latter case is acceptably small. The present maximum testing interval of 25 hr between tests is based on a conservative estimate of four failures per year per channel. It is judged that the resulting system failure rate potential of 10^{-4} per hour or 1 hr/year unprotected is acceptable; however, a shorter interval between tests is judged desirable until additional experience is gained regarding component failure rates. The test interval presently being used is 8 hr.

E. What could result from failure to detect fuel element failure promptly?

The most serious result of failure to detect fuel element failure promptly is the probability that the failure might become progressively worse. If this should happen, a relatively small incident might propagate into a larger one, and it is for this reason that the reactor is shut down via the safety system if a failure bad enough to set off the failed fuel element detector occurs.

In addition to shutdown of the reactor, the failed fuel element detectors also call for closure of the cleanup-system block valves. The intent is to confine any activity release to the primary coolant system until such time as an orderly cleanup procedure can be initiated. Any gaseous activity which escapes into the cleanup system would be carried off by the hot off-gas system, filtered, and discharged from the stack. The cleanup system has a flow which is only about 1.5% of the primary coolant flow, so even if the block valves fail to close the rate of exhaust of activity is relatively small.

Several other monitors for coolant-water activity and exhaust-gas activity are provided as described in ORNL-3572, and information from these sources would be presented to the operator starting about 20 sec after the accident.

F. Discuss accidents in which the instrumentation reacts improperly, or fails to function as intended, including that time when reactivity is being inserted at its maximum design rate.

There are a multitude of situations which could be discussed under this topic; however, it appears that these can be summarized by consideration of single or multiple failure of three elements: (1) the safety system, (2) the instrument and control system exclusive of the safety system, and (3) the op-

erator. As described in other parts of this answer, the safety system is designed to protect the reactor against failures which occur in other parts of the system, and, therefore, the only combinations of interest are those in which the safety system itself has failed. In support of this and as an example of the consequences of failure involving the addition of reactivity at its maximum rate, let us consider a startup accident.

The HFIR safety and control system design is consistent with a principle originally established by Newson[5] for the MTR and which has been applied to all ORNL reactors. This principle assumes a startup accident, originating at source level, brought about by the catastrophic failure of the startup instrumentation, the control system including interlocks, and manual operation. This failure leaves the reactor supercritical with the shim-safety plates withdrawing simultaneously at their maximum rate. The reactor safety system remains the only means of stopping the reactivity addition and of turning the excursion by releasing the shim-safety plates. One criterion for minimum required performance of the safety system is therefore the protection of the reactor core from catastrophic failure of the startup instrumentation and control system.

As indicated above, the safety system response determines the maximum allowable reactivity insertion rate by the shim plates. In the HFIR the maximum allowable rate is greater than a factor of 2 times the rate actually used. The choice of the slower rate was made on the basis of operating requirements, since this choice was well within safe limits.

The possible modes of failure include random as well as systematic failures of various components. The ORNL approach has been to design a system which is tolerant of random failures and to reduce the probability of systematic failure to the lowest practical limit. It is our opinion that the probability of safety system failure, as a result of multiple component or systematic failures, is acceptable. However, the possibility of complete failure of the safety system is conceded. If this failure occurred at a time concurrent with failure of all the rest of the instrumentation and control system and if the operator took no corrective action, the situation is such that damage to the reactor would almost certainly result. In this case, the containment system would become the remaining barrier against release of radioactivity. Recognizing this dependence on the containment system in the event of total control failure, we have designed the containment system as an independent system.

G. Discuss this choice of maximum reactivity insertion rate.

Part F of this question discussed one limitation on the maximum reactivity insertion rate, that is, that the safety system response be adequate to handle an accident in which all control elements are increasing reactivity at their maximum speed. As was pointed out, this limitation did not offer a problem in the HFIR, as other operational considerations dictated a lesser rate. As a matter of interest, the results of the analog studies are summarized in ORNL-3572, Sect. 8.8.3, and presented in somewhat greater detail in Appendix C.

---

[5]H. W. Newson, *The Control Problem in Piles Capable of Very Short Periods*, MonP-271 (Apr. 21, 1947).

The actual rate selected was a compromise of several factors. For normal operation of the reactor, both during startup and steady-state operation, there is no particular need for rapid changes in reactivity, and in fact a rather slow rate is desirable from the standpoint of observing instrument behavior during startup and from the standpoint of ease of adjustment of the rods to desired positions. This latter point is particularly of interest during the initial startup and approach-to-power tests, where many measurements are made in which the ability to accurately and easily position the control elements is of considerable interest. On the other hand, it is necessary that the rate of motion be sufficiently fast that recovery from unscheduled scrams or shutdowns can be made in the short period of time available before the reactor is poisoned out by xenon. It is also necessary that the rate be sufficiently fast that changes in xenon poisoning after recovery from the scram be at a rate small compared with the rate produced by rod motion, so that there is no question as to loss of control during this phase of operations.

Superimposed on the above considerations are certain points of design philosophy and practical experience which we have applied to ORNL reactors and which we believe are important. The first point assumes that regardless of any programming of rod motion all rods can increase reactivity at their maximum rate and that the rate must be such that the safety system can handle the ensuing transient. This consideration rules out dual- or variable-speed motors unless the maximum rate is consistent with the above. As a practical consideration, we prefer to use single-speed motors, which lead to the simplest and most trouble-free system. This imposes a penalty in recovery from a single rod scram inasmuch as the maximum rod speed is the same as if all rods were moving; however, we believe that this system is inherently safer than one which allows a rod speed based on individual rod movement.

Without belaboring this point any further, we chose a maximum rate of increase of k which would give us the desirable fine degree of control based on experience with the MTR and ORR, and which would also allow us to regain criticality after an unscheduled scram in a little over 5 min, providing that the scram was clearly false. Under these conditions we should be able to recover from a scram in all but the last three days of operation. This is not too good considering that the fuel life is only 10 to 15 days and that a core lost due to xenon in the last two or three days cannot be restarted due to the growth of samarium while the xenon is decaying. The selected rate is less than desired from this standpoint but is about as fast as we wanted to go from the standpoint of providing the desired fineness of control.

During routine startup, when there is no need for fast action, the withdrawal rate is reduced by about a factor of 5 through action of a timer which applies power to the drive motors intermittently.

29A. Discuss alternate ways* of limiting any irradiation of the public or of personnel at the Oak Ridge National Laboratory in the unlikely event of a serious accident, such as by isolation of the building and recirculation of building air through filters rather than by releasing of radioactivity through the facility stack.

---

*Further discussed in answer 46.

Before discussing various alternatives, it is necessary to emphasize that only in the extremely unlikely event that the primary containment system is breached would any significant activity be released from the primary coolant system. The main purpose of the SBHE system is to provide secondary containment should fission gases escape from the primary system. As is explained in detail in ORNL-3572, Chap. 4, and in Sects. 4 and 6 of this report, this is accomplished by removing the contaminated air from the building at a rate sufficient to guarantee inleakage at ground level. The contaminated air is then passed through filters, which effectively remove the halogens, and discharged from the 250-ft HFIR stack. As shown in Part I, the radiation doses which result from disposal of the MCA release in this way fall within the guidelines of 10 CFR 100.

The simplest alternative to the system described above is to merely shut off the SBHE fans, isolate the building, and consider the consequences of the fission gases leaking out at ground level. Because of the type of secondary containment selected and originally reviewed by the ACRS, the building was not designed to be leak-tight. It is therefore difficult to estimate what leak rate would be expected under no-flow and various atmospheric conditions and to assess how much improvement could be expected by reasonable modifications to the building. To get some feel for the problem, the downwind doses following the MCA have been calculated under the assumption that the leak rate from the building is approximately 4.17% per hour or 330 cfm from the reactor bay. It is believed that a leakage rate of this order could be achieved with appropriate changes to the doors and with the addition of automatic closures on the various penetrations. The results for iodine and for the whole-body gamma dose due to noble gases and iodines were computed for the 2-hr exposure case using "most representative" meteorological conditions. Estimates were also made for the infinite exposure case. They are shown for 2-hr and infinite exposure, respectively, in Figs. II.29.1 and II.29.2. For comparison, the MCA doses as for the case of a stack release are plotted on the same graphs.

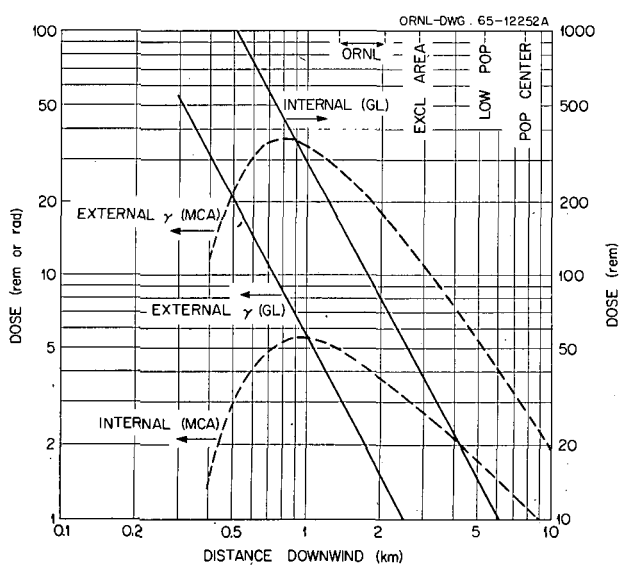

Fig. II.29.1. Comparison of Ground Release (330 ft^3/min) Doses to Present MCA 2-hr Doses.

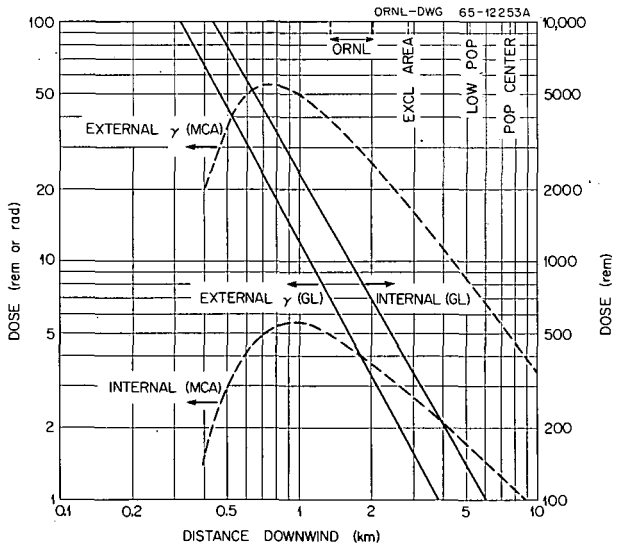

Fig. II.29.2. Comparison of Ground Release (330 ft^3/min) Doses to Present MCA Infinite Exposure Doses.

It is obvious from these results that, while the ground-level external dose values are smaller than the stack release values at some distance downwind from the site, they are considerably worse near the reactor building. The internal dose values are greater than for the stack release case for both the 2-hr exposure case and infinite exposure case for all distances of interest. This is not unexpected, as the iodine is presumed to leak from the building without filtration. Some improvement could be obtained in the 2-hr doses by relatively small decreases in the leak rate; however, to substantially reduce the infinite doses would require a very large reduction in the leak rate. It therefore appears that any decision to use this procedure would require a complete change in the containment philosophy and make it necessary to convert the HFIR building into a conventional containment vessel with very low leakage.

A second basic alternative is to continue to utilize the stack for the purpose of disposing of the fission gases, but to reduce the rate of discharge of contaminated air. This would have two beneficial effects: (1) It would increase the time for decay in the building and thus reduce the total amount of activity available for release. (2) It would decrease the rate at which activity reaches the environment and thus provide more time before a given dose is delivered at a given place.

This plan, however, has certain shortcomings. In the first place, the rate at which air is being exhausted from the stack has, in general, a relatively minor effect on the rate at which fission products from the MCA reach the stack. Despite the fact that the analysis presented in Appendix A was based in part upon uniform mixing of the fission products in the building, the fact is that, in all likelihood, any fission gases released into the pool from the reactor will be conveyed directly to the filters through the registers located along the pool perimeter. This is particularly true if the pool cover remains in place. In fact, the system was designed with this purpose in mind; and

it was for this reason that the exhaust rates used in computing the consequences of the MCA were chosen as they were: 25% at a very high rate ($\alpha = 0.5\ \text{min}^{-1}$) and 75% at a rate judged to represent a somewhat slower rate of release from the fuel ($\alpha = 0.015\ \text{min}^{-1}$) as it cooled down.

The purpose of the high exhaust rate through the filters is twofold: (1) to guarantee inleakage; and (2) to handle the normal air exhaust from the building so that the system requires no change in mode of operation between normal conditions and emergency conditions. Thus, reduction of this exhaust rate alone, during an accident, would serve to decrease the protection against outleakage while increasing the probability of malfunction during the change in mode of operation. It would have little, if any, beneficial effect on the rate of fission product release. In addition, reduction of the air flow would reduce the effective stack height and thus everywhere slightly increase the doses delivered for a given release.

One method of accomplishing a reduction of the rate of transport of fission products to the stack would be to cut off the pool-side inlet registers and remove the pool cover, thus allowing the fission gases to be released into the building, where mixing and dispersion would occur. Then a reduction in the rate of exhaust through the SBHE filters would indeed reduce the rate of fission product release if it were to be released in the pool. However, unless the building were modified into a conventional containment structure, it is safe to assume that some significant rate of exhaust will be required in order to guarantee inleakage. To get some idea of the reduction in the downwind doses which could be attained by this procedure, the peak 2-hr MCA doses which occur at 800 to 1000 m downwind and the infinite MCA doses at the low population boundary for both the internal iodine and the whole-body gamma dose have been computed under the foregoing conditions and under the assumption that the flow is reduced by a factor of 5 to about 2500 cfm. These are listed in Table II.29.1 together with the corresponding MCA doses originally presented.

Thus it can be seen that under these conditions it is possible to achieve a reduction in the peak downwind doses by a factor somewhat greater than 2, although there is little effect on the dose at the low population boundary. This reduction, however, is obtained under the assumption of a release to the reactor bay, which therefore increases greatly the hazard to personnel in the reactor building. Although modification of the system as suggested above would reduce the environmental consequences of an extremely unlikely major fission product release, any minor fission product release, a much more probably occurrence, would result in a potentially dangerous spread of contamination throughout the reactor building. Not only is the reactor building occupied during many operations which could result

Table II.29.1. Internal Iodine Doses and Whole-Body Gamma Doses Following the HFIR MCA

	Peak		Low Population Boundary	
	2-hr Iodine (rems)	2-hr Noble Gas Gamma (rads)	Infinite Iodine (rems)	Infinite Noble Gas Gamma (rads)
Original MCA dose	5.2	38	1.5	7.2
Reduced flow MCA dose	2.5	17	1.3	5.05

in such minor releases, but the necessity for cleanup and decontamination following these releases could represent a considerable loss of time and money, as well as an additional hazard to personnel engaged in this activity. The present system is specifically designed to channel any radioactive effluent originating in the reactor pool directly to the SBHE system and to minimize the spread of contamination in the reactor building itself.

It is clear from the foregoing that a ground-level release under the postulated conditions reduces the whole-body dose due to noble gases at distances from the stack greater than about 500 m. However, because there is no filtration under these conditions, the 2-hr iodine dose is increased by a factor of 30 at the ORNL site, and by a factor of 15 at the exclusion area radius. It follows that some improvement could be gained by releasing the noble gases at ground level, but at the same time filtering the iodine. Conceivably this could be done by utilizing a combination of the first and second alternatives discussed above. This combination requires that the air-handling system remain in operation and that the building air be recirculated through the filters with no net exhaust rate through the stack. Incorporation of the features required to accomplish this would require all of the changes necessary to isolate the building as in the first alternative and would also require redesign and rebuilding of the building ventilation system. The external doses would remain essentially the same as for the simple isolation case; however, the internal dose would be reduced by virtue of the filter factor for iodine removal, provided that no iodine escapes directly into the building. If a filter factor of 666 is assumed, in order to make the results comparable with the stack release MCA, and applied to the curves in Figs. II.29.1 and II.29.2, it can be seen that the internal dose is less than that for the MCA case for distances greater than about 0.45 km for the 2-hr case and about 0.8 km for the infinite case. This change appears to reduce the 2-hr internal and external doses at ORNL by factors of approximately 10. The infinite external dose is reduced by about a factor of 7 and the infinite internal dose is reduced by about a factor of 3 at ORNL.

There are several points which should be noted regarding this isolation and recirculation system. In order to obtain the above results, it was assumed that no iodine escaped into the building without first passing through the filter system. It is not clear that the assumption can be justified, and, therefore, let us examine the consequences should the accident be such as to allow the iodine to pass into the building before filtration. It is clear that the internal dose resulting will fall somewhere between that obtained with no filtration and that obtained with filtration. The effective half-life of any iodine, released in the reactor bay, due to removal by the air-handling system, assuming perfect filtration, is about 30 min. The amount of iodine which would leak from the building in 2 hr is therefore approximately one-third of that which would escape without recirculation. Inspection of the curves shows that this would result in a 2-hr internal dose at ORNL about 10 times that from the stack release MCA. The infinite release case would not be greatly different inasmuch as most of the iodine which would escape would already have done so by the end of 2 hr; therefore, the infinite internal dose at ORNL would also be about 10 times that given for the stack release MCA.

It appears from the foregoing that the major problem area for this and the first alternative is that of building leakage. This is not at all surprising, inasmuch as these alternatives may really be considered

as evaluations of the HFIR building as a conventional containment structure and it is not designed for this purpose. Provided that the leakage is not greater than assumed (i.e., no breach of the containment occurs), the doses from this last alternative would be within acceptable limits at ORNL; the internal doses would be greater than those resulting from the stack release, and the external doses would be smaller. The doses for distances closer to the HFIR building than ORNL would be much higher than those resulting from the stack release, and the building itself would be thoroughly contaminated, even in the case of a release which was of minor proportions compared with the MCA. The increase in hazard to the operating personnel and the necessity for cleanup and decontamination could present a considerable loss as well as a hazard. In summary, it appears that not only would the advantages of the HFIR containment system be lost, but there would be an increase in internal dose. The only advantage would be a reduction in external dose for distances greater than about 0.5 km. As the external dose is calculated to be adequately low for the present HFIR system, such a change does not appear desirable.

It is concluded, therefore, that all things considered, the present system of containment is superior to any that could be devised by other than a major change in containment philosophy and very substantial modifications to the building.

B. Also discuss the need for additional radiation monitoring instrumentation for the stack exhaust in order to provide information regarding the rate and quantity of radioactivity released during potential accidents.

The radiation monitoring instrumentation presently installed is designed to provide information on the amount and kind of activity released during normal operation and during situations in which the amounts released are only a small factor above that for normal operation. An in-stack monitor is provided as described in ORNL-3572, Sect. 8.7.3, which can be used to assess particulate and iodine releases over a wide range; however, this device must be removed and analyzed after an accident and therefore does not provide information during the course of an accident. It seems clear that information in addition to that provided by the presently installed equipment would be needed to evaluate the magnitude of an accident in order to make intelligent decisions regarding evacuation of the Laboratory or other nearby installations. ORNL has an area monitoring system consisting of many airborne activity particulate and fallout monitors, and this system would provide information on the magnitude and direction of movement of the activity from a significant release. The Radiation-Monitoring and -Warning System at ORNL is briefly described by L. F. Lieber in *Nuclear Safety*.[6]

In view of the fact that the gaseous waste monitoring and the emergency control center are operations conducted on a laboratory-wide basis, this question on monitoring the HFIR stack under potential accident conditions was referred to ORNL management in order to have a study made which would include these factors. This study resulted in a recommendation that a system be provided for monitoring the stack effluent under potential accident conditions. The system is to monitor the noble gas activity and the iodine activity. The detector and instrumentation requirements are currently under study, and the system will be installed as soon as the design and procurement are completed.

---

[6]L. F. Lieber, *Nucl. Safety* 6(4), 414–21 (1965).

30. Provide the latest information available relative to the effectiveness of the installed filters to remove radioactive iodine from the exhaust in the event of a fission product release accident.

As a result of the question raised concerning the efficiency of the filters with respect to the removal of methyl iodide from the effluent air stream, an investigation was initiated for the purpose of collecting and clarifying available information concerning the behavior of methyl iodide. The results of this investigation are summarized in ORNL-TM-1291.[7]

An analysis of the HFIR MCA utilizing the data obtained in this investigation leads to the conclusion that the SBHE system as presently installed provides iodine decontamination factors more than adequate to satisfy the guidelines of 10 CFR 100, but that by incorporating minor modifications it can be made to handle iodine containing the maximum amount of CH_3I with a decontamination factor substantially the same as that originally claimed.

These modifications, which are now being studied, include (1) an increase in the thickness of each of the two charcoal beds from ½ in. to 1 in., and (2) replacement of the charcoal with specially treated MSA charcoal identified as MSA 85851 charcoal. Based upon information obtained by G. W. Parker and contained in ORNL-TM-1291, it has been determined that 2 in. of this charcoal will retain about 99.5% of the methyl iodide for as long as 5 days during which air flow at the normal SBHE rate is maintained, and that over shorter periods of time (2 to 3 hr), the efficiency is greater than 99.7%.*

A conservative estimate of the maximum amount of iodine which could be present in the form of CH_3I following the HFIR MCA is 5%. Consequently, based on the above information, if the 95% of the iodine which remains as molecular iodine behaves as previously described, the 2-hr iodine doses within the exclusion area following the HFIR MCA would, because of the presence of CH_3I, be increased by about 1.7%, and the infinite doses by about 11.7%, above those given in Table I.6.1 on page 26.

It is assumed, of course, that the air flow to the filters would be shut off within a few days after the accident and that the filters would be bagged, removed, disposed of, and replaced by new filters. This procedure is facilitated by the characteristics of the containment system, which is designed to dispose of the noble gases by dilution and atmospheric dispersion, trap the iodine on the shielded filters, and then quickly reduce the radiation field in and near the building to tolerable levels.

It appears, therefore, that the HFIR filters with the suggested modifications will indeed provide the protection against iodine originally claimed.

31A. State the NDT of the pressure-vessel material and indicate how this is expected to vary during the reactor lifetime.

During procurement of the reactor vessel, samples of the actual heat-treated materials used in the fabrication of the carbon-steel components of the pressure vessel were subjected by the vendor to Charpy V-notch impact tests. The results are shown in Table II.31.1.

---

[7] R. E. Adams *et al.*, *The Release and Adsorption of Methyl Iodide in the HFIR Maximum Credible Accident*, ORNL-TM-1291 (Oct. 1, 1965).

*Answer 46 gives latest information and effects of moisture on iodine and on filters.

Table II.31.1. Results of Charpy V-Notch Impact Tests on Actual Carbon Steel Pressure Vessel Specimens

Component	Material	Integrated 20-year Fast-Neutron Dose (neutrons/cm^2)	Nil Ductility Temperature Shift (°F)	Test Temperature (°F)	Average Charpy Impact Value (ft-lb)
Shell cylinder	A212 GrB	$<10^{18}$	0	+10	17
Hemispherical head	A212 GrB	$<10^{18}$	0	+10	17
Top head	A105 GrII	$<10^{18}$	0	+10	23
Top flange	A105 GrII	$<10^{18}$	0	+10	94
Nozzle forgings:					
RH	A105 GrII	$<10^{18}$	0	+10	28
EF	A105 GrII	$<10^{18}$	0	+10	40
IC	A105 GrII	$<10^{18}$	0	+10	42
Coolant water inlet	A105 GrII	$<10^{18}$	0	+10	48
Vessel lower extension transition	A105 GrII	$<10^{18}$	0	+10	39
HB 1	A105 GrII	1.1×10^{18}	37	−20	51
HB 2	A350 GrLF3	2.9×10^{18}	80	−80	49
HB 3	A350 GrLF3	2.3×10^{18}	67	−65	38
HB 4	A105 GrII	1.1×10^{18}	37	−20	51

As part of the ORNL vessel surveillance program, Charpy V nil ductility temperature curves were determined on actual heat-treated vessel materials. From these curves, the following nil ductility temperatures for the various significant vessel parts were found:

Sample	Material	Impact Energy (ft-lb)	Nil Ductility Temperature (°F)
HB 1 & 4	A105 GrII	15	−65
HB 2	A350 GrLF3	30	−115
HB 3	A350 GrLF3	30	−85
Shell	A212 GrB	15	0

Welding procedure qualification tests included impact tests of the welds and heat-affected zones of the base metal. In no case were the impact values indicative of an NDT of more than 10°F.

It is predicted that there will be no shift in the NDT of vessel materials other than the HB nozzle materials, which are expected to experience power operation shifts over 2000-Mw years as follows:

	Initial NDT (°F)	20-Year Shift	NDT After 20 Years of 100-Mw Operation (°F)
HB 1 & 4	−65	37	−28
HB 2	−115	80	−35
HB 3	−85	67	−18
Shell	0	None	0
All other parts	≦0	None	≦0

B. How well is the flux known?

The estimated integrated 20-year fast-neutron dose was based on combined experimental* and analytical results which were corrected for difference in the neutron spectrum. It is believed that the dose rates used in the analysis are a maximum. To supplement the analysis, surveillance specimens will be used to control operation of critical areas (such as the HB nozzles and the shell girth at the reactor horizontal midplane) to maintain an NDT consistent with safe operation of the system.

C. Are there other important reactor structural members subject to considerable neutron irradiation? If so, what are the consequences of their failure?**

All other important reactor structural members are sufficiently removed from the reactor that there is no concern over radiation damage. The reactor core region support members might fall into the classification of important structural members, and they are listed in the event you wish to consider them in this category. None of these members are called on to contain high pressure, and the loads are predominantly compressive.

1. Fuel and reflector support and sleeve assembly. This item forms the connecting link between the core structure and the reactor tank. The assembly is fabricated from 304L stainless steel and is sufficiently removed from the core that there is no concern from radiation damage.
2. Reflector container and pedestal assembly. This cylindrical member is fabricated from 6061-T6 aluminum and is the supporting member for the beryllium reflector. It is bolted to the top flange of item 1 above. Although it supports the beryllium, the fast-neutron flux is quite low, as the diameter of the support is equal to or greater than the beryllium reflector. No concern over radiation damage is warranted; however, surveillance specimens for beam-tube monitoring will provide an indication of possible future damage, as they are exposed to a flux many times greater than that to which this assembly is exposed.
3. Fuel-grid support pedestal. This member provides the support for the fuel grid and fuel elements. It is in turn supported by item 1 above. The material is 304L stainless steel. No concern is warranted over radiation damage, as adequate separation from the fuel region reduces the fast-neutron flux to a relatively low level.

In addition to the above, the inner control drive bracket, while not exactly a structural member, is a crucial member. This bracket is fabricated from 304L stainless steel. The location of the bracket is sufficiently below the reactor that the neutron dose is not of concern. In addition, this bracket is

*Experimental error and safety factor discussed in answer 47.

**Failures further discussed in answer 47.

considered a part of the control element and as such is replaced each time the control element is changed.

32. State the criteria to be used in evaluating experiments which may be performed in or near the reactor.

It is standard procedure at ORNL that all experiments which are to be performed in the reactors pass a safety and operability review. This procedure will be followed in approving experiments which are conducted at the HFIR. Each experiment is reviewed by two separate groups, first by the Operations Division's Technical Assistance Department and second by ORNL's Experiment Review Committee. Each experiment is reviewed with respect to safety and operability and includes, but is not limited to, the following items:

1. Reactivity effects
2. Heat generation and dissipation
3. Radiation control
4. Containment
5. Instrumentation and control
6. Safeguard action
7. Shielding
8. Installation and removal
9. Operating procedures
10. Maintenance procedures
11. Emergency procedures
12. Harmful chemicals
13. Explosive gas mixtures
14. Floor loading
15. Fire hazards
16. Vibration
17. Effects on reactor operation (reactor shutdowns)

The criteria used in reviewing and approving experiments proposed for ORNL reactors, including the HFIR, are presented in two reports, ORNL-TM-281[8] and ORNL-TM-745.[9]

33. Indicate whether nearby facilities can be safely shut down and evacuated in the event of a severe accident at the HFIR.

All of the facilities* of the Oak Ridge National Laboratory can be safely shut down and evacuated in the event of a severe accident at the HFIR. The only nearby facility for which this might not be true is the Experimental Gas-Cooled Reactor, which will be operated for the AEC by the Tennessee Valley Authority.** The EGCR is located on the shore of Melton Hill Lake approximately 3.26 km northeast of

---

[8]C. D. Cagle, *General Standards Guide for Experiments in ORNL Research Reactors*, ORNL-TM-281 (Aug. 20, 1962).

[9]C. D. Cagle, *Considerations Involved in the Safety Review of Experiments to Be Operated in Nuclear Reactors*, ORNL-TM-745 (July 10, 1964).

*Answer 48 provides specific information for MSRE.

**The EGCR project was later terminated for other reasons.

the HFIR site. Under normal conditions, it would be necessary for the control room of the EGCR to be manned for periods of up to an hour following shutdown.

Previous calculations shown in Part I indicate that the maximum doses received in the vicinity of the EGCR following an HFIR MCA would not exceed 2.5 rems to the thyroid, 15 rads whole-body gamma, and 13 rads whole-body beta. Because the EGCR control room is located inside, is partially shielded, and is equipped with a self-contained air supply, the actual doses received by personnel remaining in this control room would be considerably lower than those quoted above.

It is planned to tie the EGCR plant into the ORNL emergency warning system so that they may be quickly informed of any incidents which may conceivably give rise to a hazardous condition. Under MCA conditions, the time required for the HFIR plume to reach the EGCR is approximately 1 hr, which gives time for emergency action to be taken.

34A. Describe how the design of future HFIR core loadings may vary from the initial core design.

The only new core design being contemplated is one which will permit a longer fuel cycle time.* This is to be accomplished by increasing the fuel loading per plate. The reactivity of the system will be maintained essentially the same as at present by adding more burnable poison. As with the present core design, every core will have a reactivity check made in a critical experiment facility prior to use in the reactor. No dimensional or mechanical changes are anticipated for the near future. However, some consideration is being given to the possibility of using different types of fuel (such as dispersed U-Al intermetallic fuel rather than U_3O_8), the use of nickel plating to reduce oxide buildup, and fuel plate reinforcement (longitudinal spacers) with the present general fuel element design. Such changes might allow even further increases in fuel cycle time.

B. By what criteria will changes in core design or operating conditions be measured for safety?

The two major criteria** by which changes in core design will be judged are the criteria for shutdown margin and the calculated power level for onset of nucleate boiling.

C. When will regulatory review be deemed appropriate?

Review by the USAEC would be deemed appropriate if any significant departure from the criteria set forth in B were proposed which would reduce the margins set forth in the descriptive report, ORNL-3572, or the operating limits.

D. Discuss steps taken in operating new core designs (including first) which will minimize the chance of fuel failure.

---

*Answer 49 discusses increased cycle-time effect on ^{131}I inventory and on after-heat removal.

**Detailed subordinate criteria discussed in answer 50.

To determine the adequacy of any new core design, including the present design, a program of gradual power increases involving several fuel elements will be used. Provision is being made for future inspection of the cooling channels after shutdown by means of remote inspection gages; analysis of nuclear noise for indications of nucleate boiling will also provide information concerning adequacy. There is, of course, no way to completely ensure that a new element design is satisfactory without operating the element at design conditions. Thus, there is a possibility that the very high-performance HFIR elements will experience some difficulty by the end of a full power cycle. Of course, we consider the probability of any difficulty to be small; however, in order to approach the design power in a conservative manner, it is our intention to operate the first core for a full cycle at about 50 Mw, the second at 75 Mw, and the third at 87.5 Mw, and thus demonstrate successful operation at successively higher power levels before going to full power.

35. Discuss the possibility that thermal expansion or damage to the beryllium reflector could affect control rod motion.

Differential thermal expansion of all core components was considered when selecting the width of the coolant channels in the control region, and therefore no problem is anticipated due to this cause. Swelling of the beryllium due to radiation damage tends to make the beryllium cylinders larger in diameter, which will increase very slightly the clearance between the control elements and the reflector. After the innermost beryllium cylinder uses up the available outward radial expansion clearance provided, the inside diameter will tend to decrease, thus decreasing the clearance between the control elements and the reflector. An analysis of MTR and ORR beryllium radiation damage data indicates that these dimensional changes occur very slowly, thus introducing no problem in the HFIR for at least six months. In addition to the routine testing of the control elements for freedom of motion and absence of friction at the beginning of every fuel cycle, a program of periodically checking control plate and beryllium dimensions without removing them from the core is planned, and a remote measuring device is being constructed for this purpose. A further precaution has been taken by placing an aluminum liner on the inner surface of the innermost beryllium cylinder, its purpose being to prevent beryllium chips, should they form, from entering the control region.

36A. Provide information as to the maximum value of the overpower scram set point and the reason that this value was chosen.

The maximum value of the overpower scram set point is 120 Mw for the heat-power scrams and 130 Mw for the ϕ/F scrams. The values were chosen on the basis of past experience, which showed that approximately this margin was needed between the operating power and scram set points if inadvertent or false scrams due to noise spikes and instrument fluctuations were to be essentially eliminated. These values limit the steady-state power level so as to prevent the onset of nucleate boiling at any time during the fuel cycle. (In this context, power transients which occur with periods no faster than 1 sec can be considered as steady-state.) The heat-power calculator response is inherently slower than the flux instrumentation and therefore less subject to spurious variations. Consequently, the heat-power trip point may be set at a lower value to take advantage of its higher accuracy

to limit the maximum value of the steady-state power. One additional factor which entered into the selection of the scram level was the fact that the HFIR system is designed to control the reactor power level during an ac power outage. The transient resulting from pump coastdown requires that some margin be allowed for the fact that the reduction in power level lags slightly behind the reduction in scram level. Figure II.17.1 shows the reduction in flow, safety trip setting, and power level during a flow coastdown.

B. Provide analyses of accidents in which this setting plays an important role.

As described in A, the scram set points limit the steady-state power level to a value below that at which the onset of nucleate boiling might occur. These settings are also adequate to prevent the onset of boiling during relatively slow transients. If one considers the behavior of a range of full-power transients starting with very slow transients and ranging to very fast transients, it will be found that different scram parameters are effective. For slow increases in power level (period >10 sec), the heat-power scrams will limit the power to the range between 120 and 130 Mw. For rates of increase between periods of about 10 sec and about 1 sec, the level scram originating from neutron flux will be the first to act, while for very short periods the rate trips will be the first to act and the level at which the scram is initiated will be decreased. The actual setting of the maximum value of the overpower scram is therefore most important for slow transients, such as might be caused by failures in the rod control system while at full power. An analysis of this type of accident is presented in Appendix C, in which it is shown that an increase of 0.05 $\Delta k/k$ per second results in a negligible transient.

37. Present a description and analysis of the hazards associated with the type of targets which may be used which are not described in the documents submitted.

At the present time, it is not contemplated to utilize targets substantially different from those described in previous submissions. Should it become necessary or desirable to make changes in the targets in the future, these changes will receive the regular internal review and, if they in any way constitute a significant change affecting safety or involve an unresolved safety question, will be submitted to ORO for approval and processing through the normal regulatory channels.

It is perhaps worth noting that the heat fluxes, reactivity worths, and potential health hazards chosen for the estimation of the consequences of an accident involving the target represent the most pessimistic values expected both for the original and for recycle targets. In addition, target rods of the HFIR design have been undergoing irradiation since early 1965 in the Savannah River high flux program.

38A. Provide results of analyses of reactivity transients considerably more severe than those previously treated, considering possible sources of such transients as control system failure, larger than expected reactivity effects associated with a central void, unexpected locally positive void effects in the core, fuel movement, etc.

The selection of reactivity accidents to be analyzed for the HFIR was based on reactivity quantities and addition rates that are accurately known as a result of conducting many experiments and as a result of intrinsic limitations. For instance, the maximum change in reactivity associated with the central tar-

get region has been measured numerous times in critical experiments, rod drive motors can move the control elements only so fast, etc. Thus, if one considers the types of accidents investigated* to be reasonable upper bounds based on the experimental data, then it follows that the proposed reactivities and their rate of insertion are also upper limits. As set fort in Part I, the analog analysis and comparison with SPERT results indicate that the HFIR can withstand the reactivity accidents which represent upper bounds with no damage. The determination of "limiting" accidents would be a monumental task which, in our opinion, would serve little purpose. In order to extrapolate from the SPERT results, it is necessary to use what we consider to be a very conservative analog model, which in the unnormalized condition predicts a small amount of melting for the most severe HFIR transient. To extend the analysis to more severe accidents would require a refinement in the analog model in order for the results to be meaningful; that is, void formation would have to be included. Since there is no initial high-power, high-pressure, high-flow-rate SPERT-type data from which to base a model on void feedback, the results from such a calculation could not be considered very reliable.

It has been suggested that we investigate the use of a model which takes void formation into account. If a satisfactory model could be found, this approach would allow us to reduce the amount of conservatism in our transient analyses and therefore obtain a better understanding of the behavior under accident conditions. As set forth before, the lack of data applicable to the HFIR operating conditions leads us to question whether we could justify the results of such calculations as being conservative. Techniques are available for incorporating void effects into analog or digital programs; however, the detailed mechanisms for void generation do not appear to be well understood. The digital analysis program which has been developed at Brookhaven National Laboratory takes into account the spatial distribution of formation and the spatial effects of the voids; however, to make calculations without being able to conclude that the results are conservative would serve little purpose. It is our opinion that a considerable effort would be required before we could assert that the results would be conservative in terms of HFIR behavior. We believe that a program should be initiated with the goal being to gain a better understanding of HFIR transient behavior; however, it appears that this will have to be done as a relatively long-range program.

B. What role do metal-water reactions play herein?**

As indicated in the answer to the first part of this question, it is not expected that fuel-plate melting or a metal-water reaction could be initiated by the reactivity accidents considered. However, if one or the other were initiated, it is possible that a portion of the fuel would be rearranged to form a more reactive configuration. It has been determined on the basis of experiments and calculations that the maximum increase in reactivity associated with uniform removal of fuel-plate material from the core is 0.025 $\Delta k/k$, which requires removal of about 30% of the core material. It seems very unlikely that this amount

*Answer 51 discusses reactivity values associated with other occurrences. More details provided in answer 55.

**More details provided in answer 55.

of material could be removed very rapidly from the core unless the transient causing the melting of the plates were much more severe than anticipated. If melting of the plates led to a metal-water reaction, the resulting expulsion of water from the core would more than cancel the reactivity effect of the expulsion of fuel-plate material. Thus, it does not appear that rearrangement of fuel by fuel-plate melting and a metal-water reaction could add significantly to an already improbable transient that would result in fuel-plate melting in the first place.

C. What is the latest information on chemical reactions involving this fuel?

The latest information* on chemical reactions involving fuel of the HFIR type is contained in ANL-7090.[10] In summary, this report on TREAT tests states:

The HFIR samples retained their platelike shape at fission energies as high as 425 cal/g, whereas the aluminum-uranium alloy fuel plates had fused into single globules at energies between ~200 and 530 cal/g. Large hemispherical cavities were apparent in the surface of the HFIR plates at energies above that sufficient to cause melting of the cladding (~200 cal/g). The appearance of the cavities suggested gas evolution.

At energies above 645 cal/g, the HFIR samples completely lost their shape. The HFIR cermet fuel samples at these energies formed one large globule that contained mostly uranium oxides, several smaller fragments of partially oxidized aluminum, and fine particulate that consisted mainly of aluminum oxide. (Previous analytical studies indicated that the aluminum oxide was mainly α-Al_2O_3.) On the other hand, the alloy plate fuel at these energies was generally found, in previous studies, to form several small fragments of aluminum, uranium, and oxides, and fine particulate oxides. In 30°C water, the amount of fine particulate formed increased as the extent of reaction of either fuel increased. In high-temperature water, each of the two types of fuel formed a single large globule that reacted extensively at high energies.

The extents of reaction of the HFIR fuel plates (as contrasted to the differences in physical behavior noted above) were quite similar to those of the alloy plates (ANL-6904).[11] In 30°C water, at low energies, only a few tenths of a percent of a plate reacted when the cladding was only partially melted, and reaction did not exceed 2.5% when the cladding was fully melted, but still retained its shape (at 425 cal/g). At higher energies, more extensive reactions occurred: at 645 cal/g, the extent of reaction was 74.6%; at 1062 cal/g, the extent of reaction was 28.4%.

In high-temperature water (285°C), more extensive reaction occurred than in the runs in 30°C water. At 413 cal/g, 11.8% of a plate reacted; while in room-temperature water, only 2.5% reaction occurred at 425 cal/g. Similarly at 658 cal/g, 91.3% of a plate reacted in the hot water, while in 30°C water, 74.6% reacted at an energy input of 645 cal/g.

---

*See also Appendix I.

[10] Argonne National Laboratory, *Reactor Development Program Progress Report, August 1965*, ANL-7090, pp. 76–78.

[11] Argonne National Laboratory, *Reactor Development Program Progress Report, May 1964*, ANL-6904.

It is postulated that at low energies where breakup does not occur or the plates do not lose their shape, the plates cannot react extensively, that is, the nature of the reaction is to form a protective oxide film, and cooling rates are sufficient to prevent ignition. The subcooled water causes an even greater suppression of the reaction as a result of a more rapid cooling rate than in the heated water. Above a threshold energy (previously determined to be 530 cal/g for the alloy plate fuel and somewhere between 425 and 645 cal/g for the HFIR fuel), flow, breakup, and ignition of the samples occur. At these higher energies, the extent of reaction is governed by the duration of burning, which in turn depends on several factors, such as particle size, depletion of the reacting fuel, and the rate of energy loss by the particles to the surroundings. Here again, the subcooled water tends to decrease the extent of reaction by providing more efficient cooling.

In addition to the test information set forth above, ANL will run four additional tests. Three of these will be run with the autoclave at 120°C and with 600 psia pressure, as being more representative of HFIR conditions. The fourth is being run in a room-temperature assembly to complete the data discussed in ANL-7090.[10] ANL also proposes to photograph samples of HFIR fuel in TREAT in the hope of obtaining additional information.

D. Is xenon burnout ever important in any possible accidents? Can the boron in the fuel ever contribute adversely to an accident?

During the most severe rapid transient studied, the duration of the transient is about 0.03 sec and the peak thermal neutron flux in the fuel is about 10^{16} neutrons cm^{-2} sec^{-1}. Thus the maximum decrease in xenon concentration is about

$$3 \times 10^6 \times 10^{-24} \times 10^{16} \times 0.03 \approx 10^{-3} = 0.1\% .$$

The greatest possible worth of the xenon during a transient is equal to the total worth of the fuel in terms of excess reactivity; this is about 0.12 $\Delta k/k$. A conservative estimate of the change in reactivity worth of the xenon during the transient yields 0.00012 $\Delta k/k$. Burnup of the boron poison would be several orders of magnitude less.*

E. Please document the spatial distribution of local void effects and provide estimates of uncertainties therein.

Average void coefficients for the inner and outer fuel elements were determined experimentally, and the radial spatial distribution was calculated. The experimental and calculated average values check very closely. A plot of the calculated radial variation is shown in Fig. II.38.1. At the beginning of a fuel cycle the radial power distribution is quite flat, except in the fuel region closest to the control region. Therefore the average coefficient should be used. Later in the fuel cycle the power density in the regions where the void coefficient tends to be less negative is less than the average due to nonuniform fuel burnup. Therefore the effective overall void coefficient would tend to be more negative.

---

*Discussed in answer 42A.

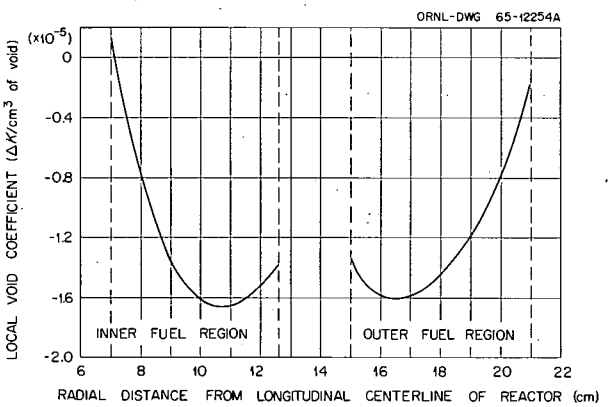

Fig. II.38.1. Void Coefficient in the HFIR for Uniform Local Void Distribution.

The void coefficient for the water gap between elements is also negative and as set forth in ORNL-3572, Sect. 7.3.4, is -0.046 in terms of the void fraction or in terms of Δk per cubic centimeter of void is -1.24×10^{-5}.

Figure 7.3.6 of ORNL-3572 shows the relationship between void fractions in the island and reactivity, with and without a target. This region has a positive coefficient for small void fractions; however, as has been indicated, there is an optimum void fraction, and the coefficient becomes negative for addition of voids in excess of the optimum. The void coefficient for the control region is also positive but quite small, being only about one-third of that in the target region.

F. Have reactivity accident studies allowed for the possibility of the return of water to the core?*

In the analog analyses the expulsion of water from the core, except by thermal expansion, was not considered. The return of water to the core follows the incident as the temperature is reduced and thus after the safety rods have been inserted.

39. What procedures will be followed if a normal removal of irradiated fuel is impossible due to fuel damage or sticking?

It has been assumed that a fuel assembly might become damaged, thus preventing normal removal of the elements, that is, one element at a time. If this should occur, it would be necessary to remove both elements simultaneously as a fuel assembly. Prior to removing a fuel assembly, it would be poisoned by inserting enriched ^{10}B steel strips into the fuel region. At least 20 such strips, 10 each in the inner and the outer element, would be inserted prior to removal.** Approximately 50 of these strips are presently

*Further discussed in answer 55G.

**Further discussed in answer 42B.

on hand. Part of the scheduled tests during the startup program was an investigation and verification of the number of strips required to remove any doubt about the fuel assembly being subcritical in any credible arrangement in the HFIR facility.

40. Discuss the reliability of the emergency air supply to the control rod drives.

Air is supplied to the rod drive motors from the main instrument air receiver. The receiver is capable of driving all four shim-safety rods through their full stroke with sufficient pressure remaining to operate the instrumentation. The receiver is supplied with air from either of two compressors. Each compressor is supplied from a normal emergency bus.

The primary purpose for incorporating fast insert air motors on the four shim-safety rods was to expedite a fast recovery of the rods following a scram. Another use for the fast insert is that of aiding the servo, whose available reactivity is limited, in reducing reactor power when ac power to the facility is interrupted.

For the first case, the lack of sufficient air would increase the probability that the reactor could not be restarted in time to override xenon. In the latter case, the lack of sufficient air could result in a scram due to failure of the air motors to insert the shim rods in response to the signal from the servo system. The reactor safety would not be compromised by loss of air to the fast insert air motors.

41A. Are there possibilities of shielding the control room so that the probability of evacuation of reactor operators can be reduced?

The HFIR control room is partially shielded by the 8-in.-thick concrete reactor building; however, this wall is penetrated by the observation gallery windows, which can be seen in Figs. 3.2.5 and 3.2.6 of ORNL-3572. The only simple way to provide additional shielding would be to block off these windows, which would prevent the operator and supervisor from having a view of the reactor bay area and which would eliminate the advantage of having a visitor gallery isolated from the containment building.

There is no advantage to having the operator remain in the control room following a serious accident, and it is not intended that he do so. For this reason it appears unnecessary to further shield the control room.

B. Are there any significant safety advantages that could be achieved with an alternate emergency control area?

There do not appear to be any significant safety advantages to having an alternate emergency control area for reactor control functions. There is a need for an emergency control center removed from the HFIR site for use during an accident, and the ORNL complex has such a center. Reference to this overall system is made in the answer to question 29B, and a brief description of the Radiation-Monitoring and -Warning System at ORNL is given in *Nuclear Safety*.[6]

APPENDIX G

USE OF TENSILE SPECIMENS

OAK RIDGE NATIONAL LABORATORY
OPERATED BY
UNION CARBIDE CORPORATION
NUCLEAR DIVISION

POST OFFICE BOX X
OAK RIDGE, TENNESSEE 37831

July 2, 1965

Mr. N. J. Palladino
333 West Park Avenue
State College, Pennsylvania 16801

Dear Sir:

We have had some difficulty in obtaining a direct answer to the questions you raised on impact properties and any impact transition of the HFIR aluminum and the use of tensile specimens to demonstrate the absence of any adverse effects by irradiation.

Aluminum, having a face-centered cubic structure, is in a group of materials which are considered as not possessing a ductile-to-brittle transition temperature. Since impact values are not commonly used with aluminum technology, there is almost a complete absence of impact data available in the literature. This even applies to the aircraft industry where impact loadings are prevalent.

In *The Properties of Metallic Materials at Low Temperatures* (John Wiley and Sons, 1950), P. Litherland Teed does present impact values of several of the complex aircraft-type alloys, none of which show any temperature effect. The alloy composition which most closely resembles type 6061 used in HFIR would be pure aluminum, the data from which are tabulated below.

Izod Impact Values Pure Aluminum[a]

Temperature (°C)	Impact Value (ft-lb)
Room	19
−40	19
−80	20
−120	21
−180	27

[a]One-inch-diameter rod rolled and annealed.

As additional evidence for the lack of a transition temperature, I am listing two sets of tensile data covering a very wide temperature region.

Tensile Properties of Heat-Treatable Wrought Aluminum Alloys at Low Temperatures[a]

Commercial Alloy and Temper	ASTM Alloy	Tensile Strength (psi)	Yield Strength (psi)	Elongation in 2 in. (%)	Reduction of Area (%)
			75°F		
61S-O	GS11A	17,700	6,800	34.8	73
-T4		40,300	21,800	30.5	57
-T6		45,100	38,800	20.6	53
			−18°F		
61S-O	GS11A	18,500	7,100	36.4	73
-T4		41,700	22,500	31.5	56
-T6		47,100	39,300	20.2	52
			−112°F		
61S-O	GS11A	20,000	7,600	40.8	74
-T4		44,100	23,200	32.5	54
-T6		49,200	41,000	21.2	52
			−320°F		
61S-O	GS11A	33,200	9,200	49.2	67
-T4		57,900	29,400	36.6	41
-T6		60,200	45,500	25.6	46

[a]F. M. Howell (Alcoa), "Low-Temperature Properties and Applications of Aluminum Alloys," *Conference on Materials and Design for Low-Temperature Service*, PB-121009, pp. 253–66.

Typical Tensile Properties (6061)[a]

	O Condition			T-6 Condition		
°F	UTS	YS	EL	UTS	YS	EL
500	5.5	4	70	10	7	50
400	9	6.5	55	18	15	28
300	16	8	30	34	31	20
75	18	8	30	45	40	17
−18	19	8.5	32	47	42	17
−112	20	9	36	48	43	18
−320	34	11	45	61	48.5	23

[a]*Aluminum Data Book*, Reynolds Metal Company, 1961, pp. 43 and 47.

The *Kaiser Aluminum Rod, Bar, and Wire Product Information Handbook*, 2nd ed., p. 4, makes the following statement: "At sub-zero temperatures, aluminum is especially valuable as it increases in strength without loss of ductility. Low temperatures make no adverse changes in other properties of aluminum. Notch sensitivity is not affected adversely and modulus of elasticity, hardness, and fatigue strength gain at low temperatures."

On page 6: "In impact strength, aluminum alloys exceed many heavier metals, weight for weight. For instance, aluminum has the ability to absorb several times as much energy, before breaking, than equivalent steel specimens."

As a more exact answer to your question, we have broken Charpy V specimens from 6061-T6. Typical broken specimens are enclosed along with a room-temperature tensile specimen. All samples show ductile-type breaks with a cup and cone fracture and reduction in area at the sides. The fracture values are shown in the following table:

Charpy V-Notch Impact Energies
6061-T6 Aluminum

Temperature (°F)	Notch[a] Orientation	Ft-Lb
76	LH	20
76	LH	22
–40	LH	19
–320	LH	23
–40	LV	13
–320	LV	14

[a]Longitudinal specimen with horizontal or vertical notch.

While the impact values on standard specimens appear to be low, they bear a direct relationship with the relative low values of the stress-strain curve and tensile strength of the material. They are not low because of a change in fracture mechanism as is the case with steels. In all cases, the fracture would be classed as a ductile fracture. For example, lead, which without question would be considered ductile at room temperature, would show an even lower value, but again one which would be related to the tensile strength.

In summary, since with type 6061 aluminum no change in deformation mechanism occurs with either testing temperature or type of test, the use of tensile specimens and tensile data would appear to be reasonable. The irradiation thimbles which are the only aluminum in the system which must sustain the system pressure were designed with the use of very conservative tensile data.

Very truly yours,

Original signed by

G. M. Adamson, Jr.
Metals and Ceramics Division

Part IIb. Safety Review Questions and Answers 42—53

ABSTRACT

Following a January 1966 meeting with the USAEC Division of Reactor Licensing to discuss the HFIR Safety Analysis, a request for additional information was made to ORNL by the USAEC. The table of contents comprises a list of the questions, with answers given in the body of this report.

Originally published as ORNL-CF-65-11-29, Supplement No. 1 (Feb. 1, 1966).

CONTENTS

42. A backup system for reactivity control has not been incorporated into the design of HFIR. Additional information, beyond that given in responses 22A and 22B, is required in the following areas:

A. Discuss the reactivity status of the reactor as a function of time after an attempted scram in which only a small fraction of the negative reactivity available in the control rods is capable of being inserted. Various initial conditions as to core lifetime, and xenon and samarium concentrations should be taken into account. The discussion should point out the amount of negative reactivity required to compensate for the temperature defect, the effect of xenon and samarium poisoning, and the times available for other action to be taken to insert additional negative reactivity into the core assuming the rods remain incapable of further insertion. 169

B. In the event the proposed insertion of poison strips into the core is, for some reason, impossible, the preparation of a liquid poison solution with subsequent injection into the core could be an alternative method of maintaining the reactor core in a shutdown status. In an emergency, how could this be done in the HFIR facility? In particular, what methods of injection are available in the present design? Would it be in the interest of safety to have written emergency procedures, available to the HFIR operating staff, which would outline steps to be taken to obtain the required poison, to prepare an adequate solution, and to inject the solution into the core in the event other methods of poisoning the core are unavailable? 171

43. Response 23B–C provided an analysis which estimated the core temperature following a step loss in pressure. The analysis assumed a mechanism for heat transfer from the core to the coolant, and the results indicated no fuel melting and no metal-water reaction. Provide an estimate of the time sequence of events which would occur in the event the assumed heat transfer mechanism were not available. In particular, at what rates might the resultant metal-water reaction proceed? How might the hydrogen generated by the reaction get to the reactor bay area? What potential is there for getting steam into the filter system following a loss-of-coolant accident with a subsequent metal-water reaction involving the core? 172

44. With respect to response 24, provide the following additional information:

A. Describe the new end cap bolts. 175

B. If the beam tube were to fail inside the reactor vessel and, subsequently, the end cap failed, what would be the maximum loss-of-coolant flow through the beam tube? What makeup flows into the reactor vessel would be available? Discuss the design and operating requirements for components to be inserted into the beam tubes, and which could limit flow through the beam tube in the event of the postulated double failure. 175

C. The probability of maintaining the integrity of the beam tube extension in the event of a beam tube failure within the reactor vessel is greater if the reactor operating pressure is not permitted to exceed the proposed operating level of 600 psi, even though the reactor coolant system has been designed for 1000 psi. Has this restriction on pressure level been considered? 178

45. If release of 100% of the noble gas inventory from the core is assumed and if fumigation meteorological conditions exist, the present method of ventilating the HFIR building could lead to doses at the site boundary in excess of standard guidelines. The alternate ways of limiting the dose considered in response 29A do not appear to provide the necessary reduction in doses. What other ways have been considered? What would be the effect on the doses? 178

46. With reference to response 30, it appears that the discussion is in conflict with the evidence given in the referenced document, ORNL-TM-1291. We have been advised that ORNL-TM-1291 did not contain the latest information available on the subject it covered. Provide the additional information necessary to support the discussion in question. 180

47. With reference to response 31B, provide an estimate of the error associated with the assumed neutron flux. With reference to response 31C, provide a discussion of the consequences of failure of the structural members mentioned in the response. 183

48. With reference to response 33, provide a discussion of the shutdown and evacuation potential at MSRE, including a summary of results of evacuation tests that may have been conducted. 184

49. With reference to response 34A, what is the maximum increase in core fission product inventory associated with the increase in fuel cycle time that could result from use of different fuels or increased loadings? 184

50. With reference to responses 34B and 34C, we have been advised by ORNL that there are many other criteria than the two mentioned which would be used to measure the safety involved in core changes and the appropriateness of regulatory review. Provide an expanded discussion of these other criteria. 185

51. Response 38A does not provide the results requested for reactivity transients considerably more severe than those previously treated. Provide the results of the analyses previously requested. 185

52. Provide a discussion of the results of operation of HFIR at power levels up to 20 Mwt. 188

53. Provide a summary of significant changes made to the facility since commencement of operation. 191

QUESTIONS AND INFORMATION REQUESTS ON THE HFIR

42. A backup system for reactivity control* has not been incorporated into the design of HFIR. Additional information, beyond that given in responses 22A and 22B, is required in the following areas:

A. Discuss the reactivity status of the reactor as a function of time after an attempted scram in which only a small fraction of the negative reactivity available in the control rods is capable of being inserted. Various initial conditions as to core lifetime, and xenon and samarium concentrations should be taken into account. The discussion should point out the amount of negative reactivity required to compensate for the temperature defect, the effect of xenon and samarium poisoning, and the times available for other action to be taken to insert additional negative reactivity into the core assuming the rods remain incapable of further insertion.

The reactivity status as a function of time has been considered for several cases of interest under the assumption that the control rods become stuck at an appropriate time to cause concern.

The first case is one in which it is desired to shut down the reactor from full power immediately following startup with fresh fuel, and the control rods only respond by reducing k a very small amount.

For this case the core is essentially clean, and fuel depletion plus the buildup of xenon will reduce the power level over the period of time required to reduce the reactivity sufficiently to compensate for the change in coolant and moderator temperatures. This amount of reactivity is about 0.003 $\Delta k/k$ (assuming no change in inlet water temperature). The number of megawatt-days required to burn up this amount of reactivity by fuel depletion alone is about 120 Mwd. Since a considerable amount of iodine and xenon would be generated during this time the number of megawatt-days would be less, and instead of just remaining critical at essentially zero power, as would be the case if only fuel depletion were considered, the decay of iodine to xenon would make the reactor subcritical. However, the eventual decay of the xenon would permit the reactor to go critical again but at a power level less than the initial power. For this case the minimum amount of negative reactivity required by control rod movement to shut the reactor down immediately would be equal to the temperature deficit, which is 0.003 $\Delta k/k$; if the reactor inlet temperature were reduced to room temperature from normal inlet temperature, a small amount of additional negative reactivity would be introduced as about 0.04% $\Delta k/k$ is removed on cooling from 120 to 80°F. Under the above conditions (clean core), the differential worth of a single safety rod is 0.0022 $\Delta k/k$ per inch. Thus, in order to reduce the power level of a clean core from 100-Mw normal operation to zero at room temperature, it would be necessary to insert a single safety rod only about 1.2 in.

The second case considered is the situation in which the reactor has run sufficiently long to have established equilibrium iodine and xenon. If a very small amount of negative reactivity is introduced, such as postulated by an attempted scram in which only a small movement is achieved, the reactor would promptly shut down due to xenon buildup. If the rods remained in this position and no other action were taken, the xenon would decay sufficiently in about $2\frac{1}{2}$ days to allow the reactor to regain criticality and proceed to a supercritical condition in which core damage would result. Two of the safety rods would have to be almost fully inserted to compensate for full xenon decay and the temperature deficit, if this situation occurred just after xenon equilibrium was reached. Later in the cycle buildup of samarium

*Further discussed in answer 60.

during the shutdown would reduce the amount of rod insertion required to keep the reactor subcritical. However, as indicated, about $2\frac{1}{2}$ days are available for inserting rods, adding other poison, and/or removing the core before criticality would be achieved as a result of xenon decay.

Late in the fuel cycle (after about 8 days for a 14-day core), the promethium concentration would be large enough so that once the reactor is shut down it could not be made critical again without withdrawing the rods beyond their position just prior to shutdown. This results from the fact that the stable samarium at that time and thereafter would be worth more than the equilibrium xenon.

Another case of interest is that in which the reactor has just been restarted after recovering from a scram. The xenon under this condition could have a worth no greater than about 0.12 $\Delta k/k$ as this is approximately the maximum excess k of a clean core. The xenon concentration would be increasing due to decay of its precursors and would continue to increase until the rate of destruction due to reactor power was equal to the xenon birth rate. This point would be reached at a power level of about 30 Mw for the case under consideration. For further increases in reactor power level the xenon concentration would begin to decrease and the control rods would have to be inserted to compensate for the increase in reactivity. The control elements normally have more than enough speed to maintain control; however, if all rods became immobile while xenon was being burned out, the reactor would become supercritical, and reactivity would be added at a rate proportional to the excess of power above 30 Mw. If no action were taken the reactor power level would increase until core damage resulted. If the power level were to be taken to 100 Mw, the rate of xenon burnup would be equivalent to a reactivity increase rate of $\sim$0.015% $\Delta k/k$ per second, which indicates that if all control elements were frozen in position only a few seconds would be available to take action before the power level increased to 130 Mw, which is the level at which safety action would normally take place. This situation is not greatly different (less than a factor of 2 in rate) from that in other high-flux reactors such as the MTR or ORR.

For this case we have always assumed that at least one method of rod insertion would be effective on at least one of the control elements. Even partial insertion of any one of the five rods would be sufficient to reduce the power level to the point where xenon buildup would complete the shutdown, thus allowing adequate time for other methods such as poison strip insertion and/or core removal to be employed. If none of the rods will move under scram conditions, force can be applied by either the normal electric drives or the fast-insert air motors. In addition, the shim regulating cylinder can be moved under electric motor drive or by a manually held air motor. If it is postulated that not any of these methods are effective and all rods are totally immovable, then the time scale is such that attempts to restart following a scram must be ruled out by administrative control or a secondary shutdown system must be provided. In our judgment it is manifestly impractical to consider ruling out any attempt to restart the reactor before the xenon has decayed, and it is also our judgment that the probability of having all control elements totally immovable is so small as to not constitute a significant risk. We do recognize the probability that at some time in the lifetime of the reactor one or more, but not all, of the control elements may become incapable of complete insertion, and for this reason and for fuel handling purposes we have provided equipment and procedures for inserting poison strips into the core. As discussed above, this technique would not be effective if all control elements became immobilized during a

recovery from a scram. The probability of having all control elements become immobilized under these conditions is quite small inasmuch as at least one of them had just demonstrated its ability to function.

B. In the event the proposed insertion of poison strips into the core is, for some reason, impossible, the preparation of a liquid poison solution with subsequent injection into the core could be an alternative method of maintaining the reactor core in a shutdown status. In an emergency, how could this be done in the HFIR facility? In particular, what methods of injection are available in the present design? Would it be in the interest of safety to have written emergency procedures, available to the HFIR operating staff, which would outline steps to be taken to obtain the required poison, to prepare an adequate solution, and to inject the solution into the core in the event other methods of poisoning the core are unavailable?

A liquid poison could easily be injected into the HFIR primary coolant system by introducing it into the suction side of the pressurizer pumps. The pressurizer system consists of two main pumps supplied with normal ac power and an emergency pump which can be supplied from either the normal power or diesel generator power. Normally one pressurizer pump is in operation with the other main pressurizer pump on standby. The emergency pump starts on failure of the normal pumps. The normal pressurizer pump flow rate is between 100 and 200 gpm, and the emergency pump will maintain a flow of 6 gpm. These pumps take their suction from a common header supplied from a 2500-gal gravity-feed head tank on the floor above. In the simplest concept, poison could be dumped into the head tank and the pressurizer pumps would inject it into the primary system. Following injection the cleanup system would be shut down to prevent removal of the poison. The primary system circulation would achieve almost complete mixing in about 2 min following injection. The above is an oversimplified description of how a system of this type could be incorporated in the HFIR; however, it would be an adequate system to prevent restart if the core were poisoned by xenon and it was only necessary to take action before the reactor could regain criticality some 2 to $2\frac{1}{2}$ days later.

The second part of this question regarded the possibility of preparing written procedures outlining the necessary steps to be taken to poison the core during the approximately $2\frac{1}{2}$ days available while the reactor is poisoned out by xenon. This approach does not seem to be particularly valuable in view of the time scale of reactivity changes during a recovery from an unscheduled scram. A very simple procedure of the type set forth would suffice to keep the reactor shut down; however, it is our opinion that if complete immobilization of the rods is postulated during xenon transients, then it follows that a secondary shutdown system must be installed, and appropriate operating procedures must be prepared that are consistent with the time behavior of the reactor system and the secondary shutdown system.

While it is our opinion that such a system is not necessary, we recognize the concern expressed by members of DRL and the ACRS in this area. In addition, we are aware of the efforts to incorporate the requirement for a secondary control means in criteria currently being reviewed for power reactors. These factors plus the expectation that such requirements may be imposed on new and existing research reactors lead us to propose that the HFIR be equipped with a liquid-poison injection system, and that operating procedures governing recovery from power reductions be established which provide adequate time

for the poison injection should the control rods become immobilized or should control of the reactor be lost in such a way as to be equivalent to immobilized control rods.

It is our intention to proceed with the design of such a system and to prepare written procedures governing recovery from power reductions which will provide reasonable assurance that the system could be effective. A program is presently being prepared for calculation of the kinetic behavior of the combined reactor and poison injection system in order to investigate the necessary programming of reactor power during restart conditions. The operating procedures will be based on this information.

We should like to point out again that we consider such a secondary shutdown system to be unnecessary in the sense that it is our opinion that the accidents in which the system might be of use are sufficiently improbable as to constitute no significant risk in operation.

43. Response 23B–C provided an analysis which estimated the core temperature following a step loss in pressure. The analysis assumed a mechanism for heat transfer from the core to the coolant, and the results indicated no fuel melting and no metal-water reaction. Provide an estimate of the time sequence of events which would occur in the event the assumed heat transfer mechanism were not available. In particular, at what rates might the resultant metal-water reaction proceed? How might the hydrogen generated by the reaction get to the reactor bay area? What potential is there for getting steam into the filter system following a loss-of-coolant accident with a subsequent metal-water reaction involving the core?

The fuel plates of an HFIR core contain approximately 85.5 kg of aluminum. Of this, 52.7 is adjacent to the fuel region and is considered available for the Al-H_2O reaction. The remaining 32.8 kg is located either in the fuel core, where it is assumed to be consumed in the U_3O_8-Al reaction, or is sufficiently remote from the fuel core so that its heating rate is significantly lowered.

The increase in heat content of the HFIR fuel due to nuclear heating has been obtained by an integration of the power decay data presented in response 23B–C. In computing the specific heat content as a function of time, illustrated in Fig. II.43.1, it has been assumed that heat transfer does take place for the first 50 msec, but that thereafter the nuclear heat is absorbed adiabatically. Moreover, it is assumed that the heat is absorbed by the entire 85.5 kg. Values of the integral are given for both the core average and the hot spot situations.

It is perfectly clear that under the assumption of adiabatic conditions the core temperature will continue to rise indefinitely. Obviously, this cannot really occur, and, at some point, the temperature rise will in fact be limited by one or more of several possible modes of heat transfer. In response 23B–C, using a conservative but rational approach, it was shown that it is extremely unlikely that a sudden pressure loss could result in the reaction of any of the core with water. If, however, one neglects the obvious contradictions involved and assumes that the conditions following the loss of pressure are indeed adiabatic and that under these conditions the metal can come in contact with sufficient water, it is possible to postulate a complete metal-water reaction.

Within 500 msec after the step loss in pressure, the primary source of heat is the decay of the fission products. This heat source will, after about two or three seconds, raise the temperature of the fuel to the melting point, at which time the volatile fission gases will start to escape from the fuel. Also, at about

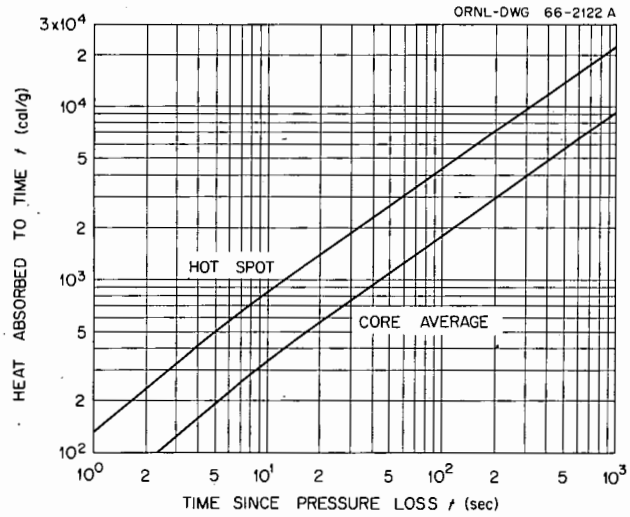

Fig. II.43.1. Energy Absorption as a Function of Time Following Pressure Loss.

this time, the reaction between U_3O_8 and aluminum is assumed to begin. This will make available an additional 61 cal per gram of aluminum. Not all of the fission product heat is absorbed by the fuel; a fraction, estimated to be about 15%, will escape in the form of gamma radiation. Consequently, the two effects – loss due to gamma radiation and loss of volatile fission products – are assumed to counterbalance the increase in heating due to the U_3O_8-Al reaction; and all three of these secondary effects have been neglected.

The extent and rate of the metal-water reaction are difficult to determine because they depend not only upon the temperature but also upon the availability of steam. As previously stated, however, it will be assumed that sufficient steam is available. One method of estimating the extent of the reaction is to attempt to apply one or more of the various isothermal rate laws to this nonisothermal situation. A second method, that utilized here, is to consider the adiabatic temperature excursion as if it were a power excursion and to apply the data obtained from excursion-type experiments. The main difference between the present case and the excursion experiments is related to the time scale of the heat-up period. Most TREAT and SL-1 data are based on periods of from 40 to 500 msec, whereas the situation under consideration here is characterized by a period of several seconds. Data[1] exist which give the extent of reaction as a function of specific heat input. On the basis of these data, it appears that for an energy input of less than 350 cal/g no significant reaction will occur. The extent of the reaction appears to increase linearly from zero at 350 cal/g to about 15% at 530 cal/g and then linearly, but with a different slope, to about 30% at 920 cal/g. Direct extrapolation would lead to the assumption of a 100% reaction at approximately 2850 cal/g. This relation is shown in Fig. II.43.2.

---

[1]L. Baker, Jr., *Nucl. Safety* 7(1), pp. 25–34 (Fall 1965).

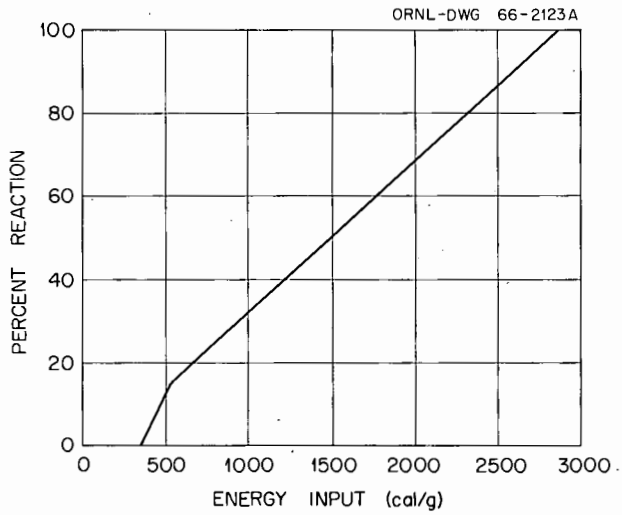

Fig. II.43.2. Extent of Metal-Water Reaction as a Function of Energy Input.

By utilizing the fact that the hot spots comprise less than 5% of the core, and by combining the information in Figs. II.43.1 and II.43.2, it is possible to deduce, based upon the foregoing assumptions, the rate at which the metal-water reaction proceeds. The results are shown in Fig. II.43.3.

The total energy available from the reaction is approximately 925 Mwsec. According to this model, about 350 Mwsec would be released in a time between 10 and 50 sec after the pressure loss. The remaining 575 Mwsec would be released over a 130-sec period at a constant rate of about 4.4 Mw. These power levels are sufficiently low so that no catastrophic damage would be anticipated.

The complete reaction could release about 2300 STP ft^3 of H_2. Approximately 875 ft^3 of this would be generated in the 10-to-50-sec interval, and the rest would be generated at a rate of about 11 cfs. In order to escape into the building the hydrogen would have to pass through several feet of water, either in the reactor pool or in the primary piping, and it would therefore be cooled. Moreover, because of the building exhaust system it would be conveyed rapidly from the building, thus reducing the possibility of ignition.

The total energy involved during the 180-sec interval – nuclear heat plus heat of reaction – is approximately 1.8×10^6 Btu. The reactor pool alone contains 6.67×10^5 lb of water. Hence this energy, if absorbed adiabatically, would increase the average water temperature by only 2.7°F. Thus there seems little possibility of any appreciable release of steam.

It would appear, therefore, that despite the absurdly conservative assumptions used to estimate the consequences, the pressure-loss accident would not result in any consequences which would materially change the previously calculated estimates of radiation doses following a 100% meltdown. Moreover, it is our contention that the foregoing analysis overestimates the fuel meltdown by at least an order of magnitude, and that our original calculations are much more representative of what could actually be expected.

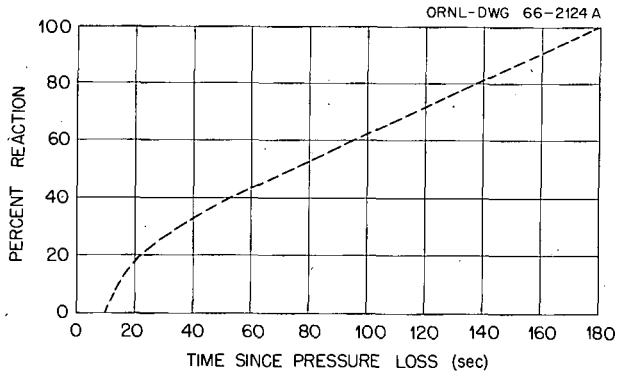

Fig. II.43.3. Metal-Water Reaction as a Function of Time.

44. With respect to response 24, provide the following additional information:

A. Describe the new end cap bolts.

The material for the new end cap bolts is ASTM-A193-62T-B7. This material has a specified minimum tensile strength of 125,000 psi and a specified minimum yield strength of 105,000 psi. Test results on the bolts we are using were obtained from Midwest Testing Laboratory by the supplier. These tests showed a minimum tensile strength of 151,000 psi and a minimum yield strength of 135,800 psi. Additional tests were performed at ORNL, and the results showed somewhat higher tensile and yield strengths than those obtained at Midwest Testing Laboratory. The operating stress in the bolts at 1000 psig internal pressure in the beam tube would be 43,750 psi.

In order to remove any question regarding our estimates that the beam tube would not be damaged and that the end caps and bolting were adequate to withstand 1000 psig internal pressure, we have hydrostatically tested one of the beam tubes, end caps, and bolts to 1500 psig. No leakage and no damage resulted.

B. If the beam tube were to fail inside the reactor vessel and, subsequently, the end cap failed, what would be the maximum loss-of-coolant flow through the beam tube? What makeup flows into the reactor vessel would be available? Discuss the design and operating requirements for components to be inserted into the beam tubes, and which could limit flow through the beam tube in the event of the postulated double failure.

As set forth in the answer to question 24, we believe that the beam tube can contain the internal pressure resulting from a rupture of the inner end even if the reactor inlet pressure were 1000 psig. In order to demonstrate that our contention was correct, we have tested a beam tube assembly to 1500 psig internal pressure without damage as described in part A of this question.

If the double failure postulated should occur, the rate of coolant loss would be limited by the internal collimator and shield plug, which would be held in place by the beam tube shutter assembly following an outward movement of about $\frac{3}{8}$ in. Calculations made of the rate of coolant flow under these

conditions and under the assumption that the collimator and shield plug were located eccentrically resulted in a flow rate of about 100 gpm at 1000 psi reactor inlet pressure. If the pressure were equal to the head of water in the pool, as would be the case after shutting down the reactor and stopping the pressurizer pump, the flow rate would be less than 10 gpm.

The design of the collimator and shield plug has been reviewed to verify that it would remain intact under conditions postulated for this accident. Like the beam tube extension, the shield plug was not designed for operation at 1000 psig; however, as was the case with the beam tube extension, the design was based on considerations other than pressure. As a result, examination of this container (plug) for external pressure application using the same ASME-type charts utilized for the beam tube design shows the allowable external operating pressure to be 360 psi. These charts are made up to include a factor of safety of 4 based on average materials, and therefore result in a minimum collapse pressure of 1440 psi. The same higher factor of safety of 6 found in examination of the beam tube design would be expected to pertain here also. Inasmuch as this vessel is not normally subjected to external pressure and is in fact at essentially zero stress, the derating of its capacity due to creep is not applicable. With the minimum expected collapse pressure being more than 500 psi greater than the maximum expected applied pressure resulting from the postulated leak from the primary system into the beam tube, the internal plug would be expected to remain intact.

Even if some buckling of the wall of the plug should occur, the cap at the inner end of the plug, which is designed to withstand 1200 psi external pressure, will remain intact and the leakage would still be limited to a rate which would only result in a reactor shutdown.

A review of the ability of the beam tube shutter to hold the beam tube collimator and shield plug in place was also made. While the results indicated that the design was adequate to accomplish this, there was essentially no safety factor. As a result of the concern expressed over this particular accident, it has been decided that a minor modification will be made to an access plug above the shutter, which will ensure a large safety factor in the ability of the shutter to restrain the collimator and shield plug should the postulated accident occur. This modification requires that an extension be welded or otherwise fastened to the end of the access plug so that the shutter will be restrained from any tendency to lift from its dowels should the collimator and shield plug exert force against it.

If a leak should occur in a beam tube, or at any other location in the primary system, the pressure-control system would sense the loss of pressure and would act to close the letdown valves which control the pressure. The normal letdown flow rate is between 100 and 200 gpm, and therefore a leak of 100 gpm would only result in a minor pressure transient while the pressure-control system readjusted to maintain pressure. If the pressure-control system did not respond sufficiently fast to prevent the pressure from dropping more than about 50 psi, the block valves would be closed by a different pressure-sensing system. These valves can shut off flow in about 0.2 sec. The pressurizer pump would continue to supply water to the reactor system at a rate dependent on the reduction in pressure below the normal pressure. Inspection of the pressurizer pump head curve, Fig. 6.2.9 in ORNL-3572,[2] shows that under

---

[2]F. T. Binford and E. N. Cramer (eds.), *The High Flux Isotope Reactor: A Functional Description, Volume I*, ORNL-3572 (May 1964; rev. Mar. 1, 1965).

typical operating conditions, that is, 600 psi inlet pressure and a letdown flow of about 150 gpm, a drop in reactor system pressure to below the scram point of 375 psi would result in a makeup flow of about 400 gpm.

For abnormal pressure reductions the standby pressurizer pump starts, and therefore a somewhat larger flow is available than indicated above. This large flow rate could not be maintained very long, as the pressurizer pump head tank is only of 2500 gal capacity and the makeup flow to this tank is only about 100 gpm from the plant process water system via the plant demineralizer and demineralized water storage tank. This is of no great consequence, as the reactor would be promptly shut down and the system depressurized to reduce the leak rate. Under depressurized conditions the pressurizer pumps would continue to supply water until stopped or until the head tank ran dry. When the pressure at the reactor inlet started to drop below a pressure equal to that in the surrounding pool, a check valve connecting the reactor tank to the pool would open and admit pool water to the primary system. In addition to the check valve, a manual valve is provided in parallel with the check valve. If it is assumed that the pressure at the reactor inlet drops to atmospheric pressure (15 psia), the 27-ft head of H_2O in the pool would provide a makeup flow rate of about 170 gpm through the check valve. If the manual valve were opened an additional 160 gpm would be available. The reactor pool contains about 30,000 gal above the inlet to these valves, and water can be added to the reactor pool at about 800 gpm from adjacent pools, should this be necessary.

The design and operating requirement for components to be inserted in the beam tubes may be summarized by stating that the design must be adequate to prevent overheating; they must be able to withstand, without leakage, the normal maximum coolant pressures (150 psig) and a vacuum for drying components; they must be made of a material which is compatible in the presence of water with the aluminum beam tubes without causing corrosion. In addition, the shielding they provide must be adequate when considered together with such external shields as are provided. All insertions into the beam tubes, including the present beam tube collimator and shield plugs, are considered to be experiments and must be reviewed by the Operations Division technical staff as set forth in the answer to question 32 and following the criteria used in reviewing and approving experiments proposed for ORNL reactors in ORNL-TM-281[3] and ORNL-TM-745,[4] copies of which have been supplied in connection with the answer.

It is not presently required that components inserted in the beam tubes be so designed to limit the flow in the event of the postulated accident; however, it is required that the design of any experiment be such that an internal pressure of 1000 psig could be applied to the interior of the beam tube without significant leakage.

---

[3]C. D. Cagle, *General Standards Guide for Experiments in ORNL Research Reactors*, ORNL-TM-281 (Aug. 20, 1962).

[4]C. D. Cagle, *Considerations Involved in the Safety Review of Experiments to Be Operated in Nuclear Reactors*, ORNL-TM-745 (July 10, 1964).

C. The probability of maintaining the integrity of the beam tube extension in the event of a beam tube failure within the reactor vessel is greater if the reactor operating pressure is not permitted to exceed the proposed operating level of 600 psi, even though the reactor coolant system has been designed for 1000 psi. Has this restriction on pressure level been considered?

We have not considered such a restriction on pressure inasmuch as the pressure level, along with reactor inlet temperature, is one of the parameters which can easily be varied as may be desired to maintain the margin between operating power level and the power level at which incipient boiling would take place.

In view of the test results set forth in the answer to part A of this question, it appears that an adequate safety factor is available even if the reactor primary system were to be operated at 1000 psig.

45. If release of 100% of the noble gas inventory from the core is assumed and if fumigation meteorological conditions exist, the present method of ventilating the HFIR building could lead to doses at the site boundary in excess of standard guidelines. The alternate ways of limiting the dose considered in response 29A do not appear to provide the necessary reduction in doses. What other ways have been considered? What would be the effect on the doses?

The whole body gamma-ray dose at the HFIR site boundary under fumigation conditions was originally estimated based upon a 50% core meltdown. Because it appeared that a release of this magnitude would not present any problem, certain extremely conservative assumptions were utilized in order to make it possible to use data already developed. These included the assumption of a 10-m/min wind speed during the inversion which precedes the fumigation condition, extremely rapid release from the stack, and an effective height of 76.2 m (the actual stack height). Moreover, because the 10-m/min wind speed is insufficient to permit the plume to reach the site boundary within 2 hr, the doses were computed for infinite exposure.

In view of the requirement to consider a 100% release, the whole body gamma doses have been recalculated using somewhat more realistic assumptions. Discussions with F. A. Gifford, Jr., and W. M. Culkowski of the Environmental Services Administration, which are summarized in a letter from Gifford to I. Speckler dated January 14, 1966, established that the model previously employed to compute the dose (response 29A) is adequate; and it has been used to obtain the information presented below. A study of wind distribution data indicates that during an inversion prior to the fumigation condition the wind speed can be expected to be no greater than $\frac{1}{2}$ to 1 mph, and that during the fumigation which may accompany the breakup of the inversion it will increase to 4 or 5 mph. This has also been confirmed by observations at ORNL.

Consequently the method previously presented in answer 1 has again been utilized. The use of F-type stability (moderately stable) for the inversion condition and C-type stability (slightly unstable) for the fumigation condition has been retained, as has the assumption of a fixed stack height $h = 76.2$ m and a rapid emission rate. The wind speed during the inversion has been chosen to be 25 m/min, which is the lowest value which will permit the plume to reach the site boundary within the 2-hr

period. (In general the dose decreases with increasing wind speed.) The wind speed during fumigation is taken to be 120 m/min, so that u_{inv}/u_{fum} is 0.208 rather than the less conservative 0.154 used in the previous calculation. Upon putting these values in the dose equation:

$$\frac{D_f}{D_i} = \sqrt{\frac{\pi}{2}}\left(\frac{u_i \sigma_{yi} \sigma_{zi}}{u_f \sigma_{yf} h}\right) e^{h^2/2\sigma_{z_i}^2},$$

it is found that at 2.82 km

$$D_f/D_i = 2.716 .$$

The 2-hr inversion dose at the site boundary for a 100% release was found to be

$$D_i = 10.9 \text{ rads} ,$$

so that the fumigation dose at the site boundary becomes

$$D_f = 10.9 \times 2.716 = 29.6 \text{ rads} .$$

It should be pointed out that this represents an extremely unlikely situation, not only because a 100% meltdown of the core is considered incredible, but also because the site boundary in question lies in a direction toward which, during inversion conditions, the wind blows less than 1% of the time. Perhaps of more interest is the 2-hr dose at the nearest site boundary which lies in the direction of the prevailing wind. This is approximately 4 km southwest of the reactor site. A calculation similar to that given above yields a whole body gamma dose due to noble gases of approximately 19.4 rads.

From this analysis it appears that it is unnecessary to consider alternate ways of limiting the ground-level radiation doses. However, these doses could be reduced if it were possible to devise a method which would decrease the rate at which the noble gases are emitted from the stack.

For many of the possible accident cases, a reduction in the total air flow through the SBHE system would not accomplish this because the escaping gases are drawn directly into the SBHE ducts under the pool cover and, instead of mixing in the building, are conveyed directly to the exhaust system. The controlling factor is not, therefore, the total air flow rate, but the rate at which the noble gases escape from the primary containment.

It appears that the only way to reduce the rate of noble gas emission from the stack is to provide some mechanism for thoroughly mixing the gases with the building air as they escape from the primary containment and concurrently to reduce the air flow from the building to some lower rate which is still sufficient to guarantee inleakage. In this way a reduction of perhaps a factor of 2 to 4 might be attained. This scheme has two distinct disadvantages. In the first place, it will magnify the effect of a minor accident by distributing the escaped fission products into the reactor building. The poolside SBHE ducts and the pool cover were conceived and designed specifically to prevent such an occurrence and to protect the operating personnel from radiation exposure due to such mishaps. Secondly, in the event of an Al-H_2O reaction it would permit hydrogen, which would otherwise be quickly disposed of to the atmosphere, to collect in the building.

One possible method of overcoming the first disadvantage would be to provide a second mode of exhaust which would divert the escaping gas into the reactor bay and simultaneously reduce the rate of exhaust to the stack. This mode would be attained through the use of high-level radiation instruments

which would actuate the appropriate equipment only when radiation levels approaching those to be expected following the MCA are present. Whether such a system could be designed and built to operate with the required degree of reliability would have to be determined. This approach would represent a major change in philosophy, as pointed out earlier, and would require a complete reexamination of the entire containment system to determine whether or not such a change would seriously compromise the overall safety of the system in order to gain a small factor in one particular area. In any case, it would not overcome the second disadvantage and would certainly serve to lower the level of operating safety presently incorporated in the design.

With respect to the CHOG system, the presence of the block valves on the pressure letdown lines already serves to contain the activity in the primary system. These valves close automatically on receiving a signal indicating a high level of radiation in the primary coolant system, and this isolates the activity within that system.

46. With reference to response 30, it appears that the discussion is in conflict with the evidence given in the referenced document, ORNL-TM-1291. We have been advised that ORNL-TM-1291 did not contain the latest information available on the subject it covered. Provide the additional information necessary to support the discussion in question.

It is our understanding that the conflict mentioned is in regard to the statement in response 30 that 2 in. of MSA 85851 charcoal will retain about 99.5% of the methyl iodide for as long as five days, during which the air flow is maintained at normal SBHE rate. ORNL-TM-1291,[5] Table 4, shows a much lower retention; however, Table 4 refers to charcoal of the type originally purchased for the HFIR. As set forth in ORNL-TM-1291 and in response 30, the charcoal is being changed from the original design to 2 in. of MSA 85851, and therefore Table 4 does not apply. Figure 2 of ORNL-TM-1291 shows the efficiency for 2-in. bed depth of MSA 85851 charcoal under HFIR accident conditions, and it was from this figure that the statement regarding 99.5% efficiency for five days was taken.

In addition to the above, several questions were asked regarding the statement on page 3 of ORNL-TM-1291 regarding the solubility of iodine in water, the effect of relative humidity on methyl iodide removal, and availability of information in addition to that contained in ORNL-TM-1291. The following information was prepared by G. W. Parker in response to these questions.

1. Solubility of Iodine in Water at 25°C

In order to reemphasize the very low order of expected release of radioiodine from the HFIR pool water, it is of most interest to refer to a paper by Diffey *et al.*[6] These authors report in summary that "when the total volume of air is the same as the volume of water through which it has passed, decontamination factors are about 100 for elemental iodine at concentrations greater than 10^{-5} g-mole/liter;

---

[5]R. E. Adams *et al.*, *The Release and Adsorption of Methyl Iodide in the HFIR Maximum Credible Accident*, ORNL-TM-1291 (Oct. 1, 1965).

[6]H. R. Diffey *et al.*, *Iodine Clean-Up in a Steam Suppression System*, CONF-650407, vol. 2, p. 776, Oak Ridge (April 1965).

1000 or more for elemental iodine at low concentrations and when sodium thiosulfate has been added to the water; 2 for methyl iodide; 100 for hydrogen iodide; and 50 for 0.06 micron diameter particles." A large increase in the partition coefficient is noted for iodine concentrations below 10^{-6} g-mole/liter of water. The above values are determined at 25°C. Slightly reducing conditions in the water such as may be contributed by a metal-water reaction or foreign impurities serve to enhance the retention in water to an extent approaching that for sodium thiosulfate solution. The data are shown in Fig. II.46.1.

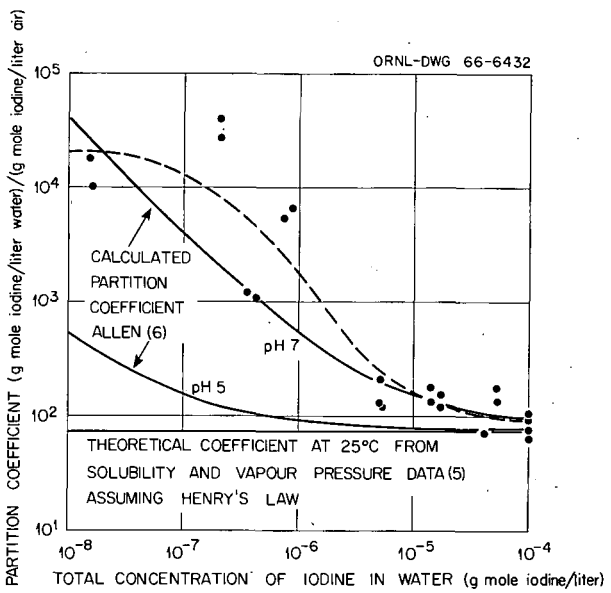

Fig. II.46.1. Effect of Iodine Concentration on the Equilibrium Partition Coefficient for Iodine at 25°C.

2. Solubility of Iodine at 100°C

At elevated temperatures, according to Griffiths,[7] two effects are noted. The first, at high iodine concentrations, is a significant reduction in the retention of iodine such that at 100°C the partition is only 10 to 1 in favor of the water when an equal volume of air is passed through. At lower iodine concentrations or in the presence of reducing impurities, the reduction of iodine and hence the decontamination coefficient will increase to values higher than those at room temperature corresponding to the increase in reduction rate.

3. Experience in Reactor Accidents Illustrating Iodine Retention in the Coolant Water

Some actual experience with this water-retention process is reported by Edwards[8] in a review of the 1952 NRX accident, in which no ^{131}I release was observed. In this case it was postulated that absorp-

[7] V. Griffiths, *The Removal of Iodine from the Atmosphere by Sprays*, British Report AHSB(S) R45 (Jan. 9, 1963).

[8] W. J. Edwards, *Fission Product Release from the NRX 1952 Accident*, Canadian Report CRDC 1177 (December 1963).

tion by the aqueous coolant appeared to have been a major factor in limiting the seriousness of fission product dispersal.

The meltdown of an ORR fuel plate in July 1963 resulted in a significant release to the water but no apparent release to the atmosphere. WTR in April 1960 also experienced a meltdown of aluminum alloy fuel under limited water flow with no reported iodine in the vapor form.

4. Retention of Methyl Iodide by Impregnated Carbons Under HFIR Conditions

Since the development of the highly efficient impregnated carbons, the removal of methyl iodide from off-gas streams by adsorption in relatively shallow beds has become routine. In Fig. II.46.2, most of the pertinent data are reflected for conditions especially pertinent to HFIR. These are an air flow of 40 fpm and 70% relative humidity. In the graph a residence time of 0.25 sec would correspond to a depth of 2 in. The indicated penetration rate is about 0.1% for the test sample of MSA carbon 85851. Other carbons and other impregnants give lower values to less than 0.0001%.

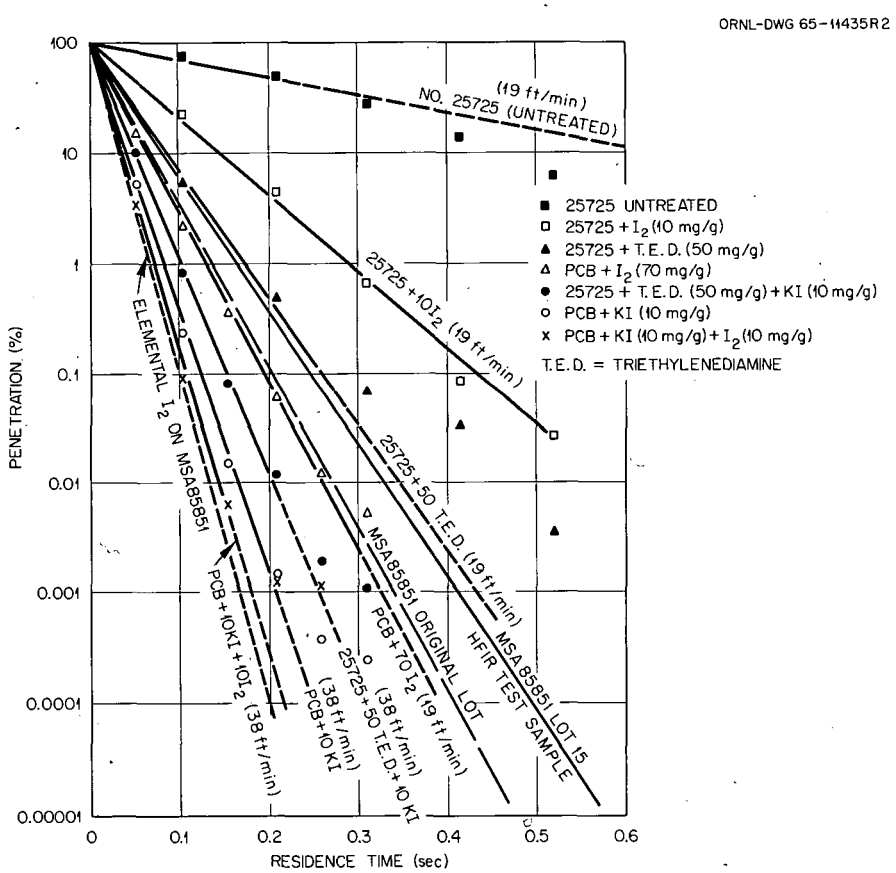

Fig. II.46.2. Effect of Residence Time on Methyl Iodide Penetration of Treated and Untreated Coconut Charcoal at 40 fpm, 25°C, and 70% Relative Humidity.

5. Effect of 100% Relative Humidity

Reference to difficulty of removal of methyl iodide at very high humidity approaching 100% is presently regarded as meaning that only a slightly longer residence time is required. In TRG 2986, Taylor and Taylor,[9] it is reported that only a 25% increase in residence time will accommodate the maximum increase in humidity and afford the same decontamination factor.

Applying this information to the MSA 85851 impregnated carbon filters, it can be seen from Fig. II.46.2 that an increase in the relative humidity from 70% to 100% would only increase the percent penetration from 0.09 to 0.31.

47. With reference to response 31B, provide an estimate of the error associated with the assumed neutron flux. With reference to response 31C, provide a discussion of the consequences of failure of the structural members mentioned in the response.

In order to obtain reasonably good estimates of the neutron fluxes for the purpose of calculating neutron damage to the reactor vessel, an experiment was conducted with a simulated HFIR core and beam tube arrangement in the ORNL Bulk Shielding Facility (Swimming Pool Reactor). Of particular interest was an investigation to determine the fast neutron fluxes at the location of the beam tube nozzles. This information was used to help determine the size of the nozzles and the material to be used.

Various detectors were used to measure the fast neutron spectrum. The accuracy associated with the measurement of the fluxes was estimated to be ±25%. However, in order to compensate for possible future contingencies, the nominal experimental fluxes were multiplied by a factor of 2 for design purposes, and as yet no further contingencies have developed.

The other structural components referred to in the answer to question 31C are far enough from the core that there is no concern about radiation damage. Furthermore, the materials are quite ductile, have been thoroughly inspected for manufacturing defects, and are subjected to very low stress levels, most of which are compressive. For these reasons the probability of failure is nil. Thus it is essentially impossible to sensibly predict a mode of failure and subsequent consequences. Perhaps it is sufficient to say that in the case of the three support assemblies mentioned, breakage and/or warpage of these components could lead to dimensional changes in the control region and thus would be a threat to satisfactory operation of the control rods, although it is very unlikely that all rods could be immobilized. If the relative radial movement took place slowly with respect to fuel cycle time, it is possible that significant dimensional changes would be detected during routine in situ inspection of core dimensions and/or during rod movement checks following each refueling.

In the case of the shim-regulating rod drive bracket (attachment between control rod and drive rod) a mode of failure and consequences are somewhat more definitive, although the probability of failure is not significantly different than that for the other cases. If the web joining the hub and the ring were to break

---

[9] R. Taylor and L. Taylor, *Progress Report on the Trapping of Methyl Iodide at High Relative Humidity*, TRG Memorandum 2986(W), not for publication.

on each side of the hub, it is possible, depending on the nature of the break, that the shim-regulating rod would fall out of the core with an acceleration of about 2 *g*. During normal operation, the most severe transient would occur with a clean core, since the differential rod worth would be large. This case has been analyzed and was found to be less severe than the flux trap void accident.

48. With reference to response 33, provide a discussion of the shutdown and evacuation potential at MSRE, including a summary of results of evacuation tests that may have been conducted.

The following information was supplied by the MSRE staff:

In the event of an emergency at a neighboring facility, such as the HFIR, requiring shutdown and evacuation of the MSRE area, and assuming the MSRE to be operating at power, normal action would be:

1. HFIR alerts Laboratory Emergency Director (LED) of emergency condition.
2. LED notifies MSRE to evacuate.
3. The MSRE local emergency director initiates evacuation plan for nonoperating personnel.[10]
4. The control room supervisor makes operating changes necessary to effectuate shutdown of the reactor. The amount of time devoted to this phase will depend on the time available. The minimum steps would be operation of the "rod scram" and "load scram" switches on the main console (about 3 sec operating time).
5. All remaining personnel evacuate from the area.

Evacuation drills have been made to check the emergency procedures. The results indicate that personnel may be evacuated from the MSRE buildings to Melton Valley Drive in about 2 min. It is estimated that evacuation of personnel from the valley to a more distant site could be effected in about 10 min by use of private vehicles.

49. With reference to response 34A, what is the maximum increase in core fission product inventory associated with the increase in fuel cycle time that could result from use of different fuels or increased loadings?

The inventory of long-lived fission products would, of course, increase with increased fuel lifetime. However, the fission products of interest, namely the noble gases and iodines, are, with the exception of ^{131}I, essentially at their saturation value after 15 days' operation. Accordingly, the saturation values for these isotopes were in the dose calculations presented in Part I.

An increase in the fuel lifetime could, at most, increase the ^{131}I inventory from 16.2 curies/kw to its saturation value of 22.3 curies/kw. This would increase the estimated internal doses due to iodine by a factor of 1.16.

The increase in heat generation due to fission product decay immediately after shutdown would, regardless of the fuel lifetime, exceed that to be expected following a 15-day lifetime by less than 5%.

---

[10] A. N. Smith, *MSRE Design and Operations Report, Part IX, Safety Procedures and Emergency Plans*, ORNL-TM-909 (June 1965).

50. With reference to responses 34B and 34C, we have been advised by ORNL that there are many other criteria than the two mentioned which would be used to measure the safety involved in core changes and the appropriateness of regulatory review. Provide an expanded discussion of these other criteria.

The criteria by which any new fuel element design will be judged safe will be essentially the same as has been used for the present fuel element design. Of course it is quite possible that some details of the criteria may change as operating experience is obtained. As pointed out in response 34, only minor changes in design are postulated for the foreseeable future. These changes will be for the purpose of extending the average life of the fuel elements to about 15 days, which was the original goal and the design basis for the HFIR. The above memo also stated that from a safety point of view the general criteria that had to be satisfied were associated with demonstrating adequate shutdown margin, and concluding on the basis of a thorough heat-transfer analysis that the incipient-boiling power level during steady-state operating conditions was equal to or greater than the scram set point. These basic general criteria can of course be broken down into numerous and perhaps more fundamental criteria such as concern: radiation damage to the fuel plates; segregation, distribution, and loading of the fuel and burnable poison; fuel plate and coolant channel dimensional tolerances; fuel plate cladding integrity (nonbonds) and surface condition (roughness, scratches, cleanliness); quality control of material; quality of assembly welds; and side plate dimensional tolerances. All of these criteria are a part of the HFIR fuel element specifications, which in principle will cover all fuel elements used in the HFIR. Wherever appropriate, the above detailed "criteria" have been included in the heat-transfer analysis and thus are considered, as indicated above, when calculating the steady-state incipient-boiling power level. Since it is the combination of these criteria rather than each one separately that determines the incipient-boiling power level, the individual criterion can be somewhat flexible.

In the event that a new form of the fuel is used, or if the fuel and burnable poison surface densities are increased significantly, or if a different type of cladding is proposed (nickel plating on aluminum cladding), suitable proof testing will have to be performed to obtain the necessary design data. This is no different than what has been done for the present core design.

Whenever significant changes are proposed in reactor core designs at ORNL, the Reactor Operations Review Committee reviews the proposed changes. In addition, the Operations Division is obligated to inform the AEC Oak Ridge Operations Office in order that the proposed change can be reviewed by the USAEC.

51. Response 38A does not provide the results requested for reactivity transients considerably more severe than those previously treated. Provide the results of the analyses previously requested.*

Following telephone discussions with Mr. Saul Levine and Mr. R. C. DeYoung of the USAEC Division of Reactor Licensing regarding this question, a telephone conversation was held with Dr. David Okrent

*Further discussed in detail, answer 55 and Appendix L.

of the Advisory Committee on Reactor Safeguards in an attempt to better define the scope and objectives of the question. Dr. Okrent stated his interpretation of the underlying philosphy as a concern as to whether or not there were possible mechanisms for introducing k which might aggravate the accidents considered. Consideration of this possibility in regard to the accidents studied and/or even somewhat larger accidents might indicate whether or not some breakpoint in accident severity might lie just above the maximum accidents previously considered. The following presents such information as we have on this subject.

If a reactivity accident were severe enough, it is possible that additional reactivity could be added as a result of fuel displacement and radial movement of the control rods. Uniform removal of fuel plate from the core increases reactivity up to the point where about 30% of the fuel plate has been removed. The maximum reactivity addition is about 2.4% $\Delta k/k$, and for relatively smaller amounts the coefficient is about $-0.113\ \Delta k/k / \Delta v/v$. Radial movement of the control rods away from the fuel region decreases the worth of the rods slightly, because reflection from the water gap between the fuel and the rods would be increased and moderation between the rods and the beryllium reflector would be decreased. Based on results obtained from critical experiments, it is estimated that the maximum decrease in rod worth would be less than 1% $\Delta k/k$.

Suppose the fuel plate begins to melt and drop out of the core at about the time the peak in power is achieved during a fast transient. At this time the safety rods are inserting negative reactivity, assuming that they started from nearly the fully withdrawn position, at a rate of about 0.25 $\Delta k/k$ per second. If it is assumed that the molten material leaves the core with the coolant velocity and that on the average it must travel one half the core length, then reactivity would be added at the rate of

$$\frac{0.113\ \Delta k/k / \Delta v/v}{0.015\ \text{sec}} \cong \frac{7.5\ \Delta k/k / \Delta v/v}{\text{sec}}.$$

Thus, the maximum fraction of the fuel plates that could melt out without causing a net increase in reactivity would be $0.25/7.5 = 0.033$. Earlier in the fuel cycle the differential rod worth is considerably greater, and thus melting of a larger fraction of the core could be tolerated without a net increase in reactivity. The maximum fuel plate fraction for this case would be about 0.20.

The rate at which reactivity might be added by radial movement of the control rods is somewhat more difficult to estimate. Radial movement of the rods could result from a pressure surge in the fuel element, in which case the pressure wave would have to travel out the bottom of the element (assuming that the outer side plate of the outer element did not rupture) to the inner surface of the inner rod, which is a complete cylinder, and through the hydraulic relief holes in this rod to reach the safety rods. In the event of such an accident, it is quite probable that the rods would be immobilized. Thus shutdown would take place as a result of core disassembly. However, the extent of the accident required to cause such a pressure surge would probably cause disassembly of the core prior to the time the rods were affected. According to SPERT test results (IDO-16806, IDO-16893),[11,12] pressures no greater than 20 psi were

[11] F. Schroeder (ed.), *SPERT Project Quarterly Technical Report, April–June 1962*, IDO-16806 (Sept. 21, 1962).

[12] F. Schroeder (ed.), *SPERT Project Quarterly Technical Report, January–March 1963*, IDO-16893 (May 20, 1963).

generated even for tests in which considerable melting took place. These pressures were measured at the ends of the element, indicating the pressure generated by moderator expansion. At the side of the core, where mass movement of the water was restricted by the fuel assembly cans, the corresponding pressures were limited to about 2 psi. Even in the case of the SPERT I 3.2-msec-period destructive test, the pressure associated with water expulsion from the core (prior to the steam explosion) was only 35 psi. For pressures of this magnitude the side plates of the HFIR fuel elements would not be stressed a significant amount in terms of radial displacement. The same is true for the inner control cylinder, which would see an order-of-magnitude lower pressure, yet has about the same wall thickness as the side plates. Since the side plates and the inner control cylinder act as buffers between the pressure generation point and the safety rods, it appears highly unlikely, even for a case in which significant fuel element damage takes place, that the safety rods would become immobile. Higher pressures can of course be developed such as the several thousand pound pressure generated by the steam explosion in the SPERT I 3.2-msec-period test. This pressure surge came after the peak in power and disassembled the core. It would appear that immobilization of the safety rods at this point would be of little consequence.

The need for considering the above secondary reactivity additions is perhaps only academic, since, as stated previously it is concluded that none of the postulated primary reactivity accidents would result in melting or significant pressure surges. This conclusion was based on an analysis of SPERT test results and a comparison between SPERT and HFIR, in which case it was found that the HFIR should experience a less severe transient for the same reactivity addition, and the particular SPERT core suffered no damage as a result of a 1.3% $\Delta k/k$ step addition. The worst reactivity addition postulated for the HFIR is 1.3% $\Delta k/k$ in 30 msec.

Another way in which a transient could be aggravated by a secondary reactivity addition would be by the formation of voids in regions having positive void coefficients. Both the flux trap and the control region have positive void coefficients. However, their heat generation rates and heat transfer characteristics, relative to those in the fuel elements, are such that boiling will occur so much sooner in the fuel element that during the postulated transients no voids would be formed in these other regions.

Although the overall void coefficient in the fuel region is strongly negative, there is a narrow region adjacent to the flux trap that has a small positive coefficient. At the beginning of a fuel cycle the power density in this region is about the same as elsewhere in the inner element and a portion of the outer element. However, as the fuel cycle proceeds, nonuniform burnup of the fuel reduces the relative power density adjacent to the flux trap, making the positive void effect less important. But even for the clean core condition the positive void effect is so small as to be negligible. If the entire positive void region were voided, the additional reactivity would be only 0.0002 $\Delta k/k$. Nevertheless, it is of interest to know how sensitive core damage is to reactivity addition. In the SPERT I (DU-12/25) tests the first signs of fuel plate damage (minor deformation) occurred with a 7-msec period, which corresponds to a step change in reactivity of about 1.5% $\Delta k/k$. In subsequent tests the period was reduced in steps to about 5 msec ($\sim$1.9% $\Delta k/k$), at which point some melting and widespread deformation of the fuel plates were observed. Thus it appears that the HFIR could survive a reactivity addition considerably in excess of the 1.3% $\Delta k/k$ on a 30-msec ramp that has been postulated.

52. Provide a discussion of the results of operation of HFIR at power levels up to 20 Mw (thermal).

On August 25, 1965, the HFIR achieved criticality for the first time, and on January 29, 1966, the power level was increased to 20 Mw. At the time of this writing (February 1, 1966), the accumulated megawatt-days at about 20 Mw are approximately 65. Operation thus far has been quite satisfactory, with no major difficulties encountered. There is no reason to believe, based on this information, that the power level should not be increased to 100 Mw.

During the period from August 25, 1965, to January 29, 1966, an extensive nuclear "zero power" experimental program was conducted for the purpose of investigating the nuclear characteristics of the actual HFIR facility,[13] for compiling generally useful data associated with the routine operation of the reactor, and for operator training. Analysis of much of the data that is pertinent to the evaluation of the nuclear characteristics is included in ORNL-CF-65-12-2.[14]

The types of experiments conducted for the purpose of investigating the nuclear characteristics are as follows (a more detailed outline is given in Table II.52.1):

1. Reactivity shutdown margins
2. Control rod reactivity differential worth
3. Fuel, fuel plate, and void reactivity coefficients for the fuel regions
4. Isothermal temperature reactivity coefficients
5. Reactivity worths of various targets and voids in the flux trap
6. Reactivity worth of water in the beam tubes
7. Reactivities associated with replacement of beryllium reflector vertical experimental facility beryllium plugs with water and with voids
8. Effect of flow and pressure on reactivity and reactivity stability
9. Reactivity worth of ^{10}B stainless steel strips in the fuel elements (secondary shutdown)
10. Power distributions
11. Response of safety system to neutron-generated signal

On January 26, 1966, the reactor was prepared for mode 2 operation (unpressurized, ~10% full flow). The system was first pressurized to 600 psi, and three-pony-motor flow (~2200 gpm) was provided. Under these conditions the power level was increased to about 2.5 Mw, with heat power calibrations being made at intermediate levels. While at 2.5 Mw the flow rate was reduced to 1850 gpm (two-pony-motor flow) and the inlet temperature was raised to 120°F (normal inlet temperature). Operation was satisfactory. Following this, the mode 2 safety set points were checked and adjusted, and effects of system pressure were investigated. No abnormalities were observed.

---

[13]Many of the nuclear characteristics had previously been investigated in HFIR critical experiments conducted at the ORNL Critical Facility (Building 9213).

[14]R. D. Cheverton and T. M. Sims, *Analysis of Selected HFIR Critical Experiment Data for Period August 25 through October 22, 1965*, ORNL-CF-65-12-2 (Dec. 1, 1965).

Table II.52.1. Chronological Outline

Date	Post Neutron Startup Procedure	Description
8/25/65	I.A	First approach to criticality
8/30/65	I.A	Measurement of the differential worth of the standard control plates
9/2/65	I.B	Confirmation of the response of the safety system to a neutron-generated signal
9/8/65	II.A and II.E	Preliminary power distribution measurement with PI+W
9/13/65	II.B	Check of shutdown margin for case IV
9/14/65	II.C	Check of shutdown margins for cases II and III
9/15/65	II.D	Check of shutdown margin for case I
9/16/65	II.F	Measurement of the differential worth of the control plates with various clean and poisoned core conditions
9/29/65	II.G and II.J	Measurement of the power distribution at various symmetrical critical plate positions
10/15/65	II.K	Poisoning of the core with ^{10}B stainless steel strips
10/20/65	II.L	Measurement of the fuel coefficient in the core
10/21/65	II.L	Measurement of the water-void coefficient in the core
12/6/65	III.A	Post shutdown noise measurements
12/7/65	III.A	Measurement of reactivity effects and shutdown margins for the production core, standard plates, and various island inserts
12/9/65	V.A	Measurement of reactivity effects and shutdown margins for the standard core, standard plates, and various island inserts
12/13/65	V.B	Measurement of reactivity effects due to changes in beryllium inserts in the reflector
12/13/65	V.B	Measurement of reactivity effects due to filling and draining the beam holes
12/16/65	IV.A	Measurement of reactivity effects and shutdown margins for the production core, production plates, and various island inserts
12/20/65	VI.A	Measurement of reactivity effects and shutdown margins for the standard core, production plates, and various island inserts
12/22/65	V.C	Check for reactivity differences between the Phase I and Phase II removable reflectors
1/11/66	VII.A	Check for any effects of water flow and pressure on reactivity
1/15/66	VII.B	Measurement of the overall isothermal temperature coefficient with the dummy flow test target
1/17/66		Special reactivity tests using the M and C first production core
1/18/66		Measurement of the overall isothermal temperature coefficient with the ^{242}Pu target
1/26/66	VII.D	Mode 2 operation (2.5 Mw)
1/28/66	VII.E	Mode 3 convective cooling test (100 kw)
1/28/66 to date	VII.F	Mode 1 operation (20 Mw)

After completing the mode 2 checks and calibrations, operation of the reactor was checked out in mode 3 (unpressurized, no forced flow). With the system depressurized (quick-opening hatch open) but with three-pony-motor flow, the reverse and level scram set points were checked and adjusted. The trip settings were then adjusted so that the reverse trip was at 135 kw (normally at 120 kw), the level trip was at 130 kw (normal), and thermocouples were provided at the ends of the fuel elements. With the coolant flow turned off the power level was slowly increased to ~130 kw. No boiling or other possibly detrimental conditions developed, and thus operation in mode 3 was considered satisfactory.

The final mode of operation investigated was mode 1 (pressurized, flux-to-flow ratio appropriate). With the system pressurized to 600 psi and with full flow (~16,000 gpm) the power level was gradually increased to 20 Mw. At intermediate steps heat power calibrations were made, and the servo performance was checked by raising and lowering the power level a few megawatts and by observing the response to xenon changes. Performance was quite satisfactory. Following these checks, two of the three operating primary pumps were shut down, reducing the flow rate to about 9500 gpm. No difficulties were encountered.

Mode 1 operation is continuing while more precise calibrations and instrument checks are being made, and while data pertaining to the transient behavior of the fission products are being obtained.

The only result from all these experiments that deviates from what was expected is that associated with the isothermal temperature coefficient. In the HFIR critical experiments the isothermal temperature coefficient was found to be slightly negative over the expected temperature range (68 to 160°F), whereas that measured in the HFIR facility was slightly positive up to about 120°F, with a maximum increase in reactivity from room temperature of 0.07% $\Delta k/k$. This constitutes no particular operating problem since the fuel region temperature coefficient is strongly negative. The difference in the two measured isothermal coefficients is attributed to a difference in the control rod drive mechanisms, a difference in the water content of the control regions, which have slightly positive coefficients, and a difference in the fuel elements (an 8-kg core with uniform burnable poison distribution was used in the original measurement).

In the zero power experiments several combinations of fuel elements, control rods, and targets were used. The fuel elements included the critical experiment element (9.4 kg of ^{235}U, 2.12 g of ^{10}B), which is referred to as the HFIRCE-3 element, the ORNL production element (9.4 kg of ^{235}U, 3.60 g of ^{10}B), and the first Metals and Controls element (9.4 kg of ^{235}U, 2.80 g of ^{10}B). The only significant difference between these elements is the loading of the ^{10}B burnable poison. Subsequent elements are presently specified to contain 2.80 g of ^{10}B.

Two sets of control rods were used: the HFIRCE-3 rods and the first production rods. With the exception of a few hydraulic relief holes these two sets of rods are identical.

The different targets used in the flux trap are listed in Table II.52.2. To avoid the possibility of voids entering the flux trap during the early experiments, two different plastic containers were used to displace the water in the flux trap. One contained the HFIRCE-3 simulated 300-g ^{242}Pu target[15] plus

[15]The HFIRCE-3 target contained ^{235}U, ^{238}U, and silver to simulate a maximum reactivity 300-g ^{242}Pu target.

Table II.52.2. Targets Used in Flux Trap

Nomenclature	Description
PI + W	Plastic container filled with water
PI + V	Plastic container with optimum void
PT + W	Plastic container with HFIRCE-3 target and filled with water
PT + V	Plastic container with HFIRCE-3 target and optimum void
DFTT	Dummy flow test target (all aluminum)
^{235}U rods	Standard target using ^{235}U, ^{238}U, and tantalum to simulate maximum heat generation rate
^{242}Pu rods	Standard target containing 248 g of ^{242}Pu, 2.5 g of ^{239}Pu, and 2.5 g of ^{241}Pu

the corresponding optimum void space; the other was provided with the optimum void space that corresponds to no target in the flux trap. Both of these plastic containers could be voided or filled with water.

Some of the more interesting results obtained during the zero power experiment, and which are not included in ORNL-CF-65-12-2, are those associated with reactivity changes resulting from flooding of the beam tubes and replacement of reflector beryllium plugs with water and voids. As shown in Table II.52.3, the reactivity changes resulting from these variations are negligible.

53. Provide a summary of significant changes made to the facility since commencement of operation.

From the standpoint of safety, the significant changes which have been made or are being planned have been discussed in the answers to previous questions. Some of the changes were started prior to the start of operation; however, they are listed below as they are considered significant:

1. replacement of the HFIR SBHE charcoal filters with MSA85851 charcoal filters having a bed depth of 2 in.,
2. replacement of the beam tube end cap bolts with bolts of high strength material,
3. addition of a wide-range radiation monitor for the reactor bay area,
4. addition of a wide-range, high-level stack monitor to provide additional information should a severe accident occur,
5. addition of an extension to the beam tube shutter access plugs for the purpose of ensuring that the shutter would restrain the beam tube plug in the event of a postulated dual accident in which the inner end of the beam tube ruptures and the outer end cap fails,
6. addition of a liquid poison injection system.

Table II.52.3. Reactivity Effects Due to Changing Experimental Facilities

Core Condition	Symmetrical Critical Position	Reactivity Change[a] (cents)
Standard core – all beryllium plugs in	16.311	
Standard core – all beryllium plugs out	16.332	−4.5
Standard core – six air-filled plugs	16.328	−4.0
Standard core – all beam holes empty	16.310	
Standard core – HB-1 filled	16.306	+1.05
Standard core – HB-1, 2 filled	16.305	+1.68
Standard core – HB-1, 2, 3 filled	16.302	+2.40
Standard core – HB-1, 2, 3, 4 filled	16.302	+2.10

[a]Rhoette reading.

In addition to the above, there have been several other changes which were made to help ensure continuous operation of the reactor or to improve the ease of operation:

7. A third fan for the SBHE system is presently being installed. This fan will operate from the normal ac power and can be considered as an installed spare to minimize the probability of having to shut down the reactor should the operating fan fail. Our criteria require that one fan be operating at all times with an operable and tested fan in standby.
8. A fourth air compressor is being added to the instrument air system to complement the two existing normal air compressors and the emergency compressor. This change is being made to reduce the maintenance requirements on the existing system and to provide greater assurance against loss of air pressure during normal operation.
9. Modifications have been made to the primary pressurizer pumps head tank and the head tank level sensor system in order to reduce the probability of air entrainment during operation and to prevent damage to the pumps should the head tank water level drop below a safe level.
10. A 10-in. bypass control valve has been added in parallel with the existing main control valve in the secondary coolant system. This valve will provide a finer degree of control than the large valve and will reduce maintenance requirements for the large valve and its operator.
11. Several minor changes have been made to the control rod actuating and selector switch systems to improve the ease in making adjustments to rod position.
    a) An additional position has been added to the rod selector switch to permit movement of control rods Nos. 1–4 without movement of No. 5 at the same time. This provision makes it easier to keep the rods balanced, that is, symmetric.
    b) The rod actuator switch has a position which allowed any selected rod to be inserted through action of the intermittent rod motion timer. This position has been changed so that continuous insertion of any rod is achieved. This change was made to provide for greater ease in making small insertions (jogs) of the control element.
    c) The intermittent timer circuit has been changed so that the timer resets itself after each intermittent action. This provision makes it easier for the operator to "jog" the rods out a very small amount, as the timer does not stop in an "off" position.

12. Although not a recent addition, no description is presented of the display instrumentation which is presently being built for the HFIR. Three sets of instruments are being provided to display the information from the three wide-range fission-chamber channels so that it will be easy for the operator to tell at a glance the approximate power level. In addition, continuous digital readout instruments are to be provided for accurately reading out the heat power level from any three of the six heat-power computers. Again, this display is being provided so that the operator can more easily verify the status of the reactor from the control console.

Part IIc. Safety Review Questions and Answers 54—60

ABSTRACT

Following the review of the preceding analyses, the Advisory Committee on Reactor Safeguards (ACRS) requested an analysis of a more severe reactivity accident than that established as credible, and without control rod action to help terminate the accident. The information in this set of questions and answers provides this analysis, considering the effect on the primary coolant system and containment building, including metal-water reactions.

Originally published as ORNL-CF-65-11-29, suppl. 2 (Aug. 15, 1966).

CONTENTS

INTRODUCTION AND SUMMARY 199

QUESTIONS AND ANSWERS 201

54. Reanalyze transient previously discussed (1.3% Δk) without control rod action. What is the extent of the metal-water reaction? Could boiling lead to a more rapid rate of increase of the reactivity? 201

55. Propose and examine mechanisms and accident conditions which might lead to the insertion of greater amounts of reactivity than 1.3% Δk. If reactivity insertions worse than that of Question 54 are found to be possible, what are the consequences to the reactor facility for the limiting insertion? Some possible examples of sources of reactivity insertion might be as follows:

A. If target overheats due to error or malfunction, could target failure of any kind, coupled with voiding (partial or complete), lead to larger reactivity insertion? 203

B. Could target become waterlogged, then fail under steam pressure during a transient induced by other causes? If so, what might the reactivity transient be? 204

C. If target coolant is closer to boiling than anticipated, could transient originating from another source lead to significantly greater energy release than that of Part I? 204

D. If flux trap is devoid of target, and flow is sharply reduced in that area, could sudden incidents of boiling or voiding lead to large reactivity insertion? 204

E. If a local meltdown in a section of the core occurs, how large must the hole get before one stops gaining reactivity? How much reactivity is involved? What is the increase in power level at the edge of the region devoid of fuel, as a function of hole size? How great is the tendency to spread as a consequence? To what extent may such a mechanism lead to autocatalytic effects and transients starting in this manner or from other sources? Are there other autocatalytic effects from fuel movement? 204

F. What pressures might be generated from local fuel melting? How much fuel failure is required to generate pressures which could move significant amounts of fuel inward (and thus gain reactivity), or which could interfere with control rod action? Does this allow for pressures from a "steam explosion" or a "water hammer"? How much reactivity could be gained by inward motion of the fuel into the flux trap? How much pressure would it take to produce such motion? Could flow blockage lead to such effects? 205

G. Are there any conditions in which water returning to a region after an explosion could lead to large reactivity insertions? For example, if fuel and water were expelled from a region due to melting, could water which rushed in thereafter cause a reactivity excursion? 205

56. What transient energy release, allowing for both total and rate of energy release, does it take to rupture the primary system (including the reactor pressure vessel) and expel significant amounts of water from the pool? What rapid reactivity insertion could lead to this energy release? On what basis is the estimate for these values made? What is the degree of uncertainty in the numbers? 205

57. What phenomena considered under Question 55 can possibly lead to transients, which when coupled with the associated chemical reaction and loss of metal during such reaction, lead to energies large enough to rupture the primary system and expel enough water, vapor, and gas from the system to threaten the integrity of the building? 206

58. Are the answers to these questions changed if no control rod motion occurs? 206

59. What would be the consequences of a reactor vessel failure, particularly with regard to impairment of the containment and failure of the pool walls? 206

60. What steps will be taken, prior to installation of the backup shutdown system, to guard against the consequences of an accident resulting from the inability to move control rods into the core? 207

APPENDIX H. The "Ultimate" Shutdown Mechanism of the HFIR 207

APPENDIX I. Energy Releases from Al-H_2O Reactions in the HFIR 210

APPENDIX J. Containment Potential of the HFIR Pressure Vessel and Primary Coolant System 227

APPENDIX K. Containment Potential of the HFIR Building 245

APPENDIX L. Detailed Discussions of Questions 54, 55, and 58 252

INTRODUCTION AND SUMMARY

Previous analyses of power excursions in the HFIR were based on a postulated maximum reactivity insertion of 1.3% $\Delta k/k$ in 0.03 sec. This accident could come about as a result of a void being swept into and remaining in the high-velocity region of the target. The power excursion resulting from this reactivity insertion would be terminated by the combined action of the negative temperature coefficients in the fuel region and the insertion of the safety plates. The kinetic studies of this accident showed that essentially no fuel melting would occur, and that no significant damage would result outside of the fuel element.

Information regarding more severe accidents is presented herein as requested by the Advisory Committee on Reactor Safeguards (ACRS). While we have evaluated many detailed aspects of reactivity behavior during the course of this investigation, the general problem is raised by question 54 in which the analysis of transients without control rod action is requested. With this restriction applied, termination of any significant reactivity insertion accident must necessarily result from core disassembly. As previously discussed it is conceivable that, as the molten fuel leaves the core region, reactivity might be increased if the appropriate geometrical conditions were achieved. Although this reactivity increase would most probably be compensated for by the generation of voids in the core region, the detailed behavior cannot be predicted with the accuracy required to show this to be the case during all stages of disassembly. For this reason, we have chosen to approach the problem in a much more general manner, in which it is shown that the energy release during a severe excursion is limited by core disassembly resulting from the energy pulse. This approach has the merit of being relatively independent of how the reactivity is introduced, that is, whether by an initiating reactivity insertion larger than our postulated maximum accident or by possible increases in reactivity resulting from core rearrangement during disassembly.

An analysis of this type of disassembly is presented in Appendix H, and the results indicate that an energy release from the nuclear excursion of 300 Mwsec represents an upper limit, if it is assumed that a flat power distribution exists. A somewhat more realistic limit of 200 Mwsec is arrived at by approximating the nonuniform power distribution of the HFIR core.

The consequence of possible energy releases from the aluminum-water reaction was discussed in the answers to previous questions. It was shown that the rate of energy release from a metal-water reaction initiated by loss-of-pressure or loss-of-coolant accidents was sufficiently low that no great concern regarding the containment was warranted. We did not previously consider the energy release from this source when the initiating accident was the postulated maximum reactivity insertion, inasmuch as the resulting excursion was not, in that case, sufficient to exceed the temperature threshold for the reaction. The present treatment includes an analysis of the quantity and rate of energy release under the assumption that it is initiated by a nuclear excursion.

Appendix I contains a discussion of the metal-water reaction mechanism. We have made the assumption that an immediate reaction and release of energy occurs for any part of the aluminum which is vaporized during the nuclear transient.

The ability of the primary containment system and in particular the ability of the reactor vessel to contain the energy release resulting from the limiting nuclear excursions and the corresponding aluminum metal–water reactions has been reevaluated. The general approach has been to consider the equation of state of the vessel and to apply physical laws and data to the distribution of energy released in excursions of various magnitudes. This analysis is presented in Appendix J. For a nuclear excursion in which it is assumed that no metal-water reaction takes place, the vessel will not rupture unless the excursion releases more than 1600 Mwsec of energy. If a prompt metal-water reaction takes place for all aluminum which is vaporized and a delayed reaction for the remaining aluminum, the vessel will not rupture unless the nuclear excursion is greater than 600 Mwsec.

Although we show that the system has adequate strength to contain the energy release estimated to be the upper limit, we have also investigated the consequences of a premature failure of the reactor vessel for the purpose of investigating the consequences of a release from the vessel into the reactor pool and from there into the reactor building – secondary containment. This analysis is contained in Appendix K.

The top of the reactor vessel is 17 ft below the surface of the water, and the center line of the reactor core is 27.5 ft below the water surface. Consequently, any escaping steam or gas will pass through at least 17 ft of water before reaching the atmosphere of the building. During this process, some of the energy contained in the hot gases will be lost to the pool water. The exact amount of energy which will be lost in this way depends upon the manner in which the gas is conveyed through the water. If the gas is broken up into many small bubbles, the heat transfer may be almost complete. On the other hand, if the gas emerges in the form of a few large bubbles, there will be considerably less heat loss to the pool. Because it is not possible to predict the exact course of the bubbles' emission, we have chosen to evaluate the consequences using the extremely conservative assumption that no heat is lost to the pool. For the limiting nuclear excursion, the pressure rise in the building is calculated to be less than 0.5 psi.

The containment features of the HFIR building were originally specified on the basis that there was no credible accident which would result in an increase in pressure in the building. This approach was consistent with the analysis of reactivity accidents, the low temperature of the primary coolant system, the absence of a pressurizer system which contained significant stored energy, etc. However, the reactor building is constructed of reinforced concrete and is designed to be a relatively low-leakage building when compared to conventional buildings. Review of the design shows that it is adequate to withstand an internal pressure of 0.8 psig without exceeding the yield stress of the reinforcing steel. The truck door on the air lock, however, would be loaded to the yield stress of the material at about 0.3 psi differential pressure.

In order to carry our investigation one step further, we have investigated the external gamma and the internal iodine doses at the downwind site boundary previously agreed to, that is, approximately 4 km from the HFIR building. Data on the consequence of a ground-level release were presented in Fig. II.29.2. These values apply to a relatively slow release, and therefore a correction was applied for decay. As before, 100% of the noble gases and 50% of the iodine were assumed to enter the building atmos-

phere; it is also assumed as before that $\frac{1}{3}$ of the iodine leaving the fuel escapes deposition and is available for leakage. If it is assumed that the limiting nuclear excursion occurs, that the reactor vessel fails prematurely, and that none of the energy is deposited in the pool, pressure will rise in the building until failure of the truck door relieves the overpressure. The location of the truck door and the geometry of the air lock are such that little if any radioactivity would escape; however, if it is assumed that a fraction escapes equal to the fraction of building air volume necessary to reduce the pressure to atmospheric (at which time the SBHE system will exhaust the rest of the activity through the filters to the stack), the calculated doses at the downwind site boundary, $\sim$4 km, are 13 rads external and 27 rems iodine for the most representative condition as previously defined.

The HFIR containment system filters are located below ground level in shielded concrete pits. The design of this system has been reviewed, and it has been determined that no damage to the filters would result from a building pressure in excess of that required to fail the building.

We believe the previously studied maximum reactivity insertion will not result in significant melting or damage by virtue of the fuel region temperature coefficient and safety rod action, and that substantially larger reactivity insertions and/or failure of the safety rods to act will not result in any significant change in the off-area consequences.

In the following section, we have prepared answers to the questions asked by the ACRS. Although we list the questions as specific questions, we have attempted to prepare answers which not only treat the specific points, but also discuss various ramifications which these points have brought to mind. Appendix L presents detailed discussions of Questions 54, 55, and 58.

QUESTIONS AND ANSWERS

54. Reanalyze transient previously discussed (1.3% Δk) without control rod action. What is the extent of the metal-water reaction? Could boiling lead to a more rapid rate of increase of the reactivity?

Several of the transients previously analyzed with the analog computer were reanalyzed with steam void reactivity feedback incorporated in the model. The correlation used for estimating steam void fraction was basically that proposed by Griffith, Clark, and Rohsenow.[1] To include proper space dependence, the core was divided into five longitudinal regions, each region having appropriate weighting factors. Typical results of these calculations are presented in Table II.L.1 of Appendix L.

In the above correlation the void fraction is approximately inversely proportional to the coolant velocity and the subcooling. Thus, for a highly subcooled, high-velocity coolant such as is the case for the HFIR, steam void reactivity feedback is not very effective in terminating power excursions. HFIR calculations made for 10% flow show that in this case steam formation is quite important.

For the 10% flow case the steam void reactivity feedback at the time of peak power is about 30% of the total negative feedback, whereas for the full flow case the corresponding steam void feedback is effectively zero. In the latter case the greatest negative feedback comes from fuel plate expansion.

---

[1] Griffith, Clark, and Rohsenow, *Void Volumes in Subcooled Boiling Systems*, Technical Report No. 12, M.I.T. (1958).

For the above calculations only the end-of-cycle cases were considered, which means that the initial differential safety rod worth was quite small. As a result the safety rods contributed very little to the termination of the excursion, their main function being to hold the reactor down after the self-shutdown mechanisms have functioned. A comparison of cases with and without control rod action shows that the difference in peak power and the plate temperatures shortly after the peak in power are quite small.

In the event that the safety rods do not scram, the power level will tend to level off at about 500 Mw, following the initial transient, in which case the plates would be film blanketed and would be increasing in temperature at the rate of about 15°F/msec. In approximately 30 msec, the pressure drop across the core would push the molten fuel plate material out the core region. The temperature increase of the aluminum, assuming it is still in contact with the fuel, would be about 450°F, which is not enough to initiate the metal-water reaction. If a steam explosion were to occur in the meantime, the ejection of material from the core would be even faster. Thus, it is not anticipated that failure of the safety rods to scram would result in a metal-water reaction from the postulated maximum reactivity insertion accident.

Several "boiling" conditions in regions having positive void coefficients have been considered as possible mechanisms for adding reactivity more rapidly than postulated for our maximum reactivity accident. The regions of interest are the flux trap, the control region, and perhaps a very narrow region in the inner fuel region adjacent to the flux trap. Positive reactivity associated with the latter is limited to about 0.02% $\Delta k/k$ and thus is negligible. Heat generation rates in the control region are relatively low, making the rate of steam formation under flow blockage conditions very low; and furthermore, the total positive reactivity associated with voids in the control region and reflector combined is only about 0.5%.

In the flux trap region, the possible reactivity addition due to boiling is quite large, but under normal conditions boiling in this region would lag far behind that in the fuel region. The abnormal conditions considered are as follows:

1. Partial flow blockage to the flux trap could cause the coolant to be on the verge of subcooled boiling, so that the initiating accident would immediately result in positive reactivity feedback.
2. Boiling within a waterlogged target rod could result in an almost instantaneous voiding of the target rod coolant.
3. Boiling and other type voiding of the target could result in target melting, which could change the metal-to-water ratio in the flux trap and thus change the size of the optimum void and associated reactivity.

In the first case, the rate of steam formation is so slow relative to the rate at which reactivity is being added by the initiating accident that the contribution to the rate is completely negligible. The total reactivity associated with the void insertion and boiling can be no greater than the 1.3% $\Delta k/k$ because of the space limitation.

The second case, target rod waterlogging, is a problem only if a rather large clearance, relative to that permitted by specifications, exists between the pellets and tube wall and/or between the ends of

adjacent pellets. The amount of energy required to burst a tube is large compared to that transferred to the water during the 30-msec ramp associated with the initiating accident. This means that the tube would not burst in time to add to the rate of reactivity insertion. After bursting, the expansion of the limited amount of high-pressure steam would not result in complete voiding of the coolant surrounding the rod, but would result in a reactivity addition of only 0.04% $\Delta k/k$ per rod, provided that there was any coolant left to displace. Thus, waterlogging of the target rods does not enhance the maximum reactivity accident.

A more likely waterlogging case is that in which an out-of-tolerance rod becomes waterlogged at low temperature. As the reactor is slowly taken to power, the trapped water will begin to boil without melting the pellet. Under some circumstances, the tube could burst and almost instantaneously add reactivity in the amount of 0.04% $\Delta k/k$ per rod and 1.1% for all 31 rods. As indicated in Table II.L.1 of Appendix L, all rods could rupture without causing melting of the fuel plates, provided that the safety rods function. If the safety rods fail to act, the results would be as previously discussed above. If this accident occurred simultaneously with the maximum reactivity accident, some localized melting might be expected with safety rod action. With no action the shutdown would proceed as previously discussed. Of course it is not very likely that very many target rods would be waterlogged and would rupture simultaneously.

For case 3, consideration was given to the situation regarding heat removal from a voided target. Since it has been assumed that the optimum void stays in place in the target during the maximum reactivity accident, it must be assumed that for some period of time there is essentially no heat transfer from the target. During the initiating 30-msec ramp, only 0.5 Mwsec of a needed 2.5 Mwsec to melt the pellets is generated, making it highly unlikely that the target rods would slump before water could return and cool them. Even if they did, there is enough target extension above the active rod that would move down with the slump and would maintain about the same metal-to-water ratio as before. Thus, no greater amount of reactivity associated with voids could be introduced.

55. Propose and examine mechanisms and accident conditions which might lead to the insertion of greater amounts of reactivity than 1.3% Δk. If reactivity insertions worse than that of Question 54 are found to be possible, what are the consequences to the reactor facility for the limiting insertion? Some possible examples of sources of reactivity insertion might be as follows:
    A. If target overheats due to error or malfunction, could target failure of any kind, coupled with voiding (partial or complete), lead to larger reactivity insertion?

This question was partially answered in the latter part of the first question. However, consider in addition the unlikely situation in which the tandem grids fail or the target melts to the extent that it flows through the grids, thus vacating the flux trap and making the trap vulnerable to the larger optimum void. The net change in reactivity from the voided maximum-fission target condition to the voided trap with no target is +1.0% $\Delta k/k$; and the corresponding reactivity change, starting with the minimum reactivity target, is 1.9% $\Delta k/k$. If the grids failed, allowing the target to be swept out with the coolant velocity while at the same time an optimum void entered, as much as 3.2% $\Delta k/k$ could be ramped in

in less than 30 msec. Such an occurrence is incredible, but even so, as explained in Appendix J, the reactor could withstand such an accident without rupture of the primary system.

B. Could target become waterlogged, then fail under steam pressure during a transient induced by other causes? If so, what might the reactivity transient be?

This is discussed in part under Question 54. In addition, we might assume that a transient is initiated by some means other than a void insertion in the flux trap. Such an event might be the failure of the inner-control-cylinder drive bracket. We have previously shown that failure of the drive bracket alone is a less severe transient than the void insertion accident. If the excursion adds enough energy to the target, the target rods could burst, adding about 0.04% $\Delta k/k$ per rod on a very fast time scale, that is, fast compared to 0.03 sec. This could cause a further increase in power and, depending on how many rods burst simultaneously, could cause melting of the core, even with safety rod action. Of course the probability of having a large number of target rods burst at the same time is very small.

C. If target coolant is closer to boiling than anticipated, could transient originating from another source lead to significantly greater energy release than that of Part I?

This is discussed in part in Question 54. There is also the possibility that an initiating accident other than the flux trap voiding could cause boiling in the target region, in which case the two would be additive. However, as indicated in the answer to Question 54, the rate at which steam can be generated in the target region is so slow relative to a significant initiating accident that the additive effect is negligible.

D. If flux trap is devoid of target, and flow is sharply reduced in that area, could sudden incidence of boiling or voiding lead to large reactivity insertion?

This is discussed in part under Questions 54 and 55A. Inadvertent operation without the target could lead to a 3.2% $\Delta k/k$ reactivity insertion on an 80-msec ramp. This could be tolerated without rupture of the primary system.

E. If a local meltdown in a section of the core occurs, how large must the hole get before one stops gaining reactivity? How much reactivity is involved? What is the increase in power level at the edge of the region devoid of fuel, as a function of hole size? How great is the tendency to spread as a consequence? To what extent may such a mechanism lead to autocatalytic effects and transients starting in this manner or from other sources? Are there other autocatalytic effects from fuel movement?

A single local cavity might very well grow in size due to power-density peaking, which can be as much as a factor of 2 greater than the local average. The maximum reactivity addition would be about 0.03% $\Delta k/k$ per spot, and the corresponding optimum hole size would be about 6 cm in diameter. A uniform removal of fuel plate would add reactivity in the amount of 2.6% $\Delta k/k$, and the corresponding removed volume would be 30%. It does not seem reasonable that this latter condition could be achieved by the former mechanism, because the increased power density around a local "flux trap" tends to make the hole grow beyond the optimum and thus results in a decrease in reactivity.

F. What pressures might be generated from local fuel melting? How much fuel failure is required to generate pressures which could move significant amounts of fuel inward (and thus gain reactivity), or which could interfere with control rod action? Does this allow for pressures from a "steam explosion" or a "water hammer"? How much reactivity could be gained by inward motion of the fuel into the flux trap? How much pressure would it take to produce such motion? Could flow blockage lead to such effects?

It does not appear that localized fuel melting would result in a steam explosion, and thus the accelerating pressures resulting from water and plate expansion, if an excursion were to exist, would be quite small. However, if several percent of the core were to be molten, it is quite possible that a steam explosion would occur. Because of the high pressures required to deflect the fuel element side plate a significant amount (see Appendix L), it is not anticipated that the tendency for inward movement of fuel would result in a significant addition of reactivity. It is more likely that movement of the safety rods would be impaired. Of course a steam explosion large enough to move significant amounts of fuel inwards or large enough to damage the safety rods, which are located beyond both the outer side plate, and the even stronger cylindrical shim-regulating rod, would disassemble the fuel element longitudinally. Thus it appears the pressure surges will only tend to shut the reactor down.

G. Are there any conditions in which water returning to a region after an explosion could lead to large reactivity insertions? For example, if fuel and water were expelled from a region due to melting, could water which rushed in thereafter cause a reactivity excursion?

If the fuel elements are stretched out longitudinally, a maximum increase in reactivity of about 6% $\Delta k/k$ could be achieved; the corresponding optimum extension of the fuel element is 35%, and of course it would be necessary for water to fill the volume vacated by the stretched fuel plate. It is not considered credible that a combination of molten plate and water-steam ejection would extend the plates without disassembly so that returning water would tend to add the 6% $\Delta k/k$. In any case, the core would be further disassembled (with energy release insufficient to rupture the pressure vessel) before the full 6% $\Delta k/k$ is added (Appendix H). A more probable but still unrealistic case is the one set forth in part E of this question, in which it is visualized that the molten metal leaves the core in a uniform manner to the extent of 30%, and the resulting space is filled with water. This could result in a reactivity addition of about 2.6%. As discussed in Appendix H, the resulting reactivity addition rate would not be instantaneous, and further disassembly would result in a reduction of reactivity.

56. What transient energy release, allowing for both total and rate of energy release, does it take to rupture the primary system (including the reactor pressure vessel) and expel significant amounts of water from the pool? What rapid reactivity insertion could lead to this energy release? On what basis is the estimate for these values made? What is the degree of uncertainty in the numbers?

The transient energy release required to rupture the primary system (including the reactor pressure vessel) has been calculated to be 1600 Mwsec from a nuclear excursion if no metal-water reaction is assumed. If a metal-water reaction is assumed, it requires a nuclear excursion of 600 Mwsec. As set forth in Appendix H we have found the limiting energy release from a nuclear excursion to be 300

Mwsec assuming a flat power distribution and 200 Mwsec if the more realistic nonuniform power distribution is assumed. The basis for the estimate on the containment potential of the reactor vessel is set forth in Appendix J. The values quoted are for nominal characteristics for the reactor vessel. We have also investigated the effects of applying a large safety factor by considering a reduction of a factor of 3 in the elongation before rupture. This results in a calculated energy input for rupture from a nuclear excursion of 600 Mwsec if no metal-water reaction is assumed and ~380 Mwsec if the metal-water reaction is considered. Even with this safety factor, the reactor vessel is adequately strong to contain the energy release of the limiting nuclear excursion plus the accompanying metal-water reaction.

57. What phenomena considered under Question 55 can possibly lead to transients, which when coupled with the associated chemical reaction and loss of metal during such reaction, lead to energies large enough to rupture the primary system and expel enough water, vapor, and gas from the system to threaten the integrity of the building?

As set forth in the Introduction and Summary, and as discussed in greater detail in Appendices H and J, we have found no phenomenon which could lead to an energy release large enough to rupture the primary system. Even if it is assumed that the primary system ruptures prematurely, as discussed in Question 59 and Appendix K, it is quite probable that no significant overpressure would occur in the building. If a significant amount of energy were transferred to the atmosphere of the building, the overpressure would be relieved through the truck-air-lock doors and no damage to the building would result. The doses calculated are within the guidelines of 10 CFR 100 at the downwind site boundary.

58. Are the answers to these questions changed if no control rod motion occurs?

For the end-of-cycle condition the safety rods do little more than shut the reactor down after the power excursion has been terminated by fuel plate expansion and moderator expansion. In the case of the maximum reactivity accident (1.3% $\Delta k/k$, 30-msec ramp) insertion of the safety rods prevents melting of the core. For more severe transients caused by much larger initial reactivity insertions the safety rods are of little use, and the case of core disassembly for shutdown is discussed in Appendix H.

59. What would be the consequences of a reactor vessel failure, particularly with regard to impairment of the containment and failure of the pool walls?

Failure of the reactor vessel during normal operation presents no particular problem with regard to either containment or the pool walls. The available stored energy in the system would be dissipated by release of about 33 gal of water, as the primary system is at an average temperature of only about 145°F.

Failure of the reactor vessel during or at the end of an excursion representing a limiting energy release case is discussed in Appendix K. No concern over damage to the pool walls is warranted as the energy release required to cause significant damage is in excess of 4500 Mwsec on a TNT explosion time scale. It is probable that no significant overpressure in the reactor bay would result from premature failure as discussed in Appendix K. However, no adequate model or experiment for dissipation of energy in the pool water has yet been obtained, and therefore, on the conservative assumption that all the available energy is transferred to the reactor bay atmosphere, the pressure could rise 0.3 psi before

failure of the truck-air-lock door would occur. The resulting dose at the downwind site boundary would not exceed the 10 CFR 100 guidelines even under this set of conservative assumptions (see Appendix K).

60. What steps will be taken, prior to installation of the backup shutdown system, to guard against the consequences of an accident resulting from the inability to move control rods into the core?

The backup shutdown system is already installed, and preliminary flow tests have been conducted to allow proper sizing of the orifice which determines the flow rate of poison from the injection system to the primary coolant system. This backup shutdown system will be operable prior to any increase in reactor power level above 20 Mw.

APPENDIX H

THE "ULTIMATE" SHUTDOWN MECHANISM OF THE HFIR

This section is divided into two parts: (1) the consideration of a hypothetical instantaneous reactivity addition of such magnitude that the resulting excursion melts, but does not boil, the aluminum in the fuel plates, the excursion being terminated by the thermal expansion of the plates, and (2) a discussion of larger reactivity additions.

At the operating pressure of the HFIR, 600 psi, the boiling point of aluminum is 3860°K (see Appendix I). If aluminum were heated from operating temperature (114°C) to this boiling point, its specific volume would increase from 0.37 ml/g to 0.665 ml/g (see Appendix I, Fig. II.I.5), that is, by 80% of its initial value. Assuming that the core can be approximated by a sphere, and that the expansion of the aluminum is accommodated by an even expansion of this sphere, the core would expand by 40%, since about half of its volume is occupied by aluminum. According to nuclear calculations (see Fig. II.H.1), this results in an 8.8% decrease in reactivity.

If a total excess reactivity of 5.1% were added instantaneously, the reactor would be super-prompt-critical by 4.4%. The Fuchs model says that the reactor shuts itself down when the compensated reactivity is twice the original prompt excess reactivity. Thus, in the present case the reactor would be shut down just short of boiling the aluminum.

The initial 4.4% prompt excess reactivity corresponds to a period of 0.8 msec, or 1.6 msec, respectively, at the beginning and the end of the fuel cycle. The energy deposited is 295 Mwsec (extrapolated from numbers given in Appendix I, Fig. II.I.5), short of the energy required to rupture the primary vessel.

The above model was deliberately made very simple, as a complicated model would not be very convincing. However, some of the simplifications deserve discussion. The thermal time constant of the HFIR fuel plates is 2 msec, much shorter than the thermal time constant for the thicker plates of the SPERT destructive test. Considerable heat flux is thus going to reach the metal-water interface much sooner in the HFIR than in the SPERT test. Such heat flux results in violent boiling, water hammer,

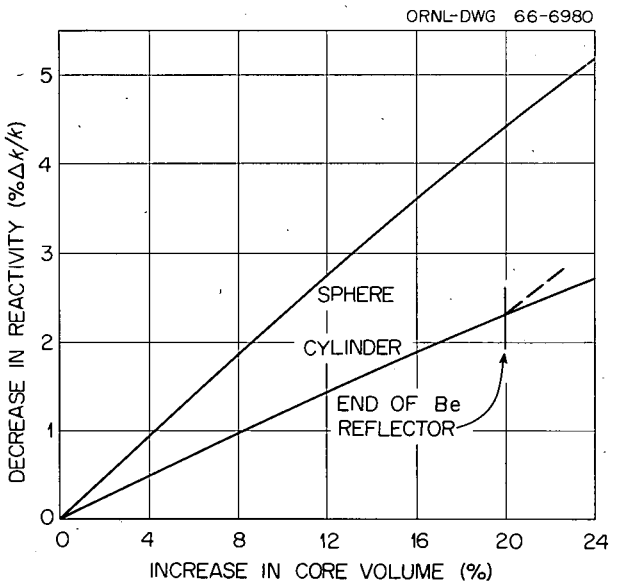

Fig. II.H.1. Decrease in Reactivity for Spherical and Cylindrical Core Expansion, Assuming Weight of Materials Remains Constant.

disruption of the molten aluminum plates, drastic increase of the heat-transfer surface, and a steam explosion; the core will probably be disassembled prior to generation of the full 295 Mwsec. Before the melting point of the aluminum is reached, the thermal expansion will largely be accommodated by the expulsion of water from the core, resulting in an increase of the metal-to-water ratio of the already undermoderated reactor and in a somewhat greater reactivity reduction than computed above on the basis of expansion with constant metal-to-water ratio. Even after the melting, the water, being lighter, might be expelled preferentially to some extent, increasing further the reactivity compensation over what was computed above.

In a short transient as visualized above, the nonfueled regions, in particular the end plates, will be heated relatively little and will retain some strength. Also the structure surrounding the core will remain rigid. The expansion will therefore not occur isotropically in all directions, as assumed above; rather, the expansion will occur preferentially in the axial direction. Such expansion results in less reactivity compensation than isotropic expansion, as long as the core remains inside the reflector, Fig. II.H.1. In the present case the expansion would be so large, however, that much of the core would be extruded outside the beryllium reflector. The resulting reactivity reduction is therefore larger than computed under the assumption of an infinitely long beryllium reflector.

It has tacitly been assumed that the temperature increase in the aluminum fuel plates is the same everywhere. This is not strictly true, partly because of the not entirely flat macroscopic power distribution, and partly because of the fact that the assumed reactor period and the thermal time constant of the fuel plates are of the same order of magnitude. Thus, some parts of the aluminum will reach the boiling point before the rest, and some vaporization of aluminum will occur at reduced reactivity com-

pensation but also with less energy deposition. Calculations made using a six-region approximation of the core showed that the boiling point would be reached at a reactivity compensation of $\sim 5.25\%\ \Delta k/k$ and an energy input of 195 Mwsec. It appears that this represents an upper limit for energy release; however, we will continue to use the 295-Mwsec value as being more conservative. The consequences of aluminum vaporization are discussed below.

With the qualifications just discussed, the reactor can be seen to be able to withstand an instantaneous reactivity addition of 5.1%. This takes care of most conceivable reactivity insertions. However, the reactor is strongly undermoderated, and substantial reactivity additions can thus, in theory at least, be inserted by decreasing the metal-to-water ratio. The conceivable mechanisms for this all seem to involve the rapid generation of steam, which expels fuel or expands the core, and the subsequent filling of the resulting void with water.

There remains, however, the question whether the water can fill the voids fast enough to even approximate an "instantaneous" reactivity addition. It has been postulated above that the aluminum can be heated to 3860°K without appreciably heating the water. This conservative assumption is, of course, never exactly fulfilled, and to the extent that it is approximated, it represents an extremely unstable situation. It is known experimentally from the SPERT destructive test that the water and hot aluminum become intimately mixed and that a violent disassembly of the core occurs. In the SPERT test this took 15 msec, and in view of the thinner fuel plates and the thinner water gap in the HFIR, it is conservative to assume that these 15 msec represent an upper limit for the time that the molten aluminum and the water can coexist without violent mixing. The question is then whether the void can be filled in a time shorter than 15 msec.

The normal cooling flow of water, assuming that it persisted after the incident that caused the void, is evidently too slow. Besides, such flow would shorten the time required for the mixing. Condensation of the steam seems out of the question on the time scale required because there are insufficient heat sinks. No mechanism is apparent for generating sufficient pressure outside the core to drive the water back in. A pressure wave, that originated in the core, cannot be reflected back with appreciable efficiency, partly because of the cylindrical, nonfocusing geometry, and partly because the pressure vessel absorbs, and transmits, some energy. If the steam bubble left the core, it could conceivably pressurize the primary system, but this again would be a slow process.

It might thus be concluded that large amounts of reactivity cannot be added fast enough to create an excursion violent enough to boil the aluminum.

However, if such large amounts of reactivity were added, the boiling of some of the aluminum would lead to intimate mixing of water with the aluminum vapor as well as with the large amount of molten aluminum.[1] The drastic increase in the heat transfer surface would cause a steam explosion. This and the aluminum-water reaction from the vaporized aluminum would cause disassembly of the core at a rate which would "outrun" any possible reactivity addition rate. This process has so far defied rigorous

---

[1]T. J. Thompson and J. G. Beckerley (eds.), *The Technology of Nuclear Safety*, sect. 6.3, pp. 704 ff., MIT Press, Cambridge, Mass., 1964.

analysis, but it should be noted that 300 Mwsec will boil 12.6% of the core at a pressure of 1 atm and 5.6% at the operating pressure of 40 atm (see Appendix J).

Even without the mixing of the aluminum and water, the vaporization of the aluminum creates pressures which would disassemble the reactor. Actually, once the boiling point is exceeded, only very little energy is needed to generate enough aluminum vapor to fill the voids associated with the disassembly. Most of the energy goes into heating the molten aluminum, and hence the saturation pressure in the hottest part of the reactor increases, and the increased pressure provides increased acceleration for the disassembly. This process, too, will eventually outrun possible reactivity insertion rates. It also cuts short the "tail" (i.e., the part of the transient after the power maximum) of an excursion caused by a hypothetical instantaneous reactivity addition.

In summary: Assuming a flat power distribution, the reactor can take a 5.1% instantaneous reactivity addition without boiling aluminum, generating only 295 Mwsec; if a nonuniform power distribution is assumed, the reactor will shut down without vaporization of aluminum following a 3.3% step in reactivity with an energy release of 195 Mwsec. This latter case is believed to represent a reasonable upper limit for energy release from the HFIR core for any reactivity input which appears possible. Larger reactivity additions than 3.3% $\Delta k/k$ can be made only relatively slowly, and the steam explosion resulting from intimate mixing of molten aluminum and water would disintegrate the core long before the reactivity addition were completed. However, if large reactivity additions could be made rapidly, the aluminum would begin to boil, and this, possibly in conjunction with a steam explosion caused by intimate mixing of water and hot aluminum and with the reaction of steam with vaporized aluminum, would disassemble the core at a rate which would outrun even a rapid reactivity addition.

APPENDIX I

ENERGY RELEASES FROM Al-H_2O REACTIONS IN THE HFIR[1]

After correlation of experimental data in the literature, we have analyzed a sequential accident model considering aluminum-water reactions in the High Flux Isotope Reactor (HFIR). The model includes the following limiting conditions with the corresponding energy releases due to the aluminum-water reaction:

1. Instantaneous heating (through a nuclear transient) of all the metal in the HFIR core to temperatures above 1700°C, triggering ignition over the entire heat transfer surface. The rate of energy release at zero time (before changes in core configuration) is 112 Mwsec/sec.
2. Disassembly of the core, including the following limiting configurations:
   a) A single sphere of molten aluminum of 46.5 cm in diameter.

[1]This investigation is based on 1×10^5 g of aluminum; the correct value for the HFIR is 7.2×10^4 g of aluminum, and the various numbers should be adjusted accordingly.

Initial rate of energy release	1.9	Mwsec/sec
Duration of ignition	2900	sec
Total energy released	1700	Mwsec

b) Molten aluminum particulates with initial diameters less than 0.336 cm.

Initial rate of energy release	0	Mwsec/sec
Duration of ignition	0	sec
Total energy released	<25	Mwsec

c) Molten aluminum particulates with initial diameter of 0.336 cm.

Initial rate of energy release	244	Mwsec/sec
Duration of ignition	0	sec
Total energy release during ignition	0	Mwsec
Total energy release during reaction	<25	Mwsec
Duration of reaction	~0.1	sec

d) Molten aluminum particulates greater than 0.336 cm with an initial diameter of D_0 cm.

Rate of energy release:

$$\frac{82}{D_0}\left(1-\frac{1.6\times 10^{-2}t}{D_0}\right)^2 \text{ Mwsec/sec .}$$

Duration of ignition:

$$t_I=\left(\frac{D_0-0.336}{1.6\times 10^{-2}}\right)\text{ sec .}$$

Total energy liberated:

$$1710\left[1-\left(\frac{0.336}{D_0}\right)^3\right]\text{ Mwsec .}$$

A review of the literature reveals that the results of previous investigations[2–7] correlate satisfactorily to provide experimental evidence on which to predict a sequential accident model involving metal-water reactions in HFIR. The analysis addresses itself to rates and extents of the metal-water

---

[2]R. E. Wilson, L. Mishler, and C. Barnes, "Metal Water Reactions: Studies of the Aluminum-Water Reaction by the Levitation-Melting Method," pp. 196–201 in *Chemical Engineering Division Summary Report, October–December 1962*, USAEC Report ANL-6648, Argonne National Laboratory, May 1963.

[3]R. E. Wilson, C. Barnes, and L. Baker, "Studies of the Aluminum-Steam Reaction by the Levitation Melting Method," pp. 233–39 in *Chemical Engineering Division Semiannual Report, January–June 1964*, USAEC Report ANL-6900, Argonne National Laboratory, August 1964.

[4]R. O. Ivins and R. Koonz, "Study of the Combustion of Aluminum in Water," pp. 338–41 in *Chemical Engineering Division Semiannual Report, July–December 1963*, USAEC Report ANL-6800, Argonne National Laboratory, May 1964.

[5]Argonne National Laboratory, *Reactor Development Program Progress Report, October 1964*, USAEC Report ANL-6965, pp. 91–92, Nov. 15, 1964.

[6]Argonne National Laboratory, *Reactor Development Program Progress Report, August 1965*, USAEC Report ANL-7090, Sept. 21, 1965.

[7]L. Baker, Jr., "Metal Water Reactions," *Nucl. Safety* 7(1), 25–44 (Fall 1965).

reactions under a variety of postulated pessimistic situations. We assumed that the reactions were initiated by a nuclear excursion and made no attempt to analyze the problem of partition of the energy released. We considered that the results of this analysis will be used as input for the problem of partition of energy which is being undertaken by other members of the group.

Basis for the Model

The justifications of our assumptions and conclusions upon which the model is based are given separately in this Appendix. The assumptions and conclusions are the following:

1. In the temperature range of 1400 to 1600°C, aluminum reacts with steam at 1 atm according to the equation:[2]

$$\frac{W}{t} = 2.5 \times 10^8 \, [\exp(-73{,}500/RT)] \text{ mg of aluminum per square centimeter per minute .}$$

   Rate of energy release calculated from this equation, using the entire heat transfer surface of the core, is only 0.3 Mwsec/sec at 1750°C, the ignition temperature for aluminum, and drops rapidly with decreasing temperature.

2. At 1750°C aluminum ignites in steam and continues to burn at temperatures in excess of 2000°C (ref. 3) when dropped in water. Under these conditions the burning rate is constant at 0.96 g of aluminum per square centimeter per minute, and the surface burning rate is independent of diameter.

3. The combustion time of pellets is given by the equation[3]

$$D_0 = 1.6 \times 10^{-2} t_c + 0.336 \, ,$$

   where D_0 is the original diameter of the particle in centimeters and t_c is the combustion time in seconds.

4. The aluminum does not burn completely, and combustion ceases as the diameter of the sphere of molten aluminum gets to 0.336 cm. Some reaction continues to occur (at lower rates) as the metal cools. Accordingly, aluminum is consumed by the reaction so that the diameter decreases from 0.336 cm (where burning stops) to 0.23 cm when reaction stops. We will consider only the combustion reaction. We will, however, make an estimate of the energy release by the chemical reaction as the particle is cooling down. Smaller aluminum particles can be forced to react only by the introduction of large inputs of energy from outside sources (such as lasers) while the reaction is taking place.[4] For particles of 360 μ in diameter, no reaction is obtained unless the input of energy is greater than 35 j (0.52 Mwsec per gram of aluminum).

5. The extent of reaction appears to be independent of the total pressure in the system (see p. 221).

6. In the combustion range, the reaction rate becomes mass-transport limited, is independent of total pressure, and is only weakly dependent on temperature. The temperature dependence is $T^{0.5+m}$, where m is less than 0.5 (see pp. 225 and 226).

Accident Conditions

We consider a most significant feature to be that the extent and the rate of reaction are profoundly affected by the original state of subdivision of the aluminum. Bearing this in mind, we have considered the following accident conditions:

1. All the aluminum in the core (1×10^5 g) is instantaneously heated to 2000°K (or above) and ignites over the entire heat transfer surface (4×10^5 cm^2).

2. After the combustion has been initiated, the molten aluminum subdivides into molten particles with an initial diameter D_0. For convenience, we have assumed the particles to be of equal size and have treated D_0 as a parameter in the analysis. As a result, we have determined reaction rates, rates of energy release, and total energy release for various configurations.

Conclusions

1. The initial rate of reaction (at time zero when combustion starts before any change in geometry has occurred):

a) Rate of consumption of aluminum in core:

$$6.4 \times 10^3 \text{ g of aluminum per second .}$$

b) Rate of energy release:

$$112 \text{ Mwsec/sec .}$$

2. After this initial condition, the rate of reaction and extent of reaction depend on the configuration that the molten aluminum assumes. A limiting case would be for the molten metal to coalesce into one initially large sphere of aluminum. If this condition prevails, the aluminum burns completely (neglecting one particle of 0.23 cm in diameter that will be left unburned) and will release all of its energy at a relatively small rate, which is limited by the unfavorable surface-to-volume ratio of the configuration.

The initial diameter of a sphere of molten aluminum of weight 1×10^5 g is 46.5 cm.

Initial rate of consumption of Al	109	g Al/sec
Initial rate of energy release	1.9	Mwsec/sec
Total energy release	1700	Mwsec
Time of reaction	2900	sec

This condition yields a large total energy release, but at very slow rates and over extended periods of time.

A second limiting condition is that the molten aluminum subdivides itself into particles smaller than 0.23 cm in diameter. If this were the case, the reaction would stop.

A third limiting case is for the aluminum to subdivide itself into particles of 0.336 cm in diameter. (Experimentally, this has been found to be the minimum size to support combustion.)[3]

Initial rate of reaction	1.43×10^4 g Al/sec
Initial rate of energy generation	244 Mwsec/sec
Duration time of ignition	0 sec
Energy liberated	<27 Mwsec

There is a gray area that cannot be described as precisely as the cases above. This area concerns the reaction as the particles are consumed from a diameter of 0.336 cm (the size below which combustion ceases) and 0.23 mm (the size below which chemical reaction ceases). This stage occurs as the particle is cooling from temperatures in excess of 2000°C, where the reaction is mass-transport limited, to the lower temperature region, where the reaction is exponential with temperature. For the worst case, however, one can rationalize that the total reaction rate is not larger than the combustion rate. The time necessary to reduce the diameter of aluminum spheres from 0.336 to 0.23 cm can be estimated from the equation in paragraph 3, page 212, as 0.11 sec. This would represent an energy release of 27 Mwsec if the initial rate of reaction of 244 Mwsec/sec (which is the maximum combustion rate obtained in the preceding paragraph) could be maintained. This small quantity of energy is not significant within the necessarily rough limitations in precision of the energy quantities we are discussing. Consequently in our subsequent discussion, we ignore the small energy contribution as the aluminum cools from combustion temperature to room temperature

We have, so far, considered the effect of particle subdivision for the case of the largest and smallest aluminum spheres and now proceed to treat the cases where the initial diameter of the spheres lies between the range 0.336 to 46.5 cm. The following equations have been used for the calculation.

Number of spheres of initial diameter D_0 into which W_0 g of molten aluminum of density ρ subdivide:

$$N_0 = 6W_0/\rho\pi D_0^3 \; ; \tag{1}$$

$$N_0 \sim (1 \times 10^5)/D_0^3$$

assuming

$$\rho \sim 2 \text{ g/cm}^3 \; , \tag{2}$$
$$W_0 = 1 \times 10^5 \text{ g} \; .$$

Diameter of spheres at t seconds after combustion starts:

$$D(t) = D_0 - 1.6 \times 10^{-2} t \text{ cm} \; . \tag{3}$$

Total rate of reaction in the core:

$$W(t) = \frac{3W_0}{D_0^3} D^2(t) \frac{dD(t)}{dt} \text{ g Al/sec} \; , \tag{4}$$

$$W(t) = +\frac{4.8 \times 10^3}{D_0} \left(1 - \frac{1.6 \times 10^{-2} t}{D_0}\right)^2 \text{ g Al/sec} \; . \tag{5}$$

Rate of energy generated:

$$P(t) = \frac{82}{D_0} \left(1 - \frac{1.6 \times 10^{-2} t}{D_0}\right)^2 \text{ Mwsec/sec} \; . \tag{6}$$

Duration of combustion is:

$$t_c = \frac{D_0 - 0.336}{1.6 \times 10^{-2}} \text{ sec} . \tag{7}$$

Fraction of aluminum unburned:

$$f = \left(\frac{0.336}{D_0}\right)^3 . \tag{8}$$

Total energy delivered by the reaction of 1×10^5 g of Al:

$$E = 1710 \left[1 - \left(\frac{0.336}{D_0}\right)^3\right] = 1710\,[1 - f] \text{ Mwsec} . \tag{9}$$

Initial rate of reaction:

$$W(0) = \frac{4.8 \times 10^3}{D_0} \text{ g Al/sec} . \tag{10}$$

Initial rate of energy generation:

$$P(0) = \frac{82}{D_0} \text{ Mwsec/sec} . \tag{11}$$

Table II.I.1 and Figs. II.I.1 and II.I.2 express the results.

Table II.I.1. Extent of Reaction and Energy Releases as Functions of Initial Particle Diameter

D_0 (cm)	f	$(1 - f)$	E (Mwsec)	t_c (sec)	$P(0)$ (Mwsec/sec)	$\bar{P}$ (Mwsec/sec)
0.336	1.0	0.0	0.0	0.0	244	0.0
0.35	0.88	0.12	205	0.88	234	233.0
0.40	0.58	0.42	720	4.00	205	180.0
0.45	0.41	0.59	1005	7.12	182	141.0
0.50	0.30	0.70	1195	10.25	164	117.0
0.60	0.175	0.825	1410	16.50	137	86.0
0.80	0.074	0.926	1580	29.00	102	55.0
1.00	0.038	0.962	1645	41.50	82	40.0
1.20	0.022	0.978	1670	54.00	68	31.0
1.50	0.011	0.989	1690	102.50	55	16.5
46.5	0.0	1.0	1710	2900.00	1.9	0.59

List of symbols:

D_0 Initial particle diameter, cm
f Fraction of aluminum not reacted
E Total energy liberated, Mwsec
t_c Time (or duration) of ignition reaction, sec
$P(0)$ Initial (or maximum) rate of energy generation, Mwsec/sec
$\bar{P}$ Average rate of energy release during the ignition reaction, E/t_c

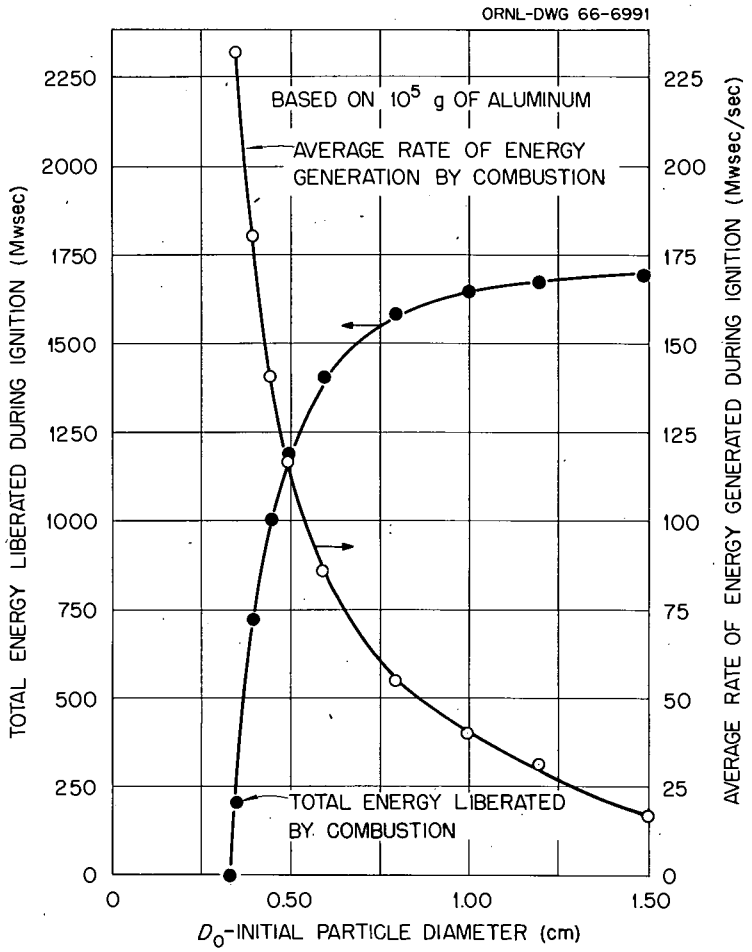

Fig. II.1.1. Energy Releases During Combustion.

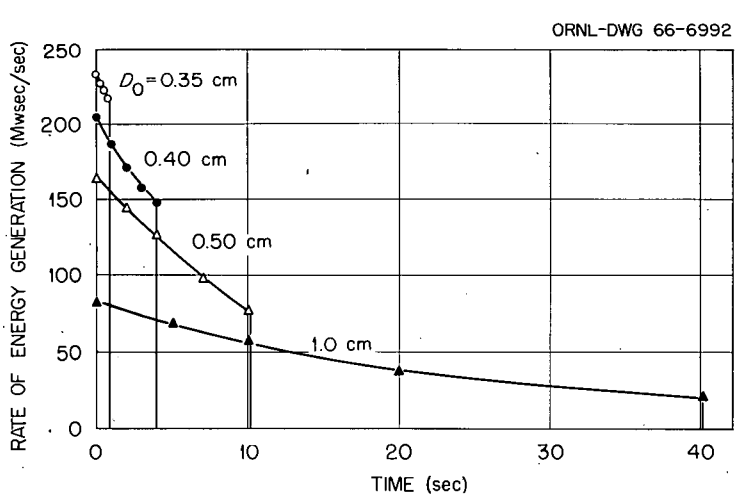

Fig. II.1.2. Rate of Energy Generation by Combustion of 10^5 g of Molten Aluminum Subdivided into Drops of Various Sizes.

Supplementary Information

Justification of $D_0 = 0.016t_c + 0.336$ as the Base Equation for Burning Calculations

The empirical equation results from data shown and discussed in ANL-6800, *Argonne National Laboratory Chemical Engineering Division Semiannual Report for July–December, 1963*, pp. 338–41, as reproduced herein. The development is straightforward. Two comments on their discussion are required.

1. Since the $Al(g) + O_2(g)$ reaction is much more energetic and therefore presumably faster, and total burning time (air and water) was used to plot the data, the 0.336-cm intercept is conservative for the diameter where burning ceases.
2. The 0.23-cm equivalent diameter sphere of aluminum remaining may well be an artifact of the $Al + O_2$ reaction during the late stages of burning on the surface of the water, since the residual oxide coating could form while the oxygen continued to react with the aluminum.

The following has been reproduced from *Argonne National Laboratory Chemical Engineering Division Semiannual Report for July–December, 1963*, ANL-6800:

---

4. Study of the Combustion of Aluminum in Water (R.O. Ivins, R. Koonz)

The sustained combustion of aluminum pellets in water has been reported by Wilson and Martin (see ANL-6379, p. 208). In these studies, small pellets of aluminum were simultaneously levitated and heated in a radio-frequency field. It was discovered that ignition occurred when the pellet temperature reached 1750°C in air. The ignition resulted in a vigorous vapor phase burning in air, which continued when the pellets were dropped into water. Burning occurred beneath the surface of water and later at the water-air interface as the pellets were buoyed up to the surface by the evolving hydrogen.

Observation of the self-sustained vapor phase combustion process prompted the present study, in which the rate of metal consumption was determined as a function of pellet size. These studies were undertaken in order to provide a basis for estimating the rate of the aluminum-water reaction in the burning regime (metal temperature greater than 1750°C).

Samples of high-purity aluminum ranging in weight from 150 to 1000 mg were levitated, heated in air until they ignited, and then dropped into room temperature water. The time which elapsed from the moment of dropping until burning ceased was measured. The results of these measurements are plotted in Figure V-8. The data points were fitted to a straight line by the method of least squares. The equation of the line was as follows:

$$D_o = 0.160\, t_c + 3.36 \qquad (6)$$

where D_o is the original diameter of the particle, in mm, and

t_c is the consumption time, in sec.

Figure V-8

CONSUMPTION OF ALUMINUM PELLETS BURNING IN WATER

(Water temperature: ≈25°C)

(Metal temperature: ≈2050°C)

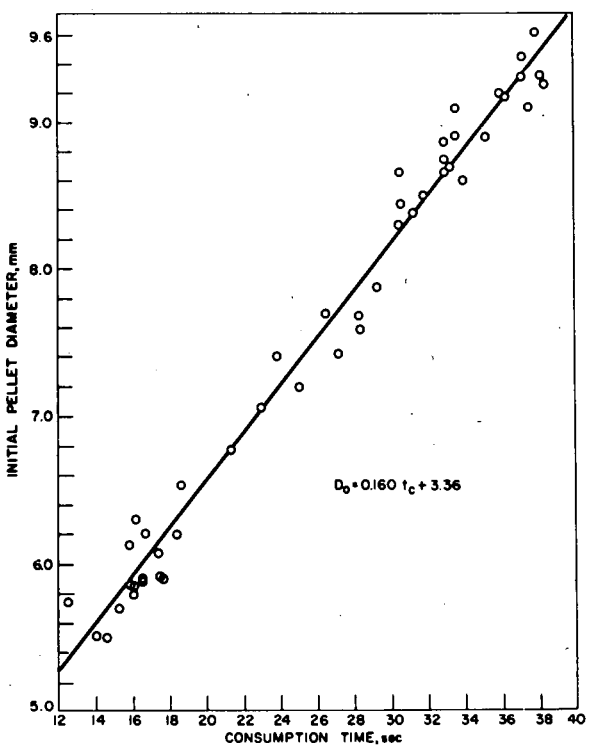

108-7191

Initially, the drops of burning aluminum sank below the water surface and would rise and sink alternately as the hydrogen bubble surrounding it would grow and break off. As the drop became smaller, it would break the water surface, releasing the hydrogen, and then sink, form a bubble, and rise again. Eventually, when the size of the drop had become small enough, it would rise to the surface and float while continuing to burn. Once burning ended, the residual metal, enclosed in an irregular oxide coating, would sink to the bottom of the water container. While the drops were burning under water, they decreased in size and the condensation of fine alumina particles was evident as a particle spray from the burning surface of the drop. The size distribution of the fine particles given off during one run is shown in Figure V-9. The distribution data was obtained by microphotography of samples of the suspended particles.

Figure V-9

PARTICLE SIZE DISTRIBUTION OF Al_2O_3 RESIDUE RESULTING FROM THE REACTION OF ALUMINUM DROPLETS AND WATER

(Geometric Mean Particle Size = 2.69 μ)

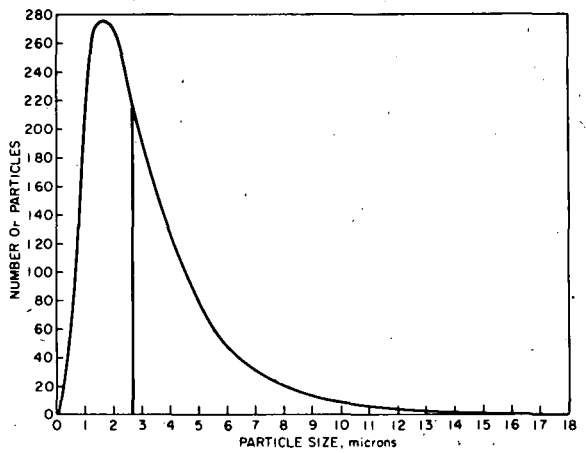

108-7192

Vapor phase burning of droplets of liquid fuels is often controlled by the rate of heat transfer from a cospherical flame front to the fuel sphere to provide the heat of vaporization and thus sustain burning.[2] The heat transfer rate for hydrocarbon fuels is usally controlled by conduction and results in a consumption time which is proportional to the square of the original droplet diameter. It can be shown, however, that if the heat transfer rate occurs predominantly by thermal radiation, a linear relationship between the consumption time and the droplet diameter is expected. The linear character of the experimental results as expressed in Figure V-8 and Equation 6 is therefore consistent with a heat transfer rate controlled by radiation. This finding is consistent with the fact that aluminum has a higher temperature of combustion than those of liquid hydrocarbon fuels and forms a solid oxide product.

The data are consistent with a simple vapor burning model, except that the straight line in Figure V-8 does not pass through the origin. This occurred primarily because the aluminum droplets did not burn to

---

[2]See, for example, Wise, H., Lorell, J. and Wood, B.J., The Effects of Chemical and Physical Parameters on the Burning Rate of a Liquid Droplet, Fifth Symposium (International) on Combustion, Reinhold Publishing Co., New York, 1955, p. 132.

completion in the water. An analysis of typical residue indicated that the equivalent of a 2.3-mm sphere remained unreacted. The experiment was also complicated by the fact that a small amount of burning occurred in air before the pellets were dropped and also that in the late stages of burning the sample was floating and therefore was in contact with both water and air. No quantitative significance, therefore, could be attached to the intercept in Figure V-8 or to the constant of 3.36 mm in Equation 6, since it could not be assumed that burning in air, under water, and at the water-air interface occurred at the same rate.

It could be assumed, however, that on the average the time of burning in air and at the water-air interface was constant for each run. This is equivalent to assuming that the droplets began burning at the water surface at a particular value of the diameter. The error incurred in including the surface burning time in the measurements, therefore, did not affect the slope of the line. It was, therefore, assumed that the slope (0.160 mm/sec) represents the burning rate of droplets submerged in room temperature water.

The calculation of the mass rate of consumption from the rate at which particle diameters decrease can be achieved as follows:

$$\frac{-dm}{A\,dt} = \frac{\rho}{\pi D^2} \frac{d\left(\frac{\pi}{6} D^3\right)}{dt} \tag{7}$$

where dm/A dt is the mass consumption rate in g aluminum/(cm^2)(min),

ρ is density of aluminum at 2000°C, 2 g/cc,

D is the diameter of the aluminum drop at any time, in cm, and

t is time, in min.

Equation 7 reduces to the following:

$$\frac{-dm}{A\,dt} = \frac{\rho}{2}\frac{dD}{dt} = 0.96 \text{ g aluminum/(cm}^2\text{)(min)}. \tag{8}$$

Combustion Ceasing at a Set Diameter

To explain the cessation of combustion at a particular diameter, we consider the geometry of the system. Surface tension forces will cause the molten aluminum to form a sphere when surrounded and burning in liquid water. The burning occurs in a film zone around the sphere, diffusion-fed by both aluminum and water vapor and populated by free hydrogen, which both thickens the film and interferes with the diffusion of the active components. The surface of the aluminum is πD_{Al}^2 and that of the vapor phase πD_v^2; the surface ratio is $\pi D_v^2/\pi D_{Al}^2$ or $(D_v/D_{Al})^2$. Radiation and conduction losses at constant thickness of the vapor layer increase as the square of the diameter ratio. Consider the following example:

Sphere Diameter (cm)	Film Thickness (cm)	Ratio $\frac{\text{Loss Surface}}{\text{Input Surface}}$
1	0.05	1.21
0.5	0.05	1.44
0.25	0.05	1.96
0.10	0.05	4.00

It is easy to see why combustion stops, since as the losses go up the aluminum temperature decreases, reducing the aluminum vapor available, which in turn decreases the energy input to the interface, and the burning ceases abruptly.

Pressure Independence of Extent of Reaction

Raw data from results reported[6] on short period fission energy inputs to samples of HFIR fuel plate may be construed as showing a greater extent of reaction with increasing pressure. If the energy input and initial conditions are used to calculate adiabatic temperature rise this apparent effect disappears as shown by plots in Fig. II.I.3.

The adiabatic temperature plot also substantiates the observations that no combustion reaction can occur below ~1450°C and that dispersal of the fuel into small pieces by internal vapor pressure will tend to limit the extent of reaction.

Initiation of the Combustion Reaction

Combustion or self-supporting reaction cannot occur until the available heat per unit of reaction surface exceeds the heat losses from the surface. Heat loss can occur by radiation, convection, and conduction.

Since we believe the reaction is aluminum vapor reacting with water vapor, we can make an energy balance in terms of calories per square centimeter per second where the reaction occurs at the aluminum surface.

From the vapor pressure of aluminum and Langmuir's equation[8] for mass vaporization into a vacuum, we can calculate the *maximum flux* of aluminum vapor available. The net heat of reaction for

$$2Al(l, T) + 3H_2O(l, 298) \rightarrow Al_2O_3(s, T) + 3H_2(g, T)$$

is about 2400 cal/g for energy input calculation. For the TREAT experiments, the only sensible loss is the radiation loss since convection cannot be established instantly. This loss is calculated for an emissivity of 1.0, but a lower value does not sensibly alter our conclusions.[9]

---

[8] S. Dushman, *Scientific Foundations of Vacuum Technique*, p. 20, Wiley, New York, 1949.

[9] H. Etherington, *Nuclear Engineering Handbook*, 1st ed., pp. 1–59, McGraw-Hill, New York, 1958.

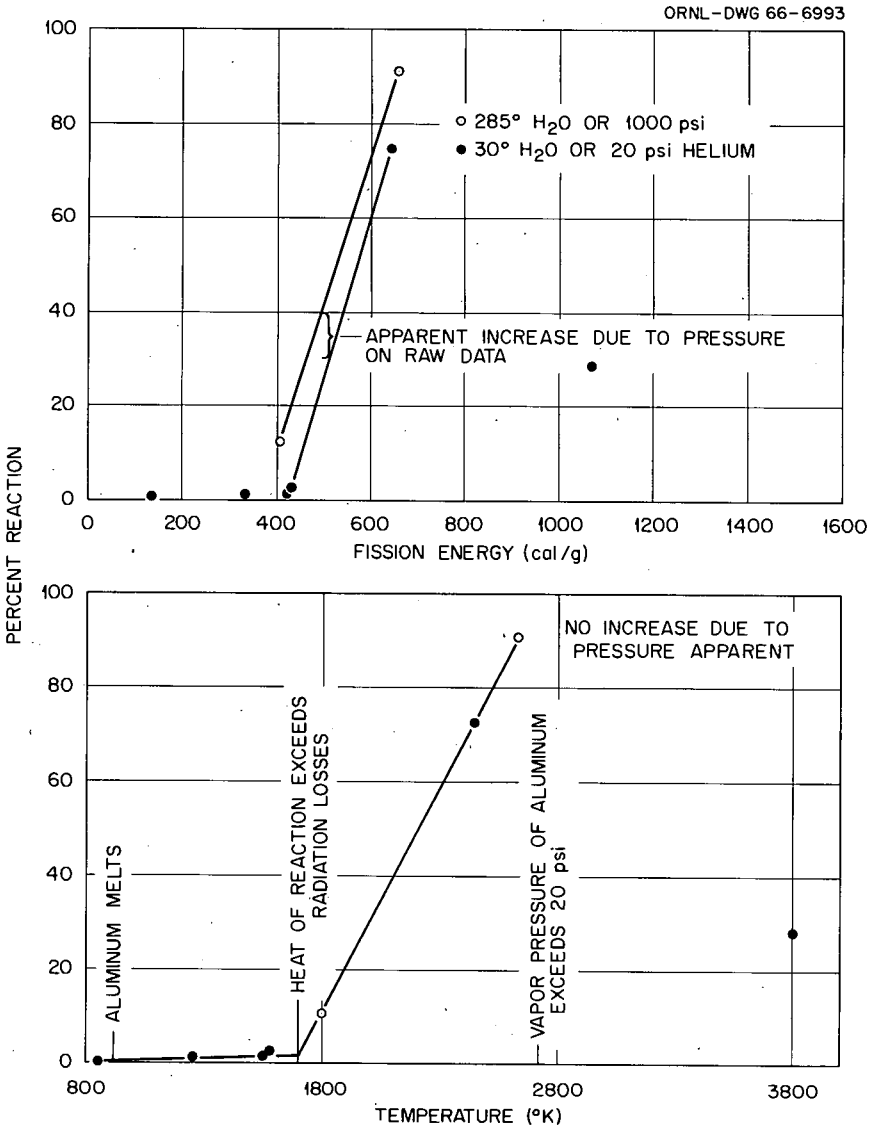

Fig. II.1.3. TREAT Results with HFIR Fuel Samples.

These values are:

Temperature (°C)	Flux of Aluminum Vapor (g cm^{-2} sec^{-1})	Heat Generated (cal cm^{-2} sec^{-1})	Radiation Loss (cal cm^{-2} sec^{-1})
1200	2.2×10^{-4}	0.5	6.2
1300	8.6×10^{-4}	2.1	8.1
1400	3.4×10^{-3}	8.1	10.3
1500	1.02×10^{-2}	24.5	12.1
1600	2.9×10^{-2}	69.6	16.1
1700	9×10^{-2}	216	19.7

It is evident that ignition should occur between 1400 and 1500°C as actually observed in TREAT. In the levitation experiments where convection was fully established this loss plus radiation was barely exceeded at 1600°C (delayed ignition) which would place the convection and conduction loss at ~ 53.5 cal cm^{-2} sec^{-1}, a perfectly reasonable number.

Observed Burning Temperature and Rate of Reaction

If we consider the system to consist of a spherical aluminum ball surrounded by a spherical flame front in turn surrounded by liquid water, we can see that conduction and radiation from the flame front is the only source of heat to vaporize the aluminum.

For the required heat transfer a thermal gradient must exist between the flame front and the aluminum. For the observed rate of burning some 20 ml of STP hydrogen is generated per square centimeter per second, and the heat flux to vaporize aluminum (1.6×10^{-2} g cm^{-2} sec^{-1}) is ~ 40 cal cm^{-2} sec^{-1}. Langmuir's equation gives this rate of delivery of vapor if the liquid is at 1900°K. An additional confirmatory observation is obtained from the levitation experiments[3] when delayed ignition is observed at 1873°K. Examination of the graph of the TREAT results (Fig. II.I.3) also reveals consistency with an ignition temperature of about 1900°K. Given flame temperature (which we change parametrically), the thermal conductivity of hydrogen, and neglecting the thermal conductivity of Al(*v*), we can calculate the film thickness between the flame zone and the aluminum surface required to supply the necessary heat flux.[10] The results of this calculation are as follows:

Flame Temperature (°K)	Heat Received from Radiation by the Aluminum (cal cm^{-2} sec^{-1})	Required Film Thickness (cm)
2000	3.6	0.4×10^{-2}
2100	7.9	1.2×10^{-2}
2200	12.7	2.0×10^{-2}
2300	18.7	3.4×10^{-2}
2400	25.4	5.8×10^{-2}

Since the hydrogen thickness is a function of rate, this shows that the reaction is self-regulating in that increases in rate thicken the film and vice versa; therefore, the rate remains sensibly constant. It should be remembered that pressure has little effect on the thermal conductivity of the gas and that heat transfer is largely independent of pressure.

The gross hydrogen generation stirs (violently) the liquid external phase, and the sensible heat of the hydrogen is largely lost to this phase without exchanging a large proportion of its heat to the incoming water vapor. The radiation losses to the external phase are appreciable, and these together with convection losses apparently combine to limit the effective flame zone temperature to the melting point of alumina (or 2313°K).

---

[10] S. Dushman, *Scientific Foundations of Vacuum Technique*, p. 60, Wiley, New York, 1949.

Effect of Temperature on Aluminum Volume on Core (Fuel Plates Only) and Vaporization Tendency of Aluminum (Figs. II.I.4 and II.I.5)

The following bases were taken for this calculation:

Total core volume	91 liters
Total volume of H_2O in core (no targets)	39 liters
Volume of solid	52 liters
Volume of fuel plates	27.4 liters
Initial density of Al at 298°K	2.7 g/cm^3
Density of solid at 932°K (mp)	2.6
Density of liquid	2.48
Density of liquid at 1000°C	2.29
Density of liquid at 1750°C	2.0

Vapor pressure of Al(*l*)

T (°C)	Vapor Pressure (atm)	
	a	*b*
2000	0.15	0.07
3000	17	7.9

[a]From Brewer's estimates.
[b]From boiling point.

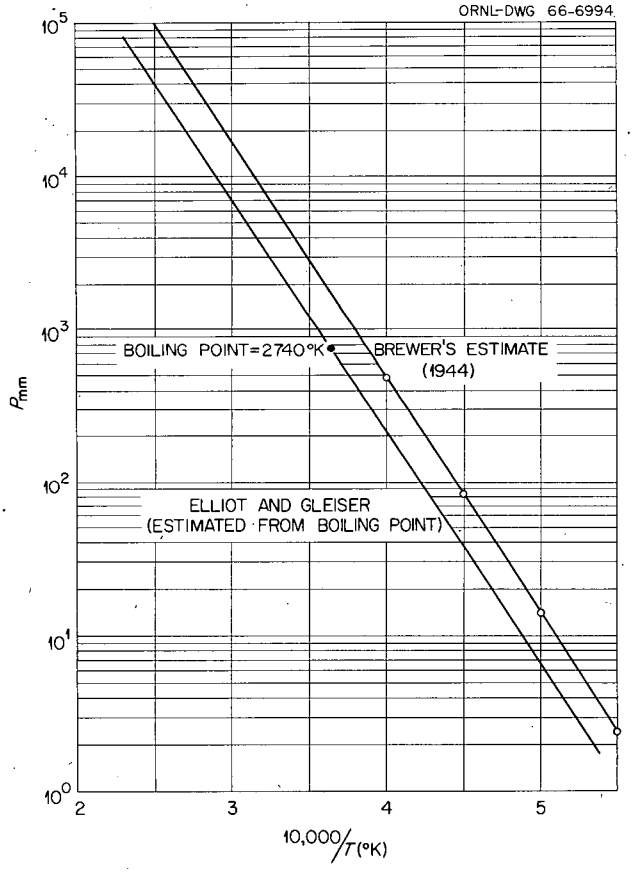

Fig. II.I.4. Vapor Pressure of Al(*l*).

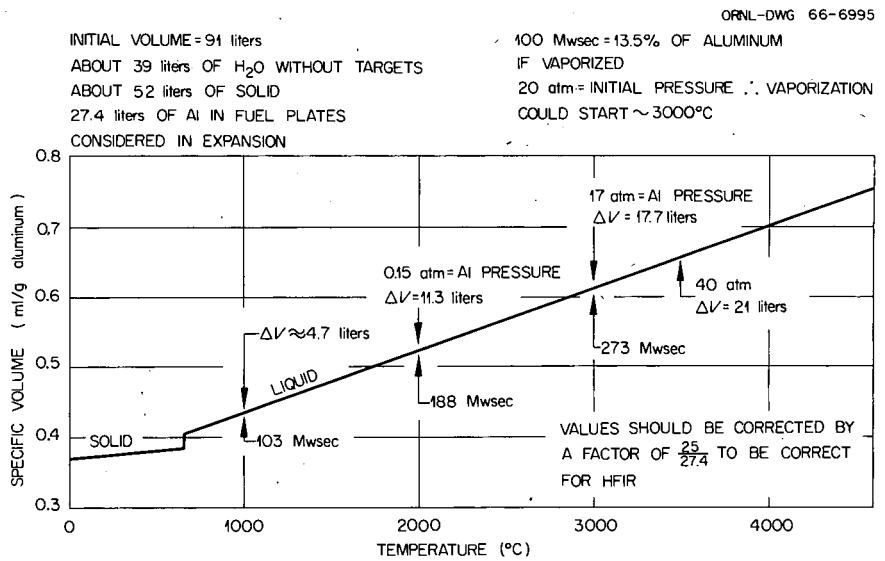

Fig. II.1.5. Specific Volume of Aluminum vs Temperature.

Rate of Reaction of Solid Aluminum with Water at High Temperatures

Model:

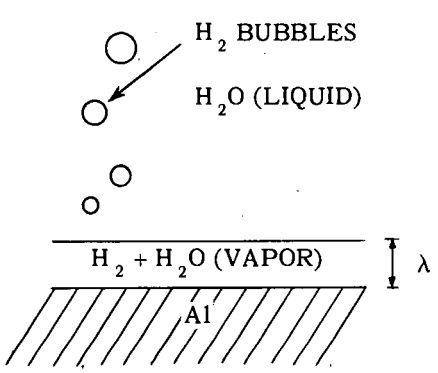

Assumption: The reaction at the surface of the Al is sufficiently rapid that a film, of thickness λ, is produced. The rate of reaction is then controlled by the transport of water vapor across the film.

Two factors control water vapor transport across the film: migration via a gaseous diffusion mechanism, and the transport of heat, in the opposite direction, which is necessary to vaporize the liquid. We first consider that the heat transfer is sufficiently fast that the governing step is diffusion-controlled. From the reaction

$$2Al + 3H_2O = Al_2O_3 + 3H_2 ,$$

we note a one-to-one correspondence between H_2O and H_2; hence the rate of generation of H_2 is equal to the rate of depletion of H_2O, which, in turn, is equal to the diffusion rate. Now

$$J_{H_2O} = \frac{D_{H_2O\text{-}H_2} p^0_{H_2O}}{RT\lambda} \text{ (moles cm}^{-2}\text{ sec}^{-1}\text{)} ,$$

where $p^0_{H_2O}$ is the vapor pressure of H_2O at the temperature T, R is the gas constant, and $D_{H_2O\text{-}H_2}$ is the diffusion coefficient of the pair H_2O-H_2. But the film thickness, on the other hand, is proportional to the rate of production of hydrogen; thus

$$\lambda = KJ_{H_2} = KJ_{H_2O} ,$$

where K is chiefly a function of geometry and external constraints. Hence

$$J^2_{H_2O} = \frac{D_{H_2O\text{-}H_2} p^0_{H_2O}}{KRT} = \frac{(pD_{H_2O\text{-}H_2})\,(p^0_{H_2O}/p)}{KRT} ,$$

where $(pD_{H_2O\text{-}H_2})$ is a function only of temperature, that is,

$$(pD_{H_2O\text{-}H_2}) = CT^{(3/2 \text{ to } 2)} .$$

But $(p^0_{H_2O}/p)$ is always less than 1; hence we can establish an upper limit by setting $(p^0/p) = 1$ and $(pD) = CT^2$; then

$$J^2_{H_2O} = (\text{const})T ,$$

or

$$J_{H_2O} = (\text{const})' T^{1/2} .$$

The rate therefore increases very slowly with temperature, since it is diffusion-controlled. Moreover, the film thickness is self-stabilizing. For example, if λ is initially too small, the increased H_2 generation pushes the liquid back; if too large, the decreased H_2 generation collapses the film. Moreover, if the reaction is thermal-conduction-controlled, then $p^0_{H_2O}$ is smaller than the vapor pressure at T = aluminum surface temperature, and the relations above become upper limits; that is, the flux will be even slower than

$$J_{H_2O} = (\text{const})' T^{1/2} .$$

Note, however, that turbulence will significantly increase the reaction rate by decreasing the film thickness.

APPENDIX J

CONTAINMENT POTENTIAL OF THE HFIR PRESSURE VESSEL AND PRIMARY COOLANT SYSTEM

This describes a model developed for estimating the effects of a nuclear excursion followed by an aluminum-water reaction on the HFIR pressure vessel and primary coolant system. The purpose is to determine a minimum upper bound of such an accident that can be contained.

The effect of a large nuclear excursion in the HFIR core would be to melt and, perhaps, vaporize a portion of the aluminum in the fuel plates. It is envisioned that the destructive effects of such an excursion would appear in two stages. The first stage, with duration measured in milliseconds, would involve rapid generation of superheated steam and exothermic reaction of any vaporized aluminum with steam to form Al_2O_3, hydrogen gas, and more steam. This first stage would conceivably disperse the remaining molten aluminum in the water. The second stage, measured in seconds, would involve diffusion–heat transfer limited burning of the molten aluminum particles that exceed the ignition temperature of about 3500°R. This reaction is also exothermic and would generate hydrogen and steam. Factors that would tend to mitigate the destructive potential of the hot gases include plastic expansion of the vessel and piping system, flow of water through the pressure relief system, collapse of steam bubbles, and dissolution of the hydrogen gas in the water.

The general approach in developing a model to describe these events has been to select experimentally based equations of state for the vessel and primary coolant system and incorporate the pressure-energy suppression mechanisms for which reliable data are available. The primary coolant system operates at high pressure (600 psi) but low temperature (~150°F); therefore, there is relatively little stored energy in the system but an efficient mechanism for transferring impulse from the gas bubbles to the walls of the container. We have avoided an involved analysis of the mechanism of energy flow in the prompt stage of the conflagration by assuming that all the available energy is transferred to the gas phase and that the gas does static, reversible work on the pressure vessel. A "TNT equivalent" shock wave would cause less strain in the vessel because of inherent inefficiencies, increased strength of the vessel under dynamic loading, and transmission of shock-wave energy through the vessel wall and into the surrounding pool.

The slower second stage of the conflagration, the delayed Al-H_2O reaction, is analyzed by taking credit for static, reversible strain work in the primary coolant system and flow of water from the system through the pressure relief valves. No credit is taken for collapse of steam bubbles or solubilization of hydrogen gas.

The calculated energy releases for marginal containment by the HFIR pressure vessel and primary coolant system are summarized in Table II.J.1. A nuclear excursion of 1600 Mwsec can be contained, based on the ultimate strength of the vessel, if there is no Al-H_2O reaction. The allowable excursion to cause $\frac{1}{3}$ ultimate strain in the vessel, a value that has been recommended for safe design to accommodate "TNT equivalent detonations," is 600 Mwsec. If the nuclear excursion causes prompt reaction of any vaporized aluminum, the allowable nuclear excursion is reduced to 610 and 380 Mwsec for ultimate strain

Table II.J.1. Energy Release by a Nuclear Excursion and Aluminum-Water Reaction for Marginal Containment by the HFIR Pressure Vessel and Primary Coolant System

This analysis takes credit for the internal energy of gaseous products, strain work on the vessel in the prompt portion of the reaction, and strain work on the piping and flow through the pressure relief system in the delayed Al-H_2O reaction

	Energy Release (Mwsec)		
	Prompt Reaction[a]		Delayed[b]
	Nuclear	Al-H_2O	Al-H_2O Reaction
Nuclear excursion, "steam explosion"	1600		
With $\frac{1}{3}$ ultimate strain[c]	600		
Nuclear excursion plus prompt Al-H_2O reaction	610	860	
With $\frac{1}{3}$ ultimate strain[c]	380	220	
Nuclear excursion plus prompt and delayed Al-H_2O reaction	610	860	4500[d]
With $\frac{1}{3}$ ultimate strain[c]	380	220	1250[d]

[a]The prompt reactions deposit 200 and 56 Mwsec of strain energy in the vessel wall, assuming ultimate strain and $\frac{1}{3}$ ultimate strain respectively.

[b]The delayed Al-H_2O reaction deposits 400 and 115 Mwsec of strain energy in the piping system, assuming ultimate strain and $\frac{1}{3}$ ultimate strain respectively.

[c]The use of $\frac{1}{3}$ the ultimate strain has been recommended for the safe design of reactor pressure vessels to accommodate "TNT equivalent detonations."

[d]This portion of the release is not possible. The potential delayed Al-H_2O energy release is only 755 Mwsec following a prompt Al-H_2O reaction of 860 Mwsec and only 1100 Mwsec following a prompt Al-H_2O reaction of 220 Mwsec.

and $\frac{1}{3}$ ultimate strain respectively. These same nuclear excursions can be tolerated if there is delayed reaction of all the remaining aluminum that is heated above the ignition temperature.

The following sections contain a description of the assumed properties of the vessel and coolant system; the model used in estimating the effects of the "steam explosion," prompt Al-H_2O reaction, and delayed Al-H_2O reaction; and a discussion of the reliability of the results.

Properties of the HFIR Pressure Vessel and Primary Coolant System

Material, strength, and dimensional properties of the HFIR pressure vessel and important components of the primary coolant system are shown in Table II.J.2. Pressure-volume relationships for the vessel and coolant system will be developed in the following sections.

Table II.J.2. Properties of the HFIR Pressure Vessel and Primary Coolant System

	Vessel	Piping	Heat Exchanger Tubing
Material	ASTM A212-B steel	304 stainless steel	304L stainless steel
Nominal yield stress, σ_e^0, psi	38,000	30,000	25,000
Nominal ultimate stress, σ_u^0, psi	70,000–85,000	80,000	70,000
Nominal ultimate strain, e_u^0	0.22	0.65	0.22
Operating temperature, T_0, °F	150	150	150
Operating pressure, P_0, psi	600	600	600
Volume, V_0, ft^3	668	485	455
Mean radius, R_i, in.	48.5	5–10	0.295
Wall thickness, X_i, in.	3	0.36–0.6	0.035
Length, ft	~14	400	270,000

HFIR Pressure Vessel

An equation of state for the A212-B HFIR pressure vessel that will underestimate the deformed volume at a given pressure was chosen on the basis of experimental data[1] of the radial strain in hydrostatically loaded A335-22 steel cylinders that were rigidly fixed at both ends. A nominal-circumferential-stress–nominal-strain relationship for the HFIR vessel was determined from the measured relationship for the A335-22 vessel by comparing published true-stress–true-strain data[1] for the two materials (Fig. II.J.1) and assuming that the nominal circumferential stress is proportional to true stress. A true stress-strain formula for A212-B steel has been reported[1] for a heat of A212-B steel that had a nominal ultimate strength of 82,000 psi and a nominal ultimate strain of 0.19:

$$\sigma = 155{,}000\ \epsilon^{0.245} .$$

In our analysis we have assumed that the A212-B steel has the minimum nominal ultimate strength (70,000 psi) and a nominal ultimate strain of 0.22. In terms of radial displacement the assumed equation of state is:

$$\left(\frac{PR_i}{X_i}\right) = 84{,}900\left[1 - e^{-60(R-R_i)/R_i}\right] , \tag{1}$$

where

P = the resisting pressure, psi,

R = deformed radius, in.

Parabolic deformation of the vessel will furnish a lower estimate of the deformed volume, V, of the vessel for a given radial strain:[1]

$$V \geqq V_0\left[1 + 1.44\left(\frac{R - R_i}{R_i}\right)\right] . \tag{2}$$

[1]M. A. Salmon *et al.*, *Studies of Reactor Containment Structures*, IITRI-578P22-14, pp. 189, 229.

ORNL DWG 66-5017

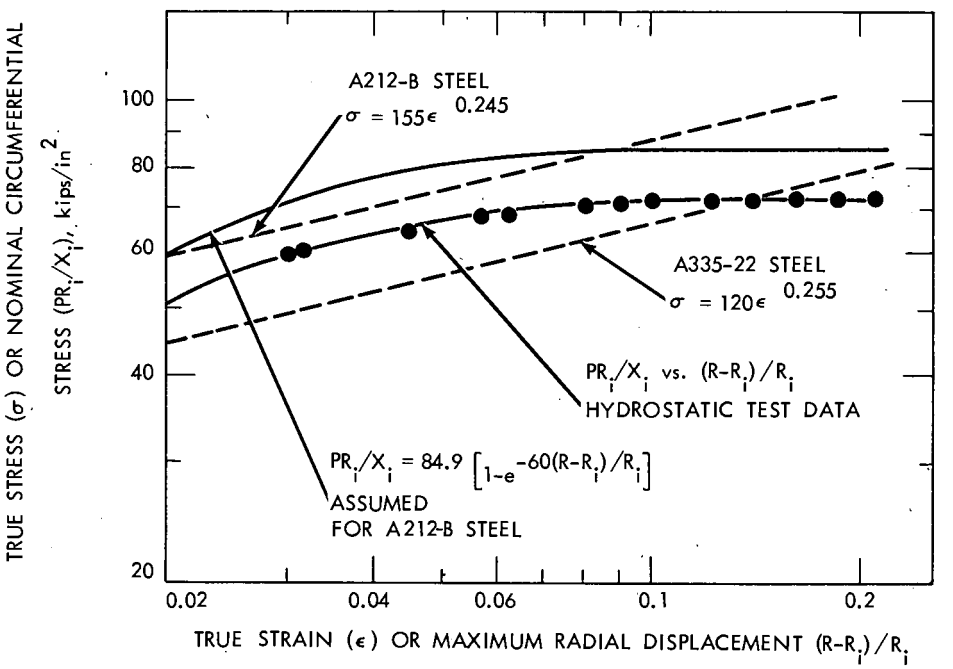

Fig. II.J.1. True Stress-Strain Relations for A335-22 and A212-B Steels and Nominal Circumferential Stress–Nominal Strain as Measured for an A335-22 Cylinder and as Assumed for the HFIR Pressure Vessel. Cylindrical vessels with rigid ends. $L/D = 2$.

An expression for the resisting pressure as a function of the incremental volume of the deformed vessel, v_v, is obtained by combining Eqs. (1) and (2):

$$P = P^*\left(1 - e^{-\lambda v_v}\right), \tag{3}$$

where

$P^* = 5250$ psi,

$\lambda = 0.0624\ \text{ft}^{-3}$,

$v_v = V - V_0$, ft^3.

The strain energy in the vessel as a function of resisting pressure is obtained as:

$$\int_0^P P\, dV = P^* v_v - \frac{P}{\lambda},\ \text{ft}^3\text{-psi}\ . \tag{4}$$

The bursting pressure and strain energy at rupture ($\epsilon_u = 0.22$) as calculated with these formulas are 5250 psi and 200 Mwsec respectively. These numbers are conservatively below those that are predicted for the actual HFIR pressure vessel. We have chosen to use the ultimate strain of the model vessel since it is our contention that for the assumed type of accident the vessel will fail by a ductile mode. In the HFIR vessel the nozzles and piping are reinforced and located in such a way that gross ductile deformation without failure is to be expected.

Primary Coolant System

Hydrostatic test data[1] are available for 304 stainless steel cylinders having a length-to-diameter ratio of 3 (Fig. II.J.2). These data were assumed to apply to the pipes in the primary coolant system because the nominal properties of the materials are essentially the same and the nominal-circumferential-stress—nominal-strain data at the crown of the bulge in a hydrostatically deformed cylindrical vessel are independent of end effects at this length-to-diameter ratio. We have assumed these same properties for the 304L stainless steel heat exchanger tubing because these tubes have greater wall-thickness-to-radius ratio and, therefore, greater bursting pressure than the 304 stainless steel piping in the system (Table II.J.3).

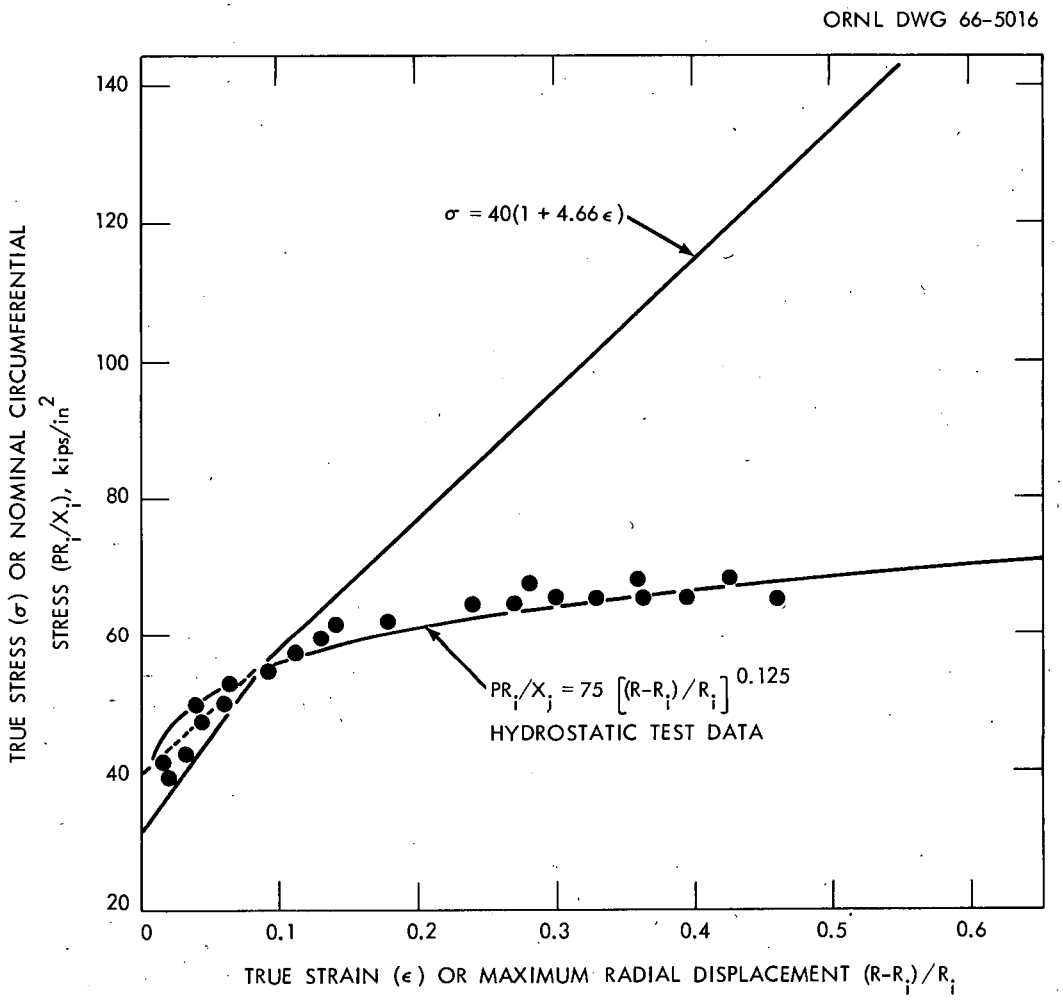

Fig. II.J.2. True Stress-Strain Relation for 304 Stainless Steel and Nominal Circumferential Stress–Nominal Strain as Measured for a Vessel Having $L/D = 3$.

Table II.J.3. Properties of the HFIR High-Pressure Coolant System

Part of System	Dimensions: Inside Diameter (in.)	Dimensions: Wall (in.)	Dimensions: Volume, V_0 (ft^3)	Ultimate Strain, ϵ_u	Bursting Pressure,[a] P_b (psi)	Incremental Volume[b] at 4350 psi (ft^3)	Strain Energy at 4350 psi[c] (Mwsec)
Heat exchanger tubing	0.555	0.035	455	0.22	7350	3	2
Pipe	10.02	0.365	55	0.65	5000	28	21
Pipe	13.13	0.438	50	0.65	4590	42	32
Pipe	15.0	0.500	40	0.65	4590	34	25
Pipe	16.88	0.562	150	0.65	4580	128	96
Pipe	18.81	0.593	190	0.65	4350	247	186
Heads, pumps			125	0.65	> 4500	50	38
Total			1065			530	400

[a] $P_b = K\epsilon_u^{0.125} X_i/\bar{R}_i$, $K = 75{,}000$ psi for pipe and tubing.
[b] $v = V_0 l\epsilon$, $l = 2.0$ for pipe and tubing.
[c] $E_s = (0.889 P_b v)(144)/0.7375 \times 10^6$.

The following function has been used to fit the nominal-circumferential-stress–nominal-strain test data:

$$\left(\frac{PR_i}{X_i}\right) = 75{,}000 \left(\frac{R - R_i}{R_i}\right)^{0.125} . \tag{5}$$

For long pipes the deformed volume, V, as a function of radial strain is given by:

$$V = V_0 \left[1 + 2\left(\frac{R - R_i}{R_i}\right)\right] . \tag{6}$$

An expression of the incremental volume of the primary coolant system, v_p, as a function of the resisting pressure, P, is obtained by combining Eqs. (5) and (6) and using the data in Table II.J.3:

$$v_p = V - V_0 = CP^8 ,$$

$$C = 4.14 \times 10^{-27} \text{ ft}^3/(\text{psi})^8 . \tag{7}$$

The strain energy in the primary coolant system as a function of resisting pressure is:

$$\int_0^P P\, dV = 0.889\, P v_p, \text{ ft}^3\text{-psi} . \tag{8}$$

The bursting pressure and ultimate strain energy of the primary coolant system are 4350 psi and 400 Mwsec. By comparison, the primary coolant system would rupture at a lower pressure but requires more energy than the pressure vessel.

The Effect of a "Steam Explosion"

If there is no metal-water reaction the minimum energy yield of a nuclear excursion to rupture the HFIR pressure vessel can be estimated using thermodynamics. It is assumed that the effect of the nuclear excursion is to instantaneously heat the aluminum. The aluminum then transfers its heat to the water, making steam at a given temperature, and doing reversible work on the pressure vessel in the process.

The equation of state of the steam is described by the ideal gas law with a compressibility factor, Z:

$$Pv = Zn_s RT \ , \tag{9}$$

where P, v, T, and n_s are the pressure, volume, temperature, and number of moles of steam.

The strain work in the vessel [Eq. (4)] as a function of resisting pressure, P, and volume of gas, v, is:

$$E_s = \text{strain work} = P^* v - P/\lambda \ .$$

Using the first law of thermodynamics and the expression for E_s, the heat, Q, that is transferred from the aluminum to the water initially at 610°R to make steam (neglecting the original volume of the water used to make steam) is:

$$\begin{aligned} Q &= n\,\Delta u + E_s \\ &= n_s\,\Delta H_v + n_s\,\bar{C}_p(T - 610) - Pv + E_s \ , \end{aligned} \tag{10}$$

Δu = the difference in internal energy between the steam and water,

$\bar{C}_p$ = the mean molal heat capacity of steam at constant pressure over the domain 610°R to T, Btu lb-mole^{-1} °R^{-1},

ΔH_v = the heat of vaporization of water $\cong$ 18,900 Btu/lb-mole.

The heat in the aluminum (5.98 lb-moles in the fuel plates) as a function of temperature, T, is given by:

$$\begin{aligned} \Delta H_{Al} &= 5.89[2970 + 7.2(T - 1080)] \ , \\ &\qquad\qquad 1080 \leqq T < 1678 \ , \\ &= 5.89[11{,}900 + 7(T - 1678)] \ , \\ &\qquad\qquad 1678 \leqq T < 6687 \ , \\ &= 5.89[48{,}400 + 127{,}260 + 4.97(T - 6687)] \ , \\ &\qquad\qquad 6687 < T \ , \end{aligned} \tag{11}$$

ΔH_{Al} = heat content of the Al above 610°R where the heat capacity of the liquid and gas (7 and 4.97 Btu lb-mole^{-1} °R^{-1}, respectively), the heat of vaporization (127,260), and other thermodynamic properties are taken from refs. 2 and 3. The boiling point of aluminum at the initial pressure (600 psi) is 6687°R.

If Q_e is the heat released in the nuclear excursion, heat is transferred only if the temperature of the aluminum is greater than or equal to the temperature of the steam:

$$Q = Q_e - Q_{al} \ . \tag{12}$$

Using thermodynamic data and compressibility factors[2–4] these equations were solved by iteration to determine the strain work done on the vessel as a function of the energy pulse of the excursion and the final steam (and aluminum) temperature. The results (Fig. II.J.3) indicate that a "steam explosion" caused by a nuclear energy pulse of 1600 Mwsec, or less, cannot do the minimum amount of work that is required to rupture the vessel. A nuclear excursion of 600 Mwsec is required to deposit $\frac{1}{3}$ the ultimate

[2] J. F. Elliot and Molly Gleiser, *Thermochemistry for Steelmaking*, pp. 16, 17, 53, 162, 176, Addison-Wesley.

[3] K. K. Kelley, *Contributions to the Data on Theoretical Metallurgy*, Bulletin 584, Bureau of Mines, pp. 10, 80 (1960).

[4] O. A. Hougen and K. M. Watson, *Chemical Process Principles Charts*, pp. 36, 37, 103, Wiley, 1946.

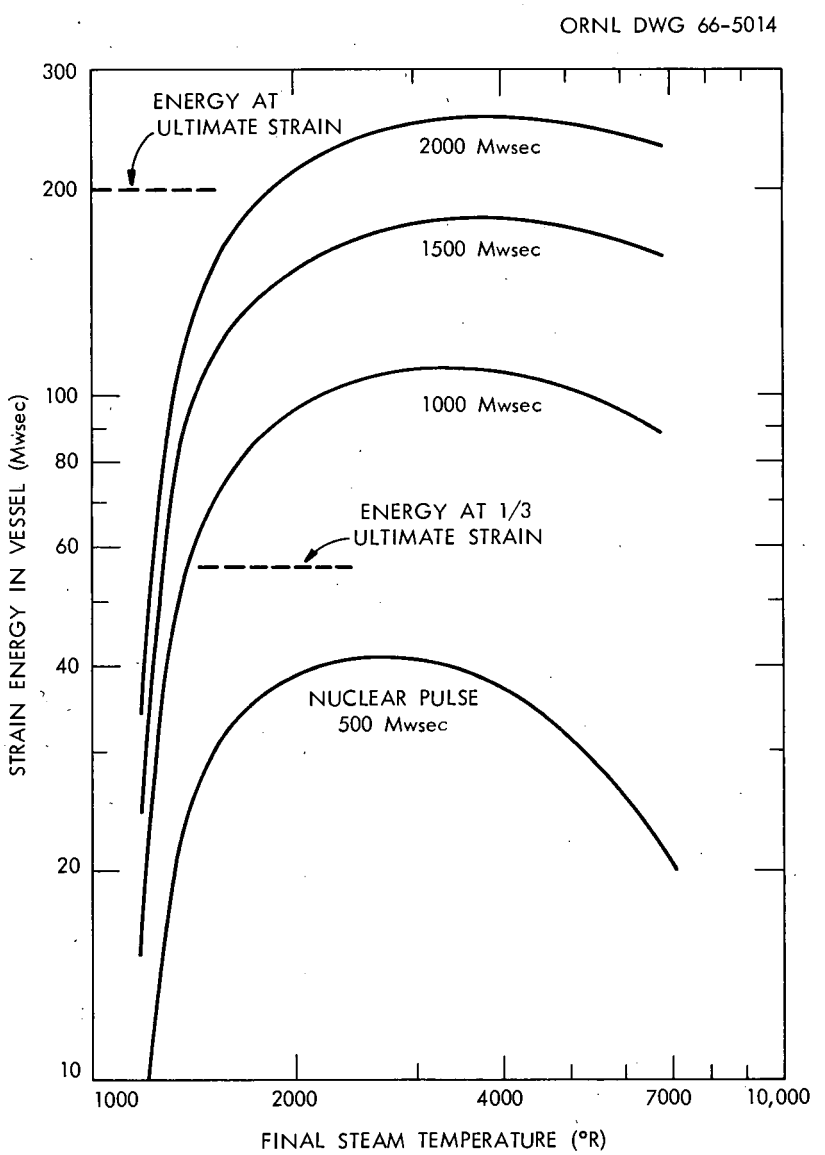

Fig. II.J.3. The Effect of Steam Temperature and Nuclear Energy Pulse on the Strain Energy in the HFIR Pressure Vessel. "Steam explosion" only – assumes no metal-water reaction.

strain energy in the vessel. For the 1600-Mwsec energy pulse the maximum strain work corresponds to a final steam-aluminum temperature of ~3500°R (2000°K). The steam temperature for maximum strain work decreases monotonically with a decrease in the magnitude of the energy pulse, approaching a minimum of 1165°R (the critical temperature of steam) for small energy pulses. The assumption that the core was heated uniformly was appropriate for this analysis, because all portions of a multiregion core would be heated to temperatures in excess of 3500°R by an energy pulse greater than 400 Mwsec.

Nuclear Excursion and Prompt Al-H_2O Reaction

In estimating the effects of a nuclear excursion followed by a prompt Al-H_2O reaction we have assumed that the effect of the nuclear excursion is to rapidly heat the aluminum in the core. Each pound-mole of aluminum that is vaporized reacts instantaneously with water initially at 610°R to form ½ mole of Al_2O_3 and ³⁄₂ moles of H_2 at 6687°R (the boiling point of aluminum at the initial pressure) and release 162,000 Btu of heat (see Table II.J.4). This heat is not available to vaporize more aluminum (because of the

Table II.J.4. Thermal Power of Al-H_2O Reaction

Reactions:

$$Al(l, T) = Al(g, T),\ \Delta H_1 = 70{,}700 \text{ cal/g-mole} \quad (1)$$

$$\tfrac{3}{2}H_2O(l, 339°K) = \tfrac{3}{2}H_2O(g, T),\ \Delta H_2 \quad (2)$$

$$Al(g, T) + \tfrac{3}{2}H_2O(g, T) = \tfrac{3}{2}Al_2O_3(S, l, T) + \tfrac{3}{2}H_2(g, T),\ \Delta H_3 \quad (3)$$

$$Al(l, T) + \tfrac{3}{2}H_2O(l, 339°K) = \tfrac{3}{2}Al_2O_3(S, l, T) + \tfrac{3}{2}H_2(g, T),\ \Delta H_4 \quad (4)$$

Temperature, T (°K)	State[a] and Enthalpy[b] (cal per mole of Al) for Reactants and Products								ΔH_4,[c] Net Heat Absorbed by Reaction (cal per gram-mole of Al)
	Reactants				Products				
	Al		³⁄₂H_2O		½Al_2O_3		³⁄₂H_2		
	State	H	State	H	State	H	State	H	
339	S, T	240	l, T	1,110	S, T	390			
1900	l, T	13,630	g, T	40,020	S, T	23,180	g, T	17,750	−71,535
2000	l, T	14,330	g, T	41,830	S, T	24,740	g, T	18,970	−69,455
2100	l, T	15,030	g, T	43,680	S, T	26,320	g, T	20,200	−67,345
2300	l, T	16,430	g, T	47,430	S, T	29,460	g, T	22,700	−63,105
2300	l, T	16,430	g, T	47,430	l, T	42,460	g, T	22,700	−50,105
3000	l, T	21,330	g, T	61,080	l, T	52,610	g, T	31,740	−35,815
3500	l, T	24,830	g, T	71,180	l, T	59,860	g, T	38,420	−25,385
3826	l, T	27,110	g, T	77,880	l, T	64,590	g, T	42,890	−18,465
3826	g, T	97,810	g, T	77,880	l, T	64,590	g, T	42,890	−89,165
4500	g, T	101,160	g, T	91,940	l, T	74,360	g, T	51,920	−73,715
5000	g, T	103,650	g, T	102,520	l, T	81,610	g, T	58,740	−62,135

[a]Solid (S), liquid (l), gas (g), and temperature (T).

[b]Enthalpy (H) with reference to an initial state of 298°K and 40 atm.

[c]At 298°F the assumed heats of formation of water and Al_2O_3 are −68,317 and −400,400 cal per gram-mole of Al respectively. The heat liberated in the reaction at 932°K (the melting point of Al) is 113,600 cal per mole of Al, assuming all reactants and products are at this temperature.

violent mixing), but rather increases the temperature of the reaction products. The analysis presented in the previous section is repeated for the steam-hydrogen mixture, but for this case it is assumed that all of the heat of reaction (162,000 Btu per pound-mole of Al), the heat in the Al_2O_3 product above 610°R, and the heat in the unvaporized aluminum and hydrogen above a given temperature is available to form steam at that temperature.

A uniform distribution of power in the aluminum has been assumed for the analysis. For nuclear excursions between 150 and 400 Mwsec the uniform distribution results in a larger total Al-H_2O reaction than a typical distribution because a larger fraction of the aluminum is heated above the ignition temperature of 3500°R. All the Al is heated above the ignition temperature by larger excursions but the uniform power distribution tends to cause larger prompt Al-H_2O reactions (Table II.J.5).

Results of the analysis (Fig. II.J.4) show that a nuclear excursion of 610 Mwsec, which initiates 860 Mwsec of prompt Al-H_2O reaction, is required to deposit the ultimate strain energy of 200 Mwsec in the vessel. This excursion deposits an additional 57 Mwsec of strain energy in the primary coolant system as the pressure is equalized (Table II.J.5). The magnitude of the nuclear excursion required to deposit $\frac{1}{3}$ the ultimate strain energy of 56 Mwsec in the vessel is 380 Mwsec. This excursion initiates 220 Mwsec of prompt Al-H_2O reaction and deposits 21 Mwsec in the primary coolant system as the pressure is equalized.

Table II.J.5. Consequences of a Nuclear Excursion and Prompt Al-H_2O Reaction in the HFIR and Initial Conditions for a Delayed Al-H_2O Reaction

Based on a flat power distribution, initial pressure 600 psi, 72.2 kg aluminum in core

Energy release, Mwsec							
Nuclear	200	300	380	500	610	750	1000
Prompt Al-H_2O[a]	0	0	220	555	860	1250	1950
Potential delayed Al-H_2O[b]	1235	1235	1100	925	755	535	140
Fraction of Al vaporized							
Flat power distribution	0	~0	0.10	0.25	0.39	0.57	0.88
Six region distribution	~0	0.056	0.12	0.26	0.37	0.51	0.74
Effect of prompt reactions							
Strain work on vessel, Mwsec	11.5	19	56[d]	130	200[e]	300	460
Maximum pressure in vessel, psi			5185		5250		
Final pressure in system,[c] psi			3150		3500		
Strain work on piping,[c] Mwsec			21		57		

[a]Resulting from Al that is vaporized.

[b]Resulting from Al above 3500°R but unvaporized.

[c]After equalization of pressure in the vessel and piping following the nuclear excursion and prompt Al-H_2O reaction.

[d]One-third ultimate strain energy of vessel.

[e]Ultimate strain energy of vessel.

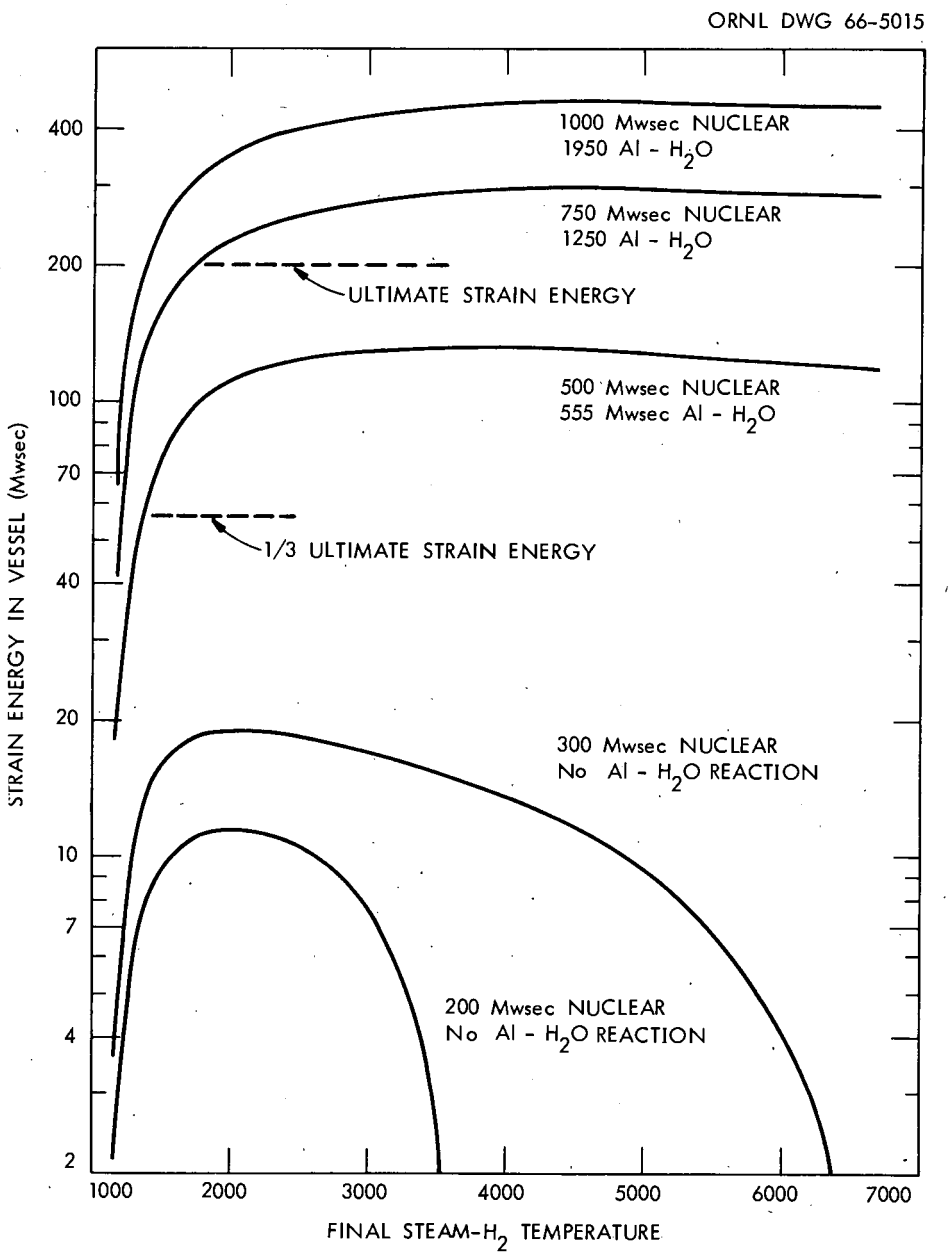

Fig. II.J.4. The Effect of Gas Temperature and Prompt Energy Release in the HFIR Pressure Vessel. The energy release is from the nuclear excursion plus prompt reaction of any vaporized aluminum.

Delayed Metal-Water Reaction

A model is developed to estimate the pressure transient and strain energy deposited in the primary coolant system by a delayed Al-H_2O reaction that follows a nuclear excursion and prompt Al-H_2O reaction of any vaporized aluminum. The following assumptions are made:

1. The nuclear excursion and prompt Al-H_2O reaction deposit either the ultimate strain energy or $\frac{1}{3}$ the ultimate strain in the vessel but leave the aluminum that is unvaporized above the ignition temperature of 3500°R. Immediately following the prompt stage of the conflagration the molten aluminum is dispersed in the water as small particles and the pressure in the vessel and system is equalized. The elastic reduction of the volume of the vessel following relaxation of the pressure is negligible. Since the piping system will fail at a lower pressure than the vessel, the net effect of the delayed aluminum-water reaction is to cause strain only in the primary coolant system.

2. The delayed metal-water reaction proceeds at a constant rate for a given assumed particle size. The average rate, duration of the reaction, and the fraction of aluminum that reacts as a function of the particle size are shown in Table II.J.6. The flame temperature of the reaction is about 3500°R (see Appendix I). The aluminum-water combustion reaction cannot be initiated at significantly lower temperatures and is diffusion-heat-transfer limited at higher temperatures. It is assumed that the Al_2O_3 and the surplus heat of reaction form steam at 3500°R. If $\bar{P}_0$ is the average power of the delayed metal-water re-

Table II.J.6. Extent of Reaction and Energy Releases as Functions of Initial Particle Diameter

D_0 (cm)	f	$(1-f)$	E* (Mwsec)	t (sec)	$P(0)$* (Mwsec/sec)	$\bar{P}_0$* (Mwsec/sec)
0.336	1	0	0	0	176	0
0.35	0.88	0.12	148	0.88	169	168
0.40	0.58	0.42	520	4	148	130
0.45	0.41	0.59	726	7.12	131	102
0.50	0.3	0.7	863	10.25	118	84.2
0.60	0.175	0.825	1018	16.50	99	61.7
0.80	0.074	0.926	1141	29	74	39.3
1.00	0.038	0.962	1188	41.50	59	28.6
1.20	0.022	0.978	1206	54	49	22.3
1.50	0.011	0.989	1220	102.50	40	11.9
46.5	0	1	1235	2900	1.4	0.425

List of symbols:

D_0 Initial particle diameter, cm

f Fraction of Al not reacted

E Total energy liberated, Mwsec

t Time (or duration) of ignition reaction, sec

$P(0)$ Initial (or maximum) rate of energy generation, Mwsec/sec, based on the heat released in the reaction at 3500°R (1940°K), 200,000 Btu per pound-mole of Al

$\bar{P}_0$ Average rate of energy release during the ignition reaction

*These values differ from those in Table II.I.1, being adjusted to the actual HFIR Al content of 72.2 kg.

action (in megawatts based on the energy release at 3500°R of 200,000 Btu per pound-mole of Al), then the production rate of hydrogen and steam is $0.00715\bar{P}_0$ and $0.0160\bar{P}_0$ lb-moles/sec respectively.

3. The work of compression of the water in the high-pressure cooling system is neglected. At the minimum bursting pressure of a portion of the system, 4350 psi, the energy stored by compression of the water in the system (1700 ft^3) is 10 Mwsec.

4. The pressure relief valves in the high-pressure system open at 1000 psi and discharge 600 gpm when the system pressure is 1100 psi. For a large nuclear excursion that will generate steam pressure at least half the bursting pressure of the vessel, it is conservative but not unduly restrictive to assume that the relief system discharges water at a constant rate determined by the pressure developed by the nuclear excursion and prompt metal-water reaction; that is, $dv/dt = 0.040P_1^{1/2}$ cfs where P_1 has units of psi.

Based on these assumptions the model may be developed as follows:

Gas-filled volume of vessel and primary coolant system:

$$v = CP^8 + k_0 P_1^{1/2} t + v_1 , \tag{13}$$

$$\frac{dv}{dt} = 8CP^7 \frac{dP}{dt} + k_0 P_1^{1/2} , \tag{14}$$

where

v = volume of gas, ft^3,

$C = 4.14 \times 10^{-27}$,

P = resisting pressure of system, psi,

P_1 = steam and hydrogen pressure following nuclear excursion, psi,

$k_0 = 0.04$,

v_1 = volume of gas formed in prompt reactions, ft^3,

t = time since beginning of metal-water reaction, sec.

Ideal gas law:[5]

$$Pv = (n_s + n_h)RT , \tag{15}$$

where n_s and n_h are pound-moles of H_2 and steam respectively.

Rate constants:

$$\frac{dn_h}{dt} = k_h ; \; n_h = k_h t + n_h^0 , \tag{16}$$

$$\frac{dn_s}{dt} = k_s ; \; n_s = k_s t + n_s^0 , \tag{17}$$

$$k_h = 7.15 \times 10^{-3} \bar{P}_0 , \text{ lb-moles } H_2/\text{sec} ,$$

$$k_s = 1.60 \times 10^{-2} \bar{P}_0 , \text{ lb-moles steam/sec},$$

[5]It is appropriate to use the ideal gas law for this model because the gas temperatures ($\gtrsim$3500°R) are well above the critical temperatures.

where

$\bar{P}_0$ = average power of metal-water reaction, Mw,

k_h = average hydrogen production rate, lb-moles/sec,

k_s = average production rate of steam at 3500°R by the Al_2O_3 reaction product and the surplus heat of reaction,

q = net heat output of metal-water reaction (assumed zero for reaction temperature of 3500°R because the surplus heat is used to make steam),

n_h^0, n_s^0 = lb-moles of hydrogen and steam formed by nuclear excursion and prompt metal-water reaction.

Conservation of mass in the gas phase:

$$\frac{dn}{dt} = k_h + k_s - 0 \,. \tag{18}$$

Conservation of energy in the gas phase:

$$\frac{d}{dt}(nu) = H_h k_h + H_s k_s + q - \frac{dw}{dt} \,, \tag{19}$$

where

$\frac{d}{dt}(nu)$ = accumulation of mass and internal energy

$$= (k_h C_v^h + k_s C_v^s)T + [(k_h C_v^h + k_s C_v^s)t + n_0^h C_v^h + n_0^s C_v^s]\frac{dT}{dt} \,,$$

H = enthalpy at 3500°R, referred to 537°R (including heat of vaporization of the steam), Btu/lb-mole,

C_p = approximate heat capacity at constant pressure of a component of the gas in the vessel

$$= \frac{H}{3500 - 537} \,, \text{ Btu lb-mole}^{-1}\ {}^\circ\text{R}^{-1} \,,$$

C_v = approximate heat capacity at constant volume of a component of the gas in the vessel $= C_p - R$, Btu lb-mole^{-1} °R^{-1},

$\frac{dw}{dt}$ = rate of work done by the gas phase

$$= \frac{P}{J}\frac{dv}{dt} = \frac{8CP^8\,(dP/dt)}{J} + \frac{(k_0 P_1^{1/2})}{J} P \,, \text{ Btu/sec} \,,$$

$J = 5.4$ ft^3 psi/Btu.

Using Eqs. (13) and (15) the volume of gas in the vessel at any time is:

$$v = \frac{(k_h t + k_s t + n_h^0 + n_s^0)RT}{P} = CP^8 + k_0 P_1^{1/2} t + v_1 \,.$$

Solving this equation for T in terms of P and t, differentiating with respect to time, substituting dT/dt in Eq. (19), and collecting terms, one obtains:

$$(\alpha - \beta P)dt = \left(\gamma P^8 + \beta \frac{C_v}{C_p} t + \delta\right) dP \ , \tag{20}$$

where

$$\alpha = (H_h k_h + H_s k_s + q)J = 5.12 \times 10^3 \overline{P}_0, \ \mathrm{ft}^3 \ \mathrm{psi\ sec}^{-1} \ ,$$

$$\beta = \frac{C_p^*}{R} k_0 P_1^{1/2} = 0.283 P_1^{1/2}, \ \mathrm{ft}^3/\mathrm{sec} \ ,$$

$$\gamma = C \ \frac{9C_v^* + 8R}{R} = 62.8 \ C, \ \mathrm{ft}^3/(\mathrm{psi})^8 \ ,$$

$$\delta = \frac{C_v^* v_1}{R} = 6.09 v_1, \ \mathrm{ft}^3 \ ,$$

$$C_p^* \cong \frac{k_h C_p^h + k_s C_p^s}{k_h + k_s} = 14.08 \ ,$$

$$C_v^* \cong C_p^* - R = 12.10 \ .$$

For the case of no pressure relief ($k_0 = 0$), this equation has the solution

$$\alpha t = \frac{\gamma}{9} (P^9 - P_1^9) + \delta(P - P_1) \ . \tag{21}$$

For the case of steady-state pressure ($dP/dt = 0$, because the rate of increase of gas volume matches the flow of water from the system) the solution is:

$$P = \alpha/\beta \ . \tag{22}$$

The general solution of Eq. (16) is:

$$t = -\gamma \sum_{n=0}^{8} \frac{P^{8-n} \alpha^n 8!}{\beta^{n+1}(8-n)! \prod_{k=0}^{n} (m + 8 - k)} + \gamma \left(\frac{\alpha - \beta P_1}{\alpha - \beta P}\right)^{C_v/C_p} \sum_{n=0}^{8} \frac{P_1^{8-n} \alpha^n \ 8 \ !}{\beta^{n+1}(8-n)! \prod_{k=0}^{n} (m + 8 - k)}$$

$$+ \frac{\gamma C_p}{\beta C_v} \left[\left(\frac{\alpha - \beta P_1}{\alpha - \beta P}\right)^{C_v/C_p} - 1\right] \ . \tag{23}$$

Results of the Metal-Water Analysis Assuming No Pressure Relief. – Using Eq. (8) the total strain work done on the primary coolant system, E_s, is a function of the maximum pressure in the transient:

$$E_s = 0.889 C P^9 \ .$$

Equation (21) may be used to determine the work done on the primary coolant system assuming no pressure relief:

$$\alpha t = \frac{\gamma}{9}(P^9 - P_1^9) + \delta(P - P_1) .$$

Multiplying through by 0.889 and converting to Mwsec the total strain energy in the primary coolant system is:

$$E_s = E_s^1 + 0.127\overline{P}_0 t - 0.000152 v_1 (P - P_1) , \tag{24}$$

where E_s^1 is the strain energy deposited in the primary coolant system by equalization of the pressure following the prompt reactions. For the nuclear excursion that deposits 200 Mwsec of strain energy in the vessel (610 nuclear, 860 prompt Al-H_2O) the initial volume of gas, pressure, and strain energy in the primary coolant system are 212 ft^3, 3500 psi, and 57 Mwsec respectively. A total delayed Al-H_2O energy release of 2700 Mwsec is required to deposit the ultimate strain energy of 400 Mwsec in the piping system. The potential delayed Al-H_2O reaction, determined by the aluminum above the ignition temperature but unvaporized, is only 755 Mwsec following a prompt Al-H_2O reaction of 860 Mwsec.

The Allowable Steady-State Delayed Metal-Water Reaction. – The allowable steady-state rate of the delayed metal-water reaction is calculated using Eq. (22). The effect of this simplification allows us to write:

$$\frac{C_p^*}{R} k_0 P^{3/2} = \alpha = 5.12 \times 10^3 \overline{P}_0 .$$

Solving for $\overline{P}_0$ and substituting the bursting pressure of the primary coolant system (4350 psi):

$$\overline{P}_0 = 16 \text{ Mw} .$$

Referring to Table II.J.6, the system, with pressure relief, could sustain a metal-water reaction of "unlimited" duration if the diameter of the molten aluminum spheres is greater than 1.4 cm.

The General Case – Transient Delayed Metal-Water Reaction with Pressure Relief. – The pressure transient and the strain energy in the primary coolant system assuming pressure relief are calculated using Eq. (24) and reaction rates as a function of molten aluminum particle size from Table II.J.6. Results of the analysis, expressed in terms of strain energy in the primary coolant system as a function of initial aluminum particle size, are shown in Fig. II.J.5. The diameter of the particle that causes maximum strain work is about 0.6 cm; smaller particles do not react so completely; pressure relief becomes important for larger particles, which react slowly. The allowable delayed Al-H_2O reactions to cause ultimate strain and ⅓ ultimate strain in the primary coolant system are 4500 and 1250 Mwsec respectively. By comparison, only 755 and 1100 Mwsec of delayed Al-H_2O reaction are potentially available for the two cases.

Comments on the Adequacy of the Model

The model that we have used for this study assumed that reversible work is done by the gaseous products of a nuclear excursion–metal-water reaction and considered essentially only three factors that would tend to negate the effects, that is, the inherent internal energy of the gas, strain work on the vessel and piping system, and flow through the pressure relief system. There are many other mechanisms

ORNL DWG 66-5019

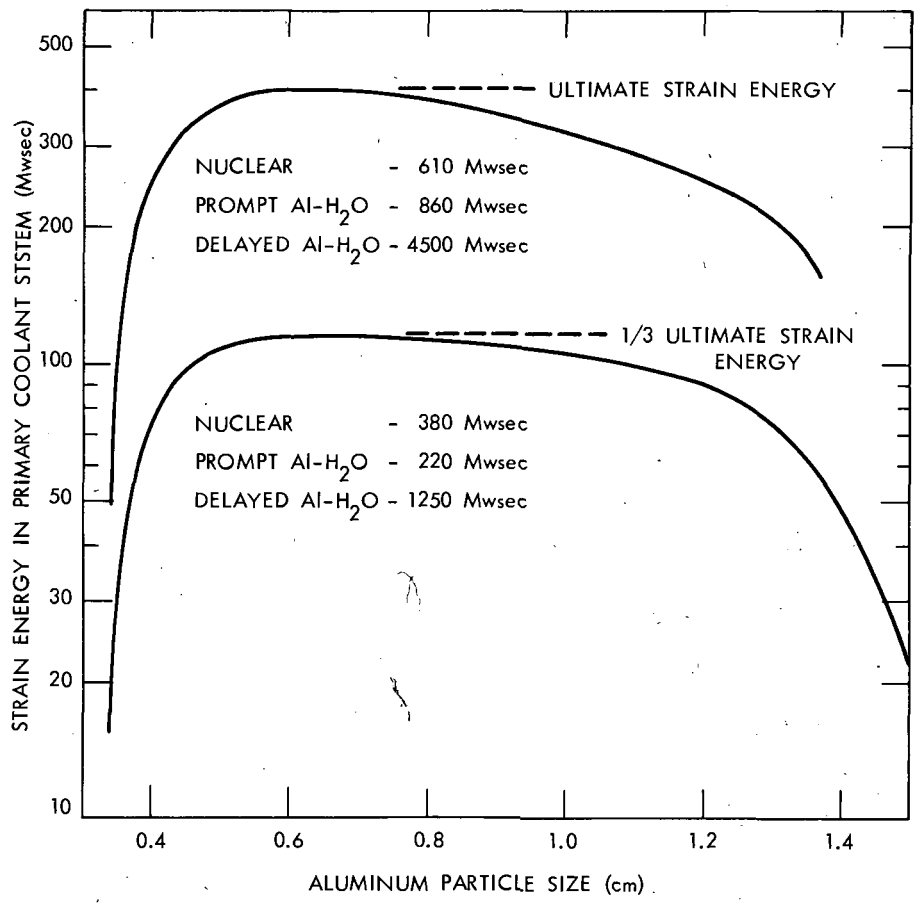

Fig. II.J.5. The Effect of Aluminum Particle Size and Magnitude of the Prompt and Delayed Energy Release on the Strain Energy Deposited in the Primary Coolant System.

that tend to make this model grossly conservative as it is applied to relatively slow reactions, such as the delayed metal-water reaction, but before we discuss these we will discuss the adequacy of the model for fast reactions by relating it to the results of high explosive tests.

The effect of exploding TNT in the HFIR pressure vessel may be estimated by analogy with experimental results[6] that were obtained by detonating pentolite in water-filled cylinders that were rigidly fixed at both ends and which had no external restraining forces. Properties of a single test that is most readily related to the HFIR are:

Vessel dimensions: 20 in. ID × 40 in. long × 1.030 in. wall

Material: 212 flange steel, nominal ultimate strength 76,200 psi, nominal ultimate strain 0.27

Pentolite charge: 4.96 lb, energy release 10.6 Mwsec, gas release 0.25 lb-mole

Maximum radial deformation: 0.23 (no rupture)

---

[6]W. R. Wise, Jr., and J. F. Proctor, *Explosion Containment Laws for Nuclear Reactor Vessels*, NOLTR-63-140, pp. 49, 71, 83 (1965).

At a nominal strain of 0.23 the 212 flange steel has approximately the same nominal stress that was assumed for the A 212-B steel in the HFIR pressure vessel. Consequently we have assumed the same equation of state [Eq. (1)]. Equations (2), (3), and (4) are also valid, but the values of P^* and λ are changed to $P^* = 8330$ psi, $\lambda = 5.73\ \text{ft}^{-3}$.

The strain energy in the vessel at the measured radial deformation (0.23) is 3.6 Mwsec for the vessel that is tamped by air. The effect of a water-filled pool in tamping the vessel is to increase the charge to cause the same deformation by at least a factor of 2 (ref. 6). Therefore, for the water-filled, water-tamped vessel the strain work efficiency of the pentolite charge is approximately 3.6/(2)(10.6) = 0.17.

A comparable strain work efficiency can be derived by the methods assumed for the present analysis. The total heat in the gas phase, Q, is

$$Q = nC_v\,(T - 530) + E_s\ , \tag{25}$$

Q = 10.6 Mwsec = 10,000 Btu,

n = moles of gas = 0.25 lb-mole,

C_v = heat capacity of the gas at constant volume $\cong$ 6.5 Btu lb-mole^{-1} °R^{-1},

T = absolute temperature of gas, °R,

$$E_s = P^*v - P/\lambda \cong nRT - P^*/\lambda\ . \tag{26}$$

By substituting Eq. (26) into Eq. (25) the temperature of the gas is found to be 4460°R. The strain work efficiency (E_s/Q) is then determined to be 0.22, which is higher than that expected for a pentolite detonation in a tamped vessel. It is observed that for either case the pentolite explosion is more efficient in producing strain energy than the "steam explosion" or Al-H_2O reaction.

The strain work efficiency should scale directly. Therefore, the pentolite charge required to impart 200 Mwsec of strain work to the HFIR pressure vessel is approximately 500 lb or 1200 Mwsec of energy. On the basis of experience with shock loading of pressure vessels it has been recommended[6] that only one-third the ultimate strain should be allowed in actual vessels as a factor of safety for nozzles and weldments. By such a procedure the maximum allowable pentolite charge would be about 330 Mwsec. We believe that it is unrealistic to apply a factor of safety of this magnitude for excursions in the HFIR vessel on the basis that the reactions will be much slower than for the detonation of high explosive; thus a smaller fraction of the total energy will appear in the shock wave (53% for pentolite) and nozzles will not be exposed to the same degree of brisance and vibration.

Factors that tend to make our model grossly conservative for slow reactions, that is, those that take place in time periods of a second or more such as the delayed Al-H_2O reaction, are as follows:

1. We have assumed no increase of the sensible heat content of the water in the pressure vessel. We know that steam bubbles will rapidly collapse and transfer sensible heat to the water but were not able to find defensible data on collapse rates at the temperatures and pressures of interest. If all the heat from a 1000-Mwsec energy pulse were transferred to the water in the vessel the temperature would increase by only 20°F and the strain energy deposited in the system would be negligible.

2. We have not assumed dissolution of the hydrogen in water. The solubility of hydrogen in water is such that all the hydrogen from the potential metal-water reaction could be dissolved.

APPENDIX K

CONTAINMENT POTENTIAL OF THE HFIR BUILDING

The Building

The type of accident which is considered is that in which the 2.67×10^3 g-moles of aluminum in the reactor core is rapidly and adiabatically heated to an extremely high temperature as the result of a fast nuclear excursion. A portion of this heat is then transferred to the water in and near the reactor core. The resulting steam which is formed then causes an increase in pressure in the reactor vessel. The situation is complicated by the fact that at temperatures above approximately 2050°K aluminum may react with steam, thus producing additional heat which will, in turn, generate more steam. It has been shown (see Appendix I) that, at temperatures below the boiling point of aluminum, this reaction proceeds relatively slowly. However, for that amount of aluminum which vaporizes, it will be assumed that the Al-H_2O reaction takes place instantly. In addition to the heat evolved, 1.5 moles of H_2 is generated per mole of Al reacted, and this is available to increase the pressure in the reactor vessel.

It is clear that no damage can result to the building unless the pressure vessel or some portion of the primary cooling system fails as a result of the energy pulse. The conditions under which this can occur have been discussed in Appendix J, which concludes that a total prompt energy release of about 1500 Mwsec is required to cause rupture of the vessel.

The reactor bay, which constitutes the secondary containment of the HFIR, contains a volume of 4.5×10^5 ft^3. Under the normal conditions – 25°C temperature and 60% relative humidity – the bay contains 5.428×10^5 moles of air and 1.07×10^4 moles of water vapor.

Assuming validity of the perfect gas law and a molar heat capacity at constant volume of 4.91 cal mole^{-1} °C^{-1}, the quantity of heat required to raise the temperature of the building atmosphere by 1°C is

$$5.535 \times 10^5 \times 4.91 = 2.718 \times 10^6 \text{ cal or } 11.4 \text{ Mwsec} .$$

Let $N_0 = 5.535 \times 10^5$ be the original number of moles of gas in the building, $p_0 = 14.7$ psi be its pressure, and $T_0 = 298$°K its temperature. Then if, at constant volume, the temperature is raised by an amount ΔT°C and the number of moles of gas or vapor is increased by an amount ΔN, it follows that the pressure will be increased by an amount

$$\Delta P = \frac{P_0}{N_0 T_0} (T_0 \, \Delta N + N_0 \, \Delta T + \Delta N \, \Delta T) . \tag{1}$$

It has been determined that no distortion of the building walls will occur for values of $\Delta P \leqq 0.8$ psi, and it is estimated that no serious disruption of the building walls would occur at twice this pressure difference; nevertheless, the former figure will be used. Upon putting $\Delta P = 0.8$ psi into Eq. (1) and solving for ΔT we obtain

$$\Delta T = 16.21 \left(\frac{1 - 3.320 \times 10^{-5} \, \Delta N}{1 + 1.807 \times 10^{-6} \, \Delta N} \right); \tag{2}$$

thus, if ΔN is zero the maximum permissible temperature increase is 16.21°C, whereas, if $\Delta N = 3.01 \times 10^4$ moles, no temperature increase can be tolerated without some distortion of the building. This relation is shown in Fig. II.K.1.

It is now necessary to consider the amounts of heat and vapor which could be supplied to the building atmosphere. The temperature of the steam formed in the reactor vessel will depend upon the total amount of energy transferred and upon the amount of water which is heated. Clearly, the more moles of water that receive a given quantity of heat, the lower will be the temperature of the steam. For example, to heat the entire contents of the reactor vessel from its original temperature, 63°C, to the boiling point at 40 atm pressure, 252°C, requires about 1.47×10^4 Mwsec of energy. On the other hand, the minimum amount of water which can be heated by transfer of energy from the aluminum is restricted by the fact that the steam cannot be generated at a higher temperature than the aluminum.

Because the actual course of events within the core during and immediately following a severe nuclear excursion is unpredictable, it is necessary to establish some criterion for determination of the steam temperature, which, in turn, permits calculation of the amount of steam generated. The work which can be done by the steam is proportional to the product, NT, of the number of moles of steam produced and its absolute temperature. Since the ability to perform work is directly related to the potential for damaging the pressure vessel, choice of a steam temperature which maximizes NT will give pessimistic results.

It has been found that for nuclear excursions in which little or no vaporization of the aluminum occurs (i.e., <225 Mwsec) and thus which do not cause rapid metal-water reactions, the appropriate value of T is 932°K. Here it is assumed that the aluminum solidifies and gives up its latent heat of fusion to the steam.

For those cases where considerable vaporization of the aluminum has occurred, the value of T which maximizes NT varies depending upon the total energy input; however, the maximum value of NT differs little from that obtained by setting $T = 2000$°K.

By using these values for the temperature and quantity of steam formed, together with the heat of reaction of the fast Al-H_2O reaction and the quantity of hydrogen which results from this reaction, it is possible to compute the composition, pressure, and heat content of the gaseous mixture in the reactor vessel. The procedure is presented in some detail in Appendix J.

If the maximum pressure reached is insufficient to rupture the system, then there is no damage to the building. On the other hand, if the internal pressure is great enough to rupture the system, the steam or steam-hydrogen mixture will escape from the vessel and may transfer heat to the building atmosphere.

There are three mechanisms by which heat will be lost from the gases before they reach the atmosphere: (1) the work required to actually rupture the vessel, (2) the work of expansion performed by the gas as it leaves the vessel, and (3) the quenching action in the reactor pool.

The first of these has been estimated to be approximately 200 Mwsec. This is the strain energy required to rupture the vessel. The effectiveness of the second mechanism depends to a large extent upon the mode of failure of the vessel. If, for example, a small nozzle fails, virtually all the energy can be expended in a relatively slow expansion as the pressure in the vessel is gradually released. On the other hand, if the failure took the form of a very large tear or rupture, the gas would undergo a very nearly

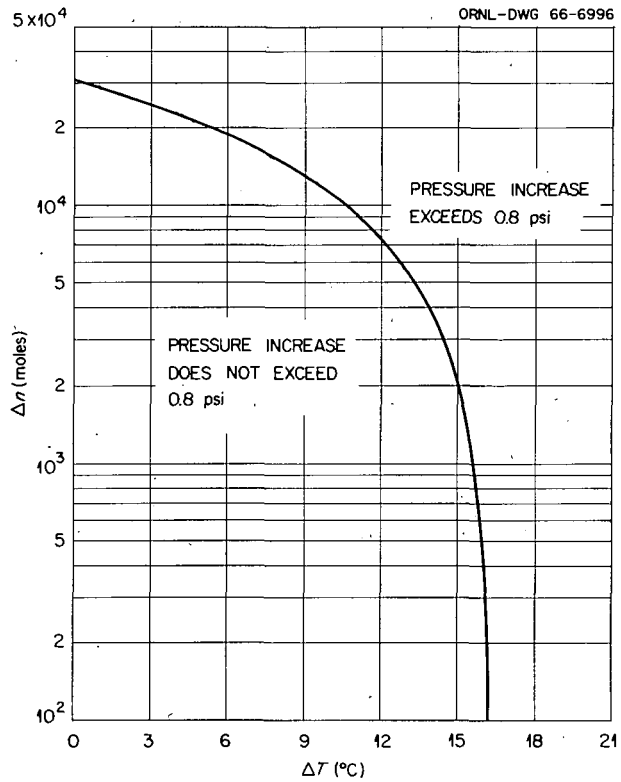

Fig. II.K.1. Moles of Steam vs Temperature Rise Required to Increase Building Pressure by 0.8 psi.

free expansion and, therefore, would do little work. Although it is believed that the mode of failure would most probably take the form of a relatively small opening, this is not completely certain, and therefore it is impossible to take credit for this type of energy loss.

The reactor vessel is located in the reactor pool, which contains approximately 80,000 gal of water, normally at about 35°C. The amount of heat required to raise the temperature of this water on the average of 1°C is 1265 Mwsec. The top of the reactor vessel is 17 ft below the surface of the water, and the center line of the reactor core is 27.5 ft below the reactor surface. Consequently, any escaping steam or hydrogen has to pass through at least 17 ft of water before reaching the atmosphere of the building. During this process, some of the energy contained in the hot gases will be lost to the pool water. The exact amount of energy which will be lost in this way depends upon the manner in which the gases are conveyed through the water. If gas is broken up into many small bubbles, the heat transfer may be almost complete. On the other hand, if the gas emerges in the form of a few large bubbles, there will be considerably less heat loss to the pool. Because it is not possible to predict the exact course of the bubble emission, the extremely conservative assumption that no heat is lost to the pool will be adopted.

Under normal conditions, the HFIR building operates at a temperature of 25°C and a relative humidity of approximately 60%. This means that the air in the building normally contains 1.07×10^4 moles of water

vapor and could accommodate 7.3×10^3 additional moles before reaching the dew point.[1] The amount of moisture which can be accommodated by the air in the building is shown as a function of temperature in Fig. II.K.2. Because of this, little, if any, of the steam will condense, and consequently its heat of vaporization is not available to raise the temperature of the building atmosphere.

The quantities of steam and hydrogen which are available as a result of various nuclear excursions have been calculated on the basis of information given in Appendix J.

In the following analysis it is assumed that each nuclear excursion considered is sufficient to rupture the pressure vessel and that all the available energy is used to instantly heat the air in the building, thus causing a step increase in pressure. The building overpressure as a function of the nuclear excursion is shown in Fig. II.K.3.

Because of the fact that the SBHE system is removing air from the reactor bay, this overpressure can persist for only a short time. The SBHE system exhausts air from the bay at a rate given by

$$E(p) = 2.65 \times 10^4 \sqrt{p - p_b} \text{ moles/min} ,$$

where p is the pressure in the reactor bay in psi and p_b is a base pressure equal to 14.258 psi. In addition to the loss through the SBHE system, there will be leakage from the building through various openings. This can be represented as

$$L(p) = K' \sqrt{p - p_a} \text{ moles/min} ,$$

where p_a is the ambient pressure and K' is a "leakage" constant which depends on the characteristics of the building. It is convenient to set $K' = 2.65 \times 10^4 a = Ka$, where a is a constant. Then the rate of loss from the building is just

[1] A 10°F increase in temperature would raise this value to 1.78×10^4 moles.

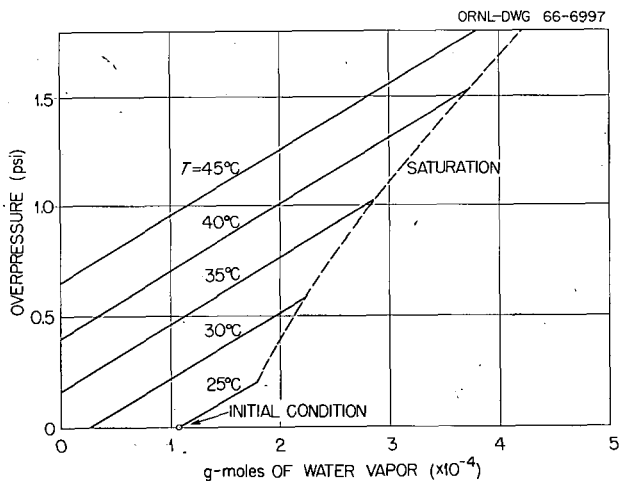

Fig. II.K.2. Moles of Water Vapor Which Can Be Accommodated by the Air in the HFIR Reactor Bay.

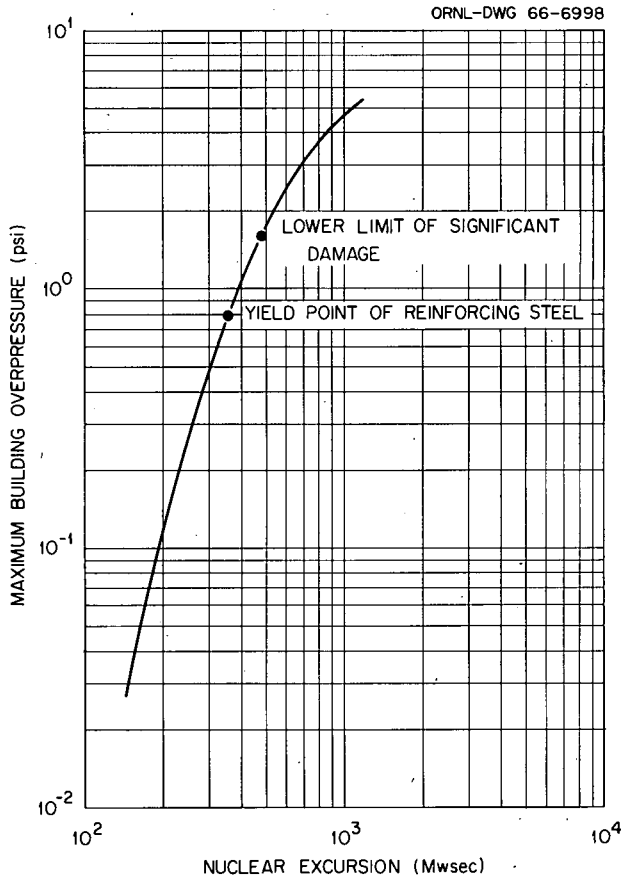

Fig. II.K.3. Maximum Building Overpressure as a Function of Nuclear Excursion Energy.

$$\dot{N}(t) = -K[\sqrt{p(t) - p_b} + a\sqrt{p(t) - p_a}] \text{ moles/min} .$$

This integral has been evaluated numerically between p_i, the initial overpressure, and p_a, the ambient pressure at which leakage to the environment ceases. The fraction of the building content which reaches the environment is given in Fig. II.K.4 as a function of the constant, a, and of the magnitude of the nuclear excursion. To clarify the significance of the parameter a, it can be easily deduced that $a = 1$ represents a building leak rate of approximately 3.37% per minute at a Δp of 0.5 psi. An infinite value of a signifies that all the overpressure escapes by leakage and none through the SBHE system.

In order to estimate the consequences of releases of this type, it is merely necessary to apply the appropriate factor from Fig. II.K.4 to the doses to be expected from a ground-level release following a 100% meltdown. These values have been calculated and appear in Fig. II.29.2.

The values given therein for ground-level doses are based upon the most representative conditions (i.e., a wind speed of 100 m/min and C stability conditions). It is assumed that a 100% meltdown occurs and that all the noble gases and 50% of the iodines are released from the vicinity of the fuel. It is further assumed that the iodine is attenuated by a factor of 3 due to washout and disposition on various surfaces.

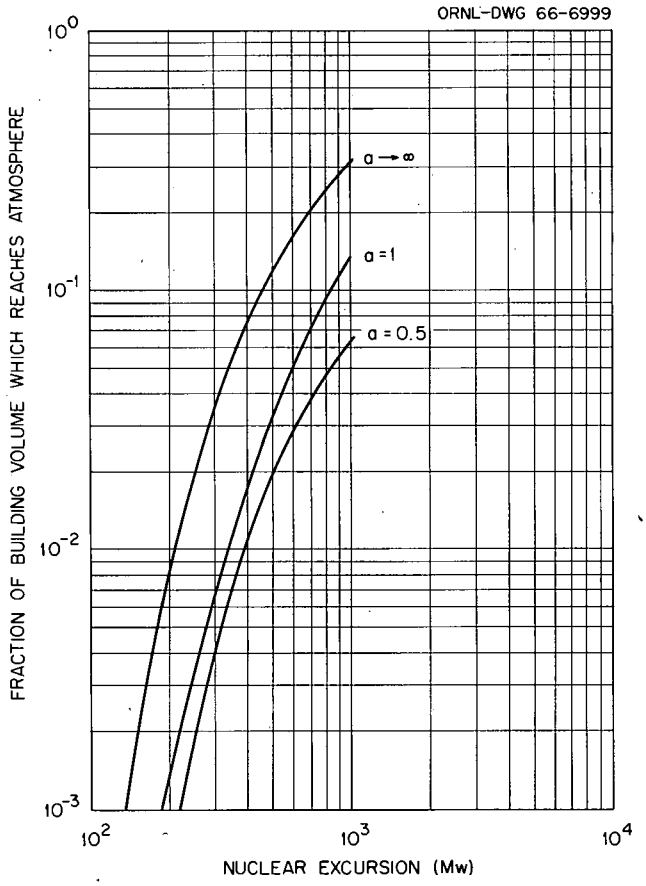

Fig. II.K.4. Fraction of Building Volume Which Escapes.

Moreover, the values given in this figure are based upon a relatively slow release rate from the building, and thus include decay during the release period. To correct this decay term for a rapid release it is necessary to multiply the noble-gas doses by ~10 and the iodine doses by a factor of ~3.5. Thus the doses to be expected from a rapid release at ground level following a 100% meltdown are as follows:

	Exclusion Area Boundary (2.8 km)	Downwind Site Boundary (4.0 km)
Noble-gas gamma dose	31 rads	16 rads
Internal I_2 dose	1350 rems	721 rems

These values contain some degree of uncertainty. For example, a wind speed of 50 m/min rather than 100 m/min would increase them by a factor of 2, whereas a wind speed of 200 m/min would decrease them by a like amount. There is also probably room for argument concerning the value of the release factor of ½, deposition factor of ⅓, and the choice of C stability conditions. Nevertheless, these values are believed to be representative of the magnitude of the doses to be expected.

Since it has been determined that the maximum possible nuclear excursion is less than 300 Mwsec, premature failure of the pressure vessel would result in an overpressure in the building of only 0.5 psi; and the appropriate factor to apply to the ground-level release, under the assumption that all of the overpressure is released to the atmosphere, is 0.035. Upon adding to this 96.5% of the stack release doses, also given in Fig. II.29.2, the doses to be expected become the following:

	Exclusion Area Boundary (2.8 km)	Downwind Site Boundary (4.0 km)
Noble-gas gamma dose	18 rads	13 rads
Internal I_2 dose	50 rems	27 rems

The foregoing estimates are believed to be conservative by a factor of at least 5. This is because of the tacit assumptions: (1) that no energy is lost from the hot gases in passing through the pool, (2) the temperature of the hot gases has a value which maximizes their energy content, and (3) all the vaporized aluminum reacts instantly with steam. Nevertheless, it seems clear that no accident will produce catastrophic off-area consequences.

The Reactor Pool

The HFIR pool is not an integral part of the reactor building in the sense that damage to the pool will result in damage to the reactor building. The only conceivable way that the reactor pool could suffer significant damage would be as the result of a severe shock wave. There does not appear to be any mechanism which could generate such a shock wave; however, it is possible to estimate the magnitude of the TNT explosion necessary to do so.

In a series of tests performed on a scale model of the Air Force Nuclear Engineering Test Reactor,[2] it was found that a 1000-Mwsec TNT explosion was required to produce significant damage to the north or shielding wall of this reactor. This wall is adjacent to the reactor vessel, which is a rectangular tank $33\frac{1}{2} \times 20\frac{1}{2}$ in. in cross section. The wall is 16 ft thick and constructed of reinforced barytes concrete. The HFIR pressure vessel is separated from the 12-ft-thick reinforced concrete pool wall by 5 ft of water. If it is assumed[3] that the shock wave is reduced by $r^{1.13}$, where r is the distance from the explosion center to the wall, and that the damage is inversely proportional to the mass of the wall, then the HFIR pool could withstand a TNT explosion equivalent to

$$1000 \times \left(\frac{5}{1}\right)^{1.13} \times \frac{12}{16} = 4600 \text{ Mwsec}$$

without suffering significant damage.

---

[2] W. E. Baker and J. D. Patterson II, *Blast Effects Test of a One-Quarter Scale Model of the Air Force Nuclear Engineering Test Reactor*, BRL-1011, Aberdeen Proving Ground, Aberdeen, Md. (March 1957).

[3] R. H. Cole, *Underwater Explosions*, Princeton University Press (1948).

Even though some cracks might appear in the concrete and water be lost thereby, this would occur after the accident was over and would not contribute significantly to the consequences. The main problem would be loss of shielding, which would make recovery operations difficult.

It is worth noting that an Atomics International report[4] based on these tests indicates that the energy release rate from a reactor excursion would be considerably less than that from an explosive. Moreover, pressures escaping from the surface of the pool were all quite low (0.6 psi in the case of the 1000-Mwsec scale test), which indicates that even for explosive-type releases there would be no blast effects in the building.

It is concluded, therefore, that no conceivable nuclear accident in the HFIR could significantly damage the reactor pool structure.

---

[4]*Summary Report on R. M. Parsons Request for Engineering Information Relative to the Model Blast Study of WADC Nuclear Engineering Test Facility*, Atomics International (Feb. 10, 1956).

APPENDIX L

DETAILED DISCUSSIONS OF QUESTIONS 54, 55, AND 58

54. Reanalyze transient previously discussed (1.3% Δk) without control rod action. What is the extent of the metal-water reaction? Could boiling lead to a more rapid rate of increase of the reactivity?

Several of the transients previously analyzed with the analog computer were reanalyzed, using a more sophisticated analog model. The new model includes an expression for steam void feedback, based on a correlation proposed by Griffith, Clark, and Rohsenow,[1] which is applicable for subcoolings as low as $\sim$20°F for the HFIR. To obtain some degree of space dependence the core was divided into five axial regions in addition to the hot spot and hot streak "cores." Proper weighting factors for coefficients were applied in each of the five regions.

The above correlation implies that the void fraction is proportional to the difference between the actual heat flux and incipient-boiling heat flux and inversely proportional to the subcooling and the square of the heat transfer coefficient. Thus, the void fraction is approximately proportional to the inverse of the coolant velocity and the subcooling. This implies that for a high-velocity, large subcooling reactor such as the HFIR, the steam void reactivity feedback will be small compared to that for the lower-coolant-velocity reactors.

Results from the above analog studies indicate that when the HFIR is operating at 10% normal flow, reactivity feedback from steam formation, prior to the peak in power, is appreciable; under full flow con-

---

[1]Griffith, Clark, and Rohsenow, *Void Volumes in Subcooled Boiling Systems*, Technical Report No. 12, M.I.T. (1958).

ditions the corresponding feedback is quite small. According to the calculated results, the greatest feedback in the latter case comes from fuel plate expansion.

A summary of the latest analog calculations made is given in Table II.L.1. In these calculations more severe accidents than the 1.3% $\Delta k/k$, 30-msec ramp were considered, and in some cases safety rod action was omitted. If one assumes that the model is reasonably correct and that some local melting can be tolerated without destroying the mechanical integrity of the rest of the element, as was the case in the SPERT experiments[2,3] with 5- and 4.6-msec periods, then it can be concluded that the HFIR can withstand the 1.3% $\Delta k/k$, 30-msec ramp accident with only a small amount of melting and no metal-water reaction. This assumes that the safety rods work. Referring to case 8, Table II.L.1, the calculated metal hot spot temperature is only 2150°F, and this does not consider a significant increase in radial conduction away from the hot spot after it is film blanketed. Since the ignition temperature for the metal-water reaction is considered to be about 3000°F, no significant reaction would take place, unless autocatalytic effects resulted in the generation of larger amounts of nuclear energy. This latter consideration is discussed later.

As stated previously the main reactivity feedback mechanism for the full-flow case is fuel plate expansion, which results in water expulsion. Thus it was not expected that small increases in safety rod differential worth and rod acceleration would significantly decrease plate temperatures (see cases 8, 14, and 17). However, to prevent a possibly large amount of core melting after the initial peak, it is necessary for the safety rods to cancel out most of the reactivity addition soon after (~10 msec) the peak in power, so that shutdown will not depend on core disassembly. Our present analog model does not include any type of core disassembly and thus cannot in itself predict what will happen without safety rod action. Furthermore, the steam void feedback correlation is not applicable for bulk boiling of the coolant. Even so, calculations were made, and some of the results are given in Table II.L.1. As indicated by a comparison of cases 8 and 9, the peak power was only slightly higher than achieved with safety rod action. The equilibrium power level achieved following the peak was 500 Mw and was achieved, following a dip to 100 Mw, about 70 msec after the peak in power. At full flow, 600 psi and 500 Mw, there would be very little, if any, bulk boiling even with good heat transfer to the water, assuming no flow instability. Of course at this power level all heat transfer surfaces would be film blanketed, causing melting of the fuel plates, at which time, if not before, the coolant pressure drop would sweep the fuel from the core region. The rate of temperature rise of the central portion of the core at 500 Mw would be about 15°F/msec. Thus, in 30 msec, about the time required to sweep the molten metal out of the core, the temperature increase of the aluminum, assuming that it is still in contact with the fuel, would be about 450°F, which is not enough to initiate the metal-water reaction.

It is of interest to consider what is happening in the core regions containing positive void coefficients, which include the flux trap, control region, and perhaps a small portion of the fuel region adjacent to the flux trap. The flux trap and control region reactivity feedback are specifically included in the analog

---

[2] F. Schroeder (ed.), *SPERT Project Quarterly Technical Report, April–June 1962*, IDO-16806 (Sept. 21, 1962).

[3] F. Schroeder (ed.), *SPERT Project Quarterly Technical Report, July–September 1962*, IDO-16829 (Feb. 28, 1963).

Table II.L.1. HFIR Analog Calculations

Case	Fuel Coolant Velocity	Initial Steady-State Power (Mw)	Safety System Differential Worth	Reactivity Accident: Reactivity	Reactivity Accident: Ramp	Peak Power (Mw)	Negative Feedback from Moderator Fuel Plate and Voids (Peak Power) (% $\Delta k/k$)	Void Feedback (Peak Power) (% $\Delta k/k$)	Integrated Power (Mwsec)	Plate Temperature, Hot Spot (Max) (°F)	Plate Temperature, Region 3 (Midcore) (Max) (°F)	Bulk Temperature, Region 5 (Outlet) (Peak Power) (°F)	Time to Peak Power (msec)	Meat Temperature, Target Average (Max) (°F)	Surface Temperature, Target Average (Max) (°F)	Bulk Temperature, Target Average (Max) (°F)
1	10%	10	8.3¢/in., 4g	1.3%	30 msec	750	0.35	0		2200	1075	210	68			
2	10%	10	8.3¢/in., 4g	1.3%	30 msec	620	0.35	0.15		1350	700	190	55			
3	10%	10	8.3¢/in., 4g	1.3%	Step	1100	0.45	0		2900	1475	225	50			
4	10%	10	8.3¢/in., 4g	1.3%	Step	740	0.3	0.2		1400	760	195	35			
5	10%	10	8.3¢/in., 4g	2.0%	Step	1940	1.1	0.9		1750	975	190	28			
6	10%	10	None	1.3%	30 msec	780	0.6	0.5		1500	775	200				
7	100%	100	8.3¢/in., 4g	1.3%	30 msec	1400	0.50	0	56	3600	1100	300	50			
8	100%	100	8.3¢/in., 4g	1.3%	30 msec	1320	0.55	Small	44	2900	1000	290	48			
9	100%	100	None	1.3%	30 msec	1450	0.6	Small	46	3000	1050	275	48			
10	100%	100	None	1.3%	30 msec in, 30 msec out	800	0.3	Small	26	1600	620	225	40			
11	100%	100	8.3¢/in., 6g	1.0%	Step	660	0.22	Small	32	2200	650	250	34			
12	100%	100	8.3¢/in., 6g	1.05%	30 msec	660	0.23	Small	32	2000	650	240	50			
13	100%	100	8.3¢/in., 6g	1.25%	60 msec	700	0.30	Small	34	2000	670	250	65			
14	100%	100	8.3¢/in., 6g	1.3%	30 msec	1250	0.50	Small	44	2800	950	280	50	540	260	130
15	100%	100	8.3¢/in., 6g	1.5%	30 msec	1820	0.70	Small	48	3200	1150	300	45	580	270	135
16	100%	100	8.3¢/in., 6g	2.0%	60 msec	2100						575		620	280	135

Conditions:
1. End of cycle
2. Mode 1 operation
3. Five axial regions
4. $h = 0$ at hot spot for $q > q_{b.o.}$
5. Temperatures above 1200°F (melting point for aluminum) must be corrected for heat of fusion as follows: $T(\text{actual}) = T(\text{calcd}) - 750°\text{F}$, if $T(\text{calcd}) > 1950°\text{F}$; $T(\text{actual}) = 1200°\text{F}$, if $1200 \leqq T(\text{calcd}) \leqq 1950°\text{F}$.

model up to the point where boiling begins. Since the initiation of boiling in these regions would lag behind that in the fuel regions (see cases 14, 15, and 16), and since boiling in the fuel region was not included in the analog model as a feedback mechanism, there was no reason to be concerned with boiling in these other regions. An exception to this lack of concern is associated with flow blockage and other extraordinary methods of generating voids in the positive coefficient regions. The worst such case appeared to be total flow blockage to the target region. In terms of reactivity addition this accident was less severe than the 1.3% $\Delta k/k$, 30-msec ramp case.

Another possibility is that the coolant temperature in the target region would be considerably higher than nominal, perhaps as a result of undetected, partial blockage of flow to the flux trap region. In such a case a transient induced by other means could cause voids through subcooled boiling and film blanketing on the target rods; this could occur before void formation in the fuel region. Suppose that the initiating accident in itself is trivial, but that the slightest increase in power initiates subcooled boiling in the target. Since about 1.3% $\Delta k/k$ is the maximum reactivity that could be added by boiling in the flux trap, and since all the high-velocity coolant would have to be removed to achieve the 1.3% $\Delta k/k$, this accident would be mild compared to the 1.3% $\Delta k/k$, 30-msec ramp accident. If this sort of feedback accompanied a void insertion accident, the total reactivity addition would be no greater than 1.3% $\Delta k/k$, but the addition rate would be greater than the addition rate associated with the initiating void by itself. However, since it is postulated that the target boiling condition existed as a result of reduced coolant velocity in the target, the initiating void would enter more slowly than usually anticipated for the maximum reactivity insertion case.

It is of some interest to consider the case of the 1.3% $\Delta k/k$, 30-msec ramp accident and the target boiling condition occurring simultaneously. Without target boiling, the amount of energy generated in the target during the time that it takes to insert the optimum void is 0.06 Mwsec, which will vaporize less than 0.1 lb of water. The optimum void represents about 3.6 lb of water; therefore, the maximum reactivity addition would be about 0.05% $\Delta k/k$. Actually only a small fraction of the 0.06 Mwsec would be transferred to the coolant during the fast transient because of the relatively long time constant in the target rods. Since the total reactivity addition cannot exceed 1.3% $\Delta k/k$, the effect of boiling in the target is quite negligible.

From an economic point of view, flow blockage to the flux trap region is of great concern because of the possibility of distributing megabucks worth of transplutonium isotopes throughout the primary system. For this reason, a special coolant inlet to the flux trap was provided which minimizes the possibility of flow blockage and gas void transport.

In the above and previous discussions concerning optimum void entrance and residency in the flux trap target, the consequences of target melting were ignored. It is obvious of course that since the optimum void associated with the high-velocity coolant in the target occupies all the forced convection coolant space, there is essentially no means for cooling the target rods once the void is in place. The amount of energy required to raise the target rod temperature to the melting temperature is about 1.4 Mwsec, and to complete melting starting from the nominal state, it is 2.5 Mwsec. By the time the peak in power occurs for the 1.3% $\Delta k/k$, 30-msec ramp case, the energy generated in the target is only 0.5

Mwsec. Since the individual rods are supported inside a "cold" tube it is not likely that they would collapse before water would return to the target area and cool the target rods. However, should the target rods either melt or crumple to the bottom of the grid support, and then if by some mechanism the optimum void were to exist in the "empty" flux trap, the net change in reactivity from the voided (1.3% $\Delta k/k$) maximum fission target condition would be about +1.0% $\Delta k/k$, making the total reactivity addition from the nominal condition 1.3 + 1.0 = 2.3% $\Delta k/k$. If instead of the maximum fission target the maximum poison target (essentially no fissioning) is in the flux trap when the postulated sequence takes place, the corresponding change in reactivity would be 1.0 + 0.9 = 1.9% $\Delta k/k$, and the total change from the nominal condition would be about 1.3 + 1.9 = 3.2% $\Delta k/k$.

The rates and times at which the above additional reactivities could be added are of course dependent on many factors. Suppose that gas bubbles of unknown origin are entering the flux trap in such a way as to maintain the optimum void whether the target is in place or not. The minimum ramp insertion time, assuming that the target could vanish in zero time, would be about 30 msec. The rate at which the target would actually slump to the bottom of the region should be slow compared to the coolant velocity. Furthermore, there should be no slumping at all unless the target is overheated, which it would not be unless the coolant velocity were considerably below normal; all of which means that slumping of the target would take place very slowly relative to the 30 msec, and the initiating void would have to enter more slowly also. In the case of the maximum poison target the heat generation rate in the target is only about 10% of that of the maximum fission target for which the coolant system is designed. Thus it is barely conceivable that the maximum poison target could slump. Another point to consider is that for reduced flow in the target region the pressure drop across the target rods is very small, reducing the likelihood of slumping. Furthermore, the grid beneath the target is such that the target could not be completely removed from the flux trap region unless it were molten to the point that it could be extruded through the $\frac{1}{4}$-in.-diam holes in the grid. It is much more likely that these holes would be plugged with the colder,non-"fuel"-bearing portions of the rod assemblies, which are located below the "hot" portion. Assuming this to be the case, the flux trap would still contain a minimum of 15 vol % of aluminum. This assumes that all the target completely slumps to the extreme bottom. In actuality, much of the aluminum, in the form of "cold" flow-tube structural material, would remain solid for quite some time, preventing the entire mass of aluminum from slumping. Thus a more realistic volume percent of aluminum in the "active" flux trap region would be about 30%, which is about the same as when the target is not damaged. The reason for this is that a non-"fueled" portion of the target rods extends several inches above the top of the fuel region, and the entire axial support for the rods is at the bottom of the target assembly below the fuel region. Thus when melting or slumping occurs, the upper "cold" material is forced into the "active" flux trap region. Therefore, it is really quite improbable that reactivities significantly in excess of the 1.3% $\Delta k/k$ could be added by a slump-type "removal" of the target.

If on the other hand the tandem grid beneath the target were to melt or otherwise become disassembled, and the control rods were inoperable, and somehow voids were continuously swept into or otherwise secured in the flux trap region, and if we assume that the coolant velocity in the flux trap region has been enhanced as a result of the removal of the tandem orificing grid, then presumably 3.2% $\Delta k/k$ could

be added in a period of time less than 30 msec. This of course, in accordance with our calculational model, would result in melting of the core, with or without rod action. Such an accident is considered incredible; however, the consequences are discussed in Appendix H.

Getting back to the subject of boiling in regions containing positive void coefficients, it is of interest to once again (response 51) consider the void coefficient in the fuel region as a function of radial position.

Although the overall void coefficient in the fuel region is strongly negative, there is a narrow region adjacent to the flux trap that has a small positive coefficient. At the beginning of a fuel cycle the power density in this region is about the same as elsewhere in the inner element and a portion of the outer element. However, as the fuel cycle proceeds, nonuniform burnup of the fuel reduces the relative power density adjacent to the flux trap, making the positive void effect less important. But even for the clean core condition the positive void effect is so small as to be negligible. If the entire positive void region were voided, the additional reactivity would be only 0.0002 $\Delta k/k$. Therefore, boiling in this region would not significantly increase the rate or total reactivity addition.

Another type of boiling is that associated with waterlogging and subsequent bursting or expansion of the target tubes, resulting from steam formation within the tubes. To examine this possibility it is necessary first to define the amount of water in the tube. In principle there is no room for water in the tubes except at the ends, where there are void spaces for the fission gases. Water in these regions would be at about the same temperature as the bulk coolant and thus would have no tendency to boil before the bulk coolant did. The differential pressure required to burst a target tube is about 1500 psi, which means that the internal pressure would be about 2000 psi, and the change in internal volume would be about 40%. If it is assumed that the increased volume is filled with saturated steam at 2000 psi (T_{sat} = 636°F), the amount of water involved would be 3.0×10^{-3} lb or 8.6×10^{-2} in.^{3}. If this water were located between the pellets and the tube wall, the diametral clearance necessary for the water would have to be about 0.011 in. Normally this clearance is less than 0.0005 in. at room temperature, since the tube is hydrostatically collapsed on the pellets during fabrication, and during operation the difference in thermal expansion between the pellet and tube brings the two in contact.

Water might also be located at the end interfaces of adjacent pellets. If all the water were located here, the accumulated spacing between the pellets would have to be about 1.7 in., or 0.049 in. per pellet. Normally this spacing is less by a factor of 20.

If by some means the above amount of water did get trapped in the target rods and resulted in rupture of the tubes, the momentary steam volume resulting from adiabatic expansion of the saturated steam to wet steam at 600 psi would be about 2.6 in.^{3} per target rod, or 81 in.^{3} for all 31 rods. This amounts to about 0.7% void and about 0.04% $\Delta k/k$ per rod. For 31 rods the increase in reactivity would be about 1.1% $\Delta k/k$.

The amount of energy per rod required in the above case to burst a target rod during a transient would be equal to the change in internal energy associated with the generation of 3.0×10^{-3} lb of saturated steam at 2000 psi pressure from the same number of pounds of saturated water at 600 psi (the water would normally be somewhat subcooled), plus the strain energy in the tube wall:

$$\Delta U + \int p\, dv = 1.8 \text{ Btu} + 0.1 \text{ Btu} = 2.0 \times 10^{-3} \text{ Mwsec per rod} .$$

The amount of energy generated in a single maximum fission target rod during the first 30 msec (reactivity insertion time) of the initiating accident is $0.06/31 = 2 \times 10^{-3}$ Mwsec. Since most of this heat would be retained in the pellet during the transient and then transferred to the coolant, the tube would not burst in time to significantly enhance the rate of reactivity addition. Before the peak in power is reached it is possible that the tube would burst, but by this time there would be no coolant water to displace, since the optimum void initiating the accident would already have displaced the water.

In the above discussion several practical aspects were ignored for the sake of investigating what appeared to be extreme cases. A more realistic analysis shows that a diametral clearance of 0.011 in. between the pellet and tube would result in melting of the pellet, whereupon the pellet would slump until making contact with the tube wall, thus relegating the leaking water to the void spaces at the end of the target rods. Because of the small exposed pellet heat transfer area associated with this water, steam formation during the transient would be negligible. If the initial power level were low enough so that the pellet did not quite melt, then water leaking in would flash and prevent further leakage.

A more practical case to consider is that in which a previously waterlogged target rod is inserted into the reactor and rather quickly taken to power, in which case it might be further assumed that the system is simultaneously subjected to our maximum reactivity insertion accident. By this method it should be possible to burst the tube, but only after the coolant has been voided, as discussed above. Therefore, the accident is not enhanced by waterlogging. On the other hand, suppose that the reactor is taken to power by normal means. At about 50 Mw, water in the target tube would begin to boil without the pellets melting, and somewhere between 50 and 100 Mw enough steam would be generated to further insulate the pellet, causing it to melt. At this point the molten metal might disintegrate, causing a steam explosion. The amount of energy in the pellet above 636°F would be about 3.2×10^{-2} Mwsec per rod, which is about ten times that required to burst the tube. This would create the optimum void almost instantaneously, making the simultaneous insertion of the maximum credible accident meaningless. According to our present analog model, such an accident would cause core damage even with safety rod action. However, it is shown in Appendix H that such an accident could not lead to rupture of the primary containment system.

If a steam explosion due to disintegration of the molten metal did not occur, but rather steam formed at a somewhat lower rate, the nearly instantaneous expansion upon rupture of the target tube would increase reactivity in the amount of 0.04% $\Delta k/k$ per rod, or about 1.1% $\Delta k/k$ for all 31 rods. According to the analog calculations (case 11, Table II.L.1), this would not cause melting of the fuel plates provided that the safety rods functioned.

The maximum reactivity addition associated with removal of water from the control region and the removable beryllium reflector region is only about 0.5% $\Delta k/k$ (see Fig. II.L.1). Furthermore, the heat generation rates in these regions are relatively low, making the steam formation rates under flow blockage conditions very low.

It is concluded on the basis of the preceding discussions that the only type of boiling accompanying the maximum reactivity insertion accident that can enhance the consequences of the accident is associated

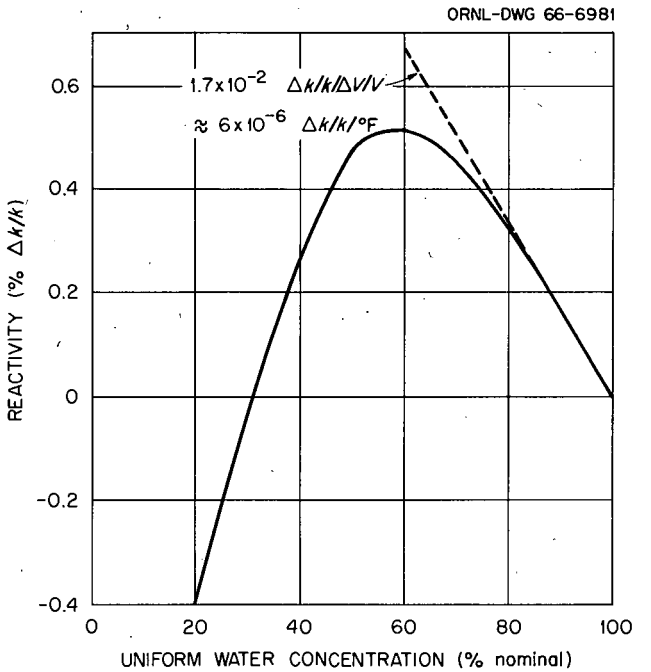

Fig. II.L.1. Reactivity vs Uniform Reduction in Control Region and Removable Beryllium Water Content (End of Cycle).

with a waterlogged target rod. Furthermore, the rod must be waterlogged at low power, and with this accomplished, the ensuing accident is initiated by taking the reactor to power either slowly or rapidly. In either event, the accident could be more severe than our maximum postulated reactivity insertion accident if all 31 rods ruptured simultaneously, but can be easily contained within the primary system.

55. Propose and examine mechanisms and accident conditions which might lead to the insertion of greater amounts of reactivity than 1.3% Δk. If reactivity insertions worse than that of Question 54 are found to be possible, what are the consequences to the reactor facility for the limiting insertion? Some possible examples of sources of reactivity insertion might be as follows:

A. If target overheats due to error or malfunction, could target failure of any kind, coupled with voiding (partial or complete), lead to larger reactivity insertion?

This question was discussed under Question 54. The conclusion is that if the pellets become molten, or nearly so (as a result of poor "bond" between pellet and tube), and are exposed to the target coolant in such a way as to disintegrate the molten material or otherwise quickly transfer the pellet heat to a portion of the water, a steam explosion could occur that would introduce the 1.3% $\Delta k/k$ in a period of time shorter than 30 msec. It is further concluded on the basis of information presented in Appendix H that this accident can be contained within the primary system.

B. Could target become waterlogged, then fail under steam pressure during a transient induced by other causes? If so, what might the reactivity be?

This is discussed in part under Question 54. In addition, we might assume that a transient is initiated by some means other than a void insertion in the flux trap. Such an event might be the failure of the inner control cylinder drive bracket. We have previously shown in response 47 that failure of the drive bracket alone is a less severe transient than the void insertion accident. If the excursion adds enough energy to the target, the target rods could burst, adding about 0.04% $\Delta k/k$ per rod on a very fast time scale, that is, fast compared to 0.03 sec. This could cause a further increase in power and, depending on how many rods burst simultaneously, could cause melting of the core, even with safety rod action. Of course the probability of having a large number of target rods burst at the same time is very small.

C. If target coolant is closer to boiling than anticipated, could transient originating from another source lead to significantly greater energy release than that of Part I?

This is discussed in part in Question 54. There is also the possibility that an initiating accident other than the flux trap voiding could cause boiling in the target region, in which case the two would be additive. However, as indicated in the answer to Question 54, the rate at which steam can be generated in the target region is so slow relative to a significant initiating accident that the additive effect is negligible.

D. If flux trap is devoid of target, and flow is sharply reduced in that area, could sudden incidence of boiling or voiding lead to large reactivity insertion?

This question is discussed in part under Question 54. In addition, consider inadvertent operation of the reactor without a target in the flux trap. The quickest way available to introduce the optimum void is with the maximum coolant velocity. The ramp time would be considerably greater than 30 msec, because removal of the target eliminates the high-velocity coolant stream, and the maximum reactivity addition would be 3.2% $\Delta k/k$ instead of the 1.3% $\Delta k/k$ associated with the target in place. Such an accident might initiate a metal-water reaction, but as discussed elsewhere there is enough negative reactivity feedback from fuel plate expansion and moderator expansion (steam explosions very likely) to prevent rupture of the primary system. Of course precautions are taken against ever operating the reactor without a target or an equivalent thereof in the flux trap.

E. If a local meltdown in a section of the core occurs, how large must the hole get before one stops gaining reactivity? How much reactivity is involved? What is the increase in power level at the edge of the region devoid of fuel, as a function of hole size? How great is the tendency to spread as a consequence? To what extent may such a mechanism lead to autocatalytic effects and transients starting in this manner or from other sources? Are there other autocatalytic effects from fuel movement?

Let it first be assumed that the melting under question does not result in water expulsion as well as fuel plate expulsion, but that water replaces the molten metal as rapidly as it is removed; otherwise there would be a decrease in reactivity rather than an increase until such time as the water could return. For a very idealized model, removal of fuel plate and replacement with water will add a maximum of 2.6% $\Delta k/k$, and the associated optimum volume of removed metal is 30% of the total fuel volume (see Fig. II.L.2). If the melting under question is localized, a flux trap effect would be created that might tend to propagate the melting at the edges of the hole as a result of flux peaking associated with the locally

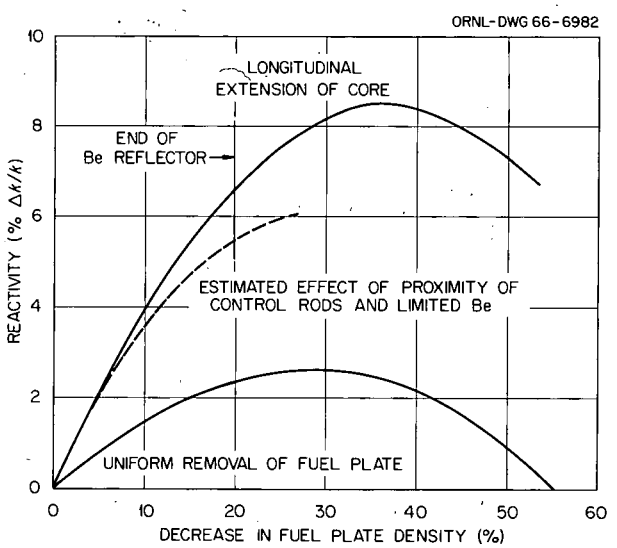

Fig. II.L.2. Reactivity vs Decrease in Fuel Plate Density Resulting from Longitudinal Extension of Core or Uniform Removal of Fuel Plate.

added water. If only one fuel plate were involved, the peaking would be very small and it is not likely that melting would be self-propagating. The increase necessary for self-propagation would depend of course on the magnitude of fuel segregation, if any, associated with the melted spot and upon other similar factors. Supposing, however, that the hole does grow; it might continue until the optimum hole size formed. The size of the optimum hole is a function of the competing effects of moderation and absorption in the water cavity; it is something less than 6 cm in diameter, which if spherical would represent about 0.2% of the core volume and thus only about 0.03% $\Delta k/k$. The reactivity would decrease if the hole grew bigger, which it probably would, because the power density at the edges of the hole is nearly doubled for holes larger than the optimum.

The only way in which a large amount of molten metal could be removed quickly from the core would be for the melting to take place at the outlet end of the core, where the metal could be easily swept away. In this case, however, the reactivity decreases immediately because the length of the core is simply being decreased without decreasing the effective metal-to-water ratio. Thus it does not seem likely that local melting could significantly enhance the consequences of a reactivity accident.

Nearly any movement of the fuel which decreases the metal-to-water ratio without completely removing fuel from the core will increase reactivity. Thus, pressure increases inside the core which tend to elongate and/or spread the core out radially could increase the reactivity provided that the driving force not only did not expel water but allowed water to enter, or if water later returned to an enlarged, but not disassembled, core. During a fast transient, expansion of the fuel plates and water generates pressures that accelerate water out of the core and apply axial and radial forces on the fuel and side plates. These forces were calculated for several transients in which essentially no steam was formed. Results of these calculations, which are presented at the end of this appendix (p. 264), indicate that for the maximum reactivity insertion

accident the maximum differential pressure generated at the horizontal midplane of the core is about 20 psi. For a 1.5%, 30-msec ramp accident the corresponding maximum pressure is 28 psi, and for a 2.0%, 30-msec ramp accident the pressure is 80 psi. These pressures are not sufficient to cause significant deflection of the side plates, but they could result in some axial displacement of the fuel plates, particularly in the latter case since the fuel plates would be molten before the pressure peaked. The extension of the fuel plate in this case would not cause an increase in reactivity because the same forces that expel the metal, preferentially expel water. However, after the core cooled down the return of water to the core would result in a more reactive core than previously existed, exclusive of the initiating accident. Of course if the initiating reactivity persisted at this time, the core would already have experienced a steam explosion, which probably would disassemble the core, making the return of water of no consequence. Under the worst possible (and very unrealistic) conditions, assuming that the fuel plates are uniformly extended an optimum distance (about 35% of the length of the core), the reactivity addition would be about 6% $\Delta k/k$ (see Fig. II.L.2). This assumes of course that enough water could return to the core, which it could not do because of the excursion that would take place after only a small part of the water returned. The conclusion of the transient would have to be disassembly by melting and a steam explosion.

Greater pressures than those mentioned above can be generated by steam explosions, which, according to results obtained from the 5-, 4.6-, and 3.2-msec SPERT I destructive tests[2–5] and experiments conducted by TRW Systems,[6] will probably occur when a rather large fraction of the core becomes molten. Since such an explosion would create accelerating pressures of several hundred or thousand psi in the fuel element, it is not likely that the core could remain critical and intact. Furthermore, it is very probable that by the time enough molten metal was formed to significantly add reactivity by its removal and replacement with water, a steam explosion would occur that would effectively disassemble the core, preventing the above more reactive core from being created. As discussed in another section the steam explosions can be tolerated without rupture of the primary system.

F. What pressures might be generated from local fuel melting? How much fuel failure is required to generate pressures which could move significant amounts of fuel inward (and thus gain reactivity), or which could interfere with control rod action? Does this allow for pressures from a "steam explosion" or a "water hammer"? How much reactivity could be gained by inward motion of the fuel into the flux trap? How much pressure would it take to produce such motion? Could flow blockage lead to such effects?

According to the data presented in ANL-7152[7] and the 5- and 4.6-msec SPERT I tests,[2,3] small amounts of molten aluminum will not disintegrate and cause a steam explosion. However, as indicated by the 3.2-msec SPERT I test[4,5] and the TRW experiments,[6] when perhaps several percent of the core

---

[4] F. Schroeder (ed.), *SPERT Project Quarterly Technical Report, October–December 1962*, IDO-16890 (May 17, 1963).

[5] F. Schroeder (ed.), *SPERT Project Quarterly Technical Report, January–March 1963*, IDO-16893 (May 20, 1963).

[6] Thompson, Ramo, and Wooldridge Systems, *Kinetic Studies of Heterogeneous Water Reactors Quarterly Progress Report for Period Ending June 30, 1965*, USAEC Report STL 372-22 (July 30, 1965).

[7] Argonne National Laboratory, *Reactor Development Program Progress Report, January 1966*, ANL-7152 (Feb. 24, 1966).

becomes molten a steam explosion will occur. The possible results of such an explosion are the expulsion of water and fuel out the ends of the core, the direction of least resistance, and the movement of the inner side plate of the inner fuel element into the flux trap region and the outer side plate of the outer element into the control region. For static loading the collapsing pressure for the inner side plate, neglecting the additional support of the fuel plates, is about 4000 psi, and the outer side plate has a bursting pressure of about 400 psi; under static conditions the outer side plate would begin to interfere with the movement of the shim-regulating rod at a pressure just under the bursting pressure, because elastic strain is not sufficient to cause interference. During a steam explosion the accelerating pressures within the element would have to be considerably greater than those above to cause the same displacement because water in the flux trap and in the central region would also have to be accelerated. Because of the difference in the static failure pressures it is more likely that interference in the control region would occur than a collapse of the inner element inner side plate. This would be of little consequence because a steam explosion large enough to rupture the outer element outer side plate would disassemble the core.

Movement of the inner side plate of the inner element into the flux trap increases reactivity in two ways under certain conditions: (1) by displacing water from the flux trap, provided that the initiating accident was not an optimum void in the target; and (2) by decreasing the metal-to-water ratio in the inner fuel element, provided that water is available to fill the larger coolant volume.

If the inner side plate moves in enough to collapse the target to the solid condition, the maximum reactivity addition would be approximately 7% $\Delta k/k$ (see Fig. II.L.3). Since the only mechanism available for collapsing the side plate is a steam explosion, which will permanently disassemble the core axially in preference to the radial direction and will at the same time create a much larger negative reactivity feedback than can be compensated by inward radial displacement of the side plate, it appears that such movement of the side plate is of no concern.

G. Are there any conditions in which water returning to a region after an explosion could lead to large reactivity insertions? For example, if fuel and water were expelled from a region due to melting, could water which rushed in thereafter cause a reactivity excursion?

This question is discussed under Question 55E.

58. Are the answers to these questions changed if no control rod motion occurs?

For the maximum reactivity insertion accident and worse accidents, the safety rods do little more than maintain the reactor down once the self-shutdown mechanisms terminate the accident. Without safety rod action the reactor will tend to level off at a power of about 500 Mw in the 1.3% $\Delta k/k$ accident, in which case the fuel plates would melt and would be driven out of the core region in about 30 msec. During this time not enough energy would be generated, except locally perhaps, to initiate the metal-water reaction. It is also possible that a steam explosion would assist the disassembly.

In more severe accidents, disassembly by a steam explosion would occur so quickly that insertion of the safety rods would be useless. As explained in another section the primary system is capable of withstanding this means of shutdown.

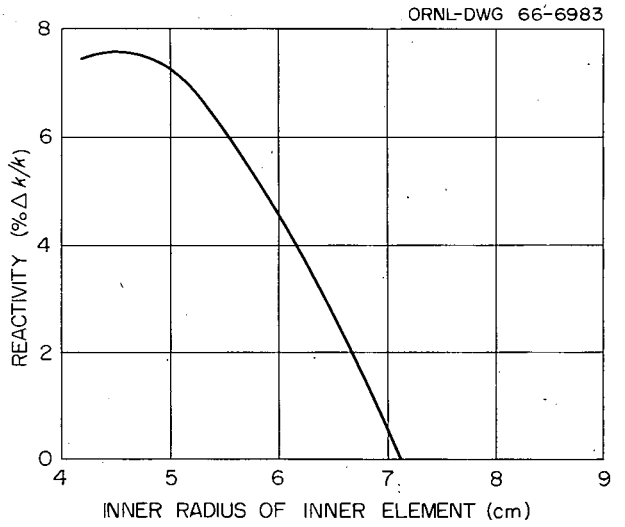

Fig. II.L.3. Reactivity vs Inward Radial Movement of Inner Element Inner Diameter (Water Content of Inner Element Increases Correspondingly).

Pressure Generated by Expulsion of Water Resulting from Water and Fuel Plate Expansion[8]

It is assumed that the forces resisting expulsion of water from a coolant channel are inertial, fluid friction, and compression of fluid in the "external" system. Neglecting compressibility of fluid within the channel, the equation for the pressure generated by a section of channel of length l_n is

$$P_n = \rho(L - \sum l_n)\frac{a(t)}{g} + \frac{4f\,v^2(t)(L - \sum l_n)}{2gD}\rho + \frac{l_n(t)\,A}{V} \times \alpha_p ,$$

where

ρ = density of the fluid,

L = effective length of channel,

l_n = incremental length of channel,

a = acceleration of interface,

g = gravitational acceleration,

v = velocity of interface,

f = friction factor,

D = hydraulic diameter of coolant channel,

A = cross-sectional flow area of all coolant channels,

V = effective vessel volume/2,

α_p = compressibility factor for water.

If the friction factor, f, is considered to be inversely proportional to the Reynolds number, so that the fluid friction term is proportional to the first power of the coolant velocity, then the total pressure at the core horizontal midplane is equal to the summation of the individual P_n's; that is, they can be superimposed. Therefore,

[8]Response 55E, as indicated in p. 261.

$$P_{\text{total}} = \sum P_n \, .$$

The change in length, Δl_n, of an incremental length l_n is obtained from

$$\Delta l_n(t) = l_n\{\alpha_w[T_w(t = t') - T_w(t = 0)] + 3\alpha_{\text{Al}}[T_{\text{Al}}(t = t') - T_{\text{Al}}(t = 0)]\} \, ,$$

where

Δl_n = increase in l_n due to expansion of plate and water in length l_n only,

T_w = water temperature as a function of time,

T_{Al} = fuel plate temperature as a function of time,

α_w = volumetric coefficient of expansion for water,

α_{Al} = linear coefficient of expansion for Al.

Based on the analog calculations, the rate of temperature rise of both the fuel plate and coolant can be represented by an exponential and a delay time, as shown in Figs. II.L.4–II.L.6:

$$\frac{\Delta l_n}{l_n} = \alpha_w \, T_w(t = 0)(e^{t/\tau} - 1)_w + 3\alpha_{\text{Al}} \, T_{\text{Al}}(t = 0)(e^{t/\tau} - 1)_{\text{Al}} \, ,$$

where the times t for the water and Al are different by the differences in delay times, and the periods, τ, are also different. Taking the first and second derivatives of this equation yields the velocity and acceleration terms.

Making the above substitutions,

$$P_n(\text{water}) = \alpha_w l_n \, T_w(0) \left\{ e_w^{t/\tau} \left[L \, \frac{(1 - \sum l_n/L)}{g} \left(\frac{\rho}{\tau_w^2} + \frac{32\mu}{D^2 \tau_w} \right) + \alpha_p \left(\frac{A}{V} \right) \right] - \alpha_p \left(\frac{A}{V} \right) \right\} ,$$

$$P_n(\text{Al}) = \alpha_{\text{Al}} l_n \, T_{\text{Al}}(0) \left\{ e_{\text{Al}}^{t/\tau} \left[L \, \frac{(1 - \sum l_n/L)}{g} \left(\frac{\rho}{\tau_{\text{Al}}^2} + \frac{32\mu}{D^2 \tau_{\text{Al}}} \right) + \alpha_p \left(\frac{A}{V} \right) \right] - \alpha_p \left(\frac{A}{V} \right) \right\} ,$$

$$P_{\text{total}} = \sum P_n(\text{Al}) + \sum P_n(\text{water}) \, ,$$

where

μ = viscosity of water,

$f = 16/\text{Re}$.

The results of the calculations are presented in Figs. II.L.7–II.L.10. They indicate that the peak pressures at the horizontal midplane are approximately 20, 28, and 80 psi for the 1.3, 1.5, and 2.0% $\Delta k/k$, 30-msec ramp accidents respectively. Figure II.L.10 shows the pressure resulting from a 5-msec period increase in plate temperature only, without limit.

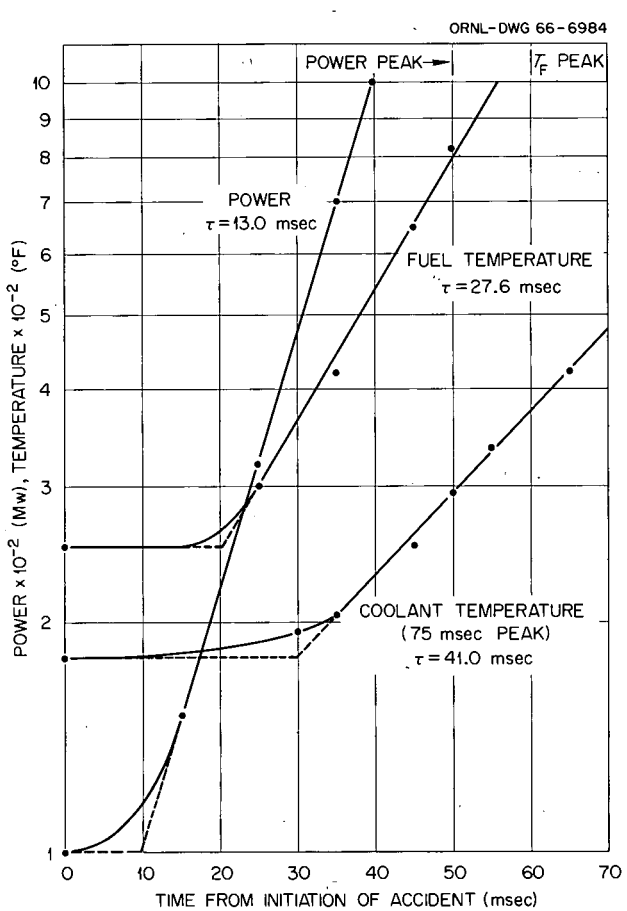

Fig. II.L.4. Power and Temperature vs Time for 1.3% $\Delta k/k$, 30-msec Ramp Reactivity Addition; End of Cycle.

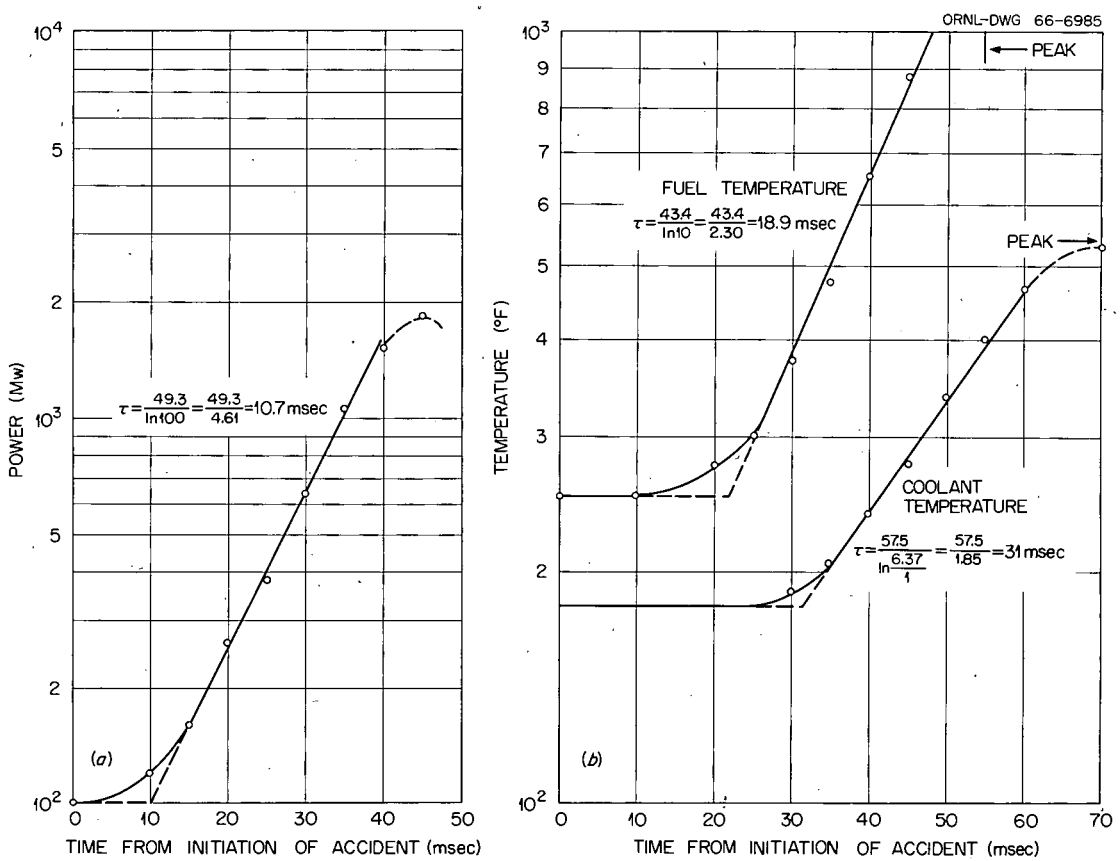

Fig. II.L.5. (*a*) **Power vs Time for 1.5% $\Delta k/k$, 30-msec Ramp Reactivity Addition; End of Cycle.** (*b*) **Temperatures vs Time for 1.5% $\Delta k/k$, 30-msec Ramp Reactivity Addition; End of Cycle.**

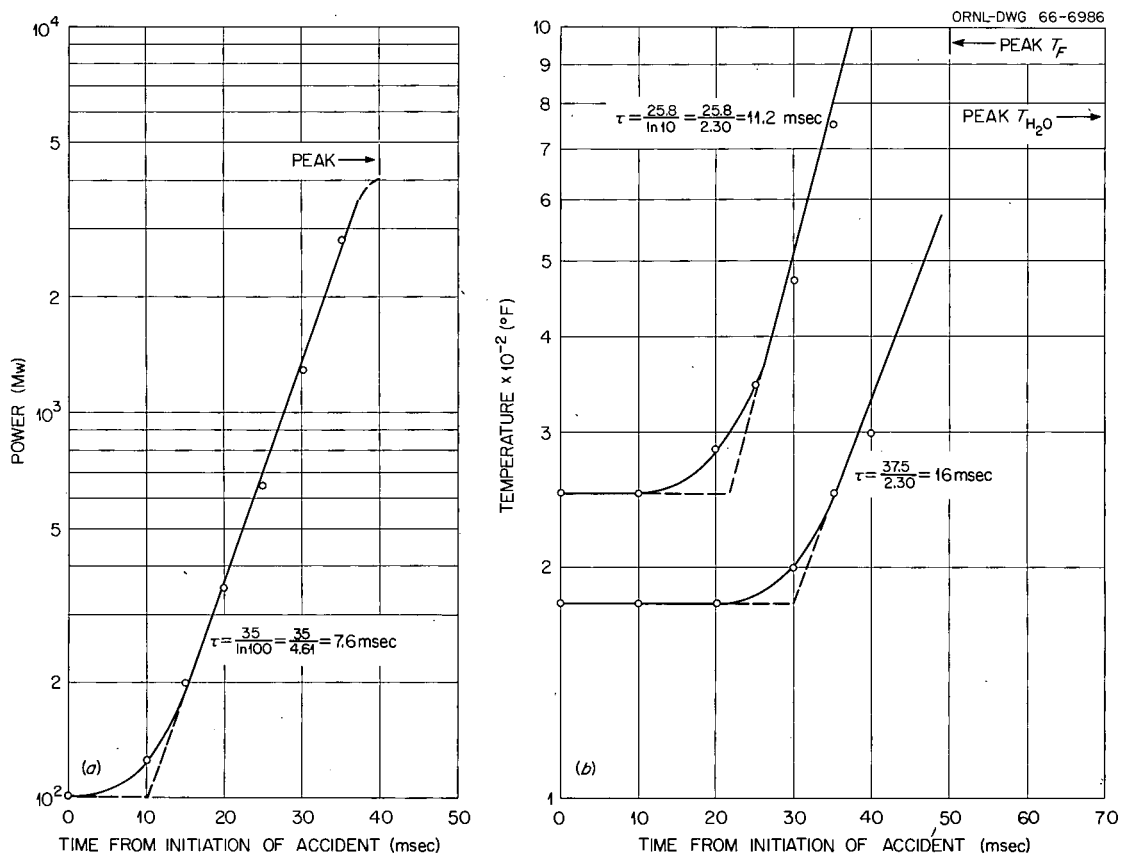

Fig. II.L.6. (*a*) **Power vs Time for 2% $\Delta k/k$, 30-msec Ramp Reactivity Addition; End of Cycle.** (*b*) **Temperatures vs Time for 2% $\Delta k/k$, 30-msec Ramp Reactivity Addition; End of Cycle.**

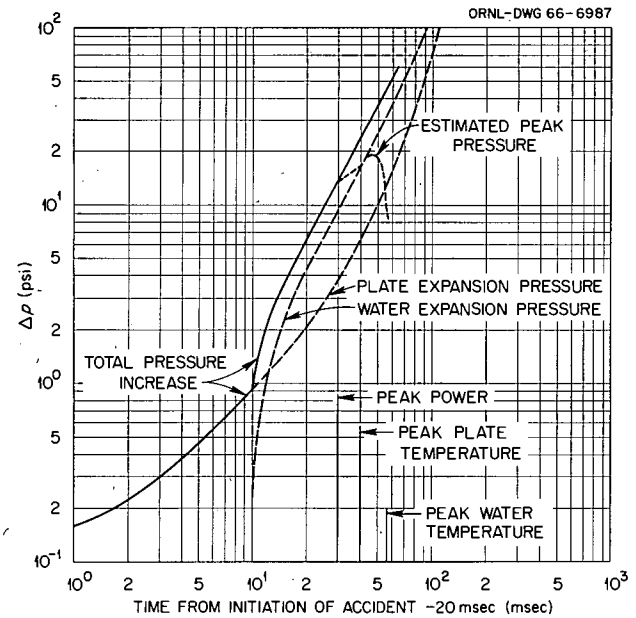

Fig. II.L.7. Increase in Pressure at Horizontal Midplane for 1.3% $\Delta k/k$, 30-msec Ramp Reactivity Addition.

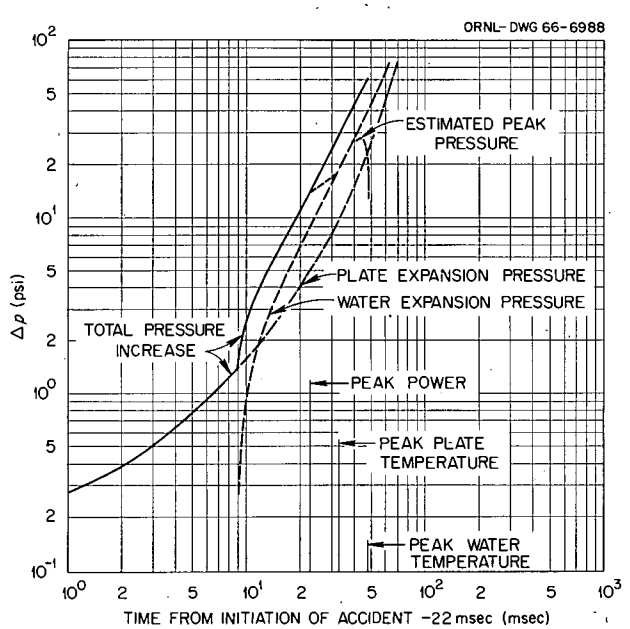

Fig. II.L.8. Increase in Pressure at Horizontal Midplane for 1.5% $\Delta k/k$, 30-msec Ramp Reactivity Addition.

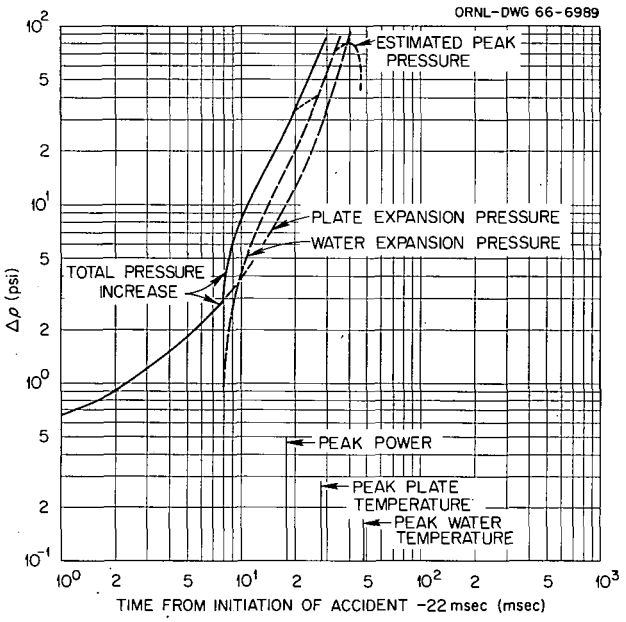

Fig. II.L.9. Increase in Pressure at Horizontal Midplane for 2.0% $\Delta k/k$, 30-msec Ramp Reactivity Addition.

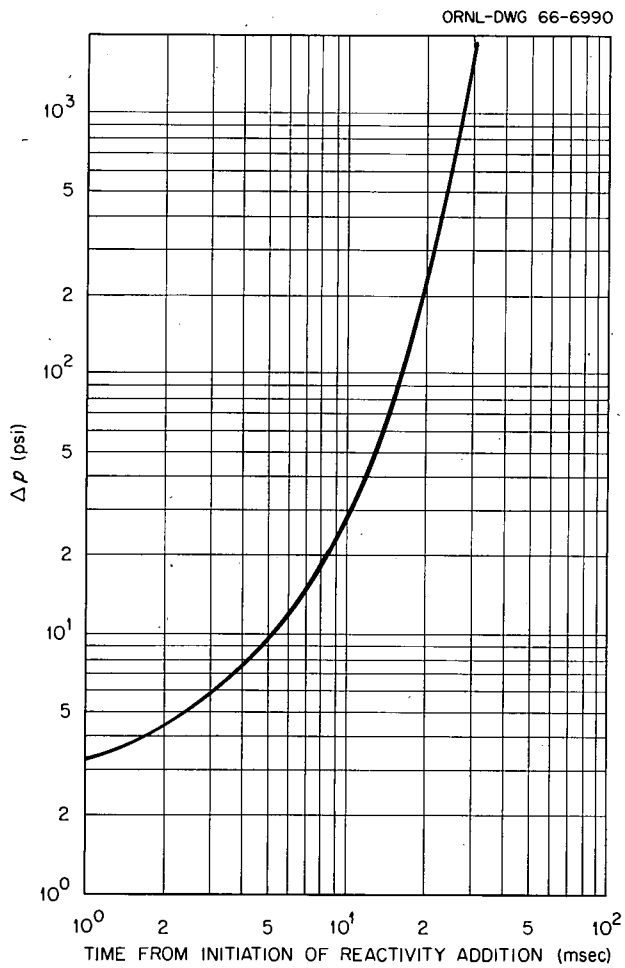

Fig. II.L.10. Increase in Pressure at Horizontal Midplane for $t = 5$ msec (All Heat in Plate).

ORNL-3573
UC-80 – Reactor Technology

INTERNAL DISTRIBUTION

1. Biology Library
2–4. Central Research Library
5. Reactor Division Library
6. Laboratory Shift Supervisor
7. Nuclear Safety Information Center
8–9. ORNL Y-12 Technical Library Document Reference Section
10–109. Laboratory Records Department
110. Laboratory Records, Record Copy
111. G. M. Adamson, Jr.
112. R. G. Affel
113. J. L. Anderson
114. D. S. Asquith
115. S. E. Beall
116. M. Bender
117. D. S. Billington
118–120. F. T. Binford
121. H. Blauer
122–131. A. L. Boch
132. E. G. Bohlmann
133. C. J. Borkowski
134. G. E. Boyd
135. W. E. Browning, Jr.
136. F. R. Bruce
137. W. D. Burch
138. O. W. Burke
139. T. J. Burnett
140. C. D. Cagle
141. A. D. Callihan
142. D. W. Cardwell
143. W. R. Casto
144. C. E. Center
145. R. D. Cheverton
146. H. C. Claiborne
147. R. L. Clark
148. W. G. Cobb
149–153. T. E. Cole
154. B. L. Corbett
155. R. A. Costner, Jr.
156. Wm. B. Cottrell
157. D. D. Cowen
158–207. J. A. Cox
208. E. N. Cramer
209. F. L. Culler
210. J. E. Cunningham
211. D. M. Davis
212. S. J. Ditto
213. G. L. Dixon
214. B. C. Duggins
215. E. P. Epler
216. W. K. Ergen
217. D. E. Ferguson
218. J. Foster
219. J. L. Fowler
220. J. H. Frye, Jr.
221. J. H. Gillette
222. R. J. Griffin
223. H. Grimac
224. W. R. Grimes
225. E. E. Gross
226. L. A. Haack
227. T. P. Hamrick
228. J. A. Harvey
229. J. W. Hill, Jr.
230. R. M. Hill, Jr.
231. L. B. Holland
232. C. F. Holloway
233. F. A. Huddleston
234. E. B. Johnson
235. J. E. Jones, Jr.
236. W. H. Jordan
237. F. B. K. Kam
238. S. I. Kaplan
239. G. W. Keilholtz
240. C. P. Keim
241. M. T. Kelley
242. W. H. Kelley, Jr.
243. M. J. Kelly
244. E. M. King
245. W. C. Koehler
246. J. A. Lane
247. C. E. Larson
248. H. A. Levy
249. A. L. Lotts
250. R. S. Livingston
251. M. I. Lundin
252. H. G. MacPherson
253. D. W. Magnuson
254. F. C. Maienschein
255–279. R. V. McCord

280. H. C. McCurdy
281. H. A. McLain
282. R. A. McNees
283. J. R. McWherter
284. E. C. Miller
285. K. Z. Morgan
286. F. H. Neill
287. J. P. Nichols
288. L. C. Oakes
289. G. R. Owens
290. G. W. Parker
291–292. R. B. Parker
293. A. M. Perry
294. K. H. Poteet
295. M. E. Ramsey
296. L. D. Roberts
297. D. P. Roux
298. E. F. Roy
299. P. Rubel
300. A. F. Rupp
301. R. L. Scott, Jr.
302. H. E. Seagren
303. T. M. Sims
304. M. J. Skinner
305. I. Spiewak
306. A. H. Snell
307. R. S. Stone
308. J. H. Swanks
309. C. A. Sweet
310. W. H. Tabor
311. E. H. Taylor
312. G. M. Watson
313. C. C. Webster
314. A. M. Weinberg
315. R. C. Weir
316. K. W. West
317. G. D. Whitman
318. M. K. Wilkinson
319. E. J. Witkowski
320. E. O. Wollan
321. G. Young

EXTERNAL DISTRIBUTION

322. Hector Barcelo, Puerto Rico Nuclear Center
323. Eric Blomberg, AB Atomenergi, Sweden
324. K. J. Bobin, Mol. Belgium
325. F. B. Buoni, Wright-Patterson Air Force Base
326. J. R. Colley, South Africa Atomic Energy Board
327–331. R. C. DeYoung, Division of Reactor Licensing, AEC-Washington
332. L. F. Franzen, Institut für Reaktorsicherheit der Technische, Koln
333. Kiyoshi Inoue, Hitachi Central Research Laboratory, Japan
334–336. T. R. Jones, Division of Research, AEC-Washington
337. Masanori Kanbara, Japan Atomic Energy Research Institute
338–342. M. Levenson, Argonne National Laboratory
343. O. D. Oner, CEKMECE Nuclear Research Center, Istanbul
344–357. H. M. Roth, Atomic Energy Commission, Oak Ridge, Tennessee
358. Milton Shaw, Division of Reactor Development & Technology, AEC-Washington
359. J. J. M. Snepvangers, Reactor Centrum Nederland
360. J. A. Swartout, 270 Park Avenue, New York 17, New York
361. R. Wakabayashi, Nippon Atomic Industry Group, Co., Ltd.
362. C. E. Winters, Union Carbide Corporation, Parma Research Center, Cleveland, Ohio
363. Karl E. Wirtz, Karlsruhe, Germany
364. A. C. Woods, Lucas Heights, Australia
365–643. Given distribution as shown in TID-4500 under Reactor Technology category (25 copies – CFSTI)